2015

Components of the Ubiquitin Proteasome System are Required for the Nonapoptotic Death of the C. Elegans Linker Cell

Jennifer Zuckerman Malin

COMPONENTS OF THE UBIQUITIN PROTEASOME SYSTEM ARE REQUIRED FOR THE NONAPOPTOTIC DEATH OF THE *C. ELEGANS* LINKER CELL

A Thesis Presented to the Faculty of

The Rockefeller University

in Partial Fulfillment of the Requirements for

the degree of Doctor of Philosophy

by

Jennifer Zuckerman Malin

June 2015

Components of the ubiquitin proteasome system are required for the nonapoptotic death of the *C. elegans* linker cell

Jennifer Zuckerman Malin, Ph. D

The Rockefeller University

Cell death is a major cell fate that promotes tissue sculpting and morphogenesis during animal development. Many developmental cell-culling events cannot be accounted for solely by caspase-dependent apoptosis, yet, alternate pathways are poorly understood. Direct evidence that caspase-independent non-apoptotic cell death pathways operate during animal development is provided by studies of the *C. elegans* linker cell. Genetic studies of linker cell death have led to the identification of genes that promote this process, including *pqn-41*, which encodes a glutamine-rich protein, as well as *tir-1*/TIR-domain and *sek-1*/MAPKK, which may function in the same pathway as *pqn-41*. The *let-7* microRNA and its indirect target, the Zn-finger transcription factor LIN-29, also promote linker cell death, and may act early in the process.

Our work suggests that components of the ubiquitin proteasome system (UPS) act to promote linker cell death. We show that LET-70, an E2 ubiquitin-conjugating enzyme, is required cell-autonomously for linker cell death. LET-70 levels, as well as those of ubiquitin and some proteasome components, increase just before linker cell death initiation. This rise is dependent on an MLL-type histone methyltransferase complex and a MAPK cascade, whose activities are required for linker cell death. The E3 ligase

components SIAH-1, RBX-1, and CUL-3 are also required for linker cell death and appear to act in the same pathway as *let-70*.

We also identify the PLZF transcription factor EOR-1, and its accessory protein, EOR-2 as major regulators of linker cell death. Our studies suggest that EOR-1/2, as well as all known regulators of the linker cell death pathway may act upstream of UPS components to promote cell death.

Our studies reveal that activation of the ubiquitin proteasome system is an important event promoting linker cell death. Given the morphological similarities between linker cell death and non-apoptotic developmental and pathological cell death in vertebrates, we raise the possibility that the proteasome may be a key mediator of vertebrate cell death.

Out of clutter, find simplicity;

From discord make harmony; and finally

In the middle of difficulty lies opportunity.

-John Archibald Wheeler, regarding Einstein's rules of work

ACKNOWLEDGMENTS

Though this thesis is my own, it is also the work—both directly and indirectly—of countless others, whose time, energy and support mean the world to me.

First, I would like to thank **Shai** for his mentorship over the past 6.5 years. His level-headedness, intelligence and wisdom—both inside and outside of the lab—have been an inspiration to me. My entire scientific approach has been informed by the way he thinks, and I cannot convey the amount of gratitude I have for what he has taught me. I am fortunate to have had his guidance.

I would also like to thank my committee chair **Hermann Steller**. Hermann's attention to detail, scientific skepticism and enthusiasm during our annual meetings pushed me to become the best scientist I could be. Hermann is also unfailingly generous, especially in suggesting experiments and offering the help of his postdocs to teach me unfamiliar techniques. His lab members, especially **Sigi Benjamin-Hong** and **Cristi Sandu**, were equally generous with their time and advice, and I am truly grateful for their help and support.

I would like to thank **Sid Strickland** for his assistance while serving on my committee. His unwavering support and optimism kept me motivated through difficult stretches in my project and I am glad to have had him as a committee member. I would also like to thank the **Dean's Office (Emily, Kristen, Marta, Stephanie and Cris)** for their assistance in simplifying the logistics of completing my thesis.

I would like to thank **Meera Sundaram** for agreeing to serve as my external committee member for my defense, and for providing strains and reagents which have been used in this thesis. I am looking forward to our scientific discussion in the coming weeks.

I would like to thank **all members of the Shaham lab, past and present**, for their guidance and support. Our meetings have truly been a breeding ground for exciting science, and I appreciate the encouragement they've given me here, especially when I've had doubts about my work. I have learned so much from all of them, and I hope that I've helped them, even in a small way, as they've all helped me. They've also made the lab a fun place to be.

I would like to give a special thanks to **Yun Lu,** whose electron micrographs appear in this thesis.

I would like to thank my **friends at Rockefeller,** for inspiring me to do the best science possible. Rockefeller is an exceptional place that has allowed me to meet people from different scientific backgrounds and I treasure our conversations, both scientific and non-scientific. They have been a great support system, and have taught me that usually, the best outlet is a potluck or a cookie swap ☺.

I would like to thank my **friends from Penn,** who have been wonderful cheerleaders, whether in New York or across the country. I'd like to give a special thanks to Alexis, Sydney and Jeremy for providing the empathy that comes from being a biology PhD student.

I would like to thank my undergraduate mentor **Elizabeth Lacy** and my high school science teacher **Terrence Bissoondial**, for introducing me to scientific research. Thank you for making biology fun and exciting, and for inspiring me to pursue science as a career.

I would like to thank my family members **(especially mom, dad, Jess, Chels and Mike)** for their love and support. Thank you for believing in me, for helping me to de-stress, and for cheering on every milestone on the path to my defense. The **Malin** family has also been an unending source of encouragement, and I am fortunate to have them in my life.

Finally, I'd like to thank my husband, **Adam,** for his limitless patience. Thank you for understanding the ups and downs inherent in pursuing a scientific career, and for making every day, whether good or bad, a little bit better.

TABLE OF CONTENTS

Chapter 6: Materials and Methods

Appendix: Potential Leads

LIST OF FIGURES

LIST OF TABLES

CHAPTER 1: Introduction

Cell death is a widespread process that is essential for life. Tissue sculpting, organ morphogenesis, and organ size control are but a few of the developmental events that utilize programmed cell death to generate a functioning adult animal (Chautan et al., 1999; Coucouvanis and Martin, 1995; Zou and Niswander, 1996). Not only is death important for development, but it is also essential to the survival of many organisms. Cell death protects the organism from environmental stressors such as radiation, and misregulation of the apoptotic pathway is associated with a number of diseases, including autoimmunity and cancer. While the hypothesis that cell death is a regulated phenomenon in animal development was first experimentally addressed in vertebrates (Hamburger and Levi-Montalcini, 1949) and insects (Lockshin and Williams, 1965), the first systematic studies aimed at deciphering the molecular program promoting cell demise employed the free-living soil nematode *Caenorhabditis elegans* (Horvitz, 2003).

Programmed Cell Death in *Caenorhabditis elegans*

The nematode *C. elegans* has proven to be an excellent system for the study of programmed cell death. The transparent cuticle of the worm facilitated the observation of cell divisions *in vivo* and allowed for the mapping of the animal's complete cell lineage, which documented a stereotyped pattern of cell divisions that creates a 959-celled organism (Kimble and Hirsh, 1979; Sulston and Horvitz, 1977; Sulston et al., 1980; 1983). From these lineage studies, it was ascertained that in the hermaphrodite, the same 131 cells consistently die during development, rounding up to be engulfed by neighboring cells. These corpses possess

characteristics of apoptotic cell death: condensed nuclear chromatin and reduced cytoplasmic volume (Kerr et al., 1972; Shaham and Horvitz, 1996a; Sulston et al., 1983). Genetic studies that were carried out characterized the molecular underpinnings of apoptosis.

Core apoptosis regulators in *C. elegans*

Most cell death in *C. elegans* is controlled by the proteins CED-3, CED-4, CED-9, and EGL-1, whose functions and interactions have been extensively analyzed. All four components of this canonical cell death pathway are conserved across disparate animal species, from nematodes to humans.

CED-3/caspase

The most downstream core component of the apoptotic cell death pathway is encoded by the *ced-3* gene. *ced-3* was initially identified in a genetic screen for *ce*ll *d*eath defective mutants using animals mutant for the *ced-1* engulfment gene, which have visible uncleared corpses. A suppressor screen for animals lacking these corpses identified the recessive mutant, *ced-3*(*n717*), in which most cells fated to die fail to do so. Characterization of the mutant revealed widespread cell death inhibition, resulting in animals with extra cells (Ellis and Horvitz, 1986). *ced-3* mutant animals are alive, suggesting that at least under laboratory conditions cell death is not essential (Ellis and Horvitz, 1986). However, some *ced-3* animals exhibit defects in chemotaxis to attractive odors, and some exhibit pronounced developmental delay (Ellis et al., 1991a), suggesting that in the wild, cell death likely confers a survival advantage.

The CED-3 protein, together with mammalian caspase-1, was the first identified member of the caspase protease family (Thornberry, 1992; Yuan et al., 1993). The active form of CED-3 derives from a precursor that is cleaved to generate three fragments. The N-terminal fragment,

which has sequence homology to caspase recruitment domains (CARD), is not required for protease activity, while the middle and C-terminal fragments associate in pairs to form a heterotetramer, which is the active protease (Huang et al., 2013; Thornberry, 1992). Protease function is effected by a cysteine residue located within an active-site pentapeptide, which cleaves target proteins after the amino acid aspartate, and biochemical studies show a further preference for cleavage after the sequence DEVD (Xue et al., 1996). Aspartate residues also define the junctions between subunits in the precursor form, and biochemical studies have revealed a role for cross-catalysis in protease autoactivation (Qi et al., 2010; Thornberry, 1992).

CED-4

Activity of CED-3 is modulated by the protein CED-4. Like those in *ced-3*, mutations in the *ced-4* gene cause inappropriate survival of somatic and germ cells fated to die during *C. elegans* development (Ellis and Horvitz, 1986). *ced-4* is similar to the mammalian cell death gene Apaf-1, and is composed of four structural domains: an N-terminal CARD domain, a nucleotide-binding domain found in NTPases, a helical domain, and a C-terminal winged-helix domain (Qi et al., 2010; Yuan and Horvitz, 1992; Zou et al., 1997). Structural studies suggest that CED-4 monomers can form an octameric complex with CED-3 that has 4-fold symmetry, in which CARD domains seem to mediate much of the contact (Qi et al., 2010). This is in contrast to the proposed hepatmer formed by Apaf-1 (Acehan et al., 2002). Although explanations based on structural data for the different stoichiometries have been put forward (Qi et al., 2010), the difference remains an intriguing mystery. The nucleotide-binding domain of CED-4, together with its overall structure, bear resemblance to AAA+ ATPases (Qi et al., 2010), although significant deviations in multimer interfaces are observed compared with *bona fide* members of this family. Nonetheless, it is intriguing and perhaps functionally relevant that the *C. elegans*

protein MAC-1, an AAA+ family ATPase, can bind CED-4 (as well as Apaf-1), and that overexpression of MAC-1 can prevent some natural cell deaths in the animal (Wu et al., 1999). The CED-4 nucleotide-binding domain binds ATP-Mg^{2+}, and, in contrast to Apaf-1, steady-state studies suggest a marked preference for ATP over dATP (Li et al., 1997; Seiffert, Vier, & Hacker, 2002). Whether ATP binding *per se*, or exchange of ADP for ATP is required for CED-4 function is still not clear.

As with CED-3, several studies suggest that CED-4 functions within dying cells to promote their demise, and is also required for ectopic postembryonic induction of cell death in cells that usually survive (Shaham and Horvitz, 1996a; Yuan and Horvitz, 1990).

Early-embryonic polyclonal CED-4 antibody staining suggests that CED-4 associates with mitochondria (Chen et al., 2000). However, a different antibody detects perinuclear staining that does not overlap with mitochondria in later embryos or in the germ line (Pourkarimi et al., 2012).

The *ced-4* genomic locus encodes at least two alternative transcripts, *ced-4*L and *ced-4*S. These differ by inclusion of an alternate splice site acceptor upstream of exon 4 of the gene, resulting in a 24 amino-acid insertion in CED-4L (Shaham and Horvitz, 1996b). Overexpression of CED-4L potently inhibits cell death, suggesting that this protein may normally function as a dominantly interfering protein that could prevent formation of the predicted CED-4S multimeric structure.

CED-9

Unlike *ced-3* and *ced-4*, the *ced-9* gene encodes a negative regulator of cell death. Increased CED-9 function, either through overexpression or by a mutation in a conserved domain, promotes survival of cells that normally die during *C. elegans* development (Hengartner

and Horvitz, 1994; Hengartner et al., 1992). Loss-of-function mutations in *ced-9* are generally lethal. Some alleles result in inappropriate and widespread death of embryonic cells not fated to die. However, strong loss-of-function mutations result in arrest very early in embryonic development with no evidence of ectopic cell death (Hengartner et al., 1992).

CED-9 protein is similar in sequence to mammalian BCL2 (B Cell Lymphoma 2) and related proteins (Hengartner and Horvitz, 1994). The protein consists of seven alpha helices. Helix 1 corresponds to sequences that comprise BCL2 homology region 4 (BH4) in other BCL2 family members, but is not conserved in the primary sequence of CED-9. Helix 3 comprises the BH3 domain, helices 4 and 5 make up the BH1 domain, and helices 6 and 7 overlap the BH2 domain (Woo and Jung, 2003; Yan et al., 2004). Antibody staining against CED-9 reveals that the protein is localized to mitochondria in embryos and in the germ line (Chen et al., 2000; Pourkarimi et al., 2012). It has been suggested that the C-terminal region of CED-9, which contains a transmembrane region like other BCL2 family members, contributes to this localization. Indeed, expression in *C. elegans* muscle cells of GFP fused to the transmembrane domain confers mitochondrial localization, and a GFP-CED-9 fusion protein lacking the transmembrane domain fails to localize to mitochondria (Tan et al., 2007). However, *ced-9* mutants can still be rescued by expression of cytosolic CED-9(ΔTM), or by expression of an ER-targeted CED-9 (Tan et al., 2007). Thus, the transmembrane region does not appear to be essential for function, but may facilitate mitochondrial localization.

EGL-1

Genetic screens seeking mutants regulating vulval development in *C. elegans* identified a host of genes required for egg-laying, including the cell death gene *egl-1* (Trent et al., 1983). Dominant gain-of function mutations in *egl-1* result in the inappropriate death of the two HSN

neurons that regulate hermaphrodite egg-laying (Desai et al., 1988). That these neurons normally die during male development suggested initially that *egl-1* might be involved in sex determination; however, the mutant revealed no pleiotropies that might indicate sexual transformation (Desai et al., 1988). While *egl-1*(gf)/*egl-1*(gf) mutants are 100% egg laying defective, about 30% of animals transheterozygous for an *egl-1*(gf) allele and a deletion spanning the locus lay eggs normally (Conradt and Horvitz, 1998). Using this observation, homozygous *egl-1*(gf) animals were mutagenized, and a loss-of-function mutation in the gene was obtained by screening for animals with normal egg laying. Remarkably, animals carrying such *egl-1*(lf) mutations are unable to execute the majority of developmental cell deaths in the animal, and contain many extra cells (Conradt and Horvitz, 1998).

The *egl-1* gene was cloned using complementation rescue and mapping of the loss-of-function allele of *egl-1* (Conradt and Horvitz, 1998). The predicted EGL-1 protein is only 106 amino acids long, and is homologous to the BH3 domain common to many mammalian cell death regulators (Kelekar and Thompson, 1998). By sequence, EGL-1 is most similar to the BH3-only class of cell death regulators that promote cell death in a variety of settings. This similarity is also evident in structural studies of the protein, which has been shown to adopt an amphipathic alpha helix conformation (Yan et al., 2004).

EGL-1 expression differs markedly from that of the other core apoptotic regulators in *C. elegans*. During development *egl-1* expression is upregulated in cells that die (Conradt and Horvitz, 1999; Thellmann et al., 2003), although another study suggests that the gene may also function to promote mitochondrial fusion and fission (Jagasia et al., 2005). While CED-9, CED-4, and CED-3 control stochastic germ cell death, EGL-1 appears to be dispensable (Gumienny et al., 1999), indicating that EGL-1 perhaps acts only to guarantee deterministic activation of

apoptosis. Consistent with its expression pattern, *egl-1* gene regulatory sequences are extensive, and are found both upstream and downstream of the gene. The *egl-1*(gf) lesion that leads to the specific demise of the HSN neurons is a point mutation in a regulatory site 5.6 kb downstream of the *egl-1* transcription unit which prevents binding of the inhibitory sex-determination factor TRA-1A (Conradt and Horvitz, 1999). In the absence of TRA-1A binding, *egl-1* is now expressed ectopically only in HSNs, leading to their removal.

Besides EGL-1, two other BH3-only proteins are made by *C. elegans*. DCT-1 is similar to mammalian BNIP3, and can cooperate with CED-3 caspase to induce cell death in cultured mammalian cells (Cizeau et al., 2000). However, a role in *C. elegans* cell death has not been established. CED-13, a protein more similar to EGL-1, is upregulated in the *C. elegans* germ line in response to radiation, and may participate in radiation-induced cell death, but does not appear to play a significant role in developmental cell death either in the soma or the germ line (Schumacher et al., 2005). Thus, unlike mammals, in which a host of BH3-only proteins controls cell death in a myriad of contexts and conditions, *C. elegans* appears to have a single member of this family dedicated to somatic developmental cell death.

The core apoptotic pathway of *C. elegans*

The current model for apoptotic cell death execution in *C. elegans* is as follows: the apoptotic cascade begins when EGL-1 inhibits the activity of CED-9. CED-9 inhibition of CED-4 is then relieved, allowing CED-4 to activate CED-3, promoting cell death (Figure 1.1). The model is supported by genetic, biochemical, and structural data, and predicts similarities and differences with pathway interactions described in mammals.

CED-4->CED-3

Genetic studies support the notion that CED-3 functions downstream of CED-4. Overexpression of CED-3 in neurons not fated to die can result in their demise, and this killing is reduced, but not eliminated, in animals harboring a *ced-4*(lf) mutation. Ectopic expression of CED-4 in the same neurons can also promote their death, however, this is nearly entirely abrogated in strong *ced-3* mutants (Shaham and Horvitz, 1996a). A parsimonious explanation for these genetic studies is that CED-4 facilitates the activity of CED-3. While direct binding of the two proteins in vivo has not yet been demonstrated, binding studies in 293T cells show that CED-4 and CED-3 can physically interact (Chinnaiyan et al., 1997a; Irmler et al., 1997). This interaction seems to occur between the CARD domain in CED-4 and the N-terminal domain of CED-3 (Chinnaiyan et al., 1997b), although binding could also be achieved in the absence of the CED-3 N-terminal domain through the L2' loop of its C-terminal subunit (Huang et al., 2013).

Steady state binding of CED-4 to CED-3 is positively correlated with activation of the caspase zymogen, or procaspase. For example, in insect cells, co-expression of CED-4 and CED-3 leads to increased caspase activity dependent on the CED-3 N-terminal domain and the ATP binding domain of CED-4 (Seshagiri and Miller, 1997; Seshagiri et al., 1998). Conversely, a CED-4 mutation disrupting a hydrophobic binding surface between CED-4 and CED-3 reduces the ability of CED-4 to stimulate CED-3 activity (Huang et al., 2013). Mutations blocking CED-4 oligomerization appear to block processing of CED-3 in cultured cells, suggesting that oligomerization is likely important for activity (Yang et al., 1998). CED-4 has also been suggested to promote the activity of the mature CED-3 caspase in vitro (Qi et al., 2010).

However, the stoichiometry of CED-4:CED-3 here is 8:2 and not 8:8 as previously predicted, raising the possibility that this complex may not be the only source of in vivo activity.

CED-9-|CED-4

The lethality observed in *ced-9*(lf) mutants is suppressed by loss-of-function mutations in either *ced-3* or *ced-4* (Hengartner et al., 1992), and cell death induced by CED-4 ectopic expression is reduced by CED-9 overexpression (Shaham and Horvitz, 1996a). These observations, coupled with the discovery that *ced-9*(gf) mutations block cell death, suggest that CED-4 and CED-3 function downstream of CED-9, and that CED-4 may be a direct target of CED-9. This hypothesis is bolstered by the demonstration that CED-9 and CED-4 physically interact (Spector et al., 1997; Wu et al., 1997), and that mutations reducing CED-9 function in vivo also reduce CED-9-CED-4 binding (Spector et al., 1997). Expression studies in the early embryo of wild-type and mutant *C. elegans* further corroborate this idea. While CED-4 protein, detected using anti-CED-4 sera, appears mitochondria-bound in wild-type animals, it is mainly localized to the nuclear periphery in *ced-9*(lf); *ced-3*(lf) double mutants in which the *ced-3* mutation is used to keep *ced-9*(lf) animals alive (Chen et al., 2000). Thus, CED-9 appears to serve as a mitochondrial anchor for CED-4.

How CED-9 inhibits CED-4 from forming an active octamer is not understood; however, X-ray crystallographic structures of CED-9 bound to CED-4 reveal a complex in which one CED-9 protein is bound to an asymmetric CED-4 dimer (Yan et al., 2005). Thus, it is possible that one mechanism by which CED-9 inhibits CED-4 activity is by preventing its oligomerization. While the contacts observed in this study are specific, they do conflict with solution studies suggesting that bacterially purified CED-9 and CED-4 form a 2:2 complex (Fairlie et al., 2006; Yan et al., 2005). Resolution of these differences is not yet at hand.

In vitro assays demonstrate that CED-9 protein can serve as a substrate for CED-3 caspase (Xue and Horvitz, 1997), raising the possibility that CED-9 might also block cell death by competitively inhibiting CED-3 caspase activity. While global overexpression of CED-9 yields broad cell survival, mutations of the CED-9 aspartate residues targeting cleavage by CED-3 reduce the ability of CED-9 to inhibit death, consistent with this model. However, such lesions could also affect protein conformation and stability. It therefore remains unclear whether CED-9 cleavage by CED-3 has physiological significance.

EGL-1-|CED-9

Genetic studies demonstrate that EGL-1 functions upstream of both CED-4 and CED-3. Specifically, ectopic expression of EGL-1 in neurons that normally live can induce their death. This killing activity is entirely blocked in animals lacking either CED-3 or CED-4 function (Conradt and Horvitz, 1998). Likewise, inappropriate death of the HSN neurons in animals carrying *egl-1*(gf) mutations is suppressed by loss-of-function mutations in *ced-3* or *ced-4* (Ellis and Horvitz, 1986).

EGL-1 also appears to function upstream of CED-9. *egl-1*(lf) mutations, which normally block programmed cell death, fail to do so in *ced-9*(lf); *ced-3*(weak lf) mutants that entirely lack CED-9 activity, suggesting that EGL-1 normally inhibits CED-9 activity (Conradt and Horvitz, 1998). CED-9 tagged with Glutathione-S-Transferase (GST) can bind to in vitro translated EGL-1 (Conradt and Horvitz, 1998), and CED-9 and EGL-1 can be co-crystallized to form a bound complex (Yan et al., 2004), raising the possibility that EGL-1 inhibition of CED-9 might occur through direct physical contact. The EGL-1-CED-9 crystal structure reveals that binding of EGL-1 results in large conformational changes to CED-9, introducing steric hindrance and

misalignment of key residues involved in CED-9-CED-4 binding. Thus, EGL-1 likely acts by preventing the association of CED-9 with CED-4.

Consistent with this idea, overexpression of EGL-1 in early embryos leads to movement of CED-4 from mitochondria to the nuclear periphery as occurs in animals lacking CED-9 (Chen et al., 2000). Titration studies with purified proteins also demonstrate dissolution of the CED-4-CED-9 complex upon addition of EGL-1 (Yan et al., 2004) but not mammalian BH3-domain proteins (Fairlie et al., 2006), as do co-immunoprecipitation studies of the proteins from cultured mammalian cells (del Peso et al., 1998). Further support for this model is provided by the CED-9 gain-of-function G169E mutation that results, in vivo, in cell survival (Hengartner and Horvitz, 1994). This mutation reduces the binding affinity of CED-9 for EGL-1 (del Peso et al., 2000; Fairlie et al., 2006; Parrish et al., 2000), and introduces a bulky amino acid into the binding pocket for EGL-1, leaving the CED-4 binding interface intact (Yan et al., 2005). Thus, blocking EGL-1 binding can allow CED-9 to remain bound to CED-4.

Regulating apoptosis

Control of *egl-1* expression

The induction of *egl-1* expression in dying cells, and the relatively large and complex regulatory region required for this expression, suggests that the decision to live or die may be mediated by cell-specific transcription factors that bind to the *egl-1* locus to promote and/or inhibit *egl-1* transcription. This appears to be the case in HSN neurons, where the sex-determination factor TRA-1A binds downstream of *egl-1* to block transcription in hermaphrodites (Conradt and Horvitz, 1999). The CEM neurons are also sexually dimorphic cells. In this case, the cells survive in males but die in hermaphrodites (Sulston et al., 1983), and

sex-specific survival here is also mediated by control of *egl-1* expression. The CEH-30 homeodomain transcription factor inhibits CEM death in males by acting with UNC-37/Groucho to block expression of *egl-1* in these cells. In hermaphrodites, the TRA-1 protein promotes CEM neuron death by inhibiting transcription of the *ceh-30* gene, thus allowing *egl-1* expression (Nehme et al., 2010; Peden et al., 2007; Schwartz and Horvitz, 2007).

Recessive mutations in the gene *ces-2*, encoding a bZIP transcription factor, and a dominant allele of the gene *ces-1*, encoding a Snail-like bHLH transcription factor, block the deaths of the NSM sister alone, or both NSM sister and I2 sister cells, respectively (Ellis and Horvitz, 1991; Metzstein and Horvitz, 1999; Metzstein et al., 1996). In the NSM sisters, survival correlates with lack of induction of a P*egl-1*::GFP reporter in the cells (Thellmann et al., 2003). CES-1 binds in vitro to Snail elements in an *egl-1* genomic fragment that is required in vivo to mediate CES-1 activity. These elements overlap with E box sequences that can bind the HLH-2 and HLH-3 transcription factors, which promote NSM death and also promote *egl-1* expression (Thellmann et al., 2003). Thus, CES-1 apparently inhibits *egl-1* expression by blocking access of HLH-2/3 to the *egl-1* promoter.

Mutations in the *ceh-34* and *eya-1* genes, both encoding homeodomain transcription factors, block the deaths of the M4 and I3 sister cells. CEH-34 and EYA-1 proteins physically interact, and CEH-34 binds to a regulatory site 5' of the *egl-1* transcription unit. In both mutants, *egl-1* expression in the M4 sister cell is abrogated (Hirose et al., 2010). The Sp1 transcription factor SPTF-3 is also required for expression of *egl-1* in and death of the M4 sister cell (Hirose and Horvitz, 2013). In a similar mode of regulation, a complex consisting of the CEH-20/Pbx1 and MAB-5/Hox transcription factors controls the death of the postembryonic cell P11.aaap. In this case, a site approximately 6 kb downstream of the *egl-1* start codon binds the CEH-20-

MAB-5 complex, and mutations in that site or in its cognate binding factors eliminate *egl-1* expression in the cell (Liu et al., 2006).

Regulation of *egl-1* expression may also govern the death of the embryonic cells ABprpppapp and ABplpppapp, whose demise appears to be weakly dependent on EGF signaling. At least one of these cells survives inappropriately in about 30% of animals deficient in either the EGF ligand LIN-3 or its receptor, LET-23/EGFR, whose site of action is not firmly established. Regardless, a ~50% reduction in the levels of a P*egl-1*::GFP reporter is seen in *lin-3*(lf) mutants (Jiang and Wu, 2014).

egl-1 is not alone

While *egl-1* is a hub for cell death decision-making, more is likely going on. In animals carrying both *ced-9*(strong lf) and *ced-3*(weak) mutations, cells destined to live do so, and only a few cells destined to die survive inappropriately (Hengartner and Horvitz, 1994). In these animals, many cells fated to die appear to die normally, as though no mutation is present. Yet, since CED-9 activity is gone, *egl-1* cannot be the relevant death effector in these cells, unless it also has a CED-9 independent function. A role for *egl-1* in starvation-induced autophagy has been proposed, based on the observation that animals homozygous for an *egl-1*(gf) mutation accumulate the autophagy marker LGG-1::dsRED even in the presence of food (Maiuri et al., 2007). However, autophagy genes are not required for cell death in *C. elegans* (Takacs-Vellai et al., 2005), making this an unlikely mechanism for cell death control. However, cell death regulators that function independently of EGL-1 have been uncovered.

In HSN neurons the EOR-1 protein, similar to the mammalian PLZF transcription factor, is required together with its novel cofactor, EOR-2, for death (Hoeppner et al., 2004; Howard and Sundaram, 2002a; Howell et al., 2010; Rocheleau et al., 2002). Neither gene promotes

expression of *egl-1*. Furthermore, the effects of *eor-1/2* mutations appear to require an intact *ced-9* gene, suggesting that EOR-1/2 may work upstream of or in parallel to CED-9 and in parallel to EGL-1. In CEM neurons, three proteins—the POU homeodomain transcription factor UNC-86, the leucyl t-RNA synthetase LRS-1, and the kinase UNC-132/PIM-1—are required for cell death (Nehme et al., 2010; Peden et al., 2007). In hermaphrodites these genes promote expression of the *ced-3* caspase gene but not of *egl-1*. In males, they promote *ceh-30* expression, and therefore indirectly inhibit *egl-1* expression.

In M4 sister cells, two proteins, GCN-1, which may be involved in controlling translation initiation factor levels, and the interacting protein ABCF-3, an AAA+ ATPase, appear to function together to promote cell death, and mutants in these genes have a weak survival defect. Here also, both proteins act independently of CED-9, and hence of EGL-1, to promote cell death (Hirose and Horvitz, 2014). The mechanism of action of this protein complex is not known, but the similarity of ABCF-3 to AAA+ ATPases raises the possibility that they may interact with CED-4.

In addition to regulating *egl-1* transcription in M4 sister cells, the SPTF-3/Sp1 protein also promotes expression of the gene *pig-1*. PIG-1, similar to MELK kinase, has been implicated in the control of a number of cell death events in *C. elegans*, and also appears to function in parallel to EGL-1 and CED-9. PIG-1 has been suggested to function in a *ced-3*–independent cell death pathway (Denning et al., 2012; Hirose and Horvitz, 2013). However, the data are also consistent with a function within the canonical cell death pathway. Indeed, PIG-1 function in asymmetric cell division has been previously described (Chien et al., 2013; Cordes et al., 2006), raising the possibility that PIG-1 may control the segregation of death effectors downstream of CED-9, such as CED-3 or CED-4. Such segregation could explain how an initially broad

expression pattern of these genes leads to the death of specific cells. Supporting this notion, the polarity proteins PAR-4/LKB1 kinase, STRAD-1/STRAD, and MOP-25/MO25 appear to function together with PIG-1 in the death of the ABplpappap cell (Denning et al., 2012).

Parallel control of death is also seen in descendents of the Pn.p blast cells that normally die in the ventral cord of early larva and in pharyngeal cells. Here, components of the conserved retinoblastoma (Rb)/E2F pathway are required for cell death and also function independently of CED-9 and likely EGL-1 (Reddien et al., 2007).

egl-1 is not always required

While *egl-1* control is essential for some cell death initiation, in some cases EGL-1 function is not required. The tail-spike cell is a binucleate cell with a posterior process believed to function as a scaffold for developing tail epithelial cells. Five hours after it is born, the tail spike cell dies (Sulston et al., 1983). While death requires *ced-3* and *ced-4*, *ced-9*(gf) mutations do not block cell death, and *egl-1*(lf) animals only have a weak defect, with about 30% exhibiting tail-spike cell survival (Maurer et al., 2007). This suggests that EGL-1-CED-9 interactions are not important for the demise of this cell. In the tail-spike cell, transcription of the *ced-3* caspase gene is temporally controlled. Expression of a P*ced-3*::GFP reporter is off until about 25 minutes before the cell rounds up and dies, suggesting that *ced-3* transcription is an important regulatory node. The transcription factor PAL-1, similar to vertebrate Cdx2, is an important regulator of tail-spike cell death. PAL-1 is required for *ced-3* expression and can bind to sequences upstream of the *ced-3* start codon in vitro. Mutations in *pal-1* also block tail-spike cell death (Maurer et al., 2007).

Besides PAL-1, the F-Box protein DRE-1 also regulates tail-spike cell death. *dre-1* mutants have inappropriately surviving tail-spike cells, and like *pal-1*, *dre-1* acts in parallel to

egl-1. However, *dre-1* requires a wild-type copy of *ced-9* to carry out its function. Genetic and protein interaction studies suggest that DRE-1 physically interacts with SKR-1/SKP, which controls protein ubiquitylation, to promote cell death. DRE-1 also interacts with CED-9, which may, therefore, be its in vivo target (Chiorazzi et al., 2013).

egl-1(lf) and *ced-9*(gf) mutations block germ cell death in response to ionizing radiation (Gartner et al., 2000); however, as in the tail-spike cell, neither mutation affects normal physiological cell death in the germ line. Other regulators appear to take charge here. Mutants in *pax-2* and *egl-38*, encoding Pax2/5/8 family transcriptional regulators, have increased rates of germ cell death. Overexpression of these genes reduces germ line apoptosis (Park et al., 2006). Mosaic analysis shows that *egl-38* is required in the germline for germ cell survival, and RT-PCR, deletion, and chromatin immunoprecipitation studies suggest that both *egl-38* and *pax-2* act by activating *ced-9* transcription (Park et al., 2006). This function may also extend to embryonic cell death, as *egl-38* and *pax-2* single mutants also have increased cell corpses in embryos.

The Rb pathway also plays a role in developmental germ cell death control. LIN-35/Rb appears to inhibit *ced-9* transcription in these cells, while the DP homolog DPL-1, and the E2F-like EFL-2 promote transcription of *ced-3* and *ced-4* (Schertel and Conradt, 2007). Another tumor control pathway, the RAS/MAPK signaling pathway, also appears to be important. Mutations in the *let-60*/Ras, *lin-45*/Raf, and *mek-2* and *mpk-1* MAPK genes block germ cell death (Gumienny et al., 1999), and also lead to other developmental defects in the germ line, suggesting that they likely act early in cell fate determination.

The engulfment genes and their roles in cell death

Two parallel and partially-redundant pathways control recognition of dying cells (Ellis et al., 1991b). One consists of the membrane receptor CED-1, which appears to recognize the lipid phosphatidylserine on the surface of dying cells (Zhou et al., 2001b), CED-6, an adaptor protein that may function in signal transduction (Liu and Hengartner, 1999; 1998), and CED-7, a membrane ABC transporter that may be involved in phosphatidylserine presentation (Wu and Horvitz, 1998). CED-1 and CED-6 function in the engulfing cell, and CED-7 is required in both dying and engulfing cells. Unlike CED-1 and CED-6, CED-7 is required only in the soma, whereas the phospholipid scramblase PLSC-1 exposes phosphatidylserine in dying germ cells (Venegas and Zhou, 2007). The other pathway consists of the proteins CED-2/CrkII, CED-5/Dock180, CED-10/Rac, and CED-12/Elmo (Gumienny et al., 2001; Reddien and Horvitz, 2000; Wu et al., 2001; Zhou et al., 2001a). CED-2, -5, and -12, appear to function together to regulate CED-10 activity. CED-10 likely acts to control assembly of the actin cytoskeleton during the extension of engulfing cell protrusions around the dying cell.

Once an apoptotic cell has been incorporated into a phagosome within the engulfing cell, a series of events alter the phagosomal surface, culminating in lysosomal targeting. Phosphatidylinositol 3-phosphate (PtdIns(3)P) coats the phagosomal membrane, allowing binding of BAR-domain sorting nexins to recruit lysosomes (Lu et al., 2011a). In parallel, RAB-5, which binds initially to the phagosomal surface, is replaced by RAB-7, through activity of the SAND-1 and CCZ-1 complex (Kinchen and Ravichandran, 2010; Nieto et al., 2010), and phagolysosome formation ensues through activities of the conserved HOPs complex (Kinchen et al., 2008) and the proteins UNC-108/RAB2 and RAB-14, which promote acidification of the compartment (Guo et al., 2010; Mangahas et al., 2008).

While engulfment has generally been viewed as independent of cell death execution, some observations suggest a more intimate connection. In animals carrying weak *ced-3* caspase mutations, some cells destined to die in the developing ventral cord of *C. elegans* larvae succumb and are removed, while others survive inappropriately. Occasionally, cells that by DIC microscopy appear to have initiated apoptosis recover and survive (Hoeppner et al., 2001). In these mutants, cells fated to die teeter on the edge between life and death. Remarkably, in animals homozygous for mutations in genes controlling engulfment, significantly more cells survive and develop (Reddien et al., 2001). These results demonstrate that at least under some conditions, engulfment may promote cell death. Similarly, in *C. elegans* males, the cells B.alapaav and B.arapaav have been reported to survive in *ced-1* and *ced-2* mutants, presumably because they fail to be engulfed by the P12.pa cell (Hedgecock et al., 1983).

CED-3 substrates

While caspase enzymology and activity have been studied in *C. elegans* and many other organisms, the mechanism by which these aspartyl-specific cysteine proteases bring upon cellular demise is an enduring mystery. Are there many or few relevant targets? Are there many or few cellular processes that must be blocked or activated to ensure cell death? While a plethora of vertebrate caspase substrates have been described (Poreba et al., 2013), their relevance to cell death is poorly understood. One exception is the ICAD DNase inhibitor, whose inactivation by caspase-mediated cleavage leads to DNA degradation in mammalian cells (Enari and Sakahira, 1998; Liu et al., 1998). Proteins related to ICAD or the active nuclease CAD/DFF40 are not encoded by the *C. elegans* genome. However the *C. elegans* DNAse II homolog NUC-1 does play a key role in DNA degradation during apoptosis (Hevelone and Hartman 1988; Sulston,

1976; Wu et al., 2000). *C. elegans* apoptotic DNA is cleaved into 10 bp fragments (Aruscavage et al., 2010); *nuc-1* mutants lack these fragments and accumulate larger DNA fragments in dying cells, as well as undegraded bacterial DNA in the gut (Aruscavage et al., 2010; Sulston, 1976). *nuc-1* mutant embryos stained using the TUNEL method (Gavrieli et al., 1992) display an accumulation of DNA ends (Wu et al., 2000), suggesting that NUC-1 degrades TUNEL-positive intermediates produced by another nuclease. One candidate may be the microRNA-processing Dicer in *C. elegans.* Dicer can be cleaved by CED-3 and may, surprisingly, participate in DNA cleavage (Nakagawa et al., 2010). It is therefore possible that a DNA degradation system analogous to that in mammals is targeted by caspases in *C. elegans*.

Cell death pathways in *Drosophila*

Drosophila homologs of the core apoptotic pathway exist and are similar in function to those in *C. elegans*. BCL2 genes identified in *Drosophila* include Buffy and Debcl (Colussi et al., 2000; Quinn et al., 2003); Dark is the fly Apaf-1 homolog (Rodriguez et al., 1999); and a number of caspases are required to carry out apoptotic death in the organism. No BH3-only gene has been identified in the *Drosophila* genome (Lomonosova and Chinnadurai, 2008).

Although *Drosophila* apoptotic genes are functionally conserved with those in *C. elegans*, their regulatory mechanisms are quite different (Figure 1.1). First, there are more caspase genes—there are seven in the *Drosophila* genome—and their functions are subdivided into two classes. The first class of *Drosophila* caspases are "initiator"/apical caspases (Dronc/Strica/Dredd); these proteins are characterized by long prodomains. Little is known about Strica's role as an initiator caspase, but recent analysis of mutants suggests that it may work redundantly with Dronc to regulate apoptosis during cell competition in "Minute" cells, and may

also regulate cell death during oogenesis (Baum et al., 2007; Kale et al., 2015). Dronc appears to be the main initiator caspase, as evidenced by its ability to bind and be processed by Apaf-1/Dark (Chen et al., 1998; Dorstyn et al., 1999; Kanuka et al., 1999). The remaining caspases are "executioner"/downstream caspases (Drice, Dcp-1, Decay, and Damm), which have shortened N-terminal domains, and whose cleavage by initiator caspases causes conformational changes that allow them to digest specific substrates required for death (Dorstyn et al., 1999; Fraser and Evan, 1997; Kornbluth and White, 2005). Drice appears most essential for apoptosis, as Drice null mutant animals experience lethality by the pupa stage (Muro et al., 2006), while flies carrying homozygous null mutations of Dcp-1 appear healthy, with mild defects in starvation-induced germline cell death (Laundrie et al., 2003).

While the fly genome does contain BCL2 homologs—the anti-apoptotic Buffy and the proapoptotic Debcl—they appear not to be essential for most developmental cell deaths in the organism, as mutants harboring small deletions in Buffy and Debcl loci show wild-type patterns of cell death and appear physiologically normal (Colussi et al., 2000; Quinn et al., 2003; Sevrioukov et al., 2007). Further experiments using full knock-out mutants of Buffy and Debcl corroborate this data; however, more extensive cell death characterization shows that Debcl mutant animals have extra cells in specific neuronal lineages and slightly lower viability following IR radiation treatment (Galindo et al., 2009).

Thus, BCL2 genes are required in certain apoptotic scenarios. In these circumstances, as in worms, Debcl requires intact Dark/CED-4 to function (Galindo et al., 2009). While no BH3-only homologs have been identified in *Drosophila,* a number of other gene classes have been identified as essential for regulation of developmental cell death in the fly and will be described hereafter.

Outside of the core apoptotic pathway, *Drosophila* and mammals possess a second, equally important group of proteins required for regulation of caspase activity: IAPs, or inhibitor of apoptosis proteins (Figure 1.1). Diap1, the first *Drosophila* IAP identified, was isolated in a deletion screen for enhancers of cell death using an eye-specific reaper-overexpression strain (see below) (Hay et al., 1995). Ectopic expression of Diap1 is sufficient to prevent reaper (Rpr) overexpression-induced apoptosis, and co-expression of IAPs in a caspase overexpression strain (both yeast and cell culture) is sufficient to prevent ectopic cell death, indicating that it is an important antiapoptotic regulator (Hay et al., 1995; Kaiser et al., 1998; Meier et al., 2000). IAPs were hypothesized to inhibit caspases through physical interaction; yeast two-hybrid and coimmunoprecipitation experiments have mapped the IAP binding site to their Baculovirus Repeat (BIR) domains, so called because of their homology to the antiapoptotic baculovirus protein p35 (Clem et al., 1991; Xue and Horvitz, 1995). Despite this in vitro data, very little in vivo evidence exists for direct inhibition of caspases by many IAPs. For example, though DIAP1 inhibits apoptosis in vivo in *Drosophila*, it only modestly impacts caspase activity in vitro (Devereaux et al., 1997; Yan et al., 2004b). Within the class of IAPs, a further subset of IAP genes act as E3 ubiquitin ligases (see below); these genes contain RING finger domains that allow them to ubiquitinate caspases to further prevent apoptosis (Suzuki et al., 2001; Wilson et al., 2002). Though the *C. elegans* genome contains genes with BIR domains, none of them have been implicated in cell death. However, these genes are highly conserved, and exist in mammals; the mammalian XIAP is the most well-studied of these proteins, and appears to inhibit cell death by directly binding to initiator caspases, as well as by preventing cytochrome C release (Deveraux et al., 1998; 1997; Roy et al., 1997).

Though a number of IAPs work to promote apoptosis, many other "IAPs" appear to serve a nonapoptotic function. The BIR domain-containing protein Survivin acts as a member of the chromosomal passenger complex, which promotes spindle assembly during mitosis (Jeyaprakash et al., 200). Other IAPs, such as cIAP-1, bind caspases in vitro, but do not appear to inhibit caspase activity (Eckelman and Salvesen 2006; Tenev et al., 2005). Thus, while many IAPs have conserved BIR domains required for caspase-binding, it is unclear whether some IAPs are required for induction of apoptosis.

The upstream regulators of IAPs were among the first cell death genes discovered in *Drosophila.* Reaper, hid, and grim were isolated in a screen for aberrant staining patterns of the vital dye acridine orange. These genes were mapped to the chromosomal deficiency *H99*. Homozygous deletion mutants in these genes suppress developmental cell death, and in situ hybridization experiments show that they are expressed in cells fated to die. Ectopic expression of these genes induces death which can be suppressed by p35 (Chen et al., 1996a; Grether et al., 1995; White et al., 1994). Reaper, hid, grim and their related proteins (RHGs) each possess an N-terminal IAP-binding motif (IBM) that is used to promote cell death. Analysis of various mutants and coimmunoprecipitation studies suggest that RHGs block caspase activation by competitively binding to IAP BIR domains (Goyal et al., 2000; Vucic et al., 1998; 1997). IBM-containing proteins are conserved, and related mammalian proteins—Smac/Diablo, and Omi/HtrA2—have also been isolated (Du et al., 2000; Hegde et al., 2002; Verhagen et al., 2000). A third IAP inhibitor, ARTS, does not contain an IBM motif, but directly binds XIAP and recruits the E3 ligase Siah-1 to promote IAP degradation (Gottfried et al., 2004; Bornstein et al., 2011; Garrison et al., 2010). Purified RHGs are also able to act with ubiquitin conjugating enzymes such as UbcD1 to stimulate IAP autoubiquitination in vitro, providing a second mechanism by which

they promote apoptosis (Ryoo et al., 2002; Sandu et al., 2010). Although not found in *C. elegans,* these genes are important regulators of cell death in flies and mammals.

Cell death pathways in mammals

As in *Drosophila*, a number of caspases have been identified in mammals. Three caspases (caspases-8, -9 and -10) in mammals are initiator caspases, and three (caspases -3, -6, and -7) are executioner caspases (Nicholson et al., 1995; Parrish et al., 2013). The remaining caspases are required for processes such as cytokine processing and keratinocyte specification, and thus play a limited role in apoptosis (Parrish et al., 2013). As in the worm and the fly, co-immunoprecipitation experiments using purified proteins suggest that Apaf-1 binds caspases to promote cell death; however, unlike the worm/fly, binding is Cytochrome C and dATP dependent (Li et al., 1997). Structural studies suggest that in the worm, CED-4 monomers can form an octameric complex with CED-3 that has 4-fold symmetry, in which CARD domains seem to mediate much of the contact (Qi et al., 2010). While the apoptosome in *Drosophila* also appears to form an octamer in electron cryo-microscopy studies (Yu et al., 2006), mammalian experiments propose an Apaf-1 heptamer (Acehan et al., 2002). Although explanations based on structural data for the different stoichiometries have been put forward (Qi et al., 2010), the difference remains an intriguing mystery.

BCL2 genes are regulated differently in mammals than in invertebrates. As in the fly, the mammalian genome contains antiapoptotic as well as proapoptotic BCL2 genes. These proteins also localize to the mitochondria, as visualized with GFP-tagged proteins in cell culture, immunofluorescence, membrane fractionation and immuno-EM experiments (Hockenbery et al., 1990; Krajewski et al., 1993; Wolter et al., 1997). BCL2 family members have been suggested to

form membrane pores, and in vitro experiments demonstrate that they can assemble into channels of variable conductivity (Antonsson et al., 1997; Basanez and Sharpe, 2002). CED-9 can also associate with lipid membranes in vitro, inducing changes in membrane permeability, and this association appears independent of the C-terminal transmembrane domain (Tan et al., 2011). Whether pore formation is required for the in vivo function of CED-9, or any BCL-2 family member, is an important outstanding question. The components of the core apoptosis pathway and their signs of interaction appear conserved from *C. elegans* to humans. Nonetheless, even within the core pathway, distinctions are obvious. In mammals, though the BCL2-related protein Diva/Boo can bind Apaf-1 (Inohara et al., 1998; Song et al., 1999), this seems to be the exception. Most BCL2 family proteins appear to control Apaf-1 activity by regulating the release of cytochrome C, an Apaf-1 activating factor, from the mitochondrial outer membrane (Zou et al., 1997). To date, no evidence implicating cytochrome C in *C. elegans* apoptosis has been revealed. Indeed, the cytochrome C binding domain in Apaf-1 appears not to be present in CED-4 (Li et al., 1997). Unlike CED-4, which is bound to mitochondria in at least some stages of *C. elegans* development, Apaf-1 is localized to the cytoplasm in a variety of cell types (Hausmann et al., 2000), consistent with a different mode of activation.

Cytochrome C release also appears not to be required for many cell deaths in *Drosophila.* siRNAs directed against the cytochrome C homologs DC3 and DC4 have no impact on expression levels or processing of caspases in *Drosophila* larvae, nor do they impact rates of apoptosis in BG2 cells (Dorstyn et al., 2004). Furthermore, ectopic expression of DC3 and DC4 in BG2 cells has no effect on caspase activity as visualized by DEVD-amc fluorescence. This is especially interesting in light of the finding that *Drosophila* Dark coimmunoprecipitates with cytochrome C in SL2 cells (Rodriguez et al., 1999). Despite this, cytochrome C fails to interact

with the *Drosophila* apoptosome and is not required for its assembly (Yu et al., 2006), so it appears that the use of cytochrome C to activate Apaf-1 for programmed cell death is not a phenomenon found in invertebrates.

Despite this evidence, cytochrome C appears to be required for other caspase-dependent developmental events in the fly, such as developmental cell deaths in the retina, as well as sperm individualization. *cyt-c-d* mutations cause a small but significant delay in superfluous interommatidial and perimeter ommatidial cell deaths in the drosophila eye, as well as an extra bristle in the scutellum (Mendes et al., 2006). This mutation appears not to alter ATP levels or overall retinal development, indicating that it is likely impacts cell death. Also, the observations that overexpression of the caspase inhibitor p35 causes male sterility in vivo, as well as that dApaf-1, drICE and dronc are detected in individualization complexes using immunofluorescence suggest that spermatogenesis is a caspase-dependent process whose molecular biology resembles that of apoptosis. The fact that P element insertions in the *cyt-c-d* locus cause male sterility indicates that in certain instances, cytochrome C may be used to activate caspases in the fly (Arama et al., 2003). More work is needed to determine the relative importance of cytochrome C release in fly developmental apoptosis.

Whether mitochondria in general play a role in *C. elegans* cell death is also unclear. Some mitochondrial factors have been examined, including endonuclease G (CPS-6) (Parrish et al., 2001), Apoptosis Inducing Factor (WAH-1) (Wang et al., 2002), and the mitochondrial fission and fusion proteins DRP-1 and FZO-1 (Breckenridge et al., 2008; Jagasia et al., 2005; Lu et al., 2011b). While animals carrying lesions in the genes encoding these factors have been reported in some cases to have cell death defects, the effects are rather weak. It is therefore unclear whether any of these proteins specifically interact with the cell death machinery or if the

effects are due to more generic changes in cell state. Mutations in core apoptotic components do not obviously affect mitochondrial shape, fission, or fusion in homozygous early embryos (Breckenridge et al., 2009). Perhaps more relevant, however, in dying cells, mitochondrial fragmentation is observed, is dependent on *egl-1*, and is blocked by a *ced-9*(gf) allele (Jagasia et al., 2005). Importantly, fission is independent of *ced-3* and *ced-4*. Thus, while mitochondrial fragmentation is not required for cell death, it does accompany the process.

Unlike in *Drosophila,* BH3 protein expression is an important apoptotic regulatory mechanism in mammals. Here, however, the activation mechanism for BH3 proteins is less straightforward. While some BH3 proteins are transcriptionally activated (as is the case with p53 upregulation of Puma expression), other BH3 proteins are constitutively expressed and require post-translational modifications to become activated (Nakano and Vousden, 2001) (See also Ubiquitination and PCD). One example of this is the BH3 protein BIK, which displays phosphorylation at a number of sites in HeLa cells as viewed by western blotting. HeLa cells transfected with mutant BIK lacking these sites show less cell death than those transfected with wild-type BIK, indicating that this modification is required for BIK-mediated apoptotic function (Verma et al., 2001).

Ordering of the intrinsic apoptotic pathway also differs between worms and mammals (Figure 1.1). Overexpression of the antiapoptotic BCL2 genes BCL-2, BCL-XL or MCL-1 in MEFs successfully reduces the number of Annexin V-positive cells (a proxy for PS exposure) in lines stably expressing BID, BIM or PUMA, indicating that BCL2 genes can act “backwards” to inhibit BH3 function. Furthermore, as in vitro-translated BCL-2 successfully coimmunoprecipitates with BIM, activated BID (tBid) and PUMA, it is likely that this inhibition comes from direct physical interaction (Kim et al., 2006).

Another difference between *C. elegans* and flies/mammals lies in death initiation (Figure 1.1). Though not found in *C. elegans,* members of the tumor necrosis factor (TNF) superfamily, such as Fas and TNFα, are important cell-extrinsic regulators of programmed cell death (Trauth et al., 1989). The mechanism of Fas and TNF-activated signaling is as follows: in mammals, Fas ligand (FasL) activates the Fas receptor by binding to its cysteine-rich domain. Because the ligand is expressed as a homotrimer (as evidenced by structural studies), it causes clustering of the receptor (Kischkel et al., 1995; Schneider et al., 1997). This clustering allows Fas to bind to specifically interact with accessory proteins such as FADD via their death domains (DED), and the sum of these interactions forms what is known as the Death Inducing Signaling Complex (DISC) (Chinnaiyan et al., 1995; Kischkel et al., 1995). TNF signaling is fairly analogous to Fas signaling, substituting FasL, FasR, and FADD for TNFα, TNFR, and TRADD, respectively (Hsu et al., 1995). Components of both complexes interact with caspase-8, allowing for cross-activation of effector caspases (Boldin et al., 1996; Fernandes-Alnemri et al., 1996; Srinivasula et al., 1996; Wang et al., 2008).

Though no Fas homolog has been identified in *Drosophila*, recent studies show that *Drosophila* uses its own TNF-mediated death pathway involving the homolog TNF ligand homolog Eiger and the TNF receptor Wengen (Kanda et al., 2002). UAS-Eiger promotes cell death in a JNK- and DRONC-dependent, but Dredd independent manner; thus, unlike the mammalian TNF, the fly TNF receptor induces effector caspase activation without requirement for initiator caspases (Moreno et al., 2002). Though cell culture experiments across mammalian cell types show that Jun kinase is upregulated in response to Fas induction and genotoxic stressors, responses vary greatly between cell types, suggesting that JNK is not likely a main effector of extrinsic apoptosis in mammals (Chen et al., 1996b).

Recent studies show that extrinsic apoptotic signaling is important in fly models of cell death during injury and development. JNK and Reaper immunostainings in dying leg tissue colocalize, and their combined expression is required for proper *Drosophila* leg morphogenesis, indicating that TNF may play a role in coordinated cell death during tissue reorganization (Manjón et al., 2007). TNF/Eiger is also required for transmission of apoptosis-induced apoptosis, another coordinated cell death event. Apoptosis induced via ectopic reaper/hid expression in the presence or absence of p35 in the posterior wing disc of the fly can induce apoptosis in more anterior cells, indicating that flies can propagate long-range signals to extrinsically induce apoptosis; this phenomenon is abrogated when Eiger RNAi is supplied, suggesting that this pathway is also TNF-dependent (Pérez-Garijo et al., 2013).

Ubiquitination and programmed cell death

As mentioned above, a number of the components in the apoptotic pathway are members of the ubiquitin pathway. Ubiquitin is a 76-amino acid protein that post-translationally modifies substrates through an isopeptide linkage with one of its lysines for purposes of signaling activation or protein degradation (Ciechanover et al., 1980; Hershko et al., 1979; 1983; 1984). Ubiqutination begins with the creation of an ATP-dependent thioester linkage between ubiquitin and the E1 ubiquitin-activating enzyme (Schulman and Harper, 2009). In *C. elegans* this action is mediated by UBA-1, its sole E1 (Kipreos, 2005). Following this step, the E1 transfers the ubiquitin to the E2 ubiquitin-conjugating enzyme via another thioester bond on the E2's conserved cysteine moiety (Ye and Rape, 2009). There are 22 ubiquitin conjugating-enzymes in

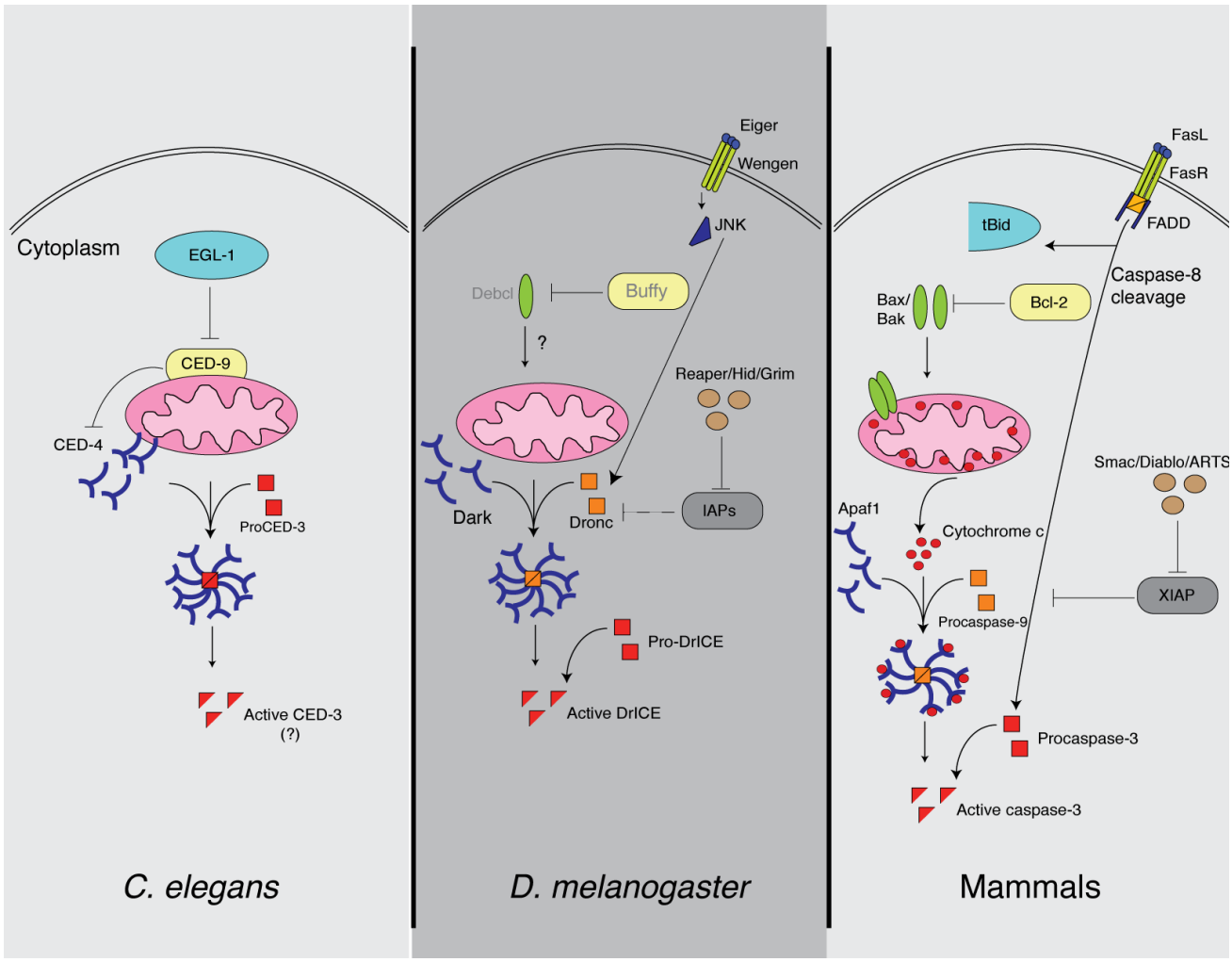

Figure 1.1. Programmed cell death is highly conserved between different species. Though - differences are apparent in cell death programs between worms, flies and humans, by and large, the mechanisms are conserved. Many apoptotic events begin with the inactivation of an antiapoptotic BCL2-like protein (yellow) by a BH3 inhibitor (blue). This prevents the BCL2 protein from inhibiting Apaf1 (indigo). Activation of Apaf-1 in the presence or absence of cytochrome c (red circles) induces formation of the apoptosome (spoked object), a structure that processes inactive caspase (squares) into its active form. The sum of the proteolytic output due to caspase activity causes apoptotic death. In other apoptotic events, death is induced via competitive RHG protein (tan circles) binding to inhibitor of apoptosis proteins (gray), which relieves caspase inhibition. Finally, apoptosis can be extrinsically induced via TNFα signaling, which processes initiator caspases into their active forms (Adapted from Parrish et al., 2013).

the *C. elegans* genome (Kipreos, 2005). The E2 finally transfers ubiquitin to a substrate through a peptide linkage; this transfer is made via interaction with a substrate-bound E3 ubiquitin ligase, of which there are hundreds in the *C. elegans* genome (Kipreos, 2005) (Figure 1.2). The type of E3 used specifies the mechanism of transfer; HECT E3 ligases transfer the ubiquitin from the E2 to the substrate, whereas RING finger and U-box E3s facilitate ubiquitin transfer to the substrate by bringing it into close proximity with the E2 (Kipreos, 2005). RING finger E3s are the most numerous type of ubiquitin ligase and also are diverse in form; monomeric E3s catalyze ubiquitination on their own, while cullin-based E3 ligases act in a multisubunit complex containing a RING E3 bound to a number of different components that vary depending on the cullin used (Deshaies and Joazeiro, 2009). Cul1 E3 complexes utilize a Skp and F-box in addition to the RING and cullin, while Cul3 E3 complexes use a BTB protein in substitution for both the Skp and F-box (Kipreos, 2005). In order to tag proteins, ubiquitin binds its substrates using either its amino terminus, or one of seven lysines that exist within the protein. Mass spectrometry analysis has mapped out the multiple forms of ubiquitination: monoubiquitination (a single ubiquitin added to a protein), multi-monoubiquitination (single ubiquitins added along a protein), homogenous and branched ubiquitin chains (e.g. a row of K48 linkages; a branch of K48 linkages); and mixed ubiquitin chains (a row of ubiquitins, each binding through a different lysine residue) (Komander and Rape, 2012). Thus, the residue used and the nature of the linkages

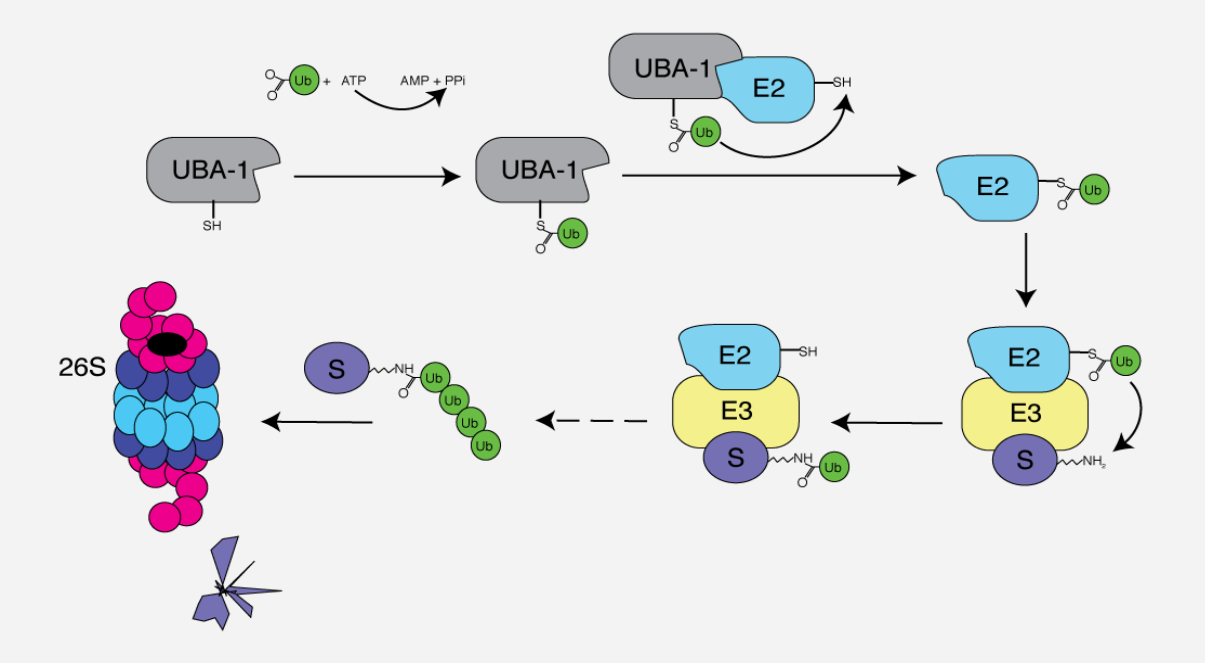

Figure 1.2. The ubiquitin proteasome pathway. Ubiquitin is first bound to an E1 activating enzyme (UBA-1) through an ATP-dependent thioester bond. Ubiquitin is transferred from the E1 to the E2 through a second thioesterification event. The E3 binds the substrate to be ubiquitinated (purple) and shuttles it to the E2. The E2 transfers the ubiquitin to the E3 via a peptide bond. Multiple rounds of ubiquitination tags proteins for degradation for the 26S proteasome (19S regulatory particle: magenta; α/β subunits of 20S core particle, violet and cyan).

determines the fate of the substrate. K48 linkages are the most common in all organisms as visualized by quantitative proteomic experiments, and their concentration in the cell drastically increases with proteasome inhibition, indicating that they are used to tag proteins for proteasomal degradation (Xu et al., 2009). K63 linkages are multifarious in function: they can signal DNA damage, as RAP80 physically interacts with K63-polyubiquitin chains, and as RAP80 mutants have defective BRCA targeting to DNA damage sites in 293T cells (Sobhian et al., 2007); they can also tag proteins for degradation, as in vivo tagging of a known substrate of the E3 ligase Rsp5 in yeast shows that K63-linked chains are detectable in the proteasome (Saeki et al., 2009); and they can target substrates to lysosomes, as surface Plasmon Resonance curves for the lysosomal targeting ESCRT complex shows that ESCRT preferentially binds K63 (Ren and Hurley, 2010). K11 is less well studied, but transfection of HA-Ub-K11 in HEK293T cells causes APC/C dependent ubiquitination of E2F1 when immunoprecipitated in the presence of a proteasome inhibitor, indicating that K11 modifications can signal for proteasomal substrate degradation (Budhavarapu et al., 2012). Finally, recent work has underscored the importance of "linear ubiquitination" mediated by M1 linkages, which is used to regulate signaling through TNF and other pathways (Gerlach et al., 2011; Rieser et al., 2013). The repertoire of ubiquitin linkages is far more diverse than is outlined here; other linkages such as K27 and K29 have been observed, but their functions are poorly understood.

Ubiquitination enzymes regulate a number of steps in developmental and nondevelopmental cell deaths. As mentioned above, a number of IAPs possess RING domains that allow them to perturb apoptosis activation either through caspase degradation or caspase inhibition (Ditzel et al., 2008; Suzuki et al., 2001). These IAPs can auto-ubiquitinate to regulate their own levels, but they are also ubiquitinated separately by other ligases. For example, co-

transfection experiments and ubiquitination assays in cell culture show that the E3 ligase Nrdp1 ubiquitinates the IAP BRUCE, and that this ubiquitination causes its degradation by the proteasome. This degradation can be catalyzed in cell lines with the addition of apoptotic stimuli such as etoposide or TNFα (Qiu et al., 2004). IAPs also regulate ubiquitination of their own inhibitors; coimmunoprecipitation and ubiquitination experiments in transfected cell lines suggest that the RHG gene Smac may be ubiquitinated and degraded by cIAPs, but whether this occurs under physiological conditions has not been addressed (Hu and Yang, 2003). The use of ubiquitination to regulate IAP levels is also apparent in the caspase-dependent cellular remodeling induced during sperm individualization (see *Drosophila* pathways). Mutations in the testis-specific isoform of Cul3, the RING finger gene Roc1b, or the BTB domain protein Klhl10 reduce caspase activation during spermatogenesis. Coimmunoprecipitation experiments show that all three physically interact, and that Klhl10 interacts with the IAP dBruce, indicating that an intact Cullin-RING ligase (CRL) complex likely acts to regulate caspase activation through inhibition of IAPs (Arama et al., 2007). A genetic screen for genes required for sperm individualization also isolated the F-box protein Nutcracker. Like Klhl10, Nutcracker acts by physical interaction with dBruce; however, unlike Klhl10, Nutcracker interacts with a Cul1 complex to promote caspase activation (Bader et al., 2010).

The post-translational addition ubiquitin to substrates also regulates the activity of members of the core apoptotic pathway. Administration of the ERK signaling agonist 4-HT in CM3 cells induces Bim phosphorylation that is abrogated with administration of a specific ERK inhibitor. This phosphorylation causes ubiquitin-mediated degradation of Bim in an ERK-dependent manner in a translation-blocked system (Ley et al., 2003). The BH3 protein Bid also displays interesting post-translational modifications that are regulated by ubiquitin. Bid is

normally expressed as an inactive proprotein; cleavage into the active form (tBid) by caspase-8 allows it to activate cell death. In order to prevent the N-terminal regulatory region (tBid-N) from inhibiting tBid post-cleavage, tBid-N is rapidly degraded by the proteasome, as expression of HA-tBid-N in MCF-7 cells is only visible by western blot following treatment by the proteasome inhibitor MG132. This finding is especially interesting, as tBid-N possesses no lysines for ubiquitin transfer. While no E3 candidate has been identified, cell culture ubiquitination assays using various tBid-N mutants have mapped the ubiquitination site to a serine, threonine or cysteine residue in helix one of the protein (Tait et al., 2007).

Neurodegenerative cell deaths, which are often characterized by the presence of uncleared protein inclusions and aggregates, also appear to utilize ubiquitination. One of these illnesses is Parkinson's disease (PD), which causes degeneration of dopaminergic neurons in the substantia nigra. PD neurons are characterized by the accumulation of α-synuclein inclusions into cytoplasmic deposits called Lewy bodies, which stain positive for ubiquitin in immunohistochemistry experiments (Moore et al., 2005). These deposits can also inhibit proteasome activity, as substantia nigra extracts from PD patients exhibit decreased chymotrypsin activity (Tofaris et al., 2003). Mutations in E3 ubiquitin ligases and hydrolases are also associated with PD. Analysis of a German family with recessively inherited Parkinson's disease mapped the causal lesion to a missense mutation in the ubiquitin carboxy-terminal hydrolase L1 (UCH-L1), and immunostaining has shown that the protein colocalizes with Lewy bodies (Leroy et al., 1998). The same method of analysis applied to autosomal recessive juvenile Parkinson's disease identified an 84-nt in-frame deletion in the E3 ubiquitin ligase Parkin, which likely affects splicing of the gene (Kitada et al., 1998). Interestingly, patients with Parkin mutations lack the Lewy bodies found in autosomal dominant forms of Parkinson's disease,

which raises long-standing questions of whether uncleared plaques underlie disease mechanism. Another E3 implicated in the etiology of Parkinson's disease is the RING finger E3 ligase seven in absentia homologue-1 (Siah-1). Immunohistochemistry of PD brain tissues shows that Siah co-localizes with Lewy bodies (Liani et al., 2004). Consistent with this observation, co-immunoprecipitation and ubiquitination assays in rat brain lysates and cell culture show that GST-Siah-1 interacts with, colocalizes with, and ubiquitinates α-synuclein (Rott et al., 2008). Familial mutations of α-synuclein, as well as siRNA knockdown of Siah-1 lessen the levels of ubiquitination as viewed in cell culture; however, conflicting results exist as to whether this ubiquitination is helpful or toxic (Lee et al., 2007; Rott et al., 2008). Interestingly, α-synuclein is not degraded in the presence or absence of MG132, indicating that its ubiquitination may function to modify α-synuclein to transduce signaling. Siah also immunoprecipitates with and ubiquitinates the α-synuclein-binding protein synphilin-1 in HEK293 cells (Liani et al., 2004; Nagano et al., 2003). Unlike α-synuclein, synphilin-1 appears to be proteasomally degraded following ubiquitination.

Ubiquitin also appears to be an important regulator of the pathology of Alzheimer's disease (AD), which is characterized by neuron death leading to memory loss. Extracellular β-amyloid plaques and intracellular tangles composed of paired helical filaments (PHF) of the microtubule-associated protein Tau define disease pathology (Selkoe, 1991). Mass spectrophotometric analysis of plaques from an AD brain, as well as antibodies isolated that specifically stained tau paired helical filaments in Alzheimer's disease tissues show that ubiquitin is a component of AD tangles (Mori et al., 1987; Morishima-Kawashima et al., 1993). A yeast two-hybrid screen identified the RING finger E3 axotrophin as a likely modifier of tau activity; purified axotrophin ubiquitinates tau in vitro, and this ubiquitination confers a decreased

microtubule binding affinity to tau in a coimmunoprecipitation assay (Flach et al., 2014). Thus, ubiquitination of tau may be important to disease progression. Not only is tau a target of ubiquitination, but tau itself can impact proteasomal activity. Incubation of isolated proteasomes with PHF-tau isolated from AD patients causes inhibition of proteasome activity as visualized by the fluorogenic proteasome substrate suc-LLVY-MCA (Keck et al., 2003). Thus, ubiquitin proteasome system (UPS) dysfunction may be a cause as well as an effect of neurodegeneration.

The etiology of Huntington's disease (HD) and other polyQ expansion diseases such as spinocerebellar ataxia (SCA), which arise due to dominant gain-of-function mutations (CAG repeat expansion) in genes of unknown function (Group, 1993), is also characterized by ubiquitination. Neuronal intranuclear inclusions (NIIs) of huntingtin protein in the striatum and cortex of the brain are characteristic of HD pathology (DiFiglia et al., 1997). Immuno-EM staining shows that ubiquitin colocalizes with nuclear inclusions but not with cytoplasmic inclusions, and that this staining precedes the phenotypic changes that are associated with Huntington's disease (Davies et al., 1997). Yeast two-hybrid data and co-immunoprecipitation of in vitro translation products also suggest that the amino terminus of huntingtin physically interacts with the human E2 UBE2K in a manner unaffected by polyQ tract length, indicating that perhaps ubiquitination is also important to the wild-type function of huntingtin (Kalchman et al., 1996). Antisera against UBE2K localizes it to intranuclear inclusions in both HD and spinocerebellar ataxia patients, suggesting that this interaction is physiologically relevant (de Pril et al., 2007). Like Huntingtin, polyQ-expanded ataxin-1 also forms neuronal intranuclear inclusions, forming a single 2mm nuclear punctum as visualized with ataxin immunostaining in both *SCA1* transgenic mouse and *SCA1* patient neurons (Skinner et al., 1997). Ataxin aggregation is affected by ubiquitination enzymes. Mice with a deletion in the *Ube3a* HECT E3

ligase crossed to mice with an overexpression allele of *SCA1* have fewer nuclear aggregates as visualized with Ataxin-1 immunostaining. However, age-matched littermates showed extensive degeneration of the cerebellum as compared to wild-type mice or *SCA1* mutant animals alone, suggesting that prevention of aggregates alone is not sufficient to prevent disease pathology (Cummings et al., 1999). Ataxin-3, which is mutated in models of SCA, also interacts with ubiquitin chains. Coimmunoprecipitation and immunofluorescence of transfected proteins in cell culture experiments suggest that Ataxin binds to and colocalizes with ubiquitin chains through its ubiquitin interacting motif (UIM) (Donaldson et al., 2003). This domain is required for puncta formation into polyQ aggregates when transfected as GFP-fusions into HEK293 cells (Donaldson et al., 2003). Recent evidence suggests that Ataxin-3 acts as a deubiquitinating enzyme, as cells co-transfected with Ataxin-3 and the E3 ligase CHIP have substrates with shortened ubiquitin chains compared to CHIP alone (Scaglione et al., 2011).

Finally, ubiquitin appears to be important for Wallerian degeneration, in which the distal part of an axon degenerates following injury. The Wld^s mouse has a dominant mutation that causes slower post-axotomy degeneration compared to wild-type animals. Mapping experiments showed that the causal lesion is a chromosomal rearrangement that leads to the fusion of nicotinamide mononucleotide adenylyl transferase with the amino terminal half of the ubiquitination factor Ube4b (Mack et al., 2001). In vivo heterologous expression of Wld^s lacking the N-terminal Ube4b sequence abrogates Wld protective function; however, expression of a fusion protein replacing the Ube4b domain with a related AAA+ ATPase-binding domain restores protection (Conforti et al., 2009). Thus, Ube4b is likely not preventing degeneration through its usual activity. Although Ube4b ubiquitinating activity is not required for prevention of Wallerian degeneration, there are findings that underscore the importance of the UPS in

prevention of axon degeneration. UPS inhibition with the drug MG132 slows onset of Wallerian degeneration in cultured soma-deprived rat sympathetic superior ganglia (Zhai et al., 2003). Interestingly, while proteasome inhibition prevents axon degeneration, it does not slow cell body death following NGF deprivation in sympathetic neurons. This indicates that soma survival is separable from axon survival (Zhai et al., 2003). E3s are required in *Drosophila* model of axonal degeneration; ten alleles of the RING finger E3 ubiquitin ligase *highwire*, two of which were dominant gain-of-function mutations, were isolated in an X-chromosome EMS screen for mutants defective in Wallerian-like axon degeneration following axotomy of the L1 wing vein (Neukomm et al., 2014). No structure-function experiments were conducted, so more work is needed to determine how highwire impacts axon degeneration. That being said, it appears as though a number of components in the UPS play an important role in axonal degeneration.

Tissue remodeling paradigms also highlight the importance of ubiquitination. Polyubiquitin expression increases during intersegmental muscle degeneration in the moth *Manduca sexta* as visualized by Northern blot and ^{135}I-ubiquitin conjugation activity (Haas et al., 1995; Schwartz et al., 1990). While the cell death is not morphologically apoptotic, it remains to be seen whether caspases are essential to degeneration (Schwartz et al., 1993). Ubiquitin expression is also used as a proxy for thyoroxine-induced apoptosis in tadpole tails in the American bullfrog *Rana catesbeiana*. These studies indicate that ubiquitination may be important to the coordination of massive cell death during remodeling events (Phillips and Platt, 1994).

Caspase-independent cell death in *C. elegans*

Though the majority of cells in *C. elegans* die using the canonical apoptotic pathway, a number of cells die in ways that are caspase-independent. Semidominant gain-of-function mutations in the gene *lin-24*, encoding a protein with homology to *Bacillus sphaericus* mosquitocidal toxin, and *lin-33,* encoding a novel protein, cause inappropriate cell death of the Pn.p hypodermal blast cells (Galvin et al., 2008). These corpses are characterized in DIC and electron micrographs by the presence of refractile, granular nuclei, as well as ovoid refractile bodies within the cell, which likely represent disrupted mitochondria and dense membranous whorls. This death is characterized as "cytotoxic," as it is morphologically and genetically distinct from those seen in apoptotic corpses (see above) or necrotic corpses (see below). Interestingly, loss-of-function alleles in either *lin-24* or *lin-33* are able to suppress the ectopic Pn.p deaths caused by a semidominant heterozygous mutation in the other gene, indicating that the two genetically interact (Galvin et al., 2008). Furthermore, though mutations in *ced-3* fail to suppress the cytotoxic phenotype, gain-of-function mutations in *ced-9* and loss-of-function alleles of *ced-4* have a weak suppression, and homozygous loss-of-function mutations in engulfment genes *ced-2*, *-5* and *-12* cause stronger suppression, indicating that the canonical apoptotic and engulfment genes are at least partially required for death.

Though, in most cases, CED-4 is required for CED-3 activation to promote apoptosis, there are situations in which it appears that CED-3 is not required. Loss of *C. elegans* ICD-1, a protein similar to the beta-subunit of the nascent polypeptide-associated complex, results in wide-spread cell death that appears, at least in part, to be CED-4 dependent, but CED-3 independent (Bloss et al., 2003). Also, mutations in the gene *pvl-5*, whose identity is still unknown, result in cell death that is inhibited by *ced-3* mutations but not by *ced-4* alleles (Joshi

and Eisenmann, 2004). Thus, under at least some circumstances, *ced-3* and *ced-4* may operate independently.

One of the most well studied forms of nonapoptotic cell death in the worm is the necrotic death of the six touch-receptor neurons in *C. elegans.* Gain-of-function mutations in the mechanosensory sodium channel subunit-encoding gene *mec-4,* or in the related channel subunits *deg-1* and *unc-8*, cause hyperactivation of the degenerin/epithelial Na+ channels (DEG/EnaC) (Driscoll and Chalfie, 1991). Gain-of-function mutations in the nicotinic acetylcholine receptor *deg-3*, as well as activating mutations in the $G\alpha_s$ gene *gsa-1* also produces a similar phenotype (Korswagen et al., 1997; Treinin and Chalfie, 1995). Expression of these mutants in touch cells cause necrotic death visualized under DIC microscopy as cellular bloating. Ultrastructural characterization of dying touch cells as visualized by electron microscopy initially shows membrane infoldings and electron dense whorls; later stages show larger cytoplasmic vacuoles and membrane structures, with nuclear membrane infolding also observed. In the final stages, the mitochondria, Golgi and ER are degraded (Hall et al., 1997).

Genetic structure-function analysis of *mec-4* mutations showed that gain-of-function mutants likely affect ion flow due to changes in membrane-spanning subunits of the channel (Hong and Driscoll, 1994). A mutation in the pore-forming region of the *C. elegans* acetylcholine receptor a subunit (*deg-3*) causes a similar phenotype (Treinin and Chalfie, 1995).

Experiments using heterologous expression of *mec-4*(gf) in *Xenopus* oocytes and *C. elegans* touch neurons using the calcium-sensor cameleon show that MEC-4 induces an intracellular rise in Ca^{2+} levels via its own ability to conduct calcium (Bianchi et al., 2004). Electrophysiology experiments in which mutant UNC-8 channels are expressed in *Xenopus laevis* oocytes show that mutant channels hyperactivate in a manner that is blocked by increased

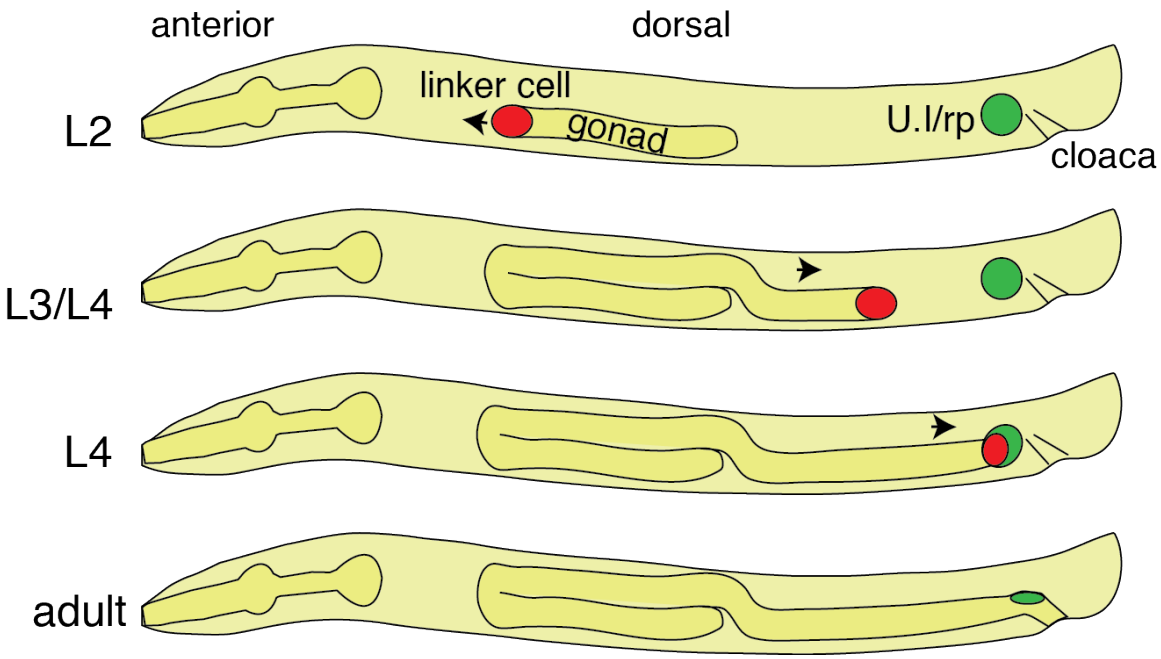

Figure 1.3. The life and death of the *C. elegans* linker cell. The linker cell is born in the center of the male in the beginning of the second larval stage (L2). The cell then undergoes a stereotypical U-shaped migration. At the end of the fourth larval stage (L4), the linker cell reaches the cloaca, rounds up and dies. The cell is engulfed by and presumably cleared by the U.l/rp rectal epithelial cells. (Reproduced by Lena Kutscher from Abraham et al., 2007).

levels of Ca^{2+}/Mg^{2+} ions in the extracellular media (Wang et al., 2013). This resultant increase in intracellular calcium levels likely activates Ca^{2+} release from the ER, as null mutations in calreticulin suppress *mec-4*(gf)-induced necrosis, and RNAi knockdown of calnexin, andmutations in the ryanodine receptor *unc-67* or the inositol 1,4,5, triphosphate receptor *itr-1* also suppress death (Xu et al., 2001). This ER release of calcium likely activates calcium-sensitive proteases such as calpains to promote degenerative death, as RNAi against various *C. elegans* calpains (*tra-3*/*clp-1*) and aspartyl proteases (*asp-3*/*asp-4*) reduce the number of vacuolated cells in *mec-4*(d) and *deg-3*(d) animals (Syntichaki et al., 2002). Degenerative cell death in *C. elegans* may be a worthwhile model for necrotic death in cases of stroke or ischemia.

Nonapoptotic developmental cell death in the *C. elegans* linker cell

The linker cell is a male-specific leader cell born in the ventral midbody in the second larval stage (L2) (Figure 1.3). The cell guides the elongation of the gonad, and upon reaching the cloacal region in the late L4 stage, it dies. Death may allow for gonad-cloaca fusion, resulting in an open germ system competent for sperm transfer during fertilization. Anecdotal reports suggested that linker cell death may require the neighboring engulfing cells, U.l/rp (Hedgecock et al., 1983); however, later studies demonstrated that the cell can die following ablation of these dedicated engulfing cells, or in animals in which the linker cell fails to migrate properly (Abraham et al., 2007). Anecdotal reports also suggested initially that linker cell death is partially dependent on *ced-3* and *ced-4* (Ellis and Horvitz, 1986). However, further studies of the genetic requirements for death, coupled with extensive morphological and ultrastructural observations revealed that linker cell death does not require *ced-3* or *ced-4*. Indeed the cell death process could proceed in its entirety in animals carrying mutations in any of the core apoptotic

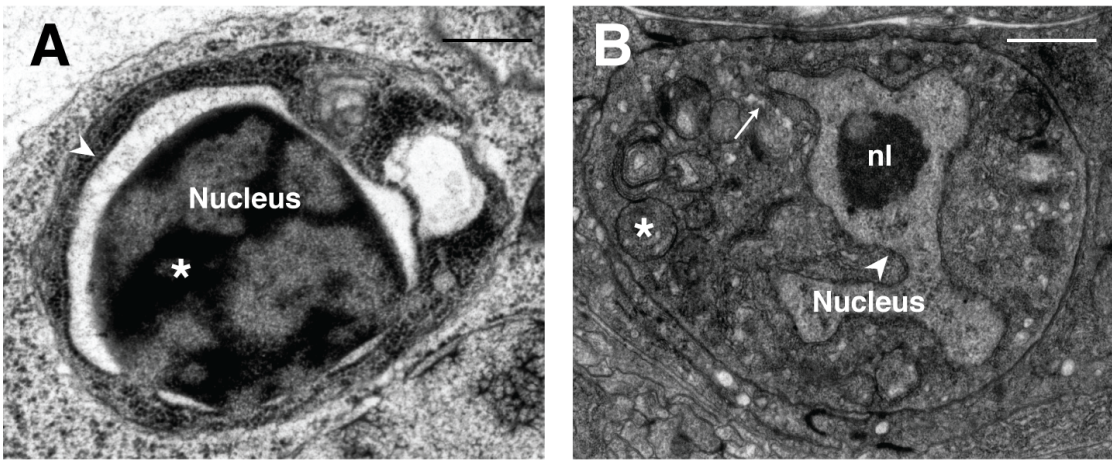

Figure 1.4. Ultrastructurally, linker cell death is nonapoptotic.

Electron micrographs of an apoptotic corpse (A) as compared to a linker cell corpse (B). Scale bar = 2μm. (A) The structural hallmarks of a linker cell corpse are compacted cytoplasm (arrowhead) and condensed chromatin. (B) The linker cell corpse displays open chromatin, but has a crenellated nucleus (arrowhead), as well as swollen ER (arrow) and mitochondria (asterisk). Electron micrographs prepared by Yun Lu.

pathway genes (Abraham et al., 2007). Thus, linker cell death proceeds by a previously unexplored mode of cell death. Consistent with these novel genetic requirements, the ultrastructural changes accompanying the cell death process are very different from those seen inapoptotic cells. While apoptosis is characterized by nuclear condensation, cytoplasmic shrinkage, and morphologically intact organelles (until the very end), the dying linker cell exhibits none of these features. Instead, the cell displays pronounced nuclear envelope invagination (crenellation), as well as swelling of endoplasmic reticulum and mitochondria (Abraham et al., 2007) (Figure 1.4). These changes are often observed in cell death during vertebrate development, and are prevalent in degenerating cells of patients with polyQ disease (Davies et al., 1997).

Genetic and molecular screens have uncovered genes involved in linker cell death. Initiation of the death process appears to be dependent on both temporal and positional cues. The LIN-29 Zn-finger transcription factor, a downstream component of the *C. elegans* heterochronic pathway controlling developmental timing, promotes linker cell demise (Abraham et al., 2007).

Two opposing Wnt pathways mediate the spatial signal (M. Kinet and S. Shaham, submitted). The Wnt LIN-44 is secreted by male tail cells and acts through the MIG-1 and CFZ-2 Frizzled-like receptors, LIT-1/Nemo-like kinase, and WRM-1/beta-catenin—all of which function in the linker cell—to inhibit linker cell death. This protective pathway is antagonized by the Wnt EGL-20, also expressed in neighboring cells, and its effectors LIN-17/Frizzled, MOM-5/Frizzled, MIG-5/Dishevelled, and BAR-1/beta-catenin. The Wnt responsive transcription factor POP-1/TCF/LEF does not appear to play a role in linker cell death (M. Kinet and S. Shaham, submitted), suggesting other possible targets. One candidate is the Q-rich protein PQN-41. A C-terminal polypeptide encoded by the locus consisting of 35% glutamine residues is

sufficient to rescue linker cell survival exhibited by *pqn-41* mutants (Blum et al., 2012). At least some PQN-41 isoforms appear to be localized to nuclei, suggesting that they could function to mediate a transcriptional output of Wnt signaling. Another candidate is the transcription factor HSF-1, which in other contexts transduces heat and stress signals to promote a protective cellular response. In the linker cell, however, *hsf-1*(lf) mutations block linker cell death, suggesting that it, instead, promotes cell dismantling (M. Kinet and S. Shaham, submitted). Supporting this observation, stress targets of HSF-1 are not induced in the linker cell. Importantly, an HSF-1 gain-of-function mutation can rescue inappropriate linker cell survival in Wnt pathway mutants, as well as almost all other tested mutants that block linker cell death (M. Kinet and S. Shaham, submitted). HSF-1, therefore, may be a key downstream regulatory node, and determining its targets is an important next step.

The kinase SEK-1 and its adaptor protein TIR-1 also promote linker cell death, and their loss can also be compensated for by the *hsf-1*(gf) allele. Genetic interaction studies suggest that these proteins might function in the same pathway as PQN-41 (Blum et al., 2012). *Drosophila* and murine homologs of TIR-1—dSarm and Sarm, respectively—have been implicated in distal axon segment degeneration following axotomy (Osterloh et al., 2012), raising the possibility that the dismantling program of the linker cell may share conserved features with non-apoptotic degenerative programs in other systems.

An RNAi screen isolated the E2 ubiquitin-conjugating enzyme *let-70* as a possible regulator of linker cell death. Our most recent work seeks to place components of the ubiquitin proteasome system within the current framework in order to better understand the molecular mechanisms underlying nonapoptotic death.

CHAPTER 2: LET-70 is an E2 ubiquitin-conjugating enzyme required for the nonapopotic death of the linker cell in *C. elegans*

SUMMARY

Apoptotic cell death has been studied extensively over the past four decades. This form of cell death requires caspase proteases (Ellis and Horvitz, 1986) and a myriad of direct and indirect caspase regulators. Caspases and other apoptotic cell death proteins are highly conserved, and regulate cell death in animals as diverse as hydra, *C. elegans*, and humans (Ellis and Horvitz, 1986). Nonetheless, it appears that caspase-dependent apoptosis may not account for many cell death events that take place during normal animal development. For example, while mice homozygous for knockout alleles of Apaf-1 tend to be lethal, about 5 percent of animals survive to adulthood, indicating that cell death in surviving mutants may proceed by an alternate mechanism (Honarpour et al., 2000). Reinforcing this notion, nearly half of spinal cord motor neurons generated during vertebrate development are normally deleted (Yamamoto and Henderson, 1999) and this process occurs unabated in the absence of caspase-3 or caspase-9 (Oppenheim et al., 2001). While caspase-independent non-apoptotic processes may play key roles in developmental cell death, the programs controlling these processes are not well understood.

Direct evidence that caspase-independent non-apoptotic cell death pathways operate during animal development is provided by studies of the *C. elegans* linker cell. Genetic studies of linker cell death led to the identification of genes that promote this process, including *pqn-41*, which encodes a glutamine-rich protein, and *tir-1*/TIR-domain and *sek-1*/MAPKK, which may function in the same pathway as *pqn-41* (Blum et al., 2012). The *let-7* microRNA and its indirect

target, the Zn-finger transcription factor LIN-29, also promote linker cell death, and may act early in the process (Abraham et al., 2007; Blum et al., 2012).

Here, we show that LET-70, an E2 ubiquitin-conjugating enzyme, is required cell-autonomously for linker cell death. LET-70 levels, as well as those of ubiquitin and some proteasome components, increase just before linker cell death initiation. This rise is dependent on an MLL-type histone methyltransferase complex and a MAPK cascade, whose activities are also required for linker cell death.

RESULTS

LET-70, an E2 ubiquitin-conjugating enzyme, is required for linker cell death

Elyse Blum and Mary Abraham, two former graduate students in the lab, performed an RNAi screen to identify genes required for linker cell death. The screen was conducted as follows: bacterial clones expressing dsRNA targeted against one of 18,132 genes were fed individually to RNAi-sensitized (*rrf-3* mutant) L1 males; two days later, the adults were scored for the inappropriate presence of a linker cell, which was tagged with a GFP-expressing reporter (Blum et al., 2012). The genes targeted by the clones represented 89% of protein-coding genes in *C. elegans*. Upon screening, the duo identified five genes required for linker cell death, one of which was *let-70* (Blum et al., 2012).

let-70 is an E2 ubiquitin-conjugating enzyme homologous to *S. cerevisiae* UBC4/5, *Drosophila* UbcD1 and human UBE2D2; pulse-chase experiments using radiolabeled amino acids in yeast suggest that members of this class of genes are required for degradation of short-lived and misfolded proteins during general cellular housekeeping, as well as following exposure to stressors such as elevated temperature (Seufert and Jentsch, 1990; Zhen et al., 1993). In

addition to this role, siRNA depletion of Ubc4/5 in yeast suggests that this class of proteins may also be required for proper ubiquitination of plasma membrane-bound proteins to allow for their cellular internalization and eventual lysosomal targeting (Umebayashi et al., 2008). LET-70 shares 94%, 97% and 78% amino acid identity with human UBE2D2, *Drosophila* UbcD1 and *Saccharomyces cerevisiae* UBC4, respectively (Figure 2.1). This conservation is functional as well, as *let-70* cDNA can rescue UBC4/5 mutants in yeast, and antibodies derived from *Drosophila* UbcD1 recognize *C. elegans* LET-70 (Zhen et al., 1993).

To better understand the role of *let-70* in linker cell death, we performed a closer characterization of the linker cell's survival following *let-70* depletion. L1 males fed bacteria expressing dsRNA targeted against *let-70* exhibit robust linker cell survival (45%; Table 2.1, Figure 2.2). Linker cell survival is characterized by the presence of an unrounded linker cell with wild-type nuclear morphology. To confirm these initial results, we examined two additional RNAi targeting fragments and obtained similar results (Table 2.1). Importantly, these two fragments do not overlap (Figure 2.2), suggesting that linker cell survival is unlikely to be a result of off-target effects. Although all three RNAi clones caused linker cell survival when administered to animals, the degree of cell survival varies based on the clone used, indicating that different dsRNAs cause different amounts of mRNA knockdown, perhaps by binding to different regions of the gene with varied intensity, or by intrinsic structural differences in the dsRNAs' abilities to disrupt translation.

In order to further characterize the phenotype caused by *let-70* loss, we examined two independent null alleles. *let-70(tm5777*) consists of a deletion 40 nucleotides upstream of to 217 nucleotides downstream of the *let-70* start codon (Figure 2.2). This removes the 5'UTR, the first

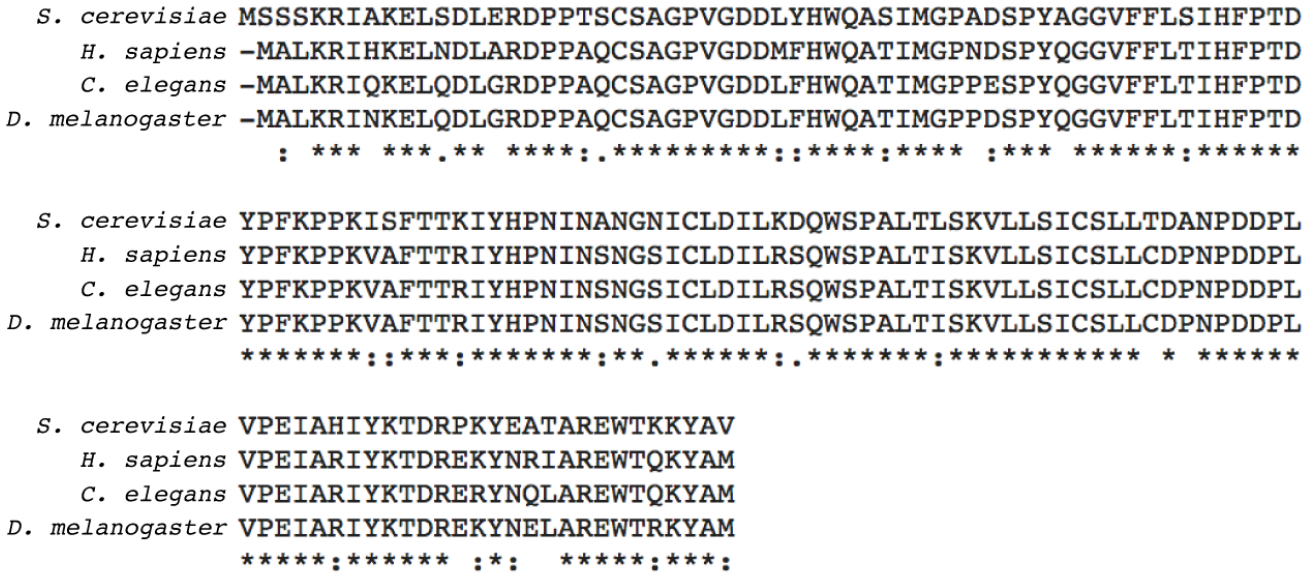

Figure 2.1. LET-70 shows high amino acid identity with human, fly, and yeast homologs.

Alignment of amino acid sequences of E2 ubiquitin-conjugating enzymes from four different species with the program Clustal Omega (Goujon et al., 2010; McWilliam et al., 2013; Sievers et al., 2011) shows that *C. elegans* LET-70 is 94%, 96% and 78% identical to human UBE2D2, to *Drosophila* UbcD1, and *Saccharomyces cerevisiae* Ubc4, respectively. Asterisk = amino acids are identical; colon= amino acids are similar (scoring >0.5 in the Gonnet PAM 250 matrix).

exon, the first intron, and part of the second intron. The second allele analyzed was *let-70*(*ns636*), which we generated using CRISPR/Cas9. This allele consists of an 87-bp deletion of nucleotides 195 to 280 within the *let-70* locus, removing part of the second exon and second intron (Figure 2.2). In both strains, live homozygous mutant animals are never generated, indicating that *let-70* is required for either proper germ cell development, or for embryogenesis. Our observations suggest that *let-70* is required for germline development. Injection of *let-70*(*tm5777*) with a fosmid containing the *let-70* locus as well as 22.1 kb upstream of and 8.3 kb downstream of the gene generates adult animals who produce no eggs (Figure 2.3), indicating that LET-70 is required for the production of healthy gametes.

Observations by the Candido lab of the *let-70*(*s689*) allele (encoding a G to A change in the splice donor site of the last intron, which induces nonsense-mediated decay of the transcript) corroborate the idea that *let-70* is required for proper embryogenesis as well as germline development. *let-70*(*s689*) mutant hermaphrodites die in early larval stages when derived from heterozygous parents, indicating that the maternal contribution of wild-type *let-70* mRNA is required during embryogenesis to produce live offspring (Zhen et al., 1996). This is supported by the fact that knockdown of *let-70* in early embryos via injection of RNAs antisense to the gene produces dead larvae and unhatched embryos (Zhen et al., 1993; 1996) Analysis of *let-70*(*s689*) mutants by the Candido lab also indicates that *let-70* is required for proper germline development, as *let-70*(*s689*) homozygote animals that do survive to adulthood are sterile with few oocytes (Zhen et al., 1996). This is bolstered by the fact that *let-70*(*s689*) animals injected with a construct containing 7kb upstream of and 6kb downstream of *let-70* are rescued for lethality but not sterility. Failure to rescue *let-70* sterility is likely caused by germline transgene-expression silencing, a commonly-occurring phenomenon in *C. elegans* (Kelly et al., 1997). *let-*

70(*s689*)-associated lethality and sterility can both be rescued by inhibition of this silencing via co-injection of the same construct mixed with N2 genomic DNA fragments (Stevens 1999).

As none of the above alleles allowed us to examine the role of *let-70* in linker cell death, we attempted to generate a viable *let-70* mutant. We utilized CRISPR/Cas9 to introduce a C-to-T point mutation predicted to cause a P61S mutation in the LET-70 protein (see Materials and Methods). Such a lesion was shown to cause temperature-sensitive UBC4 instability at 39°C in *S. cerevisiae* (Tongaonkar et al., 1999). Strikingly, we found that 57% of *let-70(ns770)*-P61S animals possess surviving linker cells, confirming that *let-70* is required for linker cell death (Table 2.1). Interestingly, linker cell survival in *let-70*(*ns770*) animals is not temperature sensitive (Table 2.1). One reason why this may be the case is that the restrictive temperature for the yeast Ubc4 temperature-sensitive allele is 39°C, a temperature at which *C. elegans* is not viable. Thus, while Ubc4 function may be compromised at 20 or 25°C, the mutation appears not to be detrimental enough to lower Ubc activity below the threshold required for the E2 to maintain general protein homeostasis. We are excited to have generated the first allele of *let-70* that does not cause embryonic or larval lethality when homozygosed, and will be conducting more experiments using it in the future. As we have only obtained the allele recently, all of the following studies utilize *let-70* RNAi instead.

To determine whether reducing LET-70 activity delays or blocks linker cell death, we examined *let-70*(RNAi A) animals (see Figure 2.2) 24 hours after linker cell death should have occurred. We found that 17% (n=100) of animals still retain a surviving linker cell. Thus, while many cells that survive early seem to eventually die (Table 2.1), about one-third of early surviving cells fail to die at a much later time point, suggesting that reducing LET-70 activity can result in a linker cell death block. Surviving linker cells in *let-70*(RNAi) animals have an

Figure 2.2. Constructs used for exploring *let-70* function. (A) Top: Locations of RNAi constructs (red lines: RNAi A/B/C), point mutations (P61S, C85S, *s689*), and deletion alleles (blue lines: *tm2777, ns636*) in relation to map of the *let-70* coding region (black rectangles= exons, white boxes= 5' or 3' untranslated regions). Middle: construct used to express *let-70*-GFP translational fusion. Includes 1.5 kb upstream of start site for promoter. Bottom: construct used to express *let-70*-GFP transcriptional fusion. Scalebar = 200bp. (B) Map of fosmid construct (black line) used to rescue *let-70*(*tm5777*) mutants (black and white gene model). *let-70* genomic locus highlighted in red. Includes *let-70* genomic sequence plus 22.1kb upstream of and 8.3kb downstream of gene. Scalebar = 2000bp.

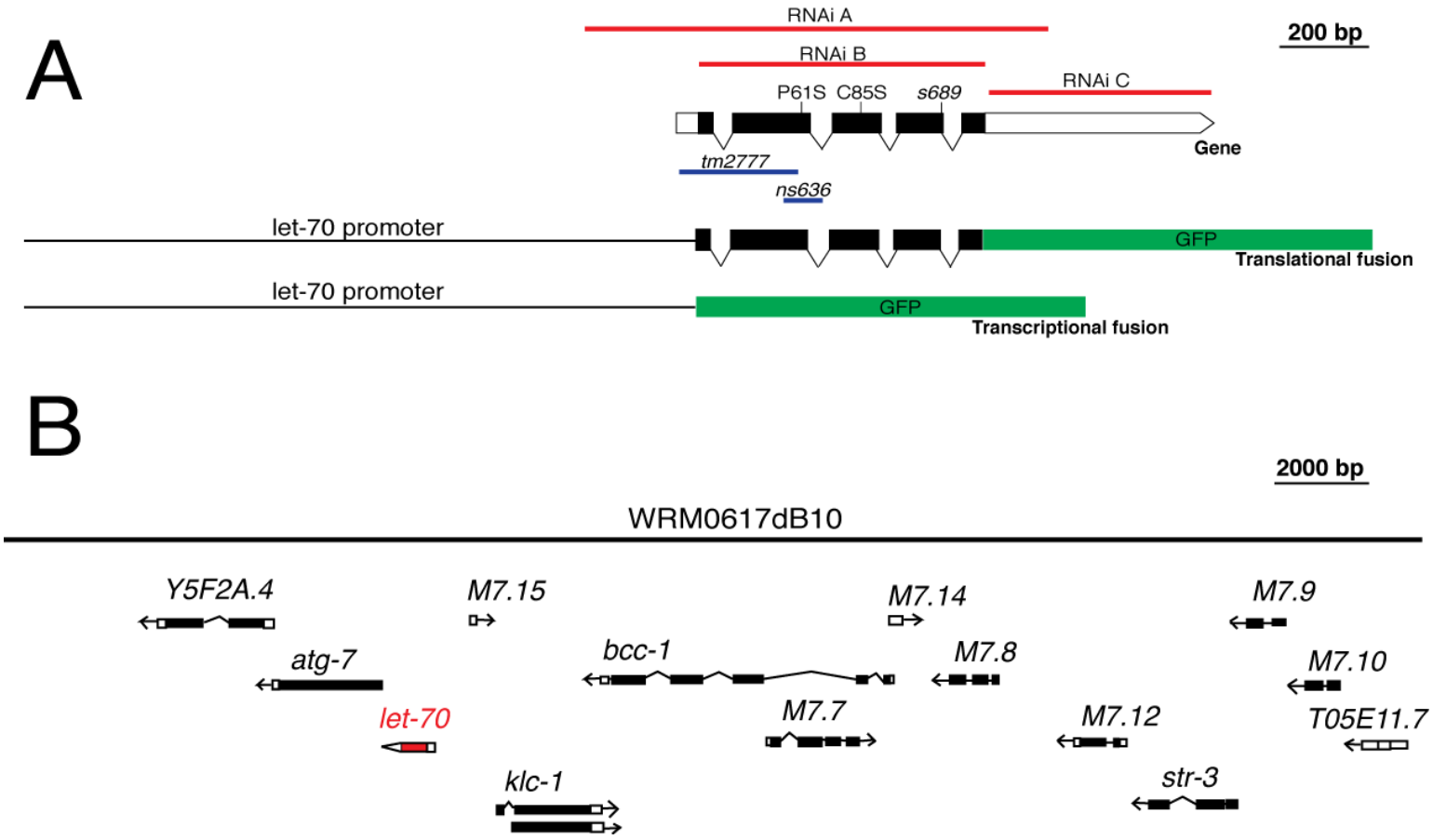
A
RNAi A
RNAi B
RNAi C
200 bp
P61S
C85S
s689
Gene
tm2777
ns636
let-70 promoter
GFP
Translational fusion
let-70 promoter
GFP
Transcriptional fusion
B
2000 bp
WRM0617dB10
Y5F2A.4
M7.15
M7.14
M7.9
atg-7
bcc-1
M7.8
M7.10
let-70
M7.7
M7.12
T05E11.7
klc-1
str-3

Figure 2.3. Deletion alleles of *let-70* are lethal. (A) DNA agarose gel containing PCR genotyping fragments from *let-70*(*tm5777*)/*nT1* balanced animals segregates only heterozygotes and no homozygous mutant *let-70* animals (549 bp= *tm5777*, 291bp = wild-type). (B) Partial DNA sequence alignment of wild-type and CRISPR/Cas9-induced *let-70*(*ns636*) alleles shows 87nt deletion in mutant. Yellow= sgRNA targeting sequence. (C) Top: Partial view of agarose gel containing PCR genotyping of 192 animals following CRISPR/Cas9 injection of wild-type embryos; one animal has an 87nt deletion in *let-70* DNA sequence (*let-70*(*ns636*)). Asterisk=*let-70(ns636)* heterozygous mutant. Bottom: DNA agarose gel containing PCR genotyping fragments from *let-70*(*ns636*) heterozygote progeny contains amplification from wild-type and heterozygous animals only, suggesting that *let-70*(*ns636*) homozygous mutant animals are lethal (519bp= wild-type, 432bp= *ns636*).

A

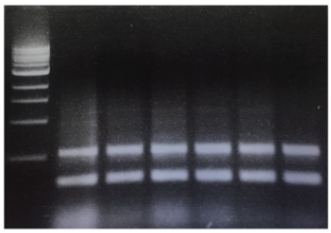

B

```
Wild-type TGTACGTTTCAGGAACTCCAAGATCTCGGCCGTGATCCACCCGCACAATGCTCCGCTGGA
    ns636 TGTACGTTTCAGGAACTCCAAGATCTCGGCCGTGATCCACCCGCACAATGCTCCGCTGGA
          ************************************************************

Wild-type CCAGTTGGTGATGATTTGTTCCATTGGCAAGCTACGATTATGGGCCCACCAGAGTGTCCC
    ns636 CCAGTTGGTGATGATTTGTTCCATTGGCAAGCTACGATTATGGGCCCACCAGAGTGTCCC
          ************************************************************

Wild-type TATCAGGGAGGT------------------------------------------------
    ns636 TATCAGGGAGGTGTCTTCTTCCTCACTATCCACTTCCCAACAGACTATCCATTCAAACCA
          ************
Wild-type ----------------------------------GTTCTTTGTTTTCTTCAGGTTGCCT
    ns636 CCAAAGGTATTGATCGAAATTGGAAAAAAATAAATTTAATTTGTTTTCTTCAGGTTGCCT
                                            * **********************
Wild-type TCACCACTCGAATTTATCATCCGAACATCAATTCAAACGGAAGCATCTGCCTTGACATTC
    ns636 TCACCACTCGAATTTATCATCCGAACATCAATTCAAACGGAAGCATCTGCCTTGACATTC
          ************************************************************
```

C

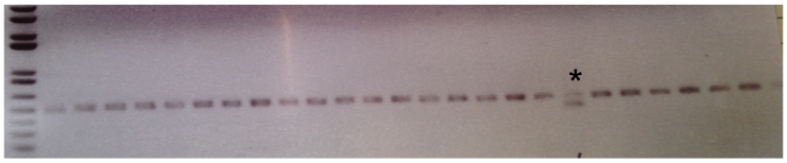

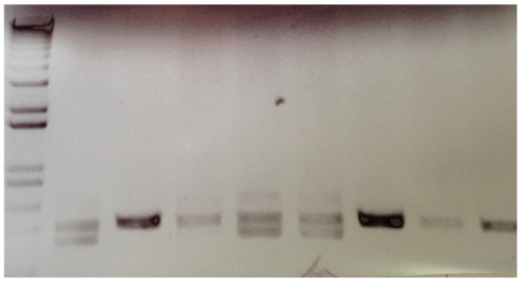

ultrastructure resembling a live linker cell (Abraham et al., 2007). Neither nuclear crenellation nor organelle swelling (as seen in *pqn-41* mutants, (Blum et al., 2012)) is evident (Figure 2.4), suggesting that LET-70 activity is required to either directly or indirectly induce morphological changes associated with linker cell death. Consistent with the idea that *let-70*(RNAi) animals have not properly initiated death, *let-70*(RNAi) surviving linker cells are not engulfed by the adjacent U.l/rp cells that normally engulf the dying linker cell (Figure 2.5).

We wondered whether *let-70* is the only E2 ubiquitin-conjugating enzyme required for linker cell death. With help from summer student Melanie Silverman, we performed RNAi against 13 E2 ubiquitin-conjugating enzymes available within the Ahringer library (out of 22 total E2 enzymes annotated in the *C. elegans* genome) to see if any had inappropriate linker cell survival when depleted. None of the other E2 enzymes caused a linker cell survival defect resembling that of *let-70* when knocked down, indicating that LET-70 likely acts specifically to promote linker cell death (Table 2.2).

LET-70 activity is required in the linker cell to promote cell death

To determine whether LET-70 functions within the linker cell to promote its demise, we performed RNAi against *let-70* in animals expressing a *let-70* cDNA under the control of regulatory DNA derived from the *mig-24* gene, which is expressed in the linker cell and not in surrounding cells (*mig-24* promoter::*let-70*) (Tamai and Nishiwaki, 2007). We used a *let-70* cDNA containing 71 silent mutations to ensure that no sequence stretch longer than 17 nt could perfectly anneal to RNAi fragments directed towards endogenous *let-70* RNA (see Materials and Methods; Figure 2.6). As shown in Table 2.1, partial rescue of linker cell survival is evident,

Table 2.1. LET-70/E2 and components of the proteasome are required for linker cell death

Genotype[a]	% LC survival[b]	% migration defect
Wild type	3 ± <1	5 ± 2
Wild type + empty vector	3 ± <1	5 ± 2
let-70(RNAi, A[c])	45 ± 2^*	58 ± 6
let-70(RNAi, B)	41 ± 13	35 ± 16
let-70(RNAi, C)	64 ± 21	64 ± 21
let-70(RNAi) + P_{LC}::*let-70* cDNA	26 ± 2^	14 ± 9
P_{LC}::*let-70* cDNA	10 ± 7	6 ± 1
let-70(RNAi) + P_{LC}::*let-70* cDNA(C85S)	52 ± 6*	48 ± 16
P_{LC}::*let-70* cDNA(C85S)	1 ± 1	0 ± 0
let-70(LC-only RNAi)	25 ± 1	0 ± 0
let-70(ns770) – P61S- 15°C	62 ± 1	15 ± 4
let-70(ns770) – P61S- 20°C	57 ± 4	9 ± 0
let-70(ns770) – P61S- 25°C	57 ± 4	10 ± 1
rpn-3(RNAi)	35 ± 1	12 ± 5
rpn-8(RNAi)	28 ± 1	26 ± 2
rpn-11(RNAi)	33 ± 2	46 ± 3
rpn-11(LC-only RNAi)	30 ± 7	5 ± 1
rpn-3 (LC-only RNAi)	32 ± 2	1 ± 1
uba-1(*it129*)	17 ± 2	1 ± 1
uba-1(LC-only RNAi)	31 ± 8	8 ± 5
ubq-1(LC-only RNAi)	23 ± 3	2 ± 2

[a]All animals contained the *rrf-3*(*pk1426*) and *him-8*(*e1489*) mutations and a *lag-2*p::gfp (*qIs56*) reporter gene to identify the linker cell, except in the LC-only experiments in which the *mig-24* promoter was used to drive an *rde-1* cDNA in *rde-1*(*ne219*); *him-8*(*e1489*); *qIs56* mutants. *rde-1*(*ne219*) mutants have 12 ± 1 % LC survival.

[b]LC, linker cell. n>79 for both linker cell survival and migration scores. *rde-1* LC RNAi strain obtained from Maxime Kinet, and integrated by Lena Kutscher. Error= SEM, except for experiments using transgenes, where error is the SD of 2-4 transgenic lines obtained. ^P>0.0001, Fisher's Exact Test; *P>0.2, Fisher's Exact Test.

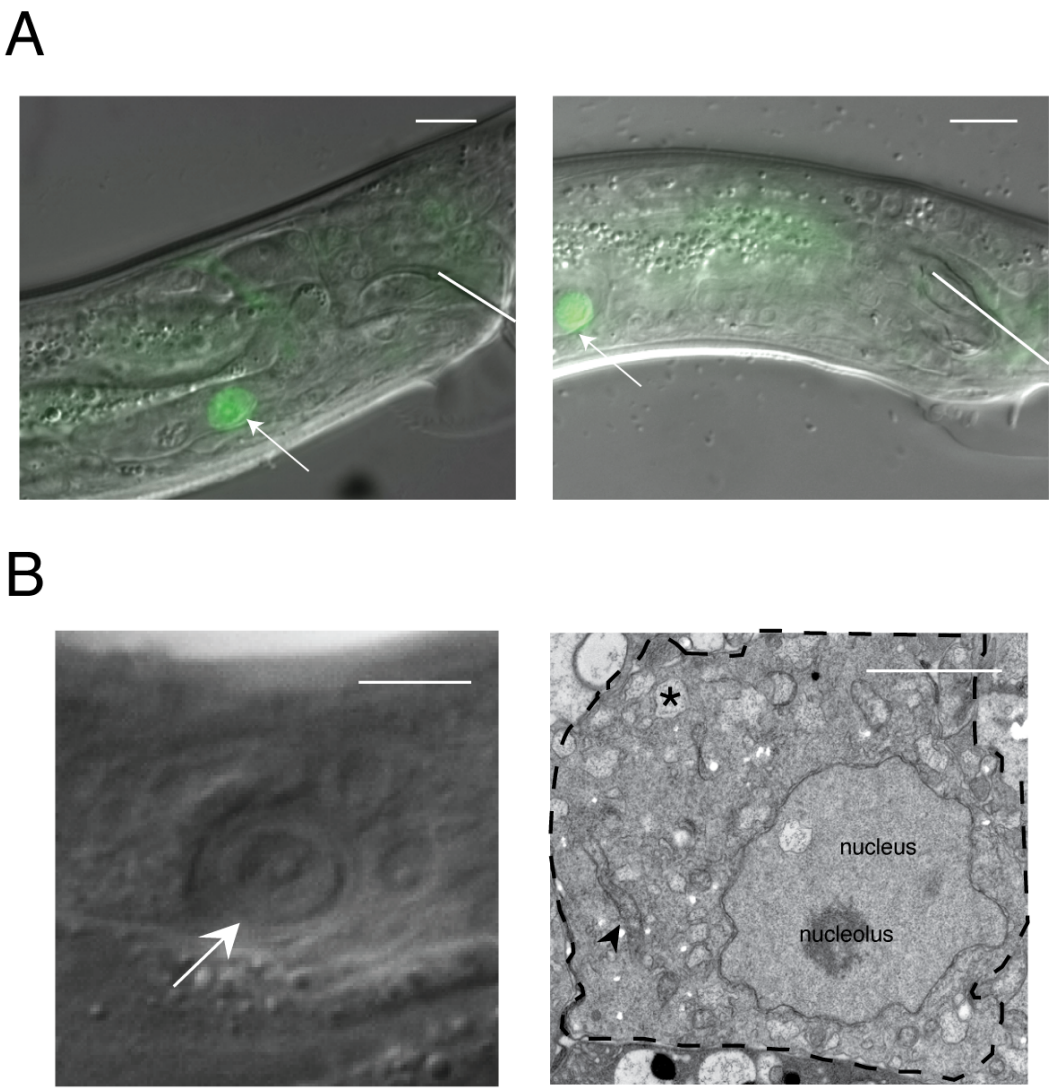

Figure 2.4. *let-70*(RNAi) animals have surviving linker cells. Animals are day one adults. For all animals, left is anterior. (A) *let-70*(RNAi) animals have incomplete linker cell migration. DIC and fluorescent merged images of *let-70*(RNAi) adult males. Left: adult male with wild-type linker cell migration. Right: adult male with inappropriately migrated linker cell. Arrowhead: linker cell. White line: cloaca. Scalebar= 10μm. (B) *let-70*(RNAi) surviving linker cells are ultrastructurally normal. Left: DIC image of surviving linker cell. Arrowhead = linker cell, scalebar= 5μm. Right: electron micrograph of cell at left. Dotted line= cell outline, asterisk= mitochondria. Arrowhead= endoplasmic reticulum. Scalebar= 2μm. Electron micrographs by Yun Lu.

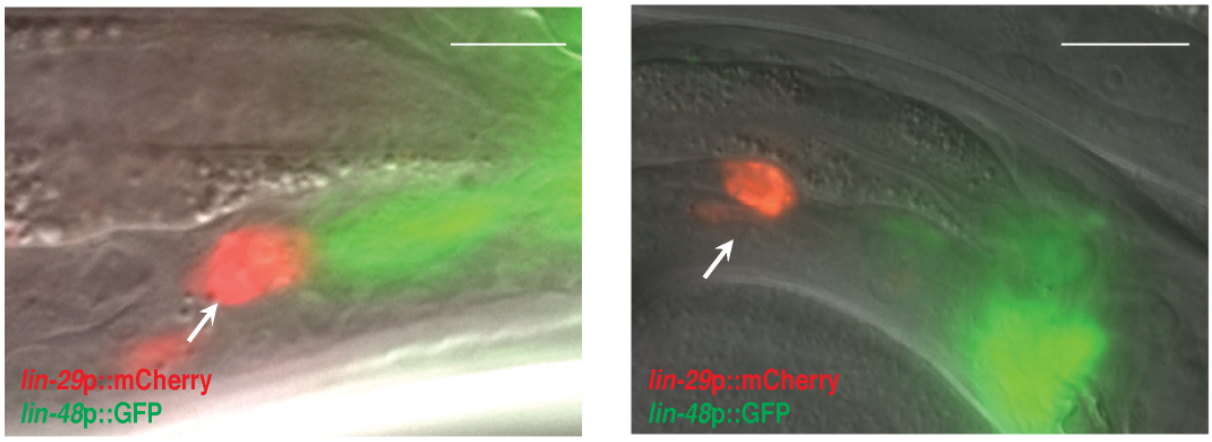

Figure 2.5. *let-70*(RNAi) animals have unengulfed linker cells.

Scalebar = 5μm at left, 10μm at right. Arrow/red cell = linker cell. Green cells= U cells. Surviving *let-70* RNAi linker cells fail to be engulfed both when at the cloaca (left) and inappropriately migrated (right).

Table 2.2. Other E2 ubiquitin-conjugating enzymes are not required for linker cell death

Genotype (RNAi)[a]	% LC survival[b]
ubc-1	7 ± 3
ubc-2/let-70	45 ± 2
ubc-6	4 ± 2
ubc-7	3 ± 2
ubc-9	1 ± 1
ubc-12	7 ± 3
ubc-19	10 ± 3
ubc-20	2 ± 2
ubc-21	2 ± 1
ubc-22	2 ± 1
ubc-23	5 ± 2
ubc-24	3 ± 2
ubc-25	3 ± 2

[a]All animals contained *rrf-3(pk1426); him-8*(*e1489*) mutations and a *lag-2*::*gfp* (*qIs56*) reporter gene to identify the linker cell.

[b]LC, linker cell. n>67, Error= SEM.

supporting the idea that LET-70 functions cell autonomously. To confirm this idea, we repeated the *let-70* RNAi studies in *rde-1* mutant animals carrying a *mig-24* promoter::*rde-1* cDNA transgene. RDE-1 is an argonaute protein required for RNAi in *C. elegans*, and in *rde-1*(*ne219*); *mig-24* promoter::*rde-1*cDNA animals RNAi is only functional in the linker cell (Figure 2.7)(Qadota et al., 2007). We found that linker cell-specific RNAi against *let-70* also prevents linker cell death (Table 2.1). We conclude, therefore, that LET-70 functions within the linker cell for linker cell death.

Of note, *let-70*(RNAi) animals often exhibit a defect in linker cell migration. Three observations suggest that migration and death are separable functions of LET-70. First, linker cell survival is sometimes observed in *let-70*(RNAi) animals with normal migration. Second, while linker cell-specific RNAi against *let-70* blocks cell death, it has essentially no effect on migration (7% migration defect (Table 2.1)). Finally, while *let-70*(P61S) mutants have surviving linker cells at roughly the same rate as *let-70*(RNAi) animals, they exhibit a much lower migration defect as compared to *let-70*(RNAi) animals (9%; Table 2.1). One possible explanation for this result is that one concentration of LET-70 protein is required for death, while another is required for migration. In this scenario, the *let-70*(P61S) mutation would cause LET-70 instability, but still provide the protein with enough functional enzymatic activity to induce cell migration. However, in this case, there would therefore not be a large enough functional pool of LET-70 to induce linker cell death. Consistent with this idea, as previously mentioned, *let-70* null mutants die as early embryos or larvae; *let-70*(P61S) mutants must therefore contain a sufficiently large pool of functional LET-70 in order to carry out homeostatic proteostasis required to survive to adulthood and propagate. Another possibility is that the RNAi against *let*

Figure 2.6. Generation of a *let-70* RNAi- rescuing cDNA generated via induced point mutations in a *C. briggsae* sequence. *let-70 C. elegans* cDNA, *let-70 C. briggsae* cDNA and *let-70 C. briggsae* + point mutations cDNA were aligned using Clustal Omega (Goujon et al., 2010; McWilliam et al., 2013; Sievers et al., 2011). Asterisk= exact DNA sequence match.

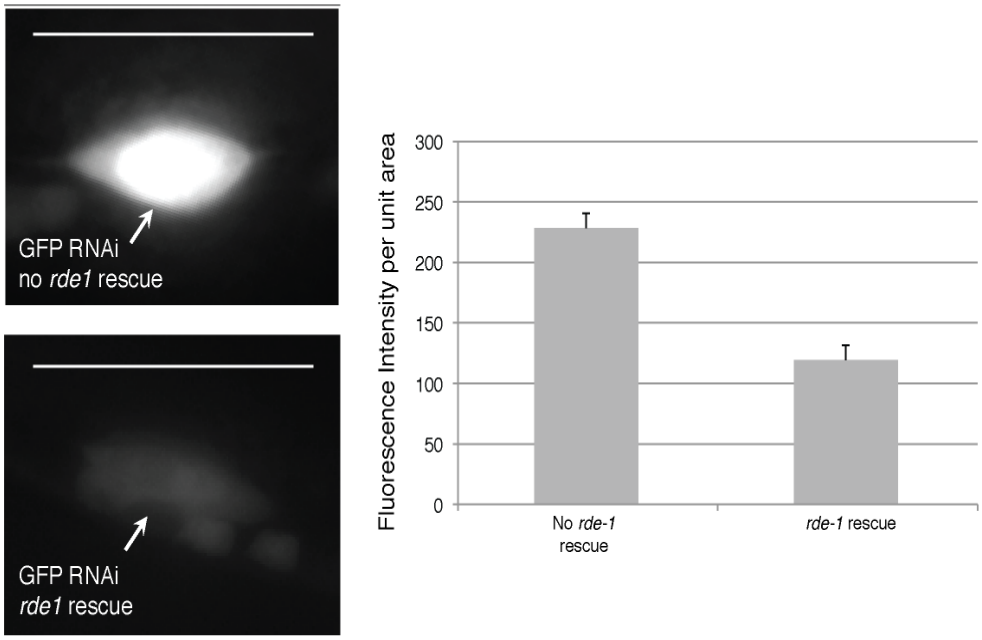

Figure 2.7. *rde-1* rescue animals knock down genes specifically in the linker cell. Top left: GFP expression is elevated in GFP(RNAi) animals without *rde-1* rescue in the linker cell. Bottom left: GFP expression is reduced in GFP(RNAi) animals with *rde-1* rescued in the linker cell. Right: Quantification of fluorescence intensity. N= 16 for each genotype. Error bars show standard deviation. P<0.0001, Student's T Test. Strain obtained from Maxime Kinet. Scalebar= 10μm.

70 causes an off-target effect; in this case, another gene, which shares sequence similarity to *let-70* in regions targeted by the RNAi, would have been knocked down in an event that impacted linker cell migration. However, this seems unlikely, as all three RNAi clones used had migration defects.

Components of the Ubiquitin Proteasome System are required for linker cell death

To determine whether LET-70 functions as part of the ubiquitin proteasome system (UPS) in the linker cell, we examined the effects of inhibiting components of the 19S regulatory subunit of the proteasome on linker cell death. Systemic RNAi against the *rpn-3*, *rpn-8*, or *rpn-11* genes result in linker cell survival in about one third of animals (Table 2.1). Furthermore, linker cell-specific RNAi against *rpn-3* and *rpn-11* result in similar inhibition (Table 2.1). Together, these data suggest that LET-70 may function in the linker cell as a component of the UPS, and demonstrate that proteasome activity is required to promote linker cell demise. We also sought to see if ubiquitin, as well as UBA-1—the sole E1 activating enzyme in *C. elegans*—were required for linker cell death. While systemic RNAi against *uba-1* is early larval lethal, weak *uba-1* mutant animals survive to adulthood. *uba-1*(*it129*) homozygous animals display a weak but significant defect in linker cell death, intimating that E1 ubiquitin-activating enzyme activity is required for linker cell death (Figure 2.8, Table 2.1). Consistent with this result, linker cell-specific RNAi against *uba-1*, as well as linker cell-specific RNAi against ubiquitin (*ubq-1*) also produces strong, significant defects in linker cell death (Table 2.1). Thus, the proper functioning of many components of the ubiquitination pathway is required to kill the linker cell.

Overexpression of *let-70, pqn-41* and/or *ubq-1* is not sufficient to kill the linker cell

As *let-70* is necessary within the linker cell for its death, we wondered whether ectopic expression of *let-70* might be sufficient to kill a related cell. Expression of *let-70* under the control of the *mig-24* promoter in the lineally related distal tip cells of hermaphrodite animals fails to induce cell death (Table 2.3). Ectopic expression of *ubq-1*, as well as simultaneous co-expression of *let-70* and *ubq-1* cDNAs also fails to induce cell death in distal tip cells, indicating that their combined expression is not sufficient to drive death (Table 2.3). Though ectopic expression of *ubq-1* cDNA is not sufficient to kill the distal tip cell, the overexpression does cause the distal tip cells to become rounded and bloated (Figure 2.9); co-expression of *let-70* cDNA with *ubq-1* instead causes the distal tip to become morphologically thin and spindly (Figure 2.9). Thus, though ectopic expression of *let-70* and ubiquitin is not sufficient to induce death, their expression may be important for regulation of overall distal tip cell character.

Previous data from our lab suggested that *pqn-41* expression is not sufficient to cause the death of a related cell. Experiments from Elyse Blum showed that the *pqn-41* genetic locus is quite complex, and is transcribed into several isoforms (Blum et al., 2012). Elyse ectopically expressed the A, B and C transcripts of *pqn-41* within the linker cells of *pqn-41*(*ns294*) animals using the *mig-24* promoter to assess their ability to rescue inappropriate linker cell survival. Elyse found that while expression of the A and B isoforms of *pqn-41* cause an increase in inappropriate survival which exceeds the mutant defect, overexpression of the *pqn-41*C isoform returns linker cell death to almost wild-type levels (Blum et al., 2012). Elyse also overexpressed each transcript under the control of the *mig-24* and *cdh-3* promoters in wild-type animals to see if either was sufficient to induce ectopic cell death in either the distal tip cells or the anchor cell,

respectively. None of the constructs caused inappropriate cell death in any worm when injected, indicating that *pqn-41* is not sufficient to kill a lineally related cell (Blum et al., 2012).

In light of this data, we wondered whether simultaneous expression of *let-70* and *pqn-41* would be sufficient to induce cell death. Heterologous expression of *mig-24*p::*let-70* in addition to either the B or C isoforms of *pqn-41* is also not sufficient to induce cell death (Table 2.3). Overexpression of the constructs, either alone or together, in touch cells under the control of the *mec-7* promoter also fails to induce death (Table 2.3).

It is interesting to speculate about why none of the above genes alone or in combination are sufficient to induce distal tip cell death. One possibility is that we have not yet identified the linker cell protein (or combination of proteins) whose expression is sufficient to kill any cell. Another possibility is that some of these proteins may be sufficient to kill, but their action is blocked by a host of protective proteins that are expressed in the distal tip cell, but not in the linker cell. Maxime Kinet has shown that components of a Wnt signaling pathway (see below) act as protective proteins that prevent linker cell death from occurring (M. Kinet, unpublished results). Given that expression of *mig-24*p::*let-70 briggsae* cDNA in the migrating linker does not induce early death, it is possible that this is the case, though one could imagine that ectopic expression of *let-70* might not be sufficient to induce death without simultaneous overexpression of ubiquitin or the proteasome.

LET-70 E2 ubiquitin-conjugating enzyme activity is required for linker cell death

Since LET-70 is homologous to E2 enzymes, we wondered whether its E2 enzymatic activity was required to promote linker cell death. To test this, we first assayed the ability of LET-70 protein to mediate ubiquitin transfer in an *in vitro* ubiquitylation assay. Incubation of

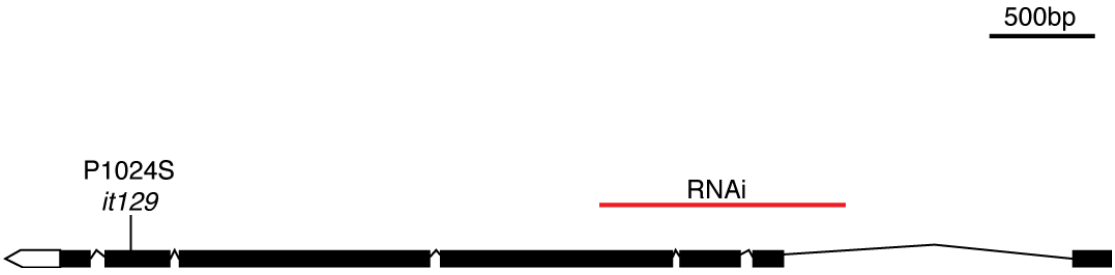

Figure 2.8. Map of mutants and RNAi used to explore *uba-1* function. RNAi (red line) and point mutation (P1024S) used to analyze *uba-1* in relation to map of *uba-1* (black boxes = exons, white box = 3'UTR), scalebar = 500bp.

Table 2.3. Overexpression of *let-70*, *pqn-41*, or *ubq-1* cDNA, either alone or in combination, is not sufficient to induce cell death

Genotype[a]	**Percentage Survival**
*lag-2*p::mCherry	100
*mig-24*p::*let-70* cDNA line 1	100
*mig-24*p::*let-70* cDNA line 2	100
*mig-24*p::*let-70* cDNA line 3	100
*mig-24*p::*let-70* + *mig-24*p::*pqn-41C* line 1	100
*mig-24*p::*let-70* + *mig-24*p::*pqn-41C* line 2	100
*mig-24*p::*let-70*::SL2::*pqn-41C* line 1	100
*mig-24*p::*let-70*::SL2::*pqn-41C* line 2	100
*mig-24*p::*let-70* + *mig-24*p::*pqn-41B*	91
*mec-4*p::gfp	100
*mec-7*p::*let-70*	100
*mec-7*p::*let-70*::SL2::*pqn-41* + *rol-6* + *mec-4*p::gfp	100
*mec-7*p::*let-70*::SL2::gfp + *mec-7*p::*pqn-41C*	100
*mig-24*p::*ubq-1*	100
*mig-24*p::*ubq-1*::SL2::*let-70*	100

[a]All animals contained a *him-8*(*e1489*) mutation. Distal tip cell constructs were co-injected with the *lag-2*p::yfp reporter gene, while touch cell constructs were co-injected with *mec-4*p::gfp.

[b]n>32

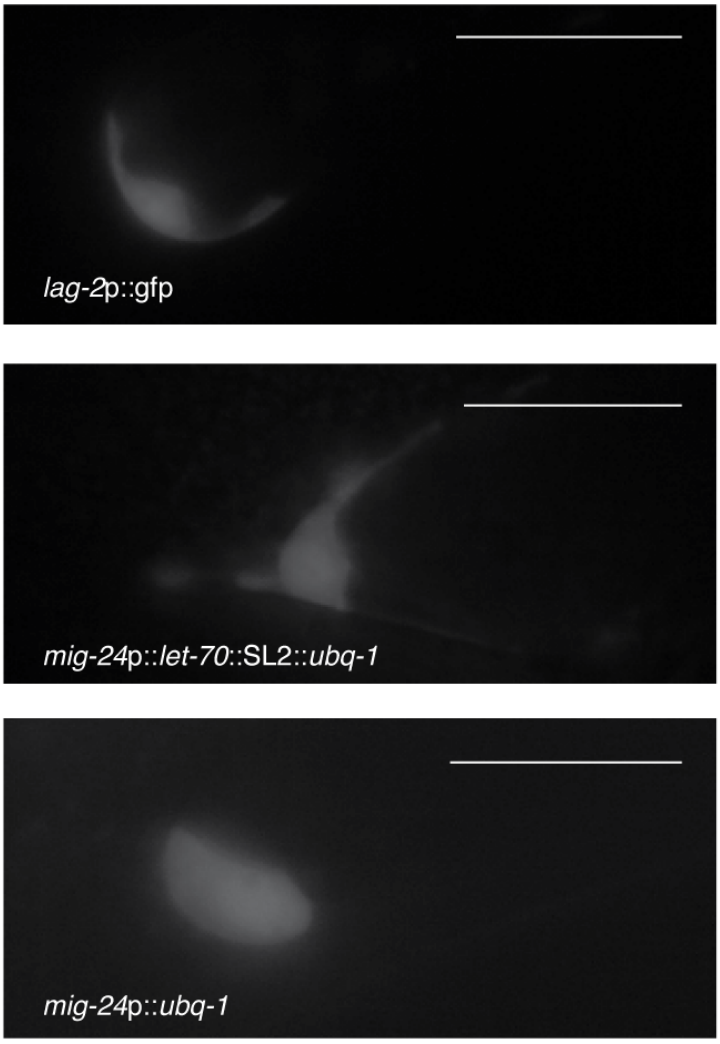

Figure 2.9. Animals overexpressing *mig-24*p::*ubq-1* or *mig-24*p::*let-70*::SL2::*ubq-1* display aberrant distal tip cell morphology. All animals are day one adults. Scalebar = 10μm. Top: *lag-2*p::gfp animals show normal distal tip cell morphology. Middle: *mig-24*p::*let-70*::SL2::*ubq-1* animals have distal tip cells with longer and mislocalized processes. Bottom: *mig-24*p::*ubq-1* animals have bloated distal tip cells without any apparent processes.

LET-70 with the *Drosophila* UBA1 E1 activating enzyme and the *Drosophila* E3 ligase DIAP1 results in DIAP ubiquitylation in the presence of ATP, magnesium ions, and ubiquitin (Figure 2.10). A similar reaction without LET-70 does not yield DIAP ubiquitylation, suggesting that LET-70 can function as an E2. To determine whether E2 activity was required in vivo, we attempted to rescue the *let-70* RNAi linker cell survival defect using a silently mutated, RNAi-resistant *let-70* cDNA that also contained a mutation predicted to change the catalytic cysteine 85 to serine. We found that this mutant cDNA, which differs from wild-type LET-70 by a single atom, is unable to rescue the linker cell survival defect of *let-70*(RNAi) animals (Table 2.2). Thus, LET-70 E2 catalytic activity is required for linker cell death.

Expression of LET-70 and other UPS components is induced within the linker cell at the time of death

To study the expression and localization of LET-70, we generated animals carrying transgenes in which GFP is fused either immediately downstream of *let-70* 5' regulatory sequences, or downstream of *let-70* coding sequences. We found that both reporters are expressed in the linker cell, and that the translational fusion reporter is evenly distributed between the nucleus and cytoplasm (Figures 2.2, 2.11). Importantly, we found that expression of neither reporter is constitutive. Rather, while GFP fluorescence is not detected during migration of the linker cell, it is induced 1-2 hours before obvious morphological features of cell death appear (Figure 2.11). This is not affected by the presence or absence of *let-70's* endogenous 3'UTR (Figure 2.11). In addition to the linker cell, *let-70*-GFP is expressed in a number of neurons including the ventral nerve cord, and what appears to be the gonadal sheath in adults. This expression is not induced during linker cell death, but rather, exists throughout the lifetime

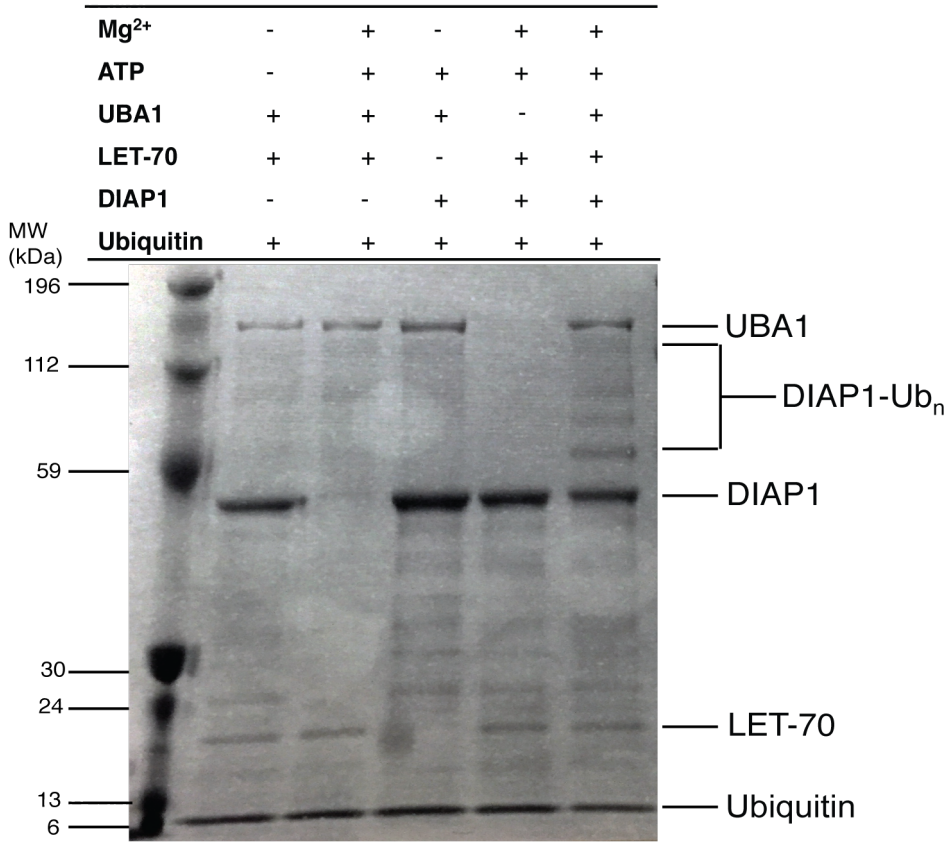

Figure 2.10. LET-70 acts as a ubiquitin-conjugating enzyme in vitro. Addition of purified 6xHis-LET-70 to *Drosophila* UBA1, DIAP1 and ubiquitin induces auto-ubiquitination of DIAP1 that is visible by Coommassie staining.

of the animal. Expression is detected in a broader range of tissues in the embryo and early larvae, where some body wall muscle expression is also visible; this expression dims by the second larval stage. We wondered whether the expression of other components of the UPS might also be induced in the linker cell with similar kinetics. Indeed, we found that *ubq-1*p::GFP and *ubq 1*p::*ubq-1*::GFP reporters are also induced in the linker cell at the time of death (Figure 2.11, 2.12). This expression pattern is also seen in animals expressing *ubq-1*p::mCherry and *ubq-1*p::*ubq-1*::mCherry reporters; however, unlike in GFP reporters, mCherry is weakly visible in migrating linker cells, indicating that *ubq-1*p::*ubq-1*::GFP may be expressed at undetectable levels in the migrating linker cell (Figure 2.11). Transcriptional fusions of the regulatory DNA 3kb upstream of the 19S proteasome subunit *rpn-3* to GFP are also induced in the linker cell upon death initiation, suggesting that expression of some UPS components may be co-regulated in the linker cell (Figure 2.11).

UPS components function downstream of SEK-1/TIR-1

To understand how UPS components cooperate with previously characterized linker cell death genes, we examined the effects of *let-70* depletion in animals carrying mutations in these genes. We found that *let-70* RNAi in *sek-1*(*ag1*) or *pqn-41*(*ns294*) mutants does not result in a significant increase in linker cell survival compared to *sek-1*(*ag1*) or *let-70*(RNAi) alone, respectively, suggesting that all three genes may function in the same pathway (Figure 2.13). We tested whether either gene could affect *let-70* or *ubq-1* reporter expression, and found that surviving linker cells in *sek-1*(*ag1*) mutants, but not in *pqn-41*(*ns294*) animals had a marked reduction in expression of both genes (Figure 2.14). Elyse Blum previously reported that *sek-1* controls expression of a *pqn-41*::GFP reporter (Blum et al., 2012). Our results, therefore, suggest

Figure 2.11. Components of the UPS are induced in the linker cell at the time of death. For all images, arrow= linker cell, scalebar =10μm. Error bar = SEM. (A) *let-70*p::*let-70*::gfp is not expressed in a migrating linker cell (left, quantification at right), but is expressed in a dying linker cell (center, quantification at right). (B) *let-70*p::gfp-*let-70* 3'UTR (left) and *let-70*p::*let-70*::gfp-*let-70* 3'UTR (right) animals express GFP in dying linker cells. (C) *ubq-1*p::*ubq-1*::gfp is not expressed in a migrating linker cell (left, quantification at right), but is expressed in a dying linker cell (center, quantification at right). (D) *ubq-1*p::*ubq-1*::mCherry is weakly expressed in a migrating linker cell, (left) but strongly expressed in a dying linker cell (right) (E) *rpn-3*p::gfp is not expressed in a migrating linker cell (left) but is expressed in a dying linker cell (right). As the constructs used in (B), (D) and (E) are extrachromosomal arrays, and are not integrated, their expression has not been quantified.

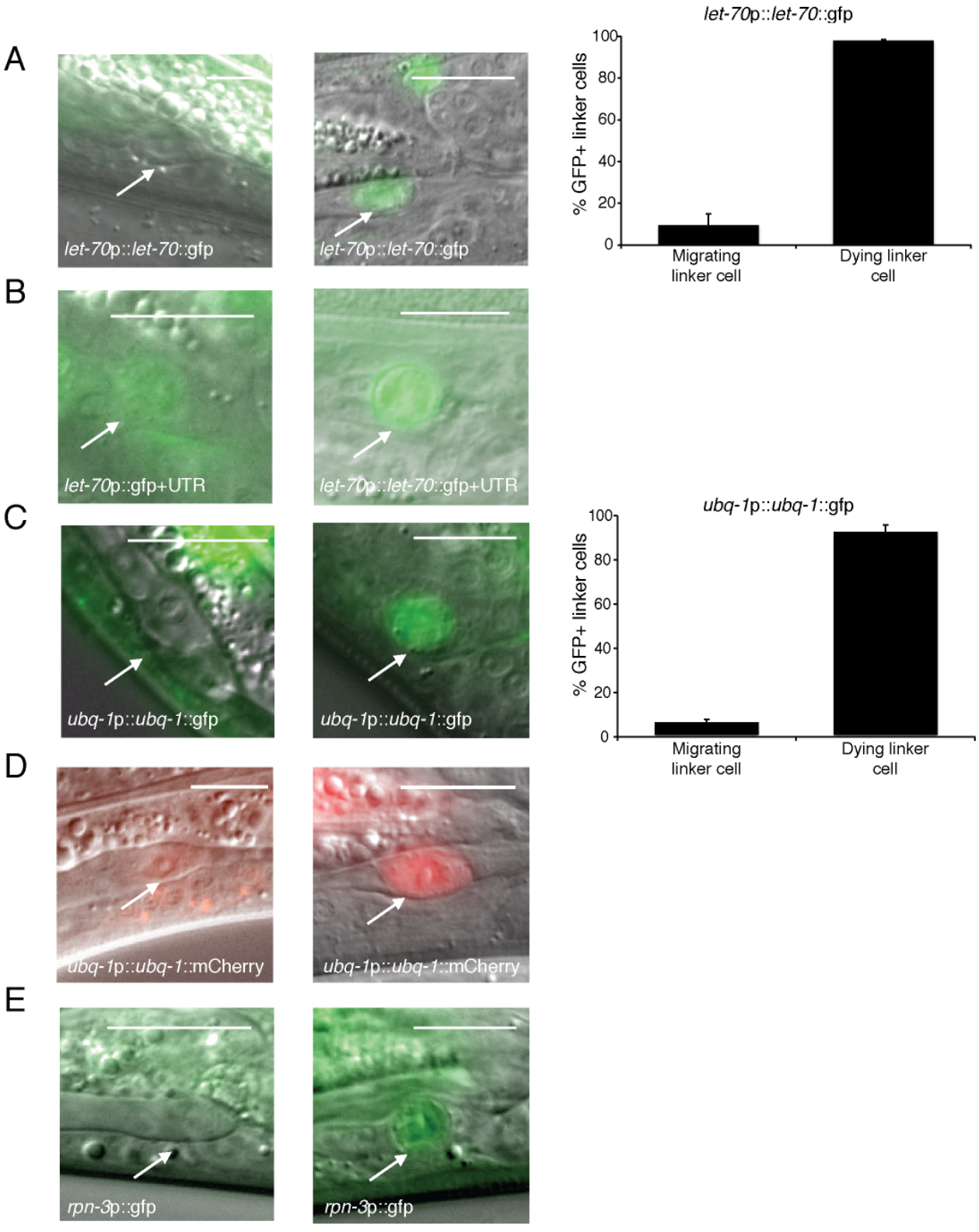
A
let-70p::let-70::gfp
let-70p::let-70::gfp
B
let-70p::gfp+UTR
let-70p::let-70::gfp+UTR
C
ubq-1p::ubq-1::gfp
ubq-1p::ubq-1::gfp
D
ubq-1p::ubq-1::mCherry
ubq-1p::ubq-1::mCherry
E
rpn-3p::gfp
rpn-3p::gfp
let-70p::let-70::gfp
% GFP+ linker cells
100
80
60
40
20
0
Migrating linker cell
Dying linker cell
ubq-1p::ubq-1::gfp
% GFP+ linker cells
100
80
60
40
20
0
Migrating linker cell
Dying linker cell

Figure 2.12. Constructs used for exploring ubiquitin function. (A) Top: Location of RNAi construct (red lines: RNAi) in relation to map of the *ubq-1* coding region (black rectangles= exons, white boxes= 5' or 3' untranslated regions, blue box= final repeat of polyubiquitin gene, gray boxes= alternatively spliced exons). Bottom: constructs used to express *ubq-1*p::*ubq-1*::gfp, *ubq-1*p::gfp, *ubq-1*p::*ubq-1*::mCherry, and *ubq-1*p::mCherry, respectively. Promoter region includes 939bp upstream of ATG. Blue box= *ubq-1* repeat 11, green box= GFP, red box = mCherry. Scalebar = 250bp. (B) DNA alignment of the 11 repeats of the *ubq-1* gene; *ubq-1* is transcribed as a polycistronic unit that is cleaved into monoubiquitins following translation. Repeat 11 was used for the translational fusion of *ubq-1* to mCherry/GFP.

A

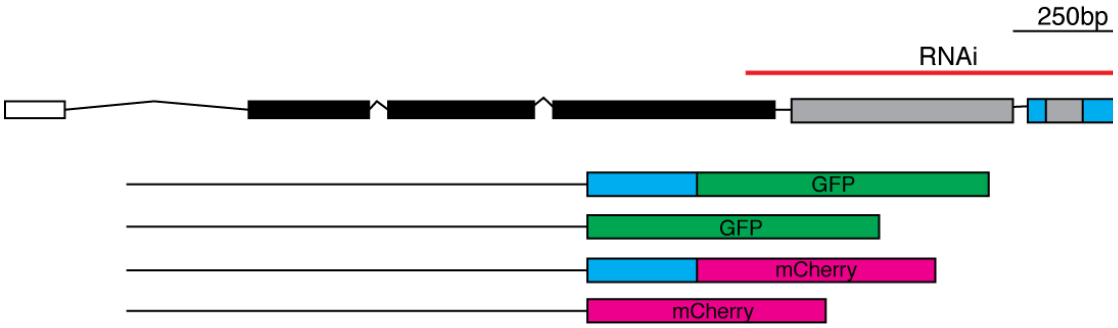

that *sek-1* may act

B

```
repeat1     ATGCAAATCTTCGTCAAAACGTTGACTGGAAAAACTATCACCCTGGAGGTGGAGGCTTCC
repeat2     ATGCAGATCTTTGTCAAGACTTTGACTGGAAAGACCATCACACTTGAAGTTGAAGCTTCC
repeat3     ATGCAGATCTTCGTCAAGACATTGACTGGAAAGACCATCACACTTGAAGTCGAAGCTTCC
repeat4     ATGCAGATCTTCGTCAAGACATTGACCGGAAAGACCATCACCCTCGAAGTCGAAGCCTCC
repeat5     ATGCAGATCTTCGTCAAGACTTTGACCGGAAAGACTATTACTCTTGAGGTTGAAGCTTCT
repeat6     ATGCAAATCTTCGTCAAGACTCTTATCGGAAAGACCATCACCCTCGAAGTCGAAGCCTCC
repeat7     ATGCAAATCTTCGTGAAGACTTTGACTGGAAAGACTATCACCCTCGAAGTCGAAGCCTCT
repeat8     ATGCAGATCTTCGTCAAGACTCTTACAGGAAAGACCATCACGCTCGAGGTGGAAGCTTCT
repeat9     ATGCAGATCTTCGTCAAGACATTGACTGGAAAGACCATCACACTTGAAGTCGAAGCCTCT
repeat10    ATGCAGATCTTCGTCAAGACATTGACCGGAAAGACCATCACCCTCGAAGTCGAAGCCTCC
repeat11    ATGCAGATCTTCGTCAAGACTTTGACTGGAAAAACCATCACTCTCGAGGTCGAAGCTTCG
            *****.***** ** **.**  * *  *****.** ** ** ** **.** **.** **

repeat1     GATACCATCGAAAATGTCAAAGCCAAGATCCAAGACAAGGAAGGAATTCCACCAGATCAG
repeat2     GACACGATCGAGAACGTCAAGGCCAAGATTCAAGACAAGGAGGGAATCCCACCAGATCAG
repeat3     GACACGATCGAAAATGTCAAGGCTAAGATTCAAGATAAAGAAGGAATCCCACCAGATCAG
repeat4     GACACCATCGAAAATGTCAAGGCCAAGATCCAAGACAAGGAAGGAATTCCACCAGATCAG
repeat5     GACACTATTGAGAACGTGAAGGCCAAGATCCAAGACAAGGAAGGTATCCCACCAGATCAA
repeat6     GATACCATCGAGAACGTGAAGGCCAAGATTCAGGACAAGGAAGGAATTCCTCCAGATCAG
repeat7     GATACCATCGAAAATGTGAAGGCCAAGATCCAAGACAAGGAAGGAATCCCACCAGATCAG
repeat8     GACACTATTGAGAACGTGAAGGCCAAGATCCAAGACAAAGAAGGTATCCCACCAGATCAG
repeat9     GATACCATCGAGAATGTGAAGGCCAAGATTCAAGACAAGGAAGGAATCCCACCAGATCAG
repeat10    GACACCATCGAAAATGTCAAGGCCAAGATCCAAGACAAGGAAGGAATTCCACCAGATCAG
repeat11    GACACCATTGAGAATGTCAAAGCCAAAATCCAGGATAAGGAGGGAATCCCACCAGATCAG
            ** ** ** **.** ** **.** **.** **.** **.**.**:** **:********.

repeat1     CAGCGTCTCATCTTCGCCGGAAAGCAGCTCGAGGACGGCCGCACCCTGTCTGACTACAAC
repeat2     CAGCGTCTTATCTTTGCTGGAAAGCAATTGGAAGATGGACGCACACTCTCTGATTACAAT
repeat3     CAAAGACTTATCTTCGCCGGAAAGCAGCTCGAGGACGGCCGCACCCTTTCGGACTACAAC
repeat4     CAGAGACTTATTTTTGCTGGAAAGCAACTCGAGGATGGCCGTACCCTTTCGGACTACAAT
repeat5     CAGCGTTTGATCTTTGCCGGAAAGCAACTCGAGGATGGCCGTACTCTCTCCGATTACAAC
repeat6     CAACGTCTCATCTTCGCTGGAAAGCAGCTCGAAGACGGCCGCACCCTTTCGGACTACAAC
repeat7     CAGCGTCTTATCTTTGCCGGAAAGCAATTGGAAGATGGGCGCACGCTCTCTGATTACAAC
repeat8     CAACGCTTGATCTTCGCCGGAAAGCAACTCGAGGATGGCCGTACCCTTTCGGACTACAAT
repeat9     CAGAGACTCATCTTCGCCGGAAAACAACTCGAAGACGGTCGTACCCTCTCCGACTACAAC
repeat10    CAGAGACTTATTTTCGCTGGAAAGCAACTCGAGGATGGCCGTACCCTTTCGGACTACAAT
repeat11    CAACGTTTGATCTTTGCTGGAAAGCAGCTCGAGGATGGACGCACTCTATCCGATTACAAC
            **..*  * ** ** ** *****.**. * **.** ** ** ** ** ** ** *****

repeat1     ATCCAGAAGGAATCTACTCTTCACTTGGTTCTTCGTCTTAGAGGAGGA---------
repeat2     ATTCAGAAAGAGTCTACTCTCCACTTGGTGCTCCGCCTCAGAGGAGGT---------
repeat3     ATCCAGAAGGAATCAACTCTTCATTTGGTTCTCCGTTTGAGAGGAGGT---------
repeat4     ATCCAGAAGGAATCAACCCTCCATTTGGTGCTCCGCCTAAGAGGAGGA---------
repeat5     ATCCAAAAGGAGTCTACTCTTCATTTGGTTCTCCGTCTCCGAGGAGGA---------
repeat6     ATCCAGAAGGAATCAACTCTTCATTTGGTTCTCCGTTTGAGAGGAGGT---------
repeat7     ATTCAGAAGGAATCTACTCTTCACTTGGTTCTCCGTCTCCGAGGAGGA---------
repeat8     ATCCAGAAGGAATCAACCCTCCATTTGGTGCTCCGTCTCAGAGGAGGT---------
repeat9     ATCCAAAAGGAGTCTACTCTTCATTTGGTTCTCCGTCTGAGAGGAGGT---------
repeat10    ATCCAGAAGGAGTCTACTCTTCATTTGGTGCTCCGTCTCAGAGGAGGT---------
repeat11    ATCCAAAAGGAGTCGACACTTCATCTCGTTCTTCGTCTTCGCGGAGGAGACATTTAA
            ** **.**.**.** ** ** **  * ** ** **  * .*.*****:
```

upstream of *let-70*, *ubq-1*, and *pqn-41* to control their expression. Supporting this idea, we also found that RNAi against the *tir-1* gene, encoding an adapter protein that functions together with *sek-1* and regulates *pqn-41* reporter expression in Elyse's hands (Blum et al., 2012), also blocks *let-70* and *ubq-1* reporter induction in the linker cell (Figure 2.14). This is reinforced by the result that *tir-1* RNAi in combination with *let-70* RNAi has the same percentage of surviving cells as *let-70* RNAi animals alone (Figure 2.14). In contrast, RNAi targeting the *lin-29* transcription factor gene (see Introduction) has a modest effect on *let-70* and *ubq-1* reporter expression, as it does on *pqn-41* reporter expression in Elyse's work (Figure 2.14)(Blum et al., 2012). *lin-29* RNAi in a *let-70*(RNAi) background produces an overall increase in linker cell survival, corroborating the above data that *lin-29* is only partially required for *let-70* expression during linker cell death (Figure 2.13).

A SET-16/MLL-type complex promotes *let-70* expression and linker cell death

To uncover the mechanism by which expression of *let-70* and other UPS genes is co-regulated in the linker cell, we assayed other genes that emerged from Elyse Blum and Mary Abraham's RNAi screen for effects on *let-70* and *ubq-1* reporter expression. One of the genes that emerged from the screen was the WD repeat domain gene *swd-2.2.* Maxime Kinet, a graduate student in the lab, found that two different RNAi constructs targeting the gene *swd-2.2* promote linker cell survival (M. Kinet, unpublished observations). As proteins related to SWD-2.2 have been identified in complex with SET-domain histone methyltransferases (Miller et al., 2001; Mohan et al., 2010), Maxime found that RNAi against SET complex proteins also has strong effects on linker cell death, with RNAi against the *set-16* gene, encoding the catalytic subunit, producing a striking survival defect of 50% (M. Kinet, unpublished observations).

Expression of *ubq-1* and *let-70* reporters is strongly reduced in *set-16*(RNAi) and *swd-2.2*(RNAi) animals (Figure 2.14). Furthermore, *swd-2.2* or *set-16* RNAi in combination with *let-70* RNAi causes no additional increase in linker cell survival above the *let-70* RNAi survival defect (Figure 2.13). Thus, we conclude that a SET-16 histone methyltransferase complex is required to induce expression of UPS components in the linker cell, thus promoting linker cell death.

The nuclear hormone receptor NHR-67 induces *let-70* expression and acts synergistically with *let-70* to promote death

A second gene that was isolated from Elyse and Mary's screen is the nuclear hormone receptor *nhr-67*. *nhr-67*(RNAi) animals exhibit inappropriate linker cell death around 61% of the time, with close to 100% of surviving linker cells failing to migrate to the cloaca (Figure 2.13). We sought to understand whether *let-70* works with *nhr-67* to promote linker cell death. Knockdown of *nhr-67* in a *let-70*(RNAi) background causes a synergistic increase in linker cell survival, with almost 90% of linker cells failing to die (Figure 2.13). Interestingly, *let-70*-GFP as well as *ubq-1*-GFP is highly expressed in surviving linker cells, indicating that *nhr-67* is either not required for proper *let-70*/*ubq-1* expression, or that *nhr-67* acts upstream to inhibit normal *let-70*/*ubq-1* expression (Figure 2.14). To distinguish between the two, we looked at *let-70*- and *ubq-1*-GFP expression in L3 animals, when GFP is normally absent in the linker cell. Surprisingly, *let-70*-GFP and *ubq-1*-GFP were both inappropriately induced in early linker cells, indicating that *nhr-67* acts upstream of *let-70* and *ubq-1* to inhibit their expression. This result seems to be counterintuitive: how can both genes be required for death while one inhibits the other? A number of answers are possible. One is that LET-70 levels are important for cell death instruction; too little LET-70 causes survival, but too much LET-70 may also cause survival.

Thus, NHR-67 may be required to properly titrate the levels of LET-70 to ensure that death is induced. A second possibility is that NHR-67, as a transcription factor, affects the expression of a number of genes at different stages in the life of the linker cell. Single-cell RNA-seq experiments have shown that this is indeed the case (Kato and Sternberg, 2009). In this model, NHR-67 would activate transcription of cell death genes while also inhibiting *let-70* to prevent early expression. Thus, loss of *nhr-67* and *let-70* may average out to increased survival.

EGL-20/Wnt, but not LIN-44/Wnt, acts upstream of LET-70 and UBQ-1 to promote their expression

Recent work from Maxime Kinet demonstrates that two opposing Wnt pathways control linker cell death (Kinet et al., submitted). He found that the EGL-20/Wnt protein promotes linker cell death by inhibiting targets of a protective LIN-44/Wnt pathway. Thus, inappropriate linker cell survival elicited by the *egl-20*(*n585*) mutation, is blocked in *lin-44*(*n1792*); *egl-20*(*n585*) double mutants (Kinet et al., submitted). We found that *lin-44*(*n1792*) mutants do not, however, suppress linker cell survival in *let-70*(RNAi) animals (Figure 2.13), similar to what Maxime saw with *sek-1*(*ag1*), *tir-1*(RNAi), and *pqn-41*(*ns294*) mutants, further supporting the notion that *let-70* functions in a common pathway with these genes in linker cell death. However, EGL-20 is required for *let-70* and *ubq-1* expression, as *egl-20(n585)* mutants prevent the expression of their GFP reporters (Figure 2.14). This indicates that LET-70 works in cooperation with the pro-death Wnt pathway, but works either in parallel to, or is inhibited by the anti-death Wnt pathway.

HSF-1 acts in the same pathway as LET-70 to promote linker cell death

Work conducted by Maxime Kinet suggests that the heat shock factor *hsf-1* is expressed in the linker cell and acts to promote linker cell death in a manner independent of its role in the heat-shock response (Kinet et al., submitted). Epistasis experiments conducted by Maxime using a gain-of-function allele of *hsf-1*(R145A) demonstrate that all of the genes that have been identified thus far to promote linker cell death appear to function, at least in part, upstream of the heat-shock factor gene *hsf-1* (Kinet et al., submitted). To examine the relationship between *let-70* and *hsf-1*, we first generated *hsf-1*(*sy441*); *let-70*(RNAi) double mutants. As shown in Figure 2.13, linker cell survival in these animals is similar to what is observed in *let-70*(RNAi) mutants alone. While neither *hsf-1*(*sy441*) nor *let-70*(RNAi) result in complete gene knockdown, the absence of strong genetic interactions suggest the genes may function in the same pathway. We sought to find out whether *hsf-1* operates upstream or downstream of *let-70*. *hsf-1*(R145A) mutants fail to rescue survival caused by *let-70*(RNAi), indicating that *hsf-1* likely operates upstream of or in parallel to *let-70* (Figure 2.13). This is corroborated by the finding that *let-70*::gfp fails to be expressed in the linker cell more than half the time when crossed to *hsf-1*(*sy441*) mutants, insinuating that *let-70* expression is at least partly dependent on HSF-1 activity (Figure 2.14). Thus, *hsf-1* may work to induce the expression of *let-70* and also to promote linker cell death.

This relationship is especially interesting, as prior analysis of the yeast *ubc4* and *ubc5* promoter region sequences has identified consensus sites where heat shock elements can bind (Seufert and Jentsch, 1990). While *let-70* transcription is not heat-inducible (Zhen et al., 1993), the *let-70* and *rpn-3* promoters—in *C. elegans* and other related nematode species—both appear to possess a highly conserved HSF consensus binding site (TTCTAGAA) about 350 bp upstream

of their ATGs (Figure 2.15). Thus, the same molecular biology mechanisms underlying UBC activation in yeast may be conserved in *C. elegans* and other nematodes (GuhaThakurta et al., 2002). Though *ubq-1* does not have a TTCTAGAA site, it does possess a highly conserved TCTAGAA site (missing the first T) around 800 bp upstream of start (Figure 2.15). This is not altogether unsurprising; non-proteolytic ubiquitination is carried out by a different set of E2s and E3s, and so ubiquitin must be transcribed in locations where *let-70* is not. These discrepancies may account for why certain linker cell death genes are required for *let-70* expression but not for ubiquitin expression (Figure 2.14).

DISCUSSION

The experiments described here provide more detail regarding linker cell death pathway mechanism. Our results are consistent with a model in which the SEK 1/MAPKK and TIR-1/TIR-domain adapter proteins, together with a histone methyltransferase complex similar to MLL3/4 and the pro-death Wnt EGL-20, act upstream of the *hsf*-1 transcription factor. HSF-1, with the help of other genes, then binds upstream of *let-70*, and at least some other UPS genes, to upregulate their expression in the linker cell. The LET-70 protein, functioning downstream of or in parallel to Wnt signals that inhibit linker cell death, then functions with downstream E3s and the proteasome to regulate ubiquitylation of (a) substrate/s.

Most, if not all, of the previously described members of the linker cell death pathway appear to act in a concerted effort to upregulate gene expression; this is supported by the observation that LET-70 and UPS expression is tightly regulated on both the temporal and spatial level. The wide number of transcription factors necessary for linker cell death may indicate that the confluence of multiple inputs could provide the “on-off” switch required to carry out linker

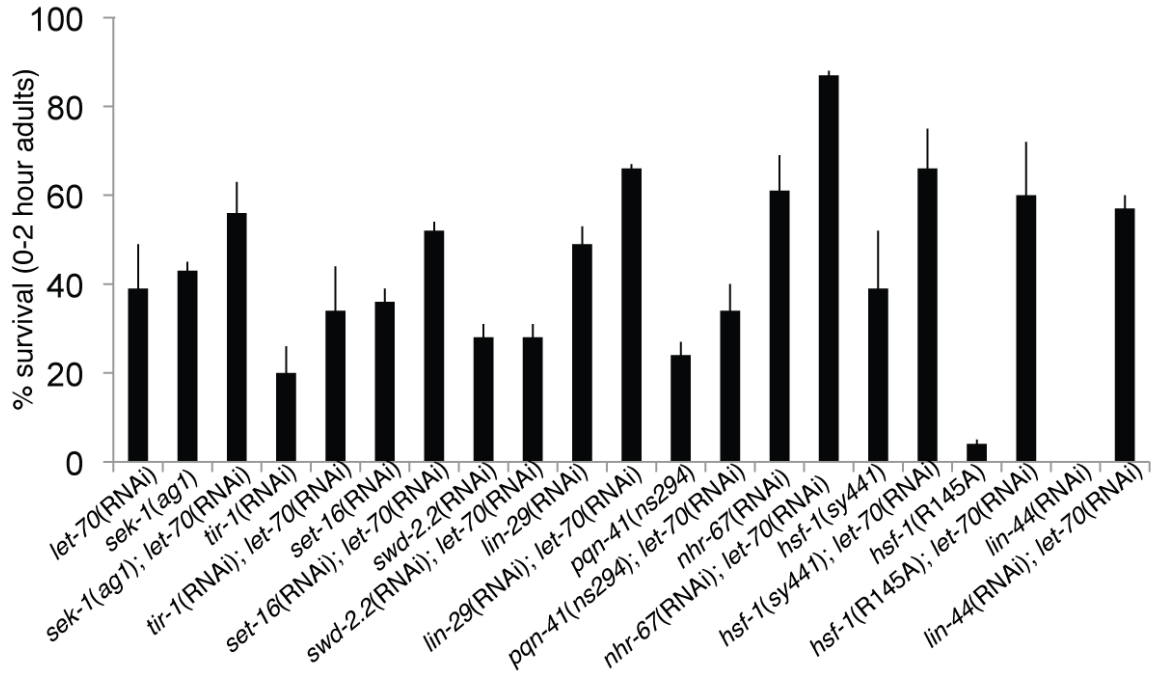

Figure 2.13. *let-70* interacts with a number of components of the linker cell death pathway. Epistasis experiments with components of the linker cell death pathway show that *let-70* works with *sek-1*/*tir-1*, *hsf-1* and *pqn-41* to promote cell death. Error bars = standard error of the mean.

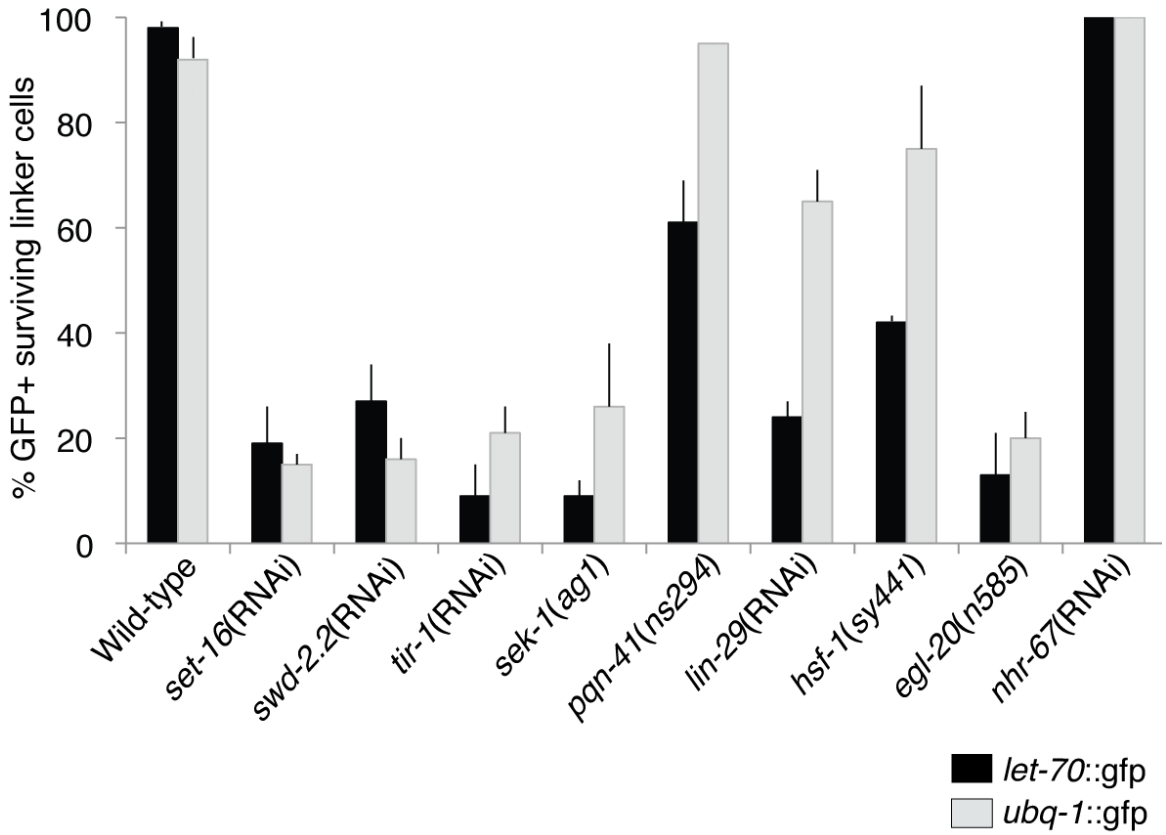

Figure 2.14. *let-70* and *ubq-1* expression is dependent on previously-described components of the linker cell death pathway.

*let-70*p::*let-70*::gfp and *ubq-1*p::*ubq-1*::gfp expression is dependent on *set-16*, *swd-2.2*, *sek-1,* and *tir-1*, but not on *pqn-41* or *nhr-67.* Expression is weakly dependent on *lin-29* and *hsf-1.* Error bars= standard error of the mean.

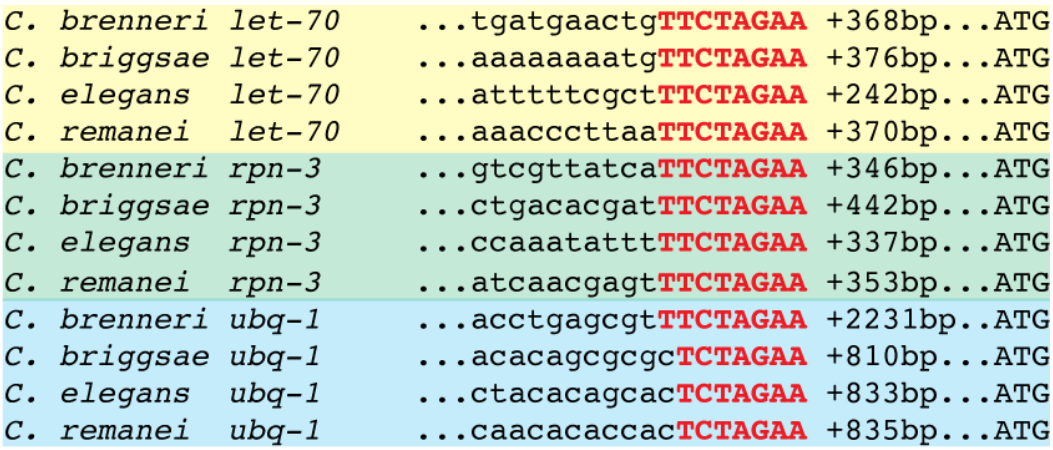

Figure 2.15. The heat shock element consensus binding site TTCTAGAA is located in the promoter region of *let-70* and *rpn-3*, and its location is conserved across related nematode species. Partial DNA alignment of the *let-70* (yellow) and *rpn-3* (green) promoters in *C. elegans* and three related nematode species shows the existence of a TTCTAGAA site (shown in red) about 350bp upstream of start (ATG). TCTAGAA sites are present in *ubq-1* (blue) promoters in *C. elegans* and related species located about 800bp upstream of start.

cell execution to completion, and the existence of TTCTAGAA motifs upstream of UPS transcriptional start sites suggests that conserved mechanisms of transcriptional activation may allow for synchronous upregulation of death components.

Temporal and spatial control of UPS induction is integral to other cellular remodeling programs such as erythropoesis. Cultured erythroblasts treated with the erythroid differentiation factor Epo show transcriptional upregulation of two E2 enzymes during red blood cell differentiation (Wefes et al., 1995). These E2s may act through the proteasome, as MG132 and lactacystin treatment of erytrhroblasts allows only half of the cells to properly differentiate (Chen et al., 2002). Spatial proteasome activity regulation is also important for proper sperm individualization; duplication events involving proteasome genes during fly evolution created testis-specific proteasome and E3 subunits which, when expressed as GFP-tagged proteins, co-localize with components of the sperm individualization complex (Arama et al., 2007; Belote and Zhong, 2009). Our data speaks to this same idea: substantial upregulation of protein degradation can be important for cell fate decisions.

Though we know that ubiquitination is required for death, we are still unsure of the mechanism by which ubiquitination executes linker cell death. It is not clear yet whether these components conduct nonspecific degradation of components that are essential to life, whether they degrade proteins that are specific to the execution of death as a specific cell fate, or whether they ubiquitinate transcription factors in order to alter the balance of certain genes required for cell death. While more experiments are needed to answer these questions, this is not altogether unsurprising; more than 25 years after the discovery of caspases, we still have a limited understanding of how caspase-directed proteolysis induces apoptotic death.

If widespread proteolytic breakdown is required for death, one can draw many parallels to the degradation induced by caspases during apoptosis. One interesting question is why caspases are not utilized for the execution of death in the linker cell. One potential idea is that the linker cell is too large, and so requires the presence of more enzymes in order to initiate cellular breakdown. Even if this is the case, however, it does not quite account for the differences underlying apoptotic and linker cell death morphologies, and that remains an intriguing mystery.

One way to answer the question of how ubiquitination regulates cell death is through careful analysis of LET-70's interactions with E3 ligases. Other research indicates that LET-70 and its homolog UBE2D2 are promiscuous E2s that interact with a number of E3s to regulate protein homeostasis (Brzovic and Klevit, 2006). We still do not know the exact repertoire of E3s required for death (see Chapters 2-3) nor do we know what substrates these E3s ubiquitinate. This remains an exciting new area for discovery.

The presence of UPS components within the roster of cell death genes is especially interesting when one notes the morphological similarities between linker cell death and neurodegenerative disease, as both display nuclear crenellation and organelle swelling (Borsello et al., 2002; Davies et al., 1997; DiFiglia et al., 1997; Pilar and Landmesser, 1976). As mentioned in the introduction, members of the UPS are also implicated in the mechanism underlying neurodegenerative disease; the E3 Parkin is mutated in familial recessive Parkinson's disease, and antibody staining shows that proteins such tau and α-synuclein are ubiquitinated in models of Alzheimer's and Parkinson's diseases. It would be interesting to see if the genetics underlying linker cell death is conserved in these processes as well.

CHAPTER 3: The seven-in-absentia homolog SIAH-1, the RING finger protein RBX-1 and the cullin CUL-3 are E3 Cullin-RING Ligase (CRL) components required for linker cell death

SUMMARY

Upon identification of *let-70* as an E2 ubiquitin-conjugating enzyme required for linker cell death, we initiated a search for E3 ligases whose inhibition also causes inappropriate linker cell survival. As mentioned in the introduction, E3 ligases provide substrate specificity to the ubiquitination reaction by binding both substrates and E2s. Thus, the discovery of an E3 ubiquitin ligase whose inhibition causes inappropriate linker cell survival might help us to isolate substrates whose degradation is required for linker cell death. Following a small RNAi screen targeting mRNA of 68 E3 ligases and other ubiquitination-related enzymes, we found that knockdown of the RING finger gene *rbx-1* and the seven-in-absentia homolog *siah-1* causes small but significant increases in inappropriate linker cell survival. As RBX-1 is a known component of cullin-RING ligase (CRL) complexes such as the Skp-Cullin-F box (SCF) complex, we also screened additional CRL components required for linker cell death, identifying the cullin CUL-3 as an important regulator of linker cell death. We show that SIAH-1 and RBX-1 act redundantly, and function together with CUL-3 in the same genetic pathway as *let-70* to promote linker cell death. The cullin CUL-3 is also necessary for linker cell death and acts cell autonomously. Unlike *let-70* or components of the proteasome, the *siah-1*, *rbx-1* and *cul-3* genes are constitutively expressed in the linker cell throughout its life and death.

RESULTS

The RING finger protein RBX-1 is required for linker cell death

As most E2 ubiquitin-conjugating enzymes require the action of E3 ligases to carry out ubiquitination, we wondered if any E3 ligases were required for linker cell death. With the help of summer student Melanie Silverman, we used RNAi to separately knock down 68 genes encoding proteins that contain domains associated with E3 enzymes (Table 3.1). While most of the genes examined have no effect when depleted, we found that RNAi against the RING finger gene *rbx-1* does promote modest linker cell survival (Table 3.2), suggesting that RBX-1 may play a role in linker cell death. 24 hours after linker cell death should have occurred, 6% of *rbx-1*(RNAi) animals still have surviving linker cells, indicating that the absence of RBX-1 likely blocks rather than delays death (Table 3.2).

RBX-1 is homologous to the mammalian protein RBX1/ROC1. It is a small, 110-amino acid protein consisting only of a RING finger domain. Yeast two-hybrid studies and coimmunoprecipitation experiments suggest that RBX1 and its homologs interact with multiprotein ubiquitination complexes such as the SCF and von Hippel-Lindau (VPL) tumor suppressor complexes (Kamura et al., 1999; Ohta et al., 1999). No viable alleles of *rbx-1* are currently available for analysis, likely because RBX-1 is required for proper chromosome condensation and migration in *C. elegans* (Sasagawa et al., 2003).

As RBX-1 appears to be required for linker cell death, we wondered if it was expressed in the linker cell. *rbx-1* promoter fusions to GFP using the first 1000 bp upstream of start express GFP in many tissues, including in the linker cell (Figures 3.1, 3.2). Thus, *rbx-1* is capable of acting in the linker cell to promote death. Unlike *let-70*p::gfp, which is induced within the linker cell at the time of death, the *rbx-1*p::gfp reporter is constitutively expressed in

the linker cell throughout all stages of the cell's development (Figure 3.2). Thus, it appears as though not all components of the ubiquitination pathway are induced at the time of death (Figures 3.1, 3.2).

In order to obtain information about RBX-1 protein localization within the linker cell, we acquired a recombineered fosmid containing the *rbx-1* gene, as well as 14kb upstream of and 13.8kb downstream of the gene, fused to GFP (Figure 3.1). Animals injected with this construct either express GFP at undetectable levels, or not at all, which prevents us from obtaining more information about its localization.

Seven-in-absentia homolog/*siah-1* mutations block linker cell death

A second gene that came out of our screen is the seven-in-absentia homolog *siah-1*. SIAH-1 is an E3 ligase with homology to mammalian Siah1 and *Drosophila* sina (Carthew and Rubin, 1990). Like many E3 ligases, it possesses a RING finger domain, which is canonically used for E2 binding (Figure 3.3)(Lorick et al., 1999). It also contains a TRAF-like domain also found in other Siah homologs, which is predicted to be used for substrate binding (House et al., 2003; 2006)(Figure 3.3).

We found that RNAi against *siah-1* causes a modest but significant linker cell death defect (Table 3.2). To confirm that *siah-1* is important for the death of the linker cell, we examined animals defective for the *siah-1*(*tm1968*) mutation, which deletes most of exon 4 of the gene and is likely a molecular null (De Arras et al., 2013; Kamura et al., 1999; Ohta et al., 1999) (Figure 3.3), and found a similar level of linker cell survival compared to *siah-1*(RNAi) animals (Table 3.2). RNAi against *siah-1* in a *siah-1*(*tm1968*) homozygous mutant background also produces the same rate of linker cell survival as *siah-1*(*tm1968*) animals alone, reinforcing

Table 3.1. Other E3 ligases and ubiquitination enzymes are not required for linker cell death

Genotype (RNAi)[a]	% Surviving LCs[b]
HECT E3s	
hecd-1	7 ± 2
D2085.4	6 ± 2
F36A2.13	2 ± 2
oxi-1	4 ± 2
wwp-1	2 ± 1
C02F5.7	6 ± 2
U-box E3s/E4s	
cyp-4/mog-6	7 ± 3
ufd-2	2 ± 1
chn-1	3 ± 2
T10F2.4	3 ± 2
Monomeric RINGs	
B0281.3	5 ± 2
B0281.8	0 ± 0
B0393.6	7 ± 3
B0416.4	3 ± 1
C01B7.6, rpm-1, rpm-3, sam-1, sad-3, syd-3	4 ± 2
C01G6.4	8 ± 2
C06A5.8	3 ± 2
rnf-1/tag-154	3 ± 1
C11H1.3	4 ± 2
lin-41	2 ± 1
C16C10.5	2 ± 1
rnf-5	7 ± 2
C17E4.3	3 ± 2
C17H11.6	0 ± 0

C18B12.4	5 ± 3
rpy-1/rap-1	3 ± 2
C26B9.6	1 ± 1
C30F2.2	2 ± 1
C32D5.10	6 ± 2
C32D5.11	3 ± 2
C32E8.1	3 ± 2
wrs-2	1 ± 1
C34F11.1	3 ± 2
brc-1	9 ± 3
C45G7.4	4 ± 2
ntl-4	0 ± 0
D2089.2	6 ± 4
prx-12	5 ± 2
F08G12.5	4 ± 4
F10D7.5	1 ± 1
F10G7.10	1 ± 1
F11A10.3	2 ± 2
F16A11.1	0 ± 0
apc-11	6 ± 3
F36F2.3	7 ± 2
F43G6.8	8 ± 3
F54B11.5	9 ± 3
nhl-1	5 ± 2
sli-1	6 ± 2
rfp-1	14 ± 3
T02C1.1	3 ± 2
sel-11	2 ± 1
apc-2 (APC E3)	5 ± 3

Other	
goa-1 (Ga protein)	2 ± 1
asp-4 (aspartyl protease)	1 ± 1
epn-1 (epsin homolog)	5 ± 4
pbs-5 (proteasome subunit b5)	2 ± 1
psa-4 (swi2/snf2 homolog)	5 ± 2
bir-1 (IAP/BIR domain)	5 ± 2
atg-7 (apg7p homolog-upstream of *let-70)*	6 ± 2
otub-1 (deubiquitylase)	6 ± 2
egl-27 (HDAC- NURD complex)	2 ± 1
lin-40 (HDAC- NURD complex)	5 ± 2
pdr-1(*gk448*) (Parkin)	5 ± 2
pdr-1 RNAi	2 ± 1

[a]All animals contained *rrf-3*(*pk1426*); *him-8*(*e1489*) mutations and a *lag-2*p::gfp (*qIs56*) reporter gene to identify the linker cell. Error, SEM.

[b]LC, linker cell. n>24

Table 3.2: *rbx-1* and *siah-1* are required redundantly for linker cell death and may act with *let-70*

Genotype (RNAi sensitized)[a]	**% Surviving Linker Cells, 0-2 hr adults**[b]	**% Migration Defect**
No RNAi	3 ± <1	5 ± 2
let-70 RNAi	45 ± 2	58 ± 6
rbx-1 RNAi	13 ± 4	2 ± 1
rbx-1 RNAi- 24 hour adults	6 ± 3	0 ± 0
let-70 RNAi, *rbx-1* RNAi	47 ± 8	33 ± 1
siah-1 RNAi	12 ± 4	1 ± 1
siah-1(*tm1968*)	14 ± 2	2 ± 1
siah-1(tm1968); siah-1 RNAi	14 ± 4	1 ± 1
siah-1(tm1968)- 24 hour adults	9 ± 4	2 ± 2
siah-1 RNAi- 24 hour adults	3 ± 2	0 ± 0
siah-1(*tm1968*)*; let-70* RNAi	35 ± 5	25 ± 2
siah-1(*tm1968*)*; rbx-1* RNAi	24 ± 8	1 ± <1
siah-1(tm1968); rbx-1 RNAi; *let-70* RNAi	41 ± 9	17 ± 3

[a]strains analyzed contained *rrf-3*(*pk1426*); *him-8*(*e1489*) mutations and a *lag-2*p::gfp (*qIs56*) reporter gene to identify the linker cell. Error, SEM.

[b]n>63

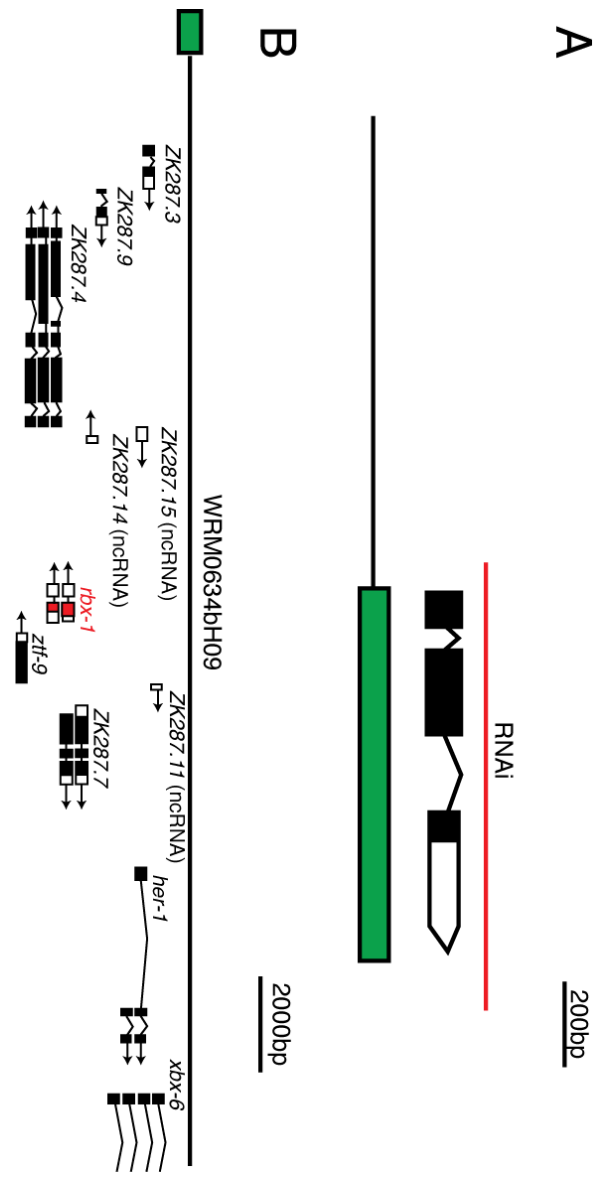

Figure 3.1. Constructs used for analysis of *rbx-1* function. For all DNA maps: Black= exons, white= 5'/3' UTR (A) Top: Location of *rbx-1* RNAi (red) in relation to a map of the *rbx-1* gene. Bottom: *rbx-1*p::gfp. Green box = GFP. Scalebar= 200bp. (B) Map of GFP-recombineered fosmid containing *rbx-1* and nearby genes. *rbx-1* gene highlighted in red. Scalebar= 2000bp.

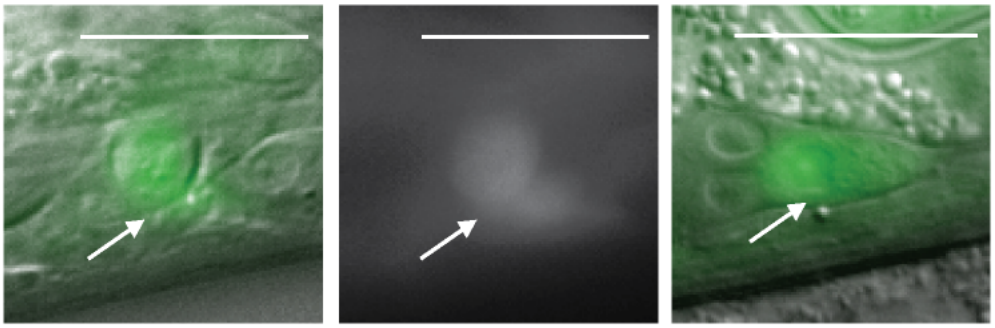

Figure 3.2. *rbx-1*p::gfp is expressed in the linker cell during migration and death.

*rbx-1*p::gfp is expressed in the linker cell while migrating and the time of death. left = merged DIC/fluorescent image of a dying linker cell at the cloaca, middle = fluorescent image of the linker cell at left, right= merged DIC/fluoresent image of a migrating linker cell. Anterior is left. Arrow= linker cell, scalebar = 10μm.

Figure 3.3. Constructs used for analysis of *siah-1* function. For all DNA maps: Black= exons, white= 5'/3' UTR, green box = GFP (A) Top: Locations of *siah-1* RNAi (red) and *siah-1*(t*m1968)* deletion allele (blue) in relation to a map of the *siah-1* gene. Middle: Map of *mig-24*p::gfp::*siah-1*. Bottom: *siah-1*p::gfp. Scalebar= 500bp. (B) Map of GFP-recombineered fosmid containing *siah-1* and nearby genes. *siah-1* gene highlighted in red. (C) Protein map of SIAH-1 region. Δ= location of amino acid sequence affected by deletion encoded by *tm1968* allele. Domains annotated below diagram. Scalebar = 50aa.

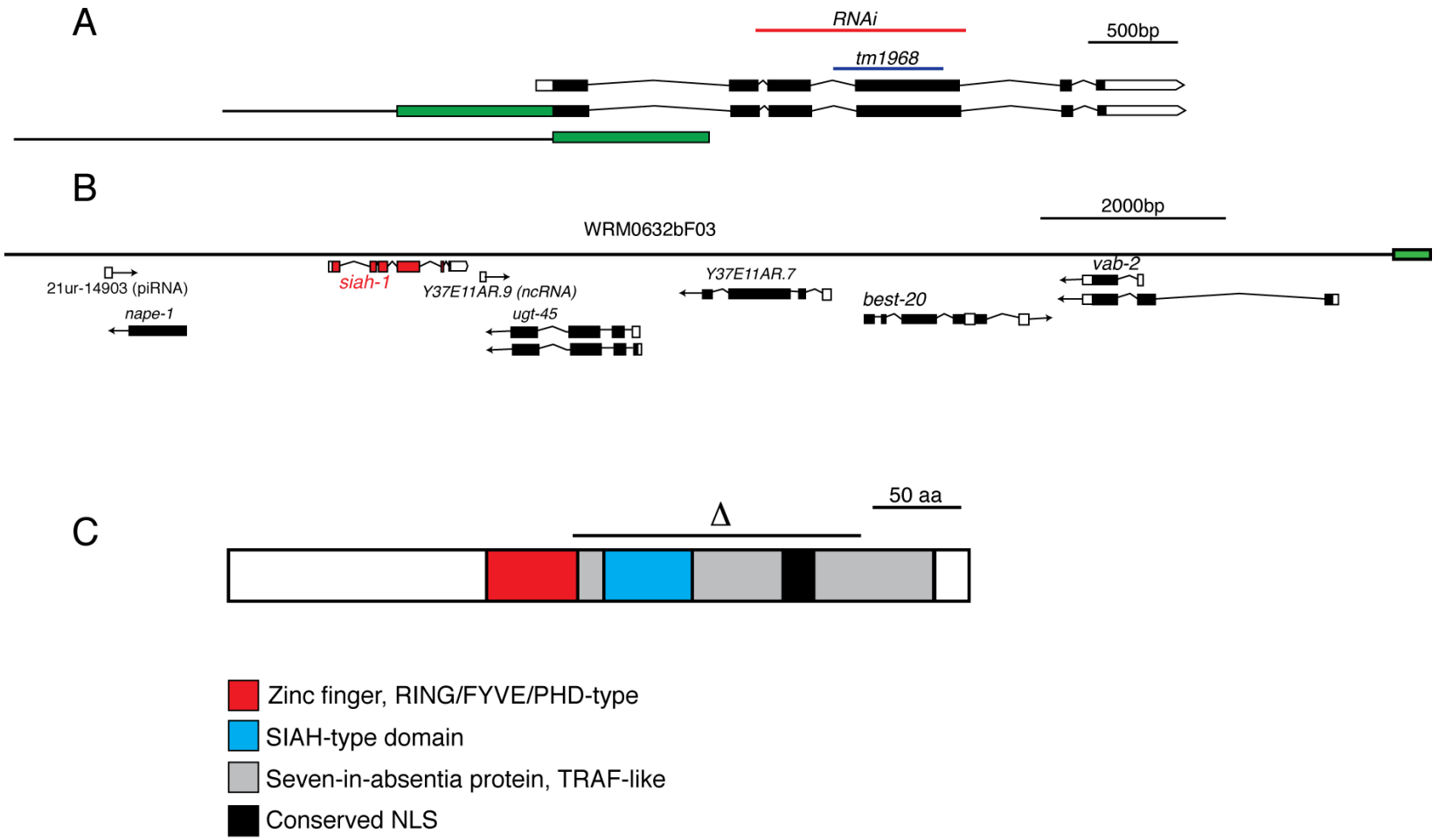
A
RNAi
500bp
tm1968
B
2000bp
WRM0632bF03
21ur-14903 (piRNA)
nape-1
siah-1
Y37E11AR.9 (ncRNA)
ugt-45
Y37E11AR.7
best-20
vab-2
C
50 aa
Δ
Zinc finger, RING/FYVE/PHD-type
SIAH-type domain
Seven-in-absentia protein, TRAF-like
Conserved NLS

the idea that *siah-1*(*tm1968*) is likely a null allele (Table 3.2). Both *siah-1*(*tm1968*) and *siah-1*(RNAi) animals exhibit a small percentage of surviving linker cells 24 hours after linker cell death should have occurred, indicating that the absence of *siah-1* likely blocks rather than delays death (Table 3.2).

SIAH-1 is expressed in the linker cell at all stages of its development

As *siah-1* mutants show cell death defects, we wondered whether *siah-1* was expressed in the linker cell. As with *rbx-1*p::gfp, animals injected with plasmids containing 3kb of upstream *siah-1* regulatory DNA fused to GFP (*siah-1*p::gfp) express GFP in many tissues including in the linker cell (Figures 3.3, 3.4). GFP expression levels within the linker cell are consistent, and do not change during migration or death. As the SIAH-1 amino acid sequence contains a conserved NLS region (Figure 3.3C), we wondered whether SIAH-1 localizes to the nucleus. We made transgenic lines expressing a plasmid containing a linker cell-specific promoter (*mig-24*p) fused to the *siah-1* cDNA followed by the GFP DNA sequence, but no visible GFP expression was detected in these animals, indicating that C-terminal GFP tags either destabilize SIAH-1 protein or reflect endogenous low levels of SIAH-1 within the cell. A reporter containing the *mig-24* promoter fused to DNA encoding GFP inserted just upstream of the *siah-1* ATG visibly expresses GFP in both the nucleus and cytoplasm of the linker cell, and its localization is invariant throughout the life and death of the linker cell (Figures 3.3, 3.4). Interestingly, though localization does not change, GFP-SIAH-1 reporter intensity is much fainter in linker cells than in distal tip cells (the hermaphrodite gonadal leader cells), and this intensity wanes as the cell dies (Figure 3.4). Thus, it appears as though SIAH-1 is maintained at

Figure 3.4. SIAH-1-GFP is expressed in the linker cell throughout the cell's lifetime. For all animals, left is anterior. Scalebar = 10mm, Arrow= linker cell. (A) *siah-1*p::gfp is expressed in the linker cell during death (left=DIC/GFP merge, middle = GFP) and migration (right, DIC/GFP merge). (B) *mig-24*p::gfp::*siah-1* is expressed in the linker cell during death (left=DIC/GFP merge, middle = GFP) and migration (right, DIC/GFP merge). (C) *siah-1*-GFP fosmid following *let-70* RNAi is expressed in the linker cell during migration; GFP localizes to mitochondria (bracket)/cytoplasm but is excluded from nucleus (asterisk) (left= DIC/GFP merge, right = GFP). (D) *siah-1*-GFP fosmid following *let-70* RNAi is expressed throughout the late linker cell corpse during death. (left= DIC + fluorescence, right = fluorescence).

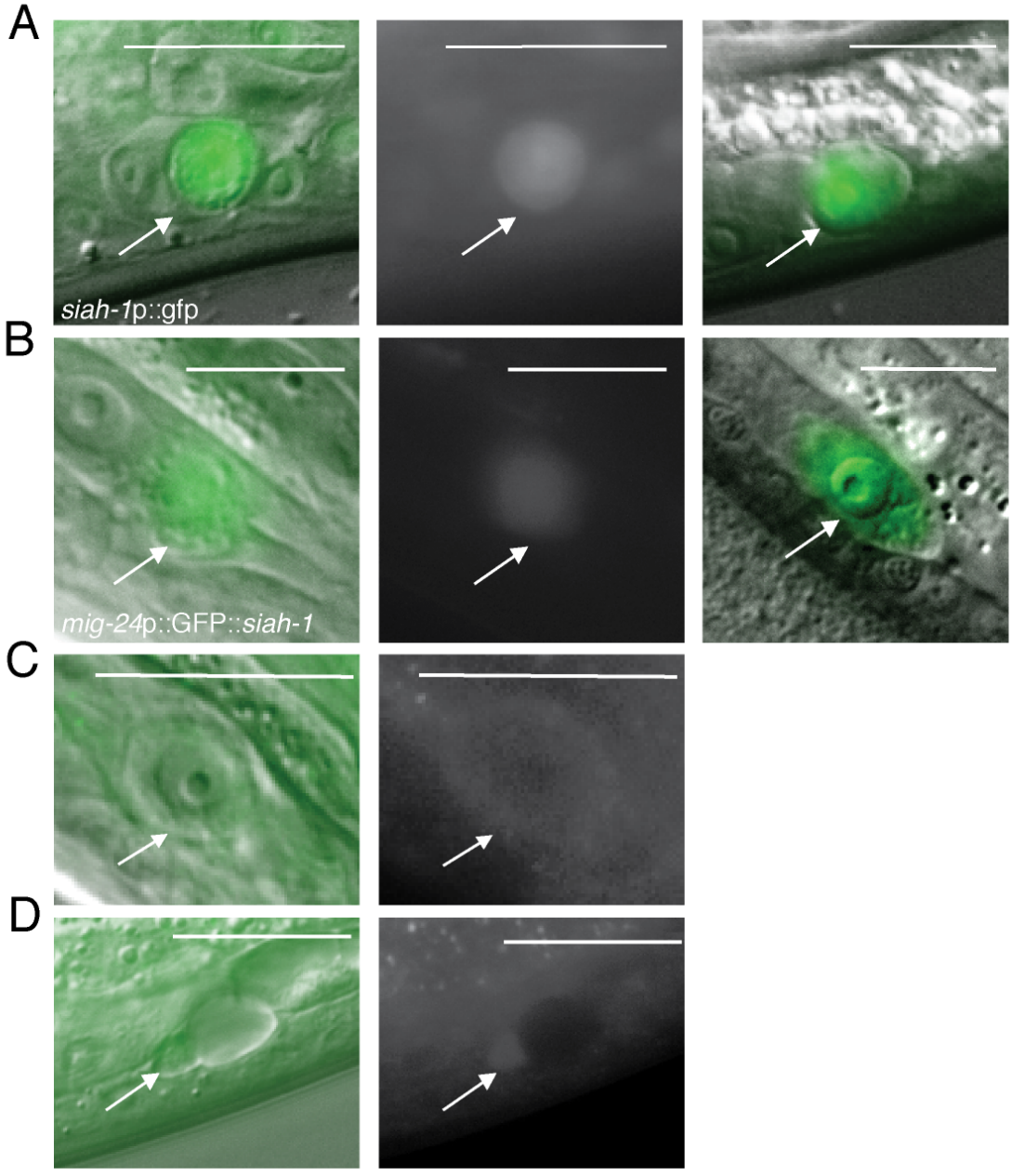
A
siah-1p::gfp
B
mig-24p::GFP::siah-1
C
D

a low level within the linker cell, and its protein concentration appears to decrease during linker cell death. We believe that this decrease may be physiologically relevant because expression of *mig-24*p::gfp reporters on their own show no change in GFP expression during death. It is still unclear whether SIAH-1 is degraded following the death of the cell, or whether degradation of SIAH is part of the mechanism required for linker cell death. Either way, this observation is surprising, as reduction of *siah-1* levels through RNAi or null mutations leads to cell survival.

SIAH-1 and RBX-1 are required redundantly for linker cell death, and act with LET-70 to promote death

As both *siah-1* and *rbx-1* mutants display inappropriate linker cell survival, we wondered whether they act in the same pathway as LET-70 to promote death. *let-70* RNAi performed in a *siah-1*(*tm1968*) mutant background causes no increase in linker cell survival above that observed in *let-70*(RNAi) animals (Table 3.2), indicating that SIAH-1 and LET-70 act in the same pathway to promote death. Combined RNAi against both *let-70* and *rbx-1* also shows no additional increase in linker cell death compared to *let-70* RNAi alone (Table 3.2). Though one could imagine a scenario where incomplete knockdown of either *let-70* or *rbx-1* causes the linker cell defect observed, the data seems to show that *let-70* and *rbx-1* also appear to act in the same pathway. In order to determine how SIAH-1 and RBX-1 interact to promote death, we performed *rbx-1* RNAi in *siah-1*(*tm1968*) mutants. Interestingly, *rbx-1*(RNAi); *siah-1*(*tm1968*) animals show a synergistic increase in linker cell survival compared to either mutant alone, indicating that SIAH-1 and RBX-1 act redundantly to promote linker cell death (Table 3.2). Furthermore, RNAi against *let-70* and *rbx-1* in *siah-1*(*tm1968*) mutants causes no further increase in linker cell death compared to *let-70* RNAi alone, corroborating the idea that SIAH-1

and RBX-1 both act with LET-70 to promote linker cell death. Therefore, LET-70 may utilize a number of E3s to ubiquitinate substrates and carry out linker cell death.

While it appears that SIAH-1 and RBX-1 act in parallel to promote linker cell death, the nature of their interaction is unknown. Do SIAH-1 and RBX-1 act in parallel as E3 monomers, as redundant subunits within the same complex or as parts of two independent complexes to promote death? Does their substrate repertoire overlap? More experiments are needed in order to understand how exactly SIAH-1 and RBX-1 function within the linker cell death pathway.

As LET-70 and RBX-1 appear to act within the same pathway, we wondered whether they are binding partners. RBX-1 and LET-70 do not appear to physically interact in a yeast two-hybrid assay (Table 3.3), nor does HA-RBX-1 or RBX-1-HA co-immunoprecipitate with MYC-LET-70 in S2 cells (Figure 3.5). Though RBX-1 and LET-70 do not appear to bind each other, we wondered whether they were able to work together to catalyze ubiquitination of a substrate. As no substrates ubiquitinated for linker cell death are known, we wondered whether RBX-1 is capable of ubiquitinating itself, as a number of E3s such as Diap1 and Siah1 are known to autoubiquitinate in vitro in other systems (Mei et al., 2007; Ryoo et al., 2002). While LET-70 is unable to induce autoubiquitination of monomeric RBX-1 (Figure 3.6), LET-70 is able to induce ubiquitination of a human Cul1 complex containing human Rbx1 (see Appendix). As RING finger proteins are implicated in mediating E2-E3 interactions within multiprotein E3 complexes, this indicates that LET-70 is capable of physically interacting with RBX-1 when it is part of a multimeric complex, and that this interaction is conserved in higher species.

As yeast two-hybrid experiments in flies and humans indicate that Siah-1 physically interacts with LET-70 homologs (Liani et al., 2004; Neufeld et al., 1998; Sasagawa et al., 2003;

Tang et al., 1997), we also wondered whether SIAH-1 and LET-70 physically interact. Yeast two-hybrid experiments fail to show any binding between LET-70 and SIAH-1, including between LET-70 and truncated SIAH domains (Table 3.3). No physical association is observed between any two linker cell death proteins tested in this assay, either (Table 3.3).

Heterologously expressed SIAH-1 and LET-70 in S2 cells do not co-immunoprecipitate (Figure 3.7). Finally, unlike mammalian Siah-1, which is able to autoubiquitinate in biochemical assays, in vitro ubiquitination experiments using bacterially purified proteins also fail to induce SIAH-1 autoubiquitination by LET-70 (Mei et al., 2007) (Figure 3.8). Thus, either the interaction between LET-70 and SIAH-1 is weak, the interaction requires members of a multi-protein complex, or most simply, the proteins do not interact.

While the lack of physical association between LET-70 and SIAH-1 is confusing, it is not altogether unexpected. E2s and E3s may be able to work with each other in a catalytic setting, but that relationship may not be strong enough to be visible in an immunoprecipitation or yeast two-hybrid assay. Furthermore, as in vitro ubiquitination assays occur in a test tube, we may be missing important co-factors required for catalytic ubiquitination of SIAH-1. Finally, despite data that mammalian Siah autoubiquitinates, perhaps SIAH-1 may not ubiquitinate itself in *C. elegans* (Carthew and Rubin, 1990; Dimitrova et al., 2010). Thus, more experiments are needed to determine whether LET-70 and SIAH-1 truly physically interact.

Anomalous interactions between SIAH-1 and LET-70 are observed

In order to better understand how LET-70 and SIAH-1 work together to promote death, we looked at how the expression of a GFP-recombineered fosmid containing 7.3kb upstream of and 20.8kb downstream of the *siah-1* genomic locus (Figure 3.3B) changes following *let-70*

Table 3.3. None of the components of the linker cell death pathway physically interact via yeast two-hybrid assay[a]

pGAD plasmids \ LexA plasmids	p53	pLexA	LET-70	LET UBC[b] domain	SIAH-1	SIAH RING[c]	SIAH SIAH[c]	SIAH TRAF[c]	RBX-1	PQN-41 C	TIR-1
T	+	-	NT[a]	NT	NT	NT	NT	NT	NT	NT	NT
pGAD	-	-	-	-	-	-	-	-	-	-	-
LET-70	NT	-	-	-	-	-	-	-	-	-	-
LET-70 UBC domain	NT	-	-	-	-	-	-	-	-	-	-
SIAH-1	NT	-	-	-	-	-	-	-	-	-	-
SIAH-1 RING domain	NT	-	-	-	-	-	-	-	-	-	-
SIAH-1 SIAH domain	NT	-	-	-	-	-	-	-	-	-	-
SIAH-1 TRAF domain	NT	-	-	-	-	-	-	-	-	-	-
RBX-1	NT	-	-	-	-	-	-	-	-	-	-
TIR-1	NT	-	-	-	-	-	-	-	-	-	-

[a]Interaction is defined as the ability of co-transformed yeast to grow on SD plates lacking adenine, leucine, histidine and tryptophan. NT= not tested

[b]UBC domain = amino acids 1-114 of LET-70 (out of 147 total)

[c]See figure 3.1 for maps of RING/SIAH/TRAF domains within SIAH-1

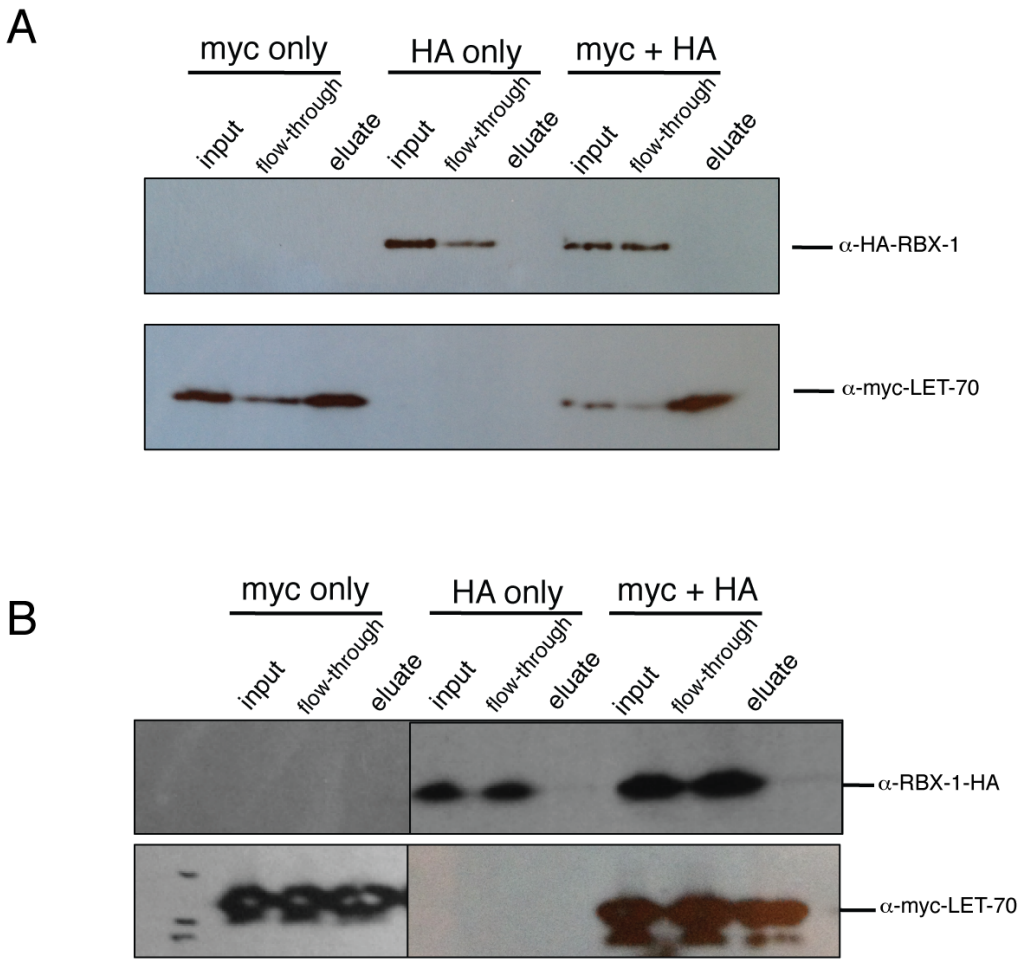

Figure 3.5. RBX-1 and LET-70 fail to co-immunoprecipitate when expressed in *Drosophila* S2 cells. *Drosophila* S2 cells were transfected with myc-LET-70 and an N/C-terminally HA-tagged RBX-1. Lysates were immunoprecipitated with anti-myc-conjugated agarose beads. Western blots stained against HA and myc to analyze protein-protein interaction. (A) HA-RBX-1 fails to interact with myc-LET-70 in S2 cells. (B) RBX-1-HA fails to immunoprecipitate with LET-70 in S2 cells.

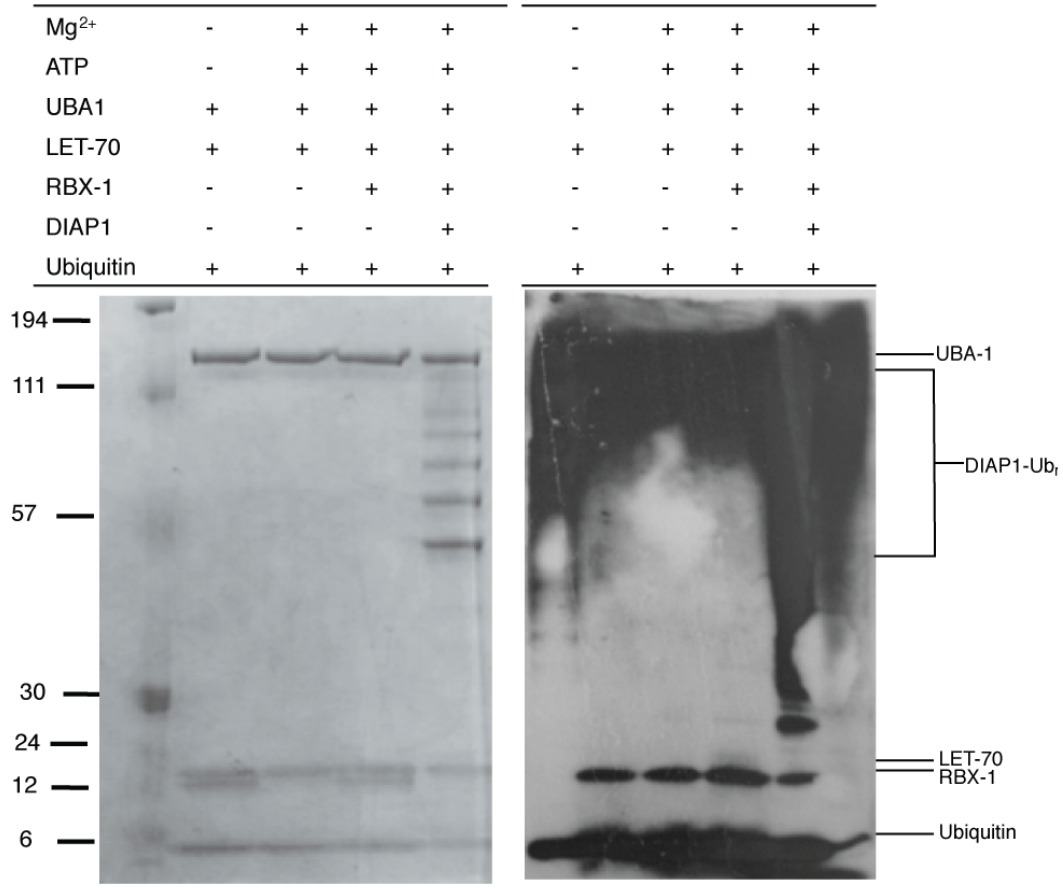

Figure 3.6. LET-70 fails to ubiquitinate monomeric RBX-1 in an in vitro ubiquitination assay. Bacterially purified 6x-His-HA-RBX-1 fails to autoubiquitinate itself when 6x-His-LET-70, HA-ubiquitin, UBA1, magnesium and ATP are added. Left: Coomassie staining of an SDS-PAGE gel. Right: Anti-HA western blot shows no HA-ubiquitin shift of HA-RBX-1.

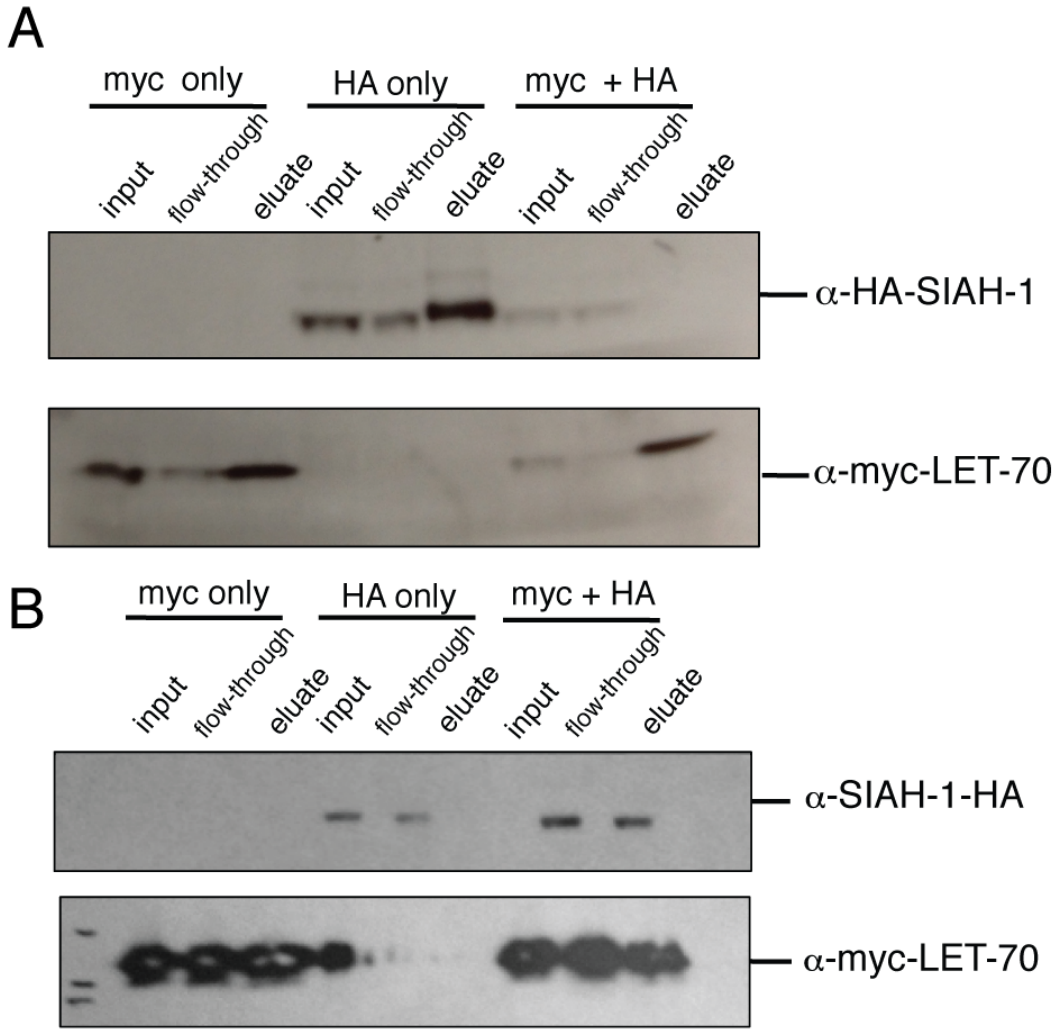

Figure 3.7. SIAH-1 and LET-70 fail to co-immunoprecipitate when expressed in *Drosophila* S2 cells. *Drosophila* S2 cells were transfected with myc-LET-70 and an N/C-terminally HA-tagged SIAH-1. Western blots stained against HA and myc to analyze protein-protein interaction. (A) HA-SIAH-1 fails to interact with myc-LET-70 in S2 cells. (B) SIAH-1-HA fails to immunoprecipitate with LET-70 in S2 cells. In both cases, myc-LET-70 was immunoprecipitated using anti-myc-conjugated agarose beads.

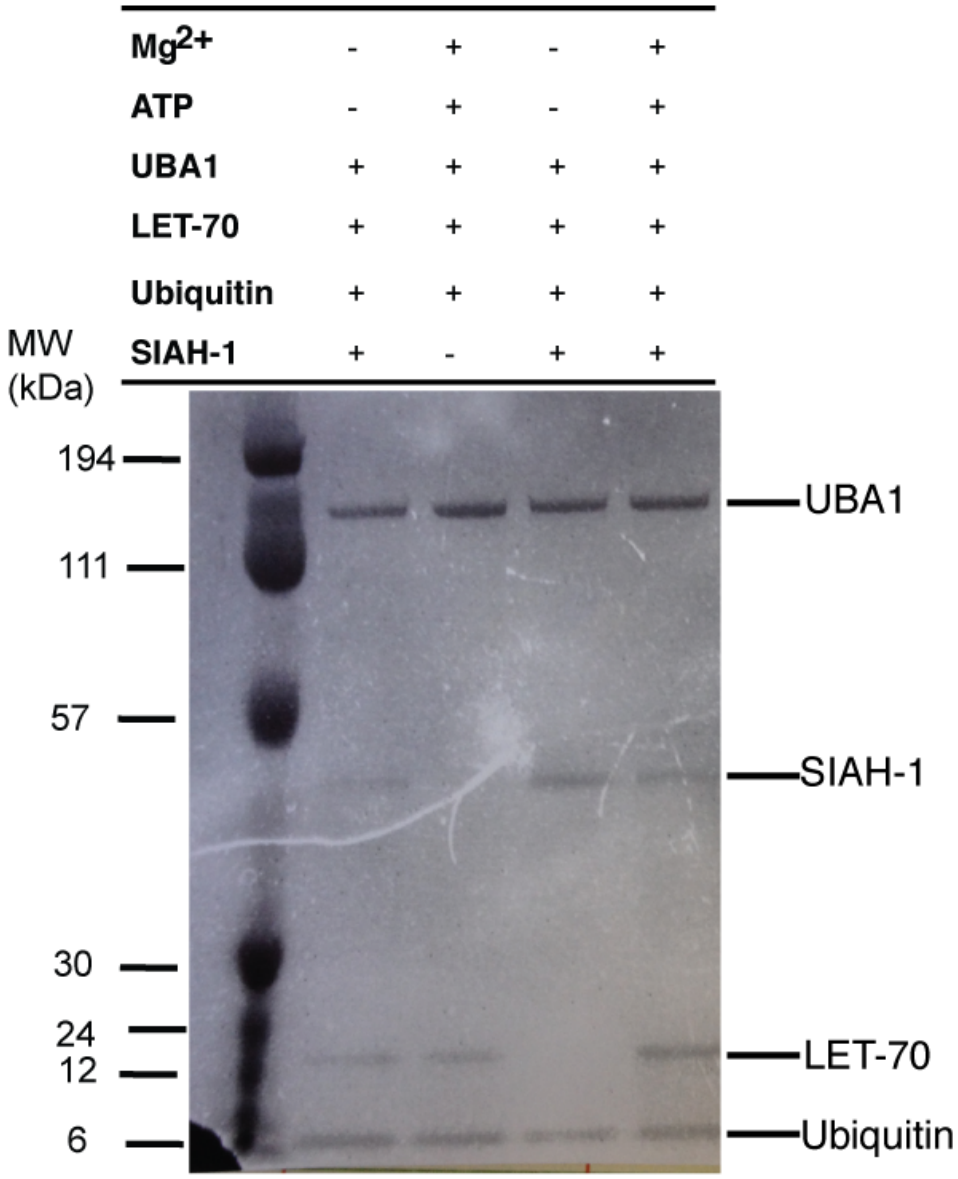

Figure 3.8. LET-70 fails to effect SIAH-1 autoubiquitination in an in vitro ubiquitination assay. Bacterially purified 6x-His-FLAG-SIAH-1 fails to autoubiquitinate itself when 6x-His-LET-70, ubiquitin, UBA1, magnesium and ATP are added. Coomassie staining of an SDS-PAGE gel.

RNAi. In wild-type animals, *siah-1*-gfp fosmid reporter expression levels are so low that they are undetectable on a compound fluorescent microscope. This GFP expression does not appreciably increase following RNAi against the proteasome subunit *rpn-3*, indicating that degradation alone may not be responsible for low GFP expression levels.

However, RNAi against *let-70* causes a visible increase in SIAH-1-GFP fosmid reporter expression, indicating that LET-70 may post-translationally regulate SIAH-1 protein levels. Interestingly, unlike other SIAH-1 reporters, fosmid-expressed SIAH-1-GFP in *let-70*(RNAi) animals is excluded from the nucleus and is diffusely localized within the cytoplasm; this exclusion persists until the cell contents have degraded (Figure 3.4). Therefore, one can conclude that either LET-70 itself impacts the subcellular localization of SIAH-1-GFP, or that SIAH-1 normally localizes solely within the cytoplasm, but that overexpression of GFP-SIAH-1 using the *mig-24* promoter forces SIAH-1 into the nucleus. One can test this hypothesis by overexpressing LET-70 in the linker cell and seeing if it changes subcellular localization of a SIAH-1-GFP reporter.

The idea that LET-70 may help to degrade or destabilize SIAH-1 is confusing, as both proteins are necessary for death. One hypothesis as to how LET-70 and SIAH-1 interact is that LET-70 ubiquitinates SIAH-1 in a nonproteolytic manner (as *rpn-3* RNAi does not impact SIAH-1 expression levels) to enable SIAH-1 to enter the nucleus to promote death. Another hypothesis would be that SIAH-1 concentration is important for death: too much SIAH-1 causes survival, but too little causes survival as well. Thus, LET-70 would be required to titrate SIAH-1 protein levels in order to promote death.

CUL-3 is required for the death of the linker cell

Cullin-RING ligases (CRLs) are multiprotein complexes that normally function to ubiquitinate substrates. As mentioned in the introduction, the composition of the CRL is dependent on the identity of the cullin used: Cul1 complexes are composed of a Skp, a Cullin, an F-box protein, and a RING finger protein, while Cul3 complexes are composed of a Cullin, a BTB/POZ protein, and a RING finger protein (Kipreos, 2005). As RBX-1 is a known component of cullin-RING ligase complexes (see above), and as in vitro and cell culture ubiquitination assays in mammals suggest that Siah1 may ubiquitinate substrates in an SCF-like complex composed of Skp1, Tbl1/Ebi, APC and SIP (Dimitrova et al., 2010; Lorick et al., 1999; Matsuzawa and Reed, 2001), we wondered whether SIAH-1 or RBX-1 acted as CRLs to promote linker cell death. We performed RNAi knockdown of all six cullin genes in the *C. elegans* genome, and found that RNAi against the *cul-3* gene results in linker cell death defects (Table 3.4, Figure 3.5). Linker cell-specific RNAi against *cul-3* also causes inappropriate linker cell survival (26%), indicating that *cul-3* expression is required within the linker cell for death (Table 3.4). Finally, reporters consisting of 3kb of regulatory DNA upstream of *cul-3* fused to GFP (*cul-3*p::gfp*,* Figures 3.9, 3.10) are constitutively expressed in the linker cell during migration and death, reinforcing the notion that CUL-3 acts in the linker cell.

CUL-3 is composed of an N-terminal cullin domain, which has been shown to facilitate interaction with BTB domains, and a C-terminal winged helix-turn-helix domain, which is implicated in RING finger binding (Figure 3.9) (Canning et al., 2013; House et al., 2003; 2006). Thus, CUL3 proteins appear to serve as the scaffold on which the BTB-CUL-RING complex is built. CUL-3 activation occurs via addition of the protein NEDD8 to the CUL-3 C-terminus (Figure 3.9); this is supported by the observation that homozygous mutants in the

Table 3.4. CUL-3 and RBX-1 promote linker cell death

Genotype[a]	% LC survival[b]
Wild type + empty vector	1 ± <1
cul-1 RNAi	12 ± 1
cul-2 RNAi	5 ± 1
cul-3 RNAi	24 ± 4
cul-3 LC-only RNAi	26 ± 1
cul-4 RNAi	7 ± 2
cul-5 RNAi	4 ± 4
cul-6 RNAi	6 ± 5
rbx-1 RNAi	15 ± 2
siah-1(*tm1968*); *cul-3* RNAi	52 ± 1

[a]All animals contained *rrf-3*(*pk1426*); *him-8*(*e1489*) mutations and a *lag-2*p::gfp (*qIs56*) reporter gene to identify the linker cell. Error, SEM.

[b]LC, linker cell. n>100

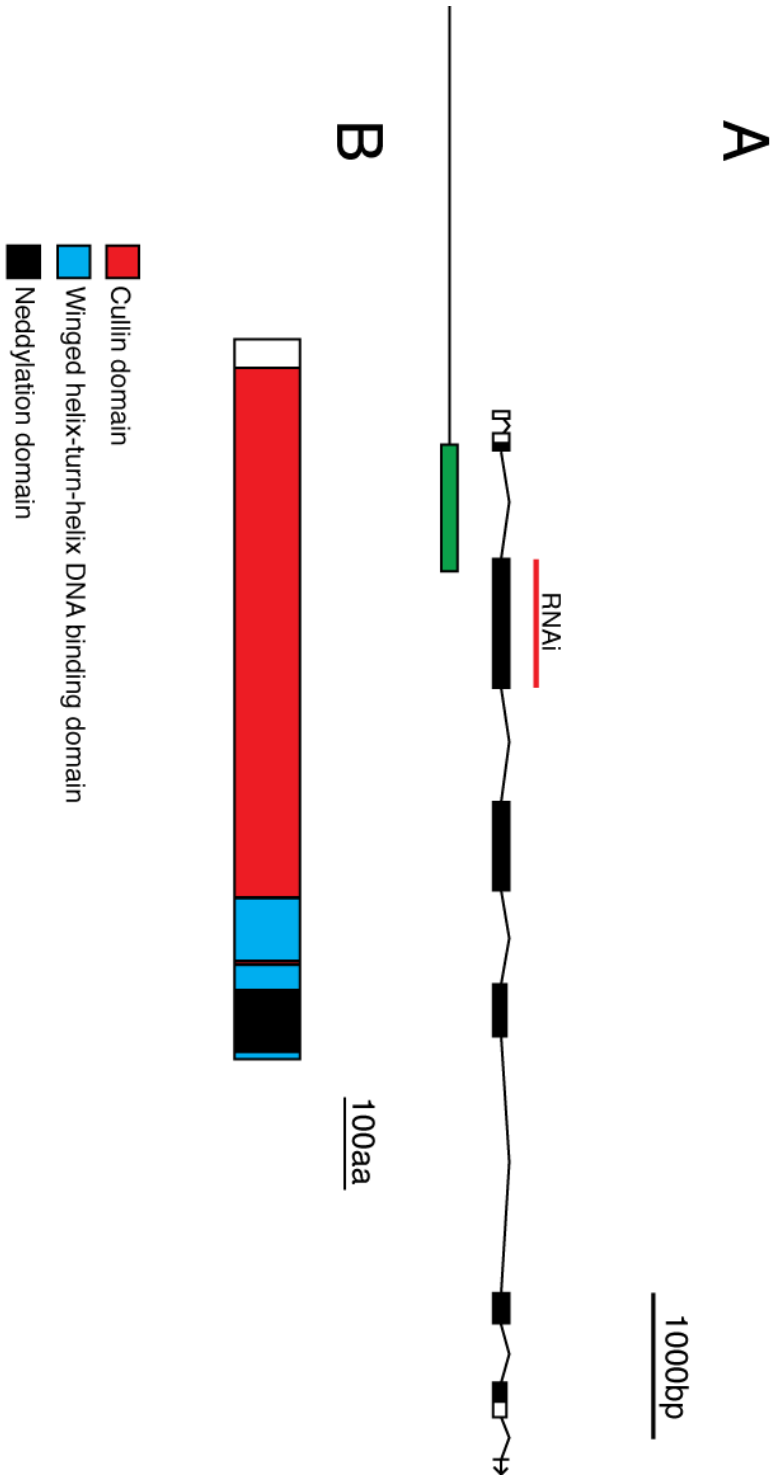

Figure 3.9. Constructs used for analysis of *cul-3* function. For all DNA maps: Black= exons, white= 5'/3' UTR (A) Top: Location of *cul-3* RNAi (red) in relation to a map of the *cul-3* gene. Bottom: *cul-3*p::gfp. Scalebar= 1000bp. (B) Protein map of CUL-3 region. Domains annotated above. Scalebar = 100aa.

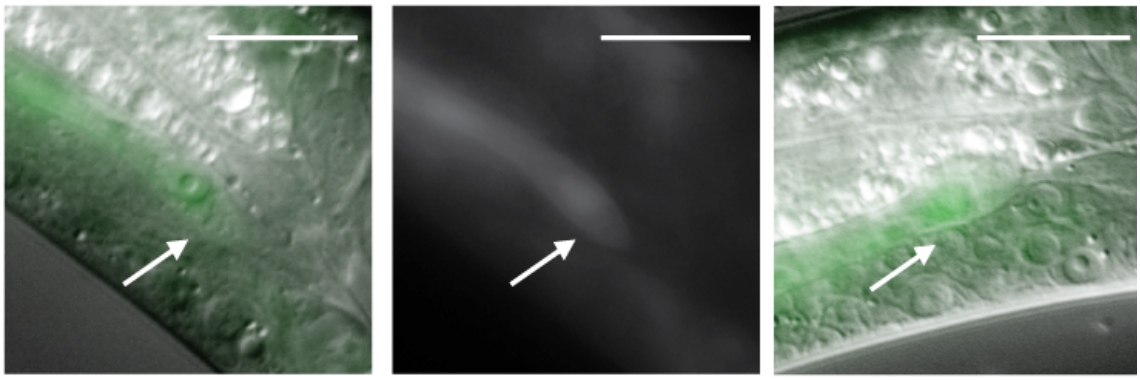

Figure 3.10. *cul-3*p::gfp is expressed in the linker cell during migration and death. left = merged DIC/fluorescent image of a dying linker cell at the cloaca, middle = fluorescent image of the linker cell at left, right= merged DIC/fluorescent image of a migrating linker cell. Anterior is left. Arrow= linker cell, scalebar = 10μm.

neddylation factor RFL-1 show the same spindle formation defects as CUL-3 RNAi animals (Kurz et al., 2002). Analysis of x-ray crystallographic structures suggests that neddylation activates CUL-3 by inducing conformational changes that allow the substrate and E2 to come into close contact (Duda et al., 2008).

We sought to determine if *siah-1* genetically interacts with *cul-3* to promote cell death. While RNAi against *cul-1* or *cul-5* shows no change in linker cell survival in a *siah-1*(*tm1968*) background, *cul-3*(RNAi); *siah-1*(*tm1968*) animals show a synergistic increase in linker cell survival compared to *siah-1*(*tm1968*) or *cul-3*(RNAi) alone (Table 3.4). Thus, one could imagine two possible models: 1) SIAH-1 and CUL-3 act in two separate complexes that are required for linker cell death. 2) SIAH-1 and CUL-3 act in a single complex; other CULs or RINGs can compensate if either is missing but if both are missing, then and essential complex required for death is removed, causing a large increase in cell survival levels. Biochemistry experiments can hopefully reveal if SIAH-1 and CUL-3 indeed act in a single CUL-RING complex to promote death.

DISCUSSION

The above results suggest that E3 ligases such as SIAH-1 and RBX-1 act as redundant members of multisubunit Cullin-RING ligase complexes with the E2 LET-70 to promote linker cell death. This model appears to share similarities with other cell death-like pathways, as CUL3-based E3 ligases are required to degrade caspase inhibitors to promote *Drosophila* sperm individualization (Arama et al., 2007), and overexpression of CUL3 in cultured mammalian cells induces non-proteolytic ubiquitination of Caspase-8 to activate cell death (Jin et al., 2009).

One potential model regarding linker cell death execution, therefore, could be that CUL-3 complexes ubiquitinate and inhibit caspase inhibitor function, thus promoting cell death. As caspase mutants fail to prevent linker cell death, this is not likely the overall mechanism. However, data from Lena Kutscher suggests that caspases may be required for proper corpse degradation downstream of linker cell death initiation (L. Kutscher, unpublished results). Thus, it is possible that E3 ligases may degrade caspase inhibitors in later stages of linker cell demise. More experiments are needed to test whether E3 inhibition prevents caspase activation during linker cell death.

In order to initiate the first steps required for linker cell death, however, E3 ligases likely ubiquitinate another group of substrates, as E3 mutants possess surviving linker cells, and not corpses. One way in which ubiquitination may be used to promote cell death is through degradation of other unidentified cell death inhibitors, thus preventing "undead" cells from inappropriately surviving. This can be seen mechanistically in models of cell cycle exit in *S. cerevisiae,* as members of the multi-subunit APC E3 ligase complex degrade S type cyclins to push the cell forward into mitotic exit (Shirayama et al., 1999). One could imagine an analogous model in linker cell death where CUL-3-RING ligases degrade substrates to push the cell from an "undead" state firmly into death.

This model would be quite interesting to test; unfortunately, the identities of the substrates ubiquitinated by SIAH-1 and RBX-1 during linker cell death are still unknown. Substrate identification would provide information as to whether E3s are acting in a signaling capacity, in a transcriptional capacity, in a protein degradation capacity, or perhaps a combination of all three. As the SIAH-1 substrate-binding motif has been elucidated (House et al., 2006), a potential starting point would be to look for proteins containing that motif.

Although *siah-1* and *rbx-1* mutants have weak survival defects, the synergistic defect exhibited by simultaneous reduction of SIAH-1 and RBX-1 expression levels suggests that there is likely E3 redundancy in the cell death pathway. The observation that linker cell survival in *rbx-1*(RNAi); *siah-1*(*tm1968*) animals does not reach the level seen in *let-70*(RNAi) animals suggests that perhaps an entire cohort of E3 enzymes is required to carry out the protein degradation required for linker cell death. As traditional biochemical approaches such as co-immunoprecipitation and yeast-two hybrids may be too insensitive to pick up binding affinities between catalytically interacting proteins, linker cell-specific RNA-seq may be able to identify other E3s that are expressed in the linker cell during death.

Finally, the fact that SIAH-1, RBX-1 and CUL-3 are maintained in the linker cell throughout its lifetime and are not induced is an interesting observation. Why only upregulate the E2, ubiquitin and the proteasome? One possible hypothesis is that RING finger E3s provide substrate-specificity without any catalytic activity. Therefore, constitutive E3 expression within the linker cell might increase the probability that a substrate-bound E3 will quickly find an E2 once linker cell death is initiated. Such a situation would allow for stringent control over death initiation timing while also maintaining efficient ubiquitination kinetics.

CHAPTER 4: EOR-1/PLZF and EOR-2 are required for the nonapoptotic death of the *C. elegans* linker cell

SUMMARY

Following the identification of CUL-3 as an important linker cell death regulator, we wondered with which BTB/POZ protein CUL-3 interacts in order to promote linker cell demise. We screened through a list of 23 BTB proteins previously shown to interact with CUL-3 and found that RNAi against the transcription factor EOR-1 causes inappropriate linker cell survival. While no evidence exists that EOR-1 acts in an E3 complex in *C. elegans*, co-immunoprecipitation experiments show that the mammalian EOR-1 homolog PLZF interacts with Cul3 in nuclei, where the complex ubiquitinates histones to transcriptionally activate lymphocyte development (Mathew et al., 2012).

Here, we analyze the role of EOR-1 in linker cell death. We show that three different *eor-1* mutants, each with lesions in different regions of the gene, exhibit inappropriate linker cell survival. An EOR-1-GFP reporter is expressed in the nucleus of the linker cell throughout its lifetime, and *eor-1* may be required in the linker cell for death. Epistasis experiments place EOR-1 in the same pathway as LET-70, RBX-1 and PQN-41. In contrast, *eor-1*; *sek-1* mutants have a larger survival defect compared to either mutant alone, indicating that they may work in parallel, while *eor-1*; *cul-3* mutants, *eor-1*; *hsf-1* mutants, and *eor-1*; *siah-1* mutants display synergistic increases in linker cell survival compared to what is observed in single mutants. *hsf-1* gain-of-function alleles are able to rescue *eor-1* mutant-associated survival, indicating that EOR-1 works upstream of HSF-1. As these results are inconsistent with the model of EOR-1

being an E3 ligase, we hypothesize that EOR-1 may be a transcriptional activator that promotes linker cell death.

RESULTS

PLZF/EOR-1 and its cofactor, the novel protein EOR-2, are required for linker cell death

As neither CUL-3 nor RBX-1 have been shown to function directly in substrate binding, we therefore wondered what substrate-recognition proteins cooperated with these E3 components to promote linker cell death. Cullin-3-RING finger ligases consist of CUL-3 bound to a RING finger-containing protein as well as a BTB/POZ domain-containing protein (Kipreos, 2005). Thus, we decided to screen for BTB-encoding genes whose absence causes linker cell survival.

We limited our search to 19 proteins previously reported to interact with *C. elegans* CUL-3 in a two-hybrid assay (Xu et al., 2003), as well as *C. elegans* homologs of KLHL10, which binds CUL-3 during *Drosophila* spermatogenesis (Arama et al., 2007). RNAi against these BTB-encoding genes identified only one, *eor-1*, whose depletion leads to significant linker cell survival (Table 4.1).

To confirm a role for *eor-1* in linker cell death, we examined linker cell survival in animals carrying viable alleles of the gene. As shown in Table 4.2, three different mutations in *eor-1* each result in inappropriate linker cell survival, with the strongest allele, *eor-1*(*cs28*), displaying 38% survival (Table 4.2). This defect is specifically caused by the *eor-1* lesion, as injection of animals with wild-type *eor-1* genomic DNA restores normal linker cell death to *eor-1*(*cs28*) mutants (Table 4.2). While linker cell-specific RNAi against *eor-1* results in a weak linker cell survival defect (Table 4.2), it is unclear whether the lack of survival observed

Table 4.1: RNAi against *eor-1*, but not other BTB domain genes, causes inappropriate linker cell survival that synergizes with *siah-1*(*tm1968*) mutations

Genotype	**LC survival**[ac]	**+ *siah-1*(*tm1968*)**[bd] **LC survival**
No RNAi	3 ± <1	14 ± 2
kel-1 RNAi	3 ± 3	12 ± 5
kel-3 RNAi	3 ± 2	NT
kel-8 RNAi	3 ± 2	NT
***eor-1* RNAi**	**14 ± 2**	**30 ± 1**
bath-15 RNAi	4 ± 2	5 ± 4
bath-40 RNAi	8 ± 3	17 ± 6
mel-26 RNAi	0 ± 0	19 ± 7
bath-42 RNAi	1 ± 1	15 ± 5
ZC239.15 RNAi	3 ± 2	6 ± 4
btb-20 RNAi	4 ± 2	20 ± 6
D2045.8 RNAi	7 ± 3	14 ± 6
inso-1 RNAi	5 ± 2	9 ± 5
R12E2.1 RNAi	7 ± 1	18 ± 3
bath-43 RNAi	4 ± 4	21 ± 1
B2081.5 RNAi	8 ± <1	13 ± 4
kel-10 RNAi	9 ± 3	13 ± 5
F47D12.7 RNAi	2 ± 2	14 ± 5
tag-147 RNAi	4 ± 2	13 ± 5
spe-26 RNAi	8 ± 3	18 ± 6
C53A5.11 RNAi	4 ± 2	14 ± 6
C53A5.6 RNAi	Arrest at L3	Arrest at L3
C53A5.9 RNAi	5 ± 2	14 ± 5
eor-2 RNAi	3 ± 2	32 ± 4

[a]strains analyzed contained *rrf-3*(*pk1426*); *him-8*(*e1489*) mutations, Error, SEM

[b]strains analyzed contained *him-5*(*e1489*) mutations, Error, SEM

[c]n>74

[d]n>35

is a result of inefficient RNAi in the cell, or from EOR-1 acting in a different cell to promote death.

Interestingly, the three mutations analyzed impact different regions of the EOR-1 protein. Genetic mapping and anti-EOR-1 staining of mutant lysates suggests that *cs28* is a null mutation caused by a 68bp deletion in the first third of the protein (Howard and Sundaram, 2002b; Howell et al., 2010); *eor-1*(*cs40*) encodes a mutation leading to an R482stop alteration in between the second and third C2H2 zinc finger domains, and likely produces a truncated protein (Howard and Sundaram, 2002b)(Figure 4.1); and *cs44* encodes a misssense mutation that induces an L81F amino acid change within the BTB domain. Coimmunoprecipitation experiments show that this mutation abrogates binding of EOR-1 to its cofactor, the novel protein EOR-2 (Howell et al., 2010). This mutation also impacts access to serine/threonine phosphoacceptor sites during ERK signaling, as shown by in vitro kinase assays (Howell et al., 2010).

Because *eor-1*(*cs44*) mutations disrupt EOR-2 binding, we wondered whether *eor-2* is also required for linker cell death. Though *eor-2*(RNAi) animals display wild-type linker cell death, mutants in *eor-2*(*cs42*)*,* encoding an early stop codon in the second exon of the gene, show significant defects in linker cell death. (Figure 4.2, Table 4.2). Thus, EOR-1 and EOR-2 likely act together to promote linker cell death.

EOR-1 encodes a protein similar to promyelocytic leukemia zinc-finger protein (PLZF), a protein that is fused to retinoic acid receptor alpha in acute promyelocytic leukemia in humans (Chen et al., 1993). Amino acid analysis suggests that EOR-1 possesses an N-terminal BTB domain which is a component of mature Cullin-RING ligases (CRLs), and a BTB and C-terminal Kelch (BACK) domain, which is hypothesized to promote substrate orientation in E3s

Table 4.2: *eor-1* and *eor-2* mutants display defects in linker cell death

Genotype[a]	**LC survival**[b]
eor-1(RNAi)	14 ± 2
eor-1(LC-only RNAi)[c]	16 ± 1
eor-1(*cs28*)	40 ± 2
eor-1(cs28) + P_{EOR-1}::*eor-1*::gfp	13 ± 1*
eor-1(*cs40*)	24 ± 3
eor-1(*cs44*)	18 ± 1
eor-2(*cs42*)	28 ± 4

[a]All animals contained a *lag-2*p::gfp (*qIs56*) reporter gene to identify the linker cell, and either *him-5*(*e1490*) mutations, except in the LC-only experiments in which the *mig-24* promoter was used to drive an *rde-1* cDNA in *rde-1*(*ne219*) *him-8*(*e1489*); *qIs56* mutants. *rde-1*(*ne219*) mutants have 12 ± 1 % LC survival. None of the strains exhibited considerable migration defects. Error, SEM, except for experiments using transgenes, where error is the SD of 3 transgenic lines obtained.

[b]n>100

Figure 4.1. Map of mutants, RNAi and gene construct used to explore EOR-1 function. For all DNA constructs, black box = exons, white box= 5'/3' UTR. (A) Location of RNAi construct (red line), deletion mutant (*cs28*, blue line), and two point mutants (*cs40, cs44*) in relation to a map of the *eor-1* coding region. Scalebar = 500bp. (B) Map of *eor-1*p::*eor-1*::gfp fusion used to analyze *eor-1* expression pattern. GFP is inserted in a unique NcoI site just after the start of the eighth exon (Howard et al., 2012). Scalebar = 500bp. (C) Map of domains located within the EOR-1 protein. Domains described in legend below diagram. Scalebar = 100aa.

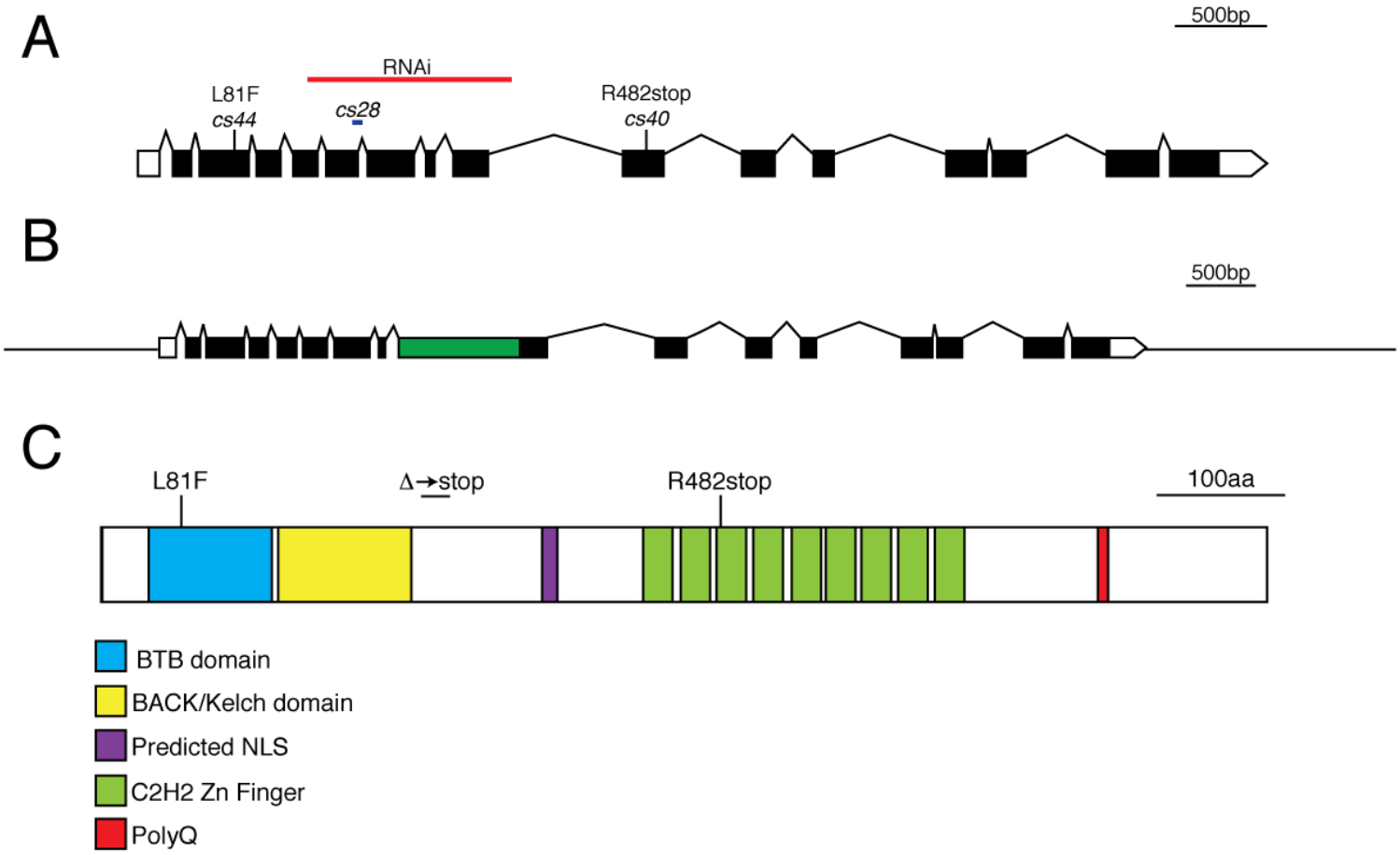
A
500bp
RNAi
L81F
cs44
cs28
R482stop
cs40
B
500bp
C
L81F
Δ→stop
R482stop
100aa
BTB domain
BACK/Kelch domain
Predicted NLS
C2H2 Zn Finger
PolyQ

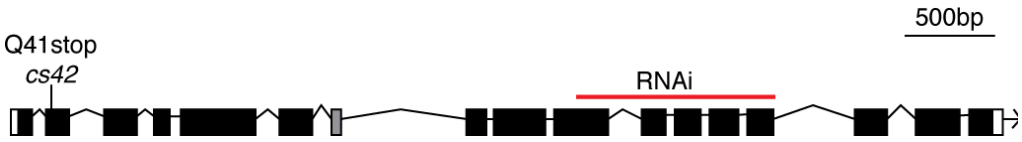

Figure 4.2. Map of mutant and RNAi construct used to explore EOR-2 function. For all DNA constructs, black box = exons, white box= 5'/3' UTR. Gray box = alternatively spliced exon. Location of RNAi construct (red line) and point mutant (*cs42*) in relation to a map of the *eor-2* coding region. Scalebar = 500bp.

(Stogios and Prive, 2004). It also contains a conserved NLS, nine consecutive C2H2 zinc fingers important for nucleotide and protein binding, and a polyQ stretch of unknown function, but which also exists in the GAGA BTB transcription factor (Agianian et al., 1999)(Figure 4.1). Though studies have shown that EOR-1 acts to induce hermaphrodite-specific neuron cell death in *C. elegans* males (see introduction), EOR-1 is also required for the proper execution of a number of cell fates; *eor-1* mutant animals exhibit neuronal function defects, excretory duct malfunction, male tail malformation, and improper hypodermal cell fate specification (Hoeppner et al., 2001; Howard and Sundaram, 2002b). These defects are likely due to EOR-1's role as the downstream node of multiple signaling pathways. As evidenced by *eor-1* mutants' abilities to suppress *pry-1*/Axin and Ras-associated phenotypes, EOR-1 acts downstream of Ras/ERK and Wnt genes to mediate signaling output (Howard and Sundaram, 2002b). This output appears to be in parallel to Hox genes, as *eor-1*; *egl-5*(Hox) double mutants display a synergistic increase in vulvaless animals observed in *egl-5* but not *eor-1* mutants, and as *eor-1* mutations fail to affect Hox reporter gene expression (Howard and Sundaram, 2002b).

EOR-1 is continually expressed in the linker cell

To determine where *eor-1* functions to promote linker cell death, we obtained an *eor-1*p::*eor-1*::gfp reporter consisting of an 8.7kb fragment including the *eor-1* coding sequence plus 1.1 kb of upstream and 1.8kb of downstream sequence, with GFP inserted into an NcoI site just before the eighth exon (Figure 4.1) (Howard and Sundaram, 2002b). Analysis of this strain shows that EOR-1 is expressed in many cells, including the linker cell (Figure 4.3). Like SIAH-1, RBX-1 and CUL-3, EOR-1 expression in the linker cell is constant throughout its lifetime, and there is no change in expression or localization during migration or death (Figure

4.3). Also, as previously shown in other cells, EOR-1-GFP exhibits nuclear localization, consistent with its role as a transcription factor (Howard and Sundaram, 2002b; Mathew et al., 2012). Thus, EOR-1 is expressed in the appropriate location to induce death.

eor-1 acts with *let-70*, *rbx-1*, and *pqn-41* in the same genetic pathway to promote linker cell death

We wondered where EOR-1 acts within the linker cell death pathway. *let-70*(RNAi); *eor-1*(*cs28*) animals exhibit the same amounts of linker cell survival as *eor-1*(*cs28*) or *let-70*(RNAi) animals alone, indicating that the two likely operate in the same pathway (Table 4.3). This is also seen with *eor-1*(*cs28*); *pqn-41*(RNAi) and *eor-1*(RNAi); *pqn-41*(*ns294*) animals, whose linker cell survival percentages are similar to that of *eor-1*(*cs28*) or *pqn-41*(*ns294*) alone. Interestingly, *eor-1*(*cs28*)*; pqn-41*(*ns294*) mutant animals are very sick; a majority of the animals on the plate exhibit larval lethality, and those that do survive to adulthood only lay one or two eggs that actually hatch. Thus, we were never able to obtain enough animals to analyze to determine how *pqn-41*; *eor-1* double mutants affect linker cell survival. Despite this, the fact that *eor-1*(*cs28*); *pqn-41*(*ns294*) animals exhibit synthetic lethality suggests that EOR-1 and PQN-41 may act redundantly to complete a process integral to the survival of the animal (Table 4.3). Given that both EOR-1 and PQN-41 contain stretches of glutamines within the protein, it is possible that both proteins function similarly to promote death.

We wondered how EOR-1 interacts with other CUL-3 complex components to promote linker cell death. 81% of *eor-1*(*cs28*); *cul-3*(RNAi) mutant males exhibit linker cell survival,

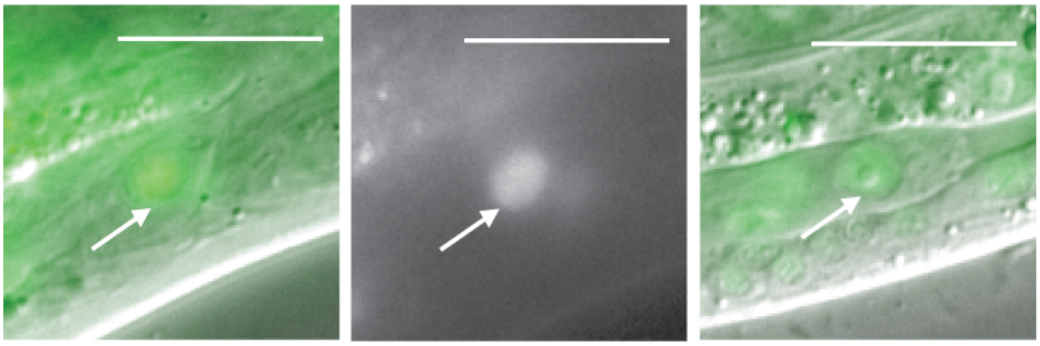

Figure 4.3. EOR-1-GFP is expressed in the linker cell during migration and death. For all animals, left is anterior. Scalebar = 10μm, Arrow= linker cell. *eor-1*p::*eor-1*::gfp is expressed in the linker cell during death (left=DIC/GFP merge, middle = GFP) and migration (right, DIC/GFP merge).

compared to 40% of *eor-1*(*cs28*) and 20% of *cul-3*(RNAi) animals, indicating that the two either work in parallel, or are required together for a joint complex (Table 4.3). This synergistic defect is also seen in *eor-1*(*cs28*)*siah-1*(*tm1968*) animals, who have around 60 percent linker cell survival compared to 40 and 20% in *eor-1*(*cs28*) and *siah-1*(*tm1968*) animals, respectively. This indicates that EOR-1 may act either in parallel with SIAH-1 and CUL-3, or that EOR-1 may act in a single complex with the two. Biochemistry experiments would be required to narrow this hypothesis. Finally, *eor-1*(*cs28*); *rbx-1*(RNAi) double mutants have the same survival defect as *eor-1*(*cs28*) animals alone, indicating that EOR-1 may act in the same pathway as RBX-1 to promote death. The basis for why *rbx-1*(RNAi)*; eor-1*(*cs28*) animals do not exhibit the synergistic survival seen with *eor-1*(*cs28*)*siah-1*(*tm1968*) or *eor-1*(*cs28*); *cul-3*(RNAi) animals is unknown; either *rbx-1* RNAi knockdown is incomplete, or the result reflects true differences in genetic interaction between the sets of genes.

Surprisingly, a number of genes that genetically interact with *let-70* do not appear to interact with *eor-1*. While *sek-1*(*ag1*); *eor-1*(*cs28)* appear to cause synthetic lethality, as no homozygous double mutants were ever recovered from crosses, 83% of *sek-1*(*ag1*); *eor-1*(RNAi) animals possess surviving linker cells compared to 59% of *sek-1*(*ag1*) or 14% *eor-1*(RNAi) animals, indicating that the two likely work in parallel. What is most intriguing, however, is the relationship of EOR-1 to HSF-1. Unlike *let-70*(RNAi); *hsf-1*(*sy441*) animals, which display roughly the same amount of survival as *let-70* or *hsf-1* single mutants, *hsf-1*(*sy441*); *eor-1*(*cs28*) animals display a synergistic increase in linker cell survival that reaches almost 90 percent. Also, unlike *let-70*(RNAi) animals that show no linker cell death rescue when crossed to the *hsf-1*(R145A) gain-of-function allele, *eor-1*(*cs28*); *hsf-1*(R145A) animals reduce *eor-1*(*cs28*)-associated linker cell survival from around 40 percent to only 20 percent

Table 4.3. *eor-1* acts in the same genetic pathway as *let-70*, *rbx-1*, and *pqn-41* to promote linker cell death

Genotype[a]	LC survival[b]
eor-1(*cs28*)	40 ± 2
eor-1(RNAi)	14 ± 2
let-70(RNAi)	60 ± 20
eor-1(*cs28*); *let-70*(RNAi)	60 ± 13
rbx-1(RNAi)	11 ± 2
eor-1(*cs28*); *rbx-1*(RNAi)	44 ± 2
cul-3(RNAi)	17 ± 4
eor-1(*cs28*); *cul-3*(RNAi)	81 ± 3
*hsf-1*R145A	4 ± 2
eor-1(*cs28*); *hsf-1*R145A	21 ± 1
hsf-1(*sy441*)	35 ± 5
eor-1(*cs28*); *hsf-1(sy441)*	86 ± 1
sek-1(*ag1*)	59 ± 13
eor-1(RNAi); *sek-1*(*ag1*)*	83 ± 5
pqn-41(*ns294*)	23 ± 1
eor-1(RNAi); *pqn-41*(*ns294*)**	28 ± 1
pqn-41(RNAi)	18 ± 5
eor-1(*cs28*); *pqn-41*(RNAi)**	53 ± 2
siah-1(*tm1968*)	14 ± 2
eor-1(*cs28*)*siah-1*(*tm1968*)	60 ± 4

[a]All animals contained a *lag-2*p::gfp (*qIs56*) reporter gene to identify the linker cell, and either *him-5*(*e1490*) mutations, Error, SEM.

[b]LC, linker cell. n>106.

**eor-1*(*cs28*); *sek-1*(*ag1*) animals were never observed.

***eor-1*(*cs28*); *pqn-41*(*ns294*) animals were very sick; most arrested at L2, and those that reached adulthood had very few progeny. As a result, the strain could never be propagated.

(Table 4.3). Thus, HSF-1 appears to act downstream of and possibly in parallel to EOR-1, while HSF-1 appears to act upstream of and in the same pathway as LET-70.

EOR-1 does not physically interact with CUL-3 or RBX-1

As genetic data seems inconsistent with the model of EOR-1 as a CUL-3 complex component, we wondered whether EOR-1 physically interacts with CUL-3 or RBX-1. One model for linker cell death is that EOR-1 localizes to the nucleus with CUL-3, RBX-1 and LET-70 to promote death via ubiquitination. As a result, we first wondered whether CUL-3 could translocate to the nucleus to promote death. Subcellular fractionation of wild-type and *eor-1*(*cs28*) animals followed by CUL-3 immunostaining suggests that CUL-3 localizes to both the cytoplasm and nucleus, and that in *eor-1*(*cs28*) mutants, slightly more CUL-3 is nuclear localized (Figure 4.4). Thus, CUL-3 and EOR-1 sometimes localize in the same subcellular compartment to promote death.

We also wondered whether EOR-1 and CUL-3 are capable of physically interacting to form a CRL complex to promote death. S2 cells transfected with tagged copies of EOR-1 and CUL-3 do not co-immunoprecipitate, nor do cells co-transfected with EOR-1 and RBX-1, or cells transfected with EOR-1, RBX-1 and CUL-3 (Figure 4.5). While the lack of interaction indicates that EOR-1 is likely not acting in a complex with CUL-3 and RBX-1, many other options may prevent the possible binding from taking place: the placement of tags may hinder physical interaction; the co-IP may be missing essential co-factors such as EOR-2 which might prevent effective pull-down; the complex may contain SIAH-1 instead of RBX-1. Therefore, more experiments must be conducted in order to confirm that EOR-1 is not a member of the Cul-RING complex required for linker cell death.

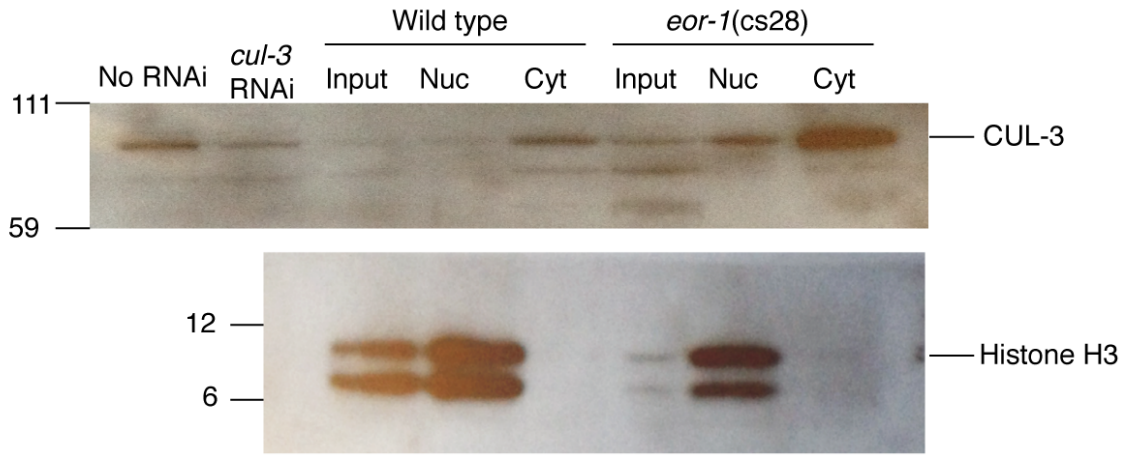

Figure 4.4. CUL-3 localizes to both the nucleus and cytoplasm in vivo. Subcellular fractionation of wild-type and *eor-1*(*cs28*) lysates were run on an SDS-PAGE gel and stained for CUL-3 (gift from L. Pintard). Histone H3 was used as a nuclear control. Nuc= nuclear fraction, cyt= cytoplasmic fraction.

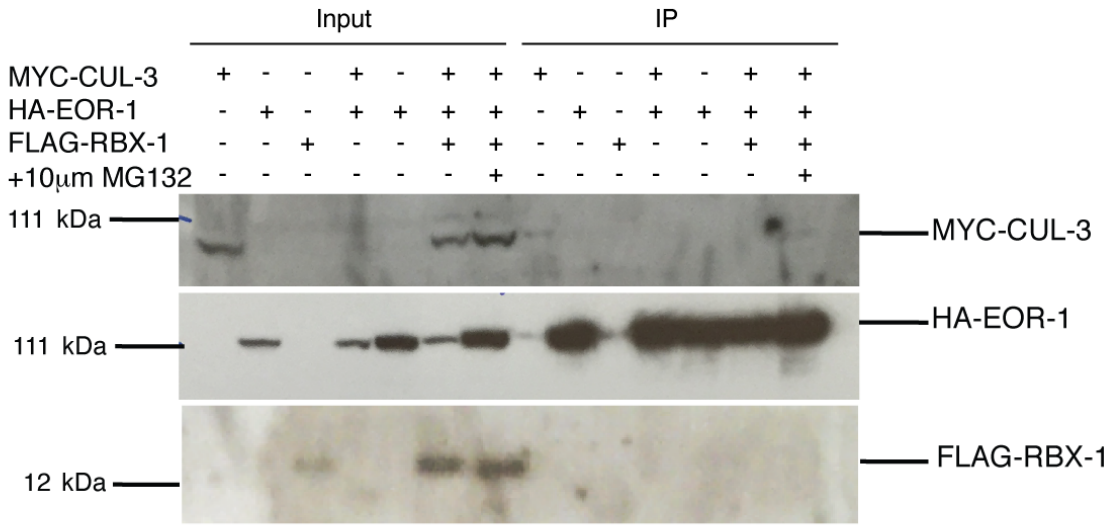

Figure 4.5. EOR-1 fails to co-immunoprecipitate with either CUL-3 or RBX-1 when expressed in *Drosophila* S2 cells. *Drosophila* S2 cells were transfected with myc-LET-70, HA-EOR-1, and MYC-FLAG-RBX-1 Lysates were immunoprecipitated with anti-HA-conjugated agarose beads. Western blots were stained against HA and myc to analyze protein-protein interaction.

EOR-1 fails to systemically affect transcriptional output of genes within the linker cell death pathway.

With this information in hand, we wondered whether EOR-1 is necessary for the transcriptional upregulation of genes important in linker cell death. Using data from the *C. elegans* modENCODE project, which compiles ChIP-seq data from transcription factors in model organisms, we performed qRT-PCR experiments using primers against linker cell death genes shown to have upstream binding sites for EOR-1: *pqn-41*, *tir-1*, *hpk-1*, *rpn-11*, *mig-5*, *lin-29*, *siah-1* and *hsf-1* (Figure 4.6). qRT-PCR experiments showed no significant fold change in transcription of any linker cell death gene tested in comparisons of wild-type versus *eor-1*(*cs28*), *eor-1*(*cs40*), or *eor-1*(*cs44*) mutants. A number of possibilities potentially underlie the reason for this negative data: (1) EOR-1 acts by altering the transcription of an as-yet undescribed gene in the linker cell death pathway. (2) EOR-1 acts to regulate transcription of these genes only on the level of the linker cell, in a manner that would not be recognized by qRT-PCR of whole animal lysates. (3) EOR-1 is acting by using a currently unknown mechanism to promote linker cell death. More experiments are needed to answer these questions.

DISCUSSION

For now, our data seems to suggest that EOR-1 acts in the same pathway as LET-70, RBX-1 and PQN-41, either in parallel or with SIAH-1 and CUL-3, upstream of and possibly in parallel to HSF-1, and in parallel to SEK-1 to promote linker cell death. As these results are inconsistent with the model of EOR-1 being a downstream effector of LET-70, EOR-1 appears to act as a transcription factor that impacts downstream signaling to promote death.

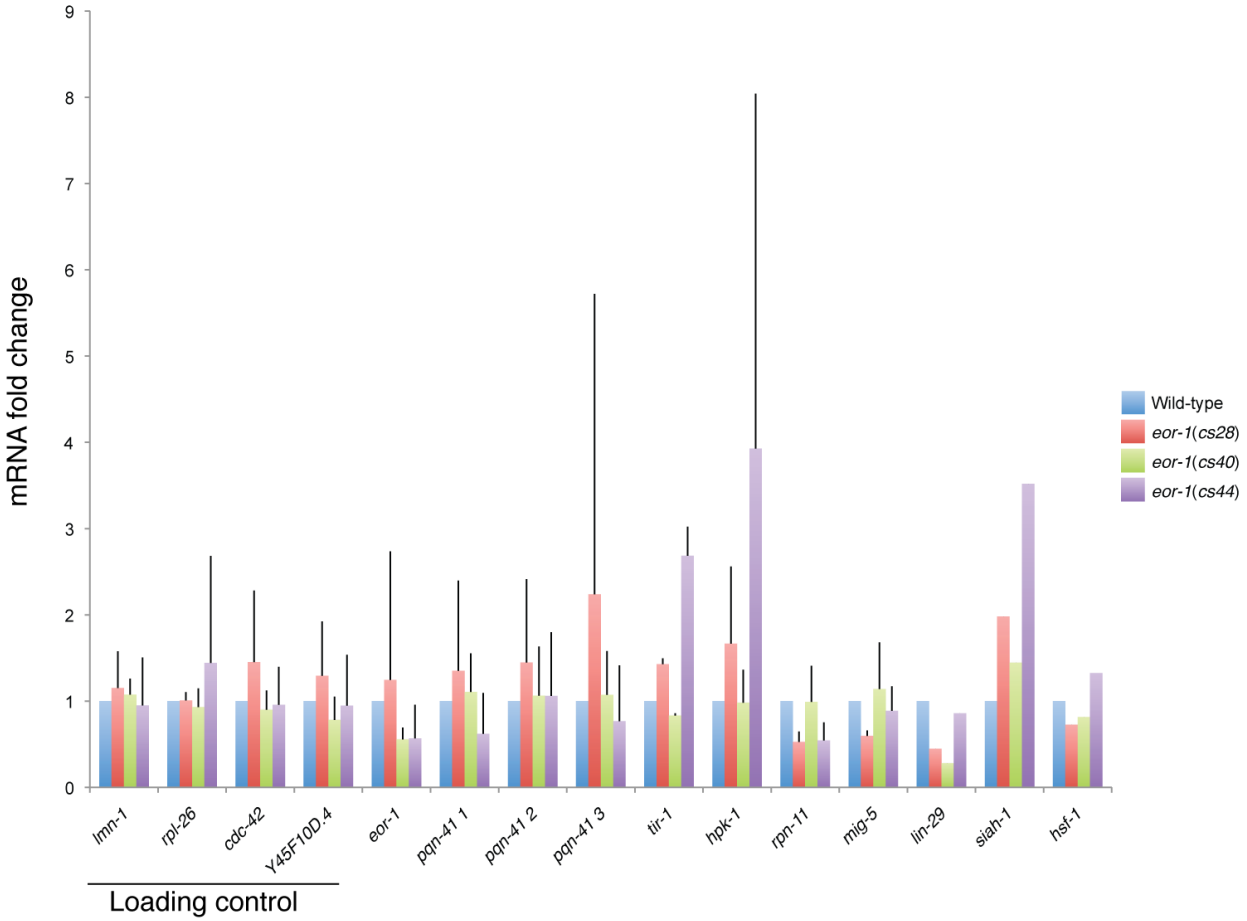

Figure 4.6. No significant changes in mRNA levels are observable in EOR-1-associated linker cell death genes between wild-type and *eor-1* mutant animals. mRNA isolated from wild-type (blue), *eor-1*(*cs28*) (red), *eor-1*(*cs40*) (green) and *eor-1*(*cs44*) (violet) animals was reverse-transcribed to cDNA and assayed for changes in gene expression using qRT-PCR. *lmn-1*, *rpl-26*, *cdc-42*, and *Y4510D.4* were used as loading controls. Each individual experiment is the sum of the average of three identical samples. Data shown is average of two to five individual experiments. Error bar= standard deviation between experiments.

Previous work on EOR-1 suggests that EOR-1 acts downstream of Wnt and Ras signaling but in parallel to Hox genes to promote cell fate decisions (Howard and Sundaram, 2002b). This observation is especially intriguing in light of observations that both Wnt proteins and the Hox protein NOB-1 are required for the death of the linker cell (M. Kinet, unpublished observations). Though we have not yet tested this hypothesis, analysis of linker cell survival in *egl-20; eor-1* and *eor-1; nob-1* mutants would help us determine whether EOR-1 is acting in a manner previously described to promote cell death.

Previous data also suggests that EOR-1 is modulated by kinase signaling (Howell et al., 2010). As mutants in the MAPKK *sek-1* cause inappropriate linker cell survival, it would be interesting to find out whether MAPKs downstream of SEK-1 phosphorylate and therefore activate EOR-1 activity. Though kinase assays might be difficult to perform given that the MAPK required for linker cell death has not been identified, one could test if EOR-1 phosphorylation site mutants have defects in linker cell survival. Furthermore, one could make phosphomimetic versions of *eor-1* and see if ectopic expression of "hyperactivated" EOR-1 can rescue specific phenotypes.

Although EOR-1 is not likely to be acting as an E3 component, it is also unknown whether EOR-1 is acting as a transcription factor. One way to test this is to see if *eor-1* mutants impact LET-70-GFP expression levels. If LET-70-GFP expression is abrogated, then one could assume that EOR-1 acts upstream to induce LET-70 expression to promote death. If EOR-1 is indeed acting as a transcription factor, then it is still unknown what other targets it activates to promote linker cell death. Linker cell-specific RNA-seq comparisons between wild-type and *eor-1*(*cs28*) animals could help to answer these questions.

If EOR-1 is not acting in a CUL-3 complex, then it is still unknown with which BTB protein CUL-3 interacts to promote death. As *eor-2*(RNAi) animals show no inappropriate survival but *eor-2*(*cs42*) animals have survival defects, it is certainly possible that we have encountered false negatives in our screens, both for Skp and BTB protein candidates. It would be worthwhile to obtain a number of mutants in these genes to see if any of them are required for linker cell death.

CHAPTER 5: Discussion and future directions

Cell death is an important molecular process required for life; its implementation allows for the promotion of tissue morphogenesis and organ sculpting, as well as the prevention of autoimmune disease and cancer. While apoptosis is canonically required for the execution of many cell deaths, prior studies of intersegmental muscle remodeling in the moth *Manduca sexta,* as well as the observation that motor neurons within the spinal cord die normally in caspase mutants, have suggested that caspases are not required for all developmental cell deaths (Oppenheim et al., 2001; Schwartz and Truman, 1982; Schwartz et al., 1990). Analysis of the genes required for *C. elegans* linker cell death supports this idea, and have made apparent a new set of genes whose absence causes inappropriate linker cell survival.

A model for linker cell death

Previous work from Elyse Blum and Mary Abraham revealed the presence of a new nonapoptotic pathway required for linker cell death. Components of this pathway included members of the heterochronic pathway, a MAP kinase cascade, and a poly-glutamine repeat protein (Abraham et al., 2007; Blum et al., 2012) (Figure 5.1). Our current work expands on this data; the experiments conducted in this thesis, as well as results from Maxime Kinet, Andrew Schwendeman and Lena Kutscher, suggest that linker cell death genes can be divided into two main classes: transcriptional activators and ubiquitin proteasome system (UPS) components. Transcription appears to require phosphorylation from SEK-1/MAPKK and TIR-1/TIR-domain adapter proteins. These proteins act together with a histone methyltransferase complex similar to MLL3/4 to either directly or indirectly activate transcription of genes such as PQN-41 and LET-70 during linker cell death (Blum et al., 2012; Figure 2.11). Components

of the Wnt signaling pathway such as EGL-20/Wnt are also required for LET-70 expression (Figure 2.14); this pathway is inhibited by an anti-death Wnt signal propagated by LIN-44/Wnt (M. Kinet, unpublished results). The homeodomain transcription factor LIN-29 and the nuclear hormone transcription factor NHR-67 appear to act in parallel to the Wnt and MLL complexes to regulate transcription of genes required for death (Figures 2.13, 2.14, 5.1). Finally, the PLZF homolog EOR-1 and its cofactor EOR-2 also appear to regulate gene expression to promote linker cell demise (see Chapter 4; Figure 5.1). Downstream of the above proteins, HSF-1 appears to activate LET-70 expression required for death, as gain-of-function alleles of HSF-1 lower survival levels of all known mutants except for *let-70*, and as sequence analysis of UPS promoter regions in *C. elegans* and other nematode species predict the existence of conserved heat shock element binding sites at a consistent distance upstream of start (M. Kinet, unpublished results; Figures 2.15; 5.1). Following transcription, the LET-70 protein appears to function with E3 components such as RBX-1, CUL-3 and SIAH-1 to regulate ubiquitylation of a substrate/s required for death (Figure 5.1). The proteasome also appears to be required for this process, as inhibition of 19S regulatory components causes inappropriate linker cell survival. Thus, degradation of unknown substrates may directly or indirectly to induce linker cell death. While this model is incomplete, it fills in a number of details regarding how cells may be executed in a non-apoptotic manner.

The UPS and cell death

The involvement of the UPS in linker cell death is quite exciting, as it is already linked to a number of cell death and cell death-related processes. In previously studied examples, the UPS seems to play a general role in cell dismantling, as seen during intersegmental muscle

remodeling during metamorphosis in moths (Schwartz et al., 1990). However, other studies suggest that the UPS plays a specific regulatory role, as in the case of caspase inhibition by IAP E3 ligases (Ditzel et al., 2008; Hay et al., 1995; Suzuki et al., 2001). The studies we present here are consistent with both of these roles but more work is needed to truly understand UPS function during death. As of now, the UPS appears to be the most downstream effector identified, but elucidation of substrates downstream of the UPS will provide more clarity regarding mechanism.

One potential candidate for a UPS substrate is the caspase CED-3. While caspases are not required to kill the linker cell, Lena Kutscher has shown that they are required for corpse degradation, and therefore may function downstream of LET-70 and the UPS (L. Kutscher, unpublished results). This would be similar to the current model for *Drosophila* sperm development, which requires caspase activity activation by the UPS to remodel sperm (Arama et al., 2007). As mentioned above, the transcriptional induction of UPS components in the linker cell just prior to the onset of cell death may also be consistent with a broader role in cellular dismantling. The purpose of this induction is, presumably, to boost levels of the protein degradation machinery. This would make sense if a specific highly abundant protein were the target, or if general cellular dismantling were required.

The relationship of linker cell death to neurodegenerative disease

Previous studies from our lab raised the possibility that linker cell death may be related to degenerative processes that promote vertebrate neuronal death. Nuclear crenellation is evident in dying linker cells and in degenerating cells in polyQ disease (Abraham et al., 2007; Davies et al., 1997; Zander et al., 2001). Glutamine-rich proteins (PQN-41 and polyQ

Figure 5.1. A model for the death of the linker cell. (Nucleus) Several transcription factors are required for linker cell death execution. Components of pro- and anti-death Wnt signaling pathways (aqua), a histone methyltransferase complex (gray) and the PLZF transcription factor EOR-1 (pink) all act upstream of the heat shock factor HSF-1 (purple). All of the above genes are required in some capacity for regulating the transcription of the E2 enzyme LET-70, as well as of ubiquitin. (Cytoplasm) During linker cell death, the E2 LET-70 acts with E3 components SIAH-1, CUL-3 and RBX-1 to cause ubiquitination of substrates, which are degraded by the 26s proteasome.

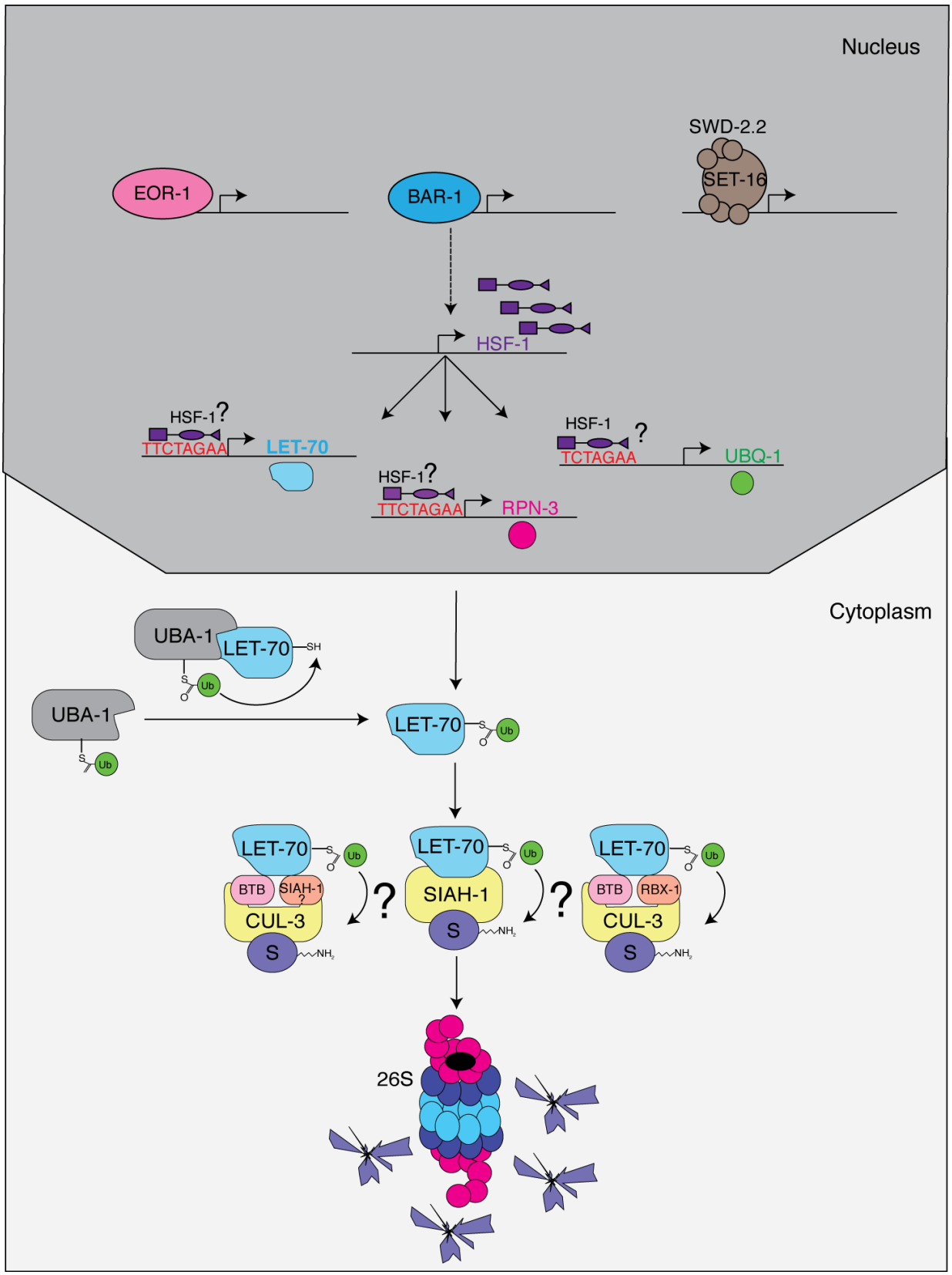
Nucleus
SWD-2.2
SET-16
EOR-1
BAR-1
HSF-1
HSF-1?
TTCTAGAA
LET-70
HSF-1
?
TCTAGAA
UBQ-1
HSF-1?
TTCTAGAA
RPN-3
Cytoplasm
UBA-1
LET-70
SH
Ub
UBA-1
Ub
LET-70
Ub
LET-70
Ub
BTB
SIAH-1
?
CUL-3
S
NH2
?
LET-70
Ub
SIAH-1
S
NH2
?
LET-70
Ub
BTB
RBX-1
CUL-3
S
NH2
26S

expansion proteins) participate in linker cell death and in polyQ-associated neurodegeneration (Blum et al., 2012; Riley and Orr, 2006). Furthermore, the TIR-1/Sarm adapter protein promotes linker cell death in *C. elegans* and degeneration of distal axonal segments following axotomy in *Drosophila* and vertebrates (Osterloh et al., 2012). Our results here implicating the UPS in linker cell death also support a connection with neurodegeneration. For example, aggregates found in polyQ-expressing cells, as in Huntingtin's disease, are heavily ubiquitylated (Kalchman et al., 1996; Liani et al., 2004). In Parkinson's disease, mutations in the E3 Parkin play an important role in disease progression, and alpha-synuclein, another key player in disease initiation, is heavily ubiquitylated (Kitada et al., 1998). The E3 SIAH-1, which we have found to play a role in linker cell death, has been implicated in a number of cell death processes (Liu et al., 2001), and has been linked to cellular toxicity induced by mutant Huntingtin protein, perhaps through nuclear shuttling of Huntingtin (Bae et al., 2006). Thus, while it is too early to draw a direct connection between linker cell death and neurodegenerative disease in humans, the emerging similarities suggest that further studies of linker cell death may provide insight into the initiation and progression of these devastating ailments.

Future Directions

Though much has been uncovered in the experiments conducted in this thesis, much remains to be known regarding the mechanisms underlying linker cell death. In the remaining paragraphs, I discuss questions that are still unanswered, as well as the experiments that will be required in the future in order to better understand how EOR-1 and UPS components promote linker cell death.

A. How is LET-70 regulated to promote linker cell death?

While epistasis experiments using *let-70* RNAi have been very informative in helping to ascertain how linker cell death is executed, we worry that spurious data may have been generated as a result of incomplete knockdown of multiple genes via RNAi. As a *let-70* allele is now available for study, all of the epistasis experiments conducted in Chapter 2 should be repeated using the *let-70*(*ns770*) allele to ensure data consistency.

In addition to repeating epistasis experiments, the cell-specific rescue experiments should also be repeated using the *ns770* allele of *let-70*. This experiment may help elucidate why *mig-24*p::*let-70 C. briggsae* transgenes only partially rescue the linker cell survival induced by *let-70* RNAi. If *mig-24*p::*let-70* transgenes provide full rescue of *let-70*(*ns770*)-associated phenotypes, then partial rescue could be attributed to RNAi-mediated inhibition of the injection construct, or other reasons such as differences in codon usage between *C. elegans* and *C. briggsae*. If injection of *mig-24*p::*let-70* transgenes into *let-70*(*ns770*) animals still provides partial rescue, then perhaps LET-70 is required at a specific concentration to induce death: too little LET-70 causes survival, but too much LET-70 may cause survival as well. Single copy insertion of a LET-70 rescuing transgene into the *C. elegans* genome using MosSCI would provide a more complete rescue if this is indeed the case.

More experiments should also be conducted to test whether HSF-1 actually induces LET-70 expression to promote linker cell death. As bioinformatic screening has identified conserved HSF-1 binding sites upstream of the *let-70* and *rpn-3* start sites (Figure 2.15), experiments should be performed that confirm that these regions are indeed required for LET-70 expression. LET-70-GFP reporters missing these sites should be generated and injected into

animals to test whether they impact LET-70 linker cell-specific expression. Furthermore, mutants lacking these sites could be generated using CRISPR/Cas9 targeting to ascertain if the resulting animals exhibit inappropriate linker cell survival. Finally, cold-competitor assays can determine whether HSF-1 is capable of binding to these sites in vitro. Such experiments would provide clarity regarding how LET-70 expression is regulated during death.

B. How do E3 ligases promote linker cell death?

1. Which E3 ligases are required?

Experiments conducted in Chapter 3 suggest that the E3 ligase components SIAH-1, RBX-1 and CUL-3 are required for the nonapoptotic death of the linker cell. As downregulation of each of these genes using RNAi or genetic mutations only provides weak inhibition of linker cell death, more studies should be conducted to ascertain whether these ligases are the only E3s required. Reverse genetic screening of the 165 monomeric E3s and roughly 100 BTBs required for death using RNAi could identify new candidates; however, one caveat of this experiment would be that RNAi knockdown may not be sufficient to disrupt the activity of all E3 components required for death, thus creating the potential for false negatives. Linker cell-specific RNA-seq could also reveal which E3 ligases are upregulated in the linker cell during death. Unfortunately, like the experiment above, it also has the possibility of false negatives; many E3s are ubiquitously expressed, and differences in E3 expression levels between the linker cell and other cells may not be readily apparent. Despite these risks, both experiments should be conducted, as they have potential to uncover novel linker cell death genes.

Further experimentation should also be carried out to determine the composition of E3 ligase complexes required for death. As epistasis experiments have been relatively uninformative thus far, biochemistry experiments should be conducted to elucidate whether SIAH-1, RBX-1 and CUL-3 act together or in separate complexes to promote death. Coimmuoprecipitation of the above proteins, or affinity purification of native complexes from lysates may also help to identify CRL members and, therefore provide more clarity regarding how E3 ligases promote death. While this may not be as physiologically relevant as immunoprecipitating complexes from the linker cell itself, the amount of worms that would be required to perform linker-cell specific coimmunoprecipitation experiments is currently prohibitive. Thus, though these experiments have limitations, they also contain the potential to be highly informative.

2. How are E3 protein levels regulated during linker cell death?

After the identity of E3 complexes required for linker cell death has been determined, more work should be conducted regarding understanding the mechanisms underlying E3 protein regulation within the linker cell death pathway. Experiments to clarify the biochemical relationship between LET-70 and SIAH-1 should be conducted, as the observation that *let-70* RNAi upregulates SIAH-1-GFP fosmid expression appears at odds with genetic data which shows that attenuation of either *siah-1* function, or both *siah-1* and *let-70* function causes inappropriate linker cell survival. One potential model is that LET-70 ubiquitinates SIAH-1 in a nonproteolytic manner (as *rpn-3* RNAi does not impact SIAH-1 expression levels) to enable SIAH-1 to enter the nucleus to promote death. To test this hypothesis, one could overexpress *let-70* in animals containing *mig-24*p::gfp::*siah-1* to determine whether this changes SIAH-1 subcellular localization in the linker cell. Overexpression experiments can also help determine

whether SIAH-1 must be localized to the nucleus to induce death. *siah-1*(*tm1968*) mutant animals could be injected with *siah-1* cDNA lacking its NLS sequence to determine whether *siah-1* overexpression fails to suppress mutant-associated linker survival. This experiment could be performed in a background with enhanced survival (such as a *siah-1(tm1968); cul-3*(RNAi) background), which would make the answer more apparent.

The relationship of SIAH-1 concentration to linker cell death should also be explored. As GFP levels observed in *mig-24*p::gfp::*siah-1* animals decline during linker cell death, one could imagine that SIAH-1 protein levels might be carefully titrated to promote death. To test this, one could overexpress *siah-1* under the control of a linker-cell-specific promoter. If upregulation of SIAH-1 prevents linker cell death in wild-type animals, then SIAH-1 levels must be diminished in order to induce death.

The experiments conducted above should also be applied to RBX-1 expression. While transcriptional reporters show that RBX-1 is expressed in the linker cell during migration and death, RBX-1-GFP fosmids provide no information regarding RBX-1 expression and localization during migration and death. One way to increase expression may be to perform *let-70* RNAi on RBX-1 reporter-expressing animals. Another idea would be to immunostain GFP-fosmid animals to amplify the weak reporter expression. Hopefully, these experiments provide more information regarding RBX-1 and SIAH-1 protein dynamics during linker cell death.

C. What substrates are degraded during linker cell death?

Though E3 ligases required for linker cell death have been elucidated, the identity of substrates ubiquitinated during linker cell death remains elusive. This would be highly informative and provide much detail regarding the mechanism required for linker cell

execution. It is still unknown whether the ubiquitination machinery modifies proteins to alter their subcellular localization or activity, or whether the machinery tags proteins for general degradation by the proteasome. Though the involvement of the UPS in linker cell death suggests that the latter is required, it does not exclude the possibility that the former is also being conducted. As multiple E3s are required for death, multiple activities may be carried out in order to execute the linker cell.

If protein degradation is required for the death of the linker cell, it is still unclear whether the UPS is acting to degrade an abundant protein required for life, or whether the UPS is enacting massive levels of nonspecific protein degradation to dismantle the cell. Identification of substrates and visualization of their dynamics as the cell dies would help to answer these questions, and would also hopefully provide answers as to why the ultrastructural details of linker cell death look so different from that of apoptotic death, especially if massive amounts protein degradation are underlying both processes.

One way to answer this question would be to take a bioinformatic approach and screen for proteins that contain a SIAH-1 substrate-binding motif, which has already been elucidated in mammalian systems (House et al 2003, 2006). One could take these identified proteins and look at expression level changes of GFP-tagged candidate genes within the linker cell in *siah-1*(*tm1968*) or *rbx-1*(RNAi) animals. While this could be quite tedious, it could possibly identify substrates required for death. Another approach would be to follow the lead of *Xenopus* researchers, who have identified numerous E3 substrates by in vitro transcribing and translating E3s in lysates and comparing the protein content of the untranslated to translated lanes (Ayad et al., 2005). This could be an interesting way to identify substrates in an unbiased manner, and also may work with LET-70 overexpression, obviating the need for an E3. Finally, as linker

cell-specific RNA-seq is becoming a reality in our lab through the efforts of Menachem Katz, Sean Wallace and Maxime Kinet, this method could potentially be applied to generate sufficient protein to look at differences in proteomic content between wild-type versus *let-70*(RNAi) linker cells. Any information regarding linker cell substrates would help to illuminate basic concepts regarding linker cell death mechanism, though if history is any indication, it may be a long time before we understand how this works; more than 25 years after the discovery of caspases, we still have no idea whether many or few targets are required for apoptotic death.

D. How does EOR-1 promote linker cell death?

As shown in chapter 4, the identification of EOR-1 as a linker cell death regulator has been a recent and exciting discovery. As EOR-1 mutants lacking C2H2 zinc finger domains, as well as mutants unable to bind EOR-2 show inappropriate linker cell survival, one might surmise that EOR-1 transcription factor activity is required for linker cell death (Table 4.2).

Though biochemistry experiments and genetic data seem to suggest that EOR-1 is not acting as an E3, a more complete biochemical analysis must be conducted to ensure that EOR-1 is not an E3 cofactor. Coimmunoprecipitation experiments should be conducted with SIAH-1 and CUL-3 in the presence or absence of EOR-2, in case EOR-2 acts as a cofactor required for E3 ligase assembly. Positive controls such as EOR-1-EOR-2 or EOR-1-EOR-1 (as EOR-1 can homodimerize (Howell et al., 2010)) coimmunoprecipitation experiments would also ensure that negative interaction data is not being generated due to too-stringent conditions.

Regardless of whether EOR-1 is an E3 cofactor or a transcription factor, more work should also be conducted to verify its position within the linker cell death pathway. Based on

the literature, one might imagine that EOR-1 acts downstream of Wnt signals and in parallel to Hox genes such to promote death (Howard and Sundaram, 2002b). As work from Maxime Kinet in the lab has shown that both Wnt signaling and the Hox gene NOB-1 are required for linker cell death, this is an interesting idea. However, for now, this is only speculation. Epistasis experiments must be conducted to confirm whether EOR-1 acts downstream of Wnt signaling to promote death.

As EOR-1 contains phosphorylation sites, tests should also be carried out to confirm whether EOR-1 is capable of being phosphorylated by components of a kinase cascade for death. As *sek-1* MAPKK mutants cause inappropriate linker cell survival, MAPKs are a possible candidate for EOR-1 phosphorylation and activation. If SEK-1 effectors do indeed phosphorylate EOR-1, then it would close long-standing questions regarding how MAP kinases act to promote cell death.

Experiments should also be conducted to ascertain whether EOR-1 works with or in parallel to components of the MLL histone methyltransferase complex required for death, as previous experiments suggest that EOR-1 can act in parallel to the PolII- recruiting Mediator complex (Howell et al., 2010). Whether EOR-1 acts as an E3 ligase or a missing piece of transcriptional machinery required for linker cell death induction, its role remains an intriguing mystery.

If EOR-1 indeed acts as a transcription factor, one would need to identify to which promoter sites it binds in order to promote linker cell death. One promising candidate for transcription factor binding would be *let-70*, a gene that can and will be easily tested. Crosses of *eor-1*(*cs28*) mutants to *let-70*p::*let-70*::gfp, as well as to reporters for other genes required for linker cell death, should be conducted, as they are an easy way to confirm EOR-1 binding

targets. In order to broaden the potential list of genes, however, one could also perform linker cell-specific RNA-seq of wild-type versus *eor-1(cs28)* mutant animals to ascertain which transcripts are up- or down-regulated in the absence of EOR-1. This list could provide more detail regarding the genes required for linker cell death, and help to clarify the mechanism behind how linker cell death is executed.

Closing comments

The studies outlined here suggest that developmental nonapoptotic cell death programs exist. In the case of the linker cell, ubiquitin proteasome components are transcriptionally upregulated during death of the linker cell, in a manner that shows resemblance to cellular remodeling programs such as spermatogenesis and erythropoeisis. While more experiments need to be conducted, the work carried out here delineates the importance of protein degradation during cell death, and indicates that it may be one of the more downstream components of the linker cell death pathway.

CHAPTER 6: MATERIALS AND METHODS

Strains

C. elegans strains were cultured using standard methods (Brenner, 1974) and were grown at 20°C. Wild-type animals were the Bristol N2 subspecies. The following alleles were crossed to *qIs56* V(Siegfried and Kimble, 2002), an integrated GFP transgene that acts as a linker cell reporter, and *him-8*(e1489) IV or *him-5*(e1490) V (Hodgkin et al., 1979), to increase the percentage of males in the population.

LGI: *hsf-1*(*sy441*) (Hajdu-Cronin et al., 2004)

LGII: *lin-29*(*n333*)(Ambros and Horvitz, 1984); *rrf-3*(*pk1426*)(Simmer et al., 2002)

LGIII: *pqn-41*(*ns294*)(Blum et al., 2012)

LGIV: *siah-1*(*tm1968*) (Japanese National BioResource Project), *eor-1*(*cs28;cs40;cs44*)(Rocheleau et al., 2002)*; let-70*(*ns636;ns770;tm5777*) (Japanese National BioResource Project); *uba-1*(*it129*)(Kulkarni and Smith, 2008)*; egl-20*(*n585*)(Maloof et al., 1999)

LGV: *rde-1*(*ne219*) (Tabara et al., 1999)

LGX: *sek-1*(*ag1*) (Kim et al., 2002), *eor-2*(*cs42*) (Rocheleau et al., 2002)

RNAi experiments

RNAi was performed by feeding on the strains indicated (Blum et al., 2012). Bleached embryos from gravid hermaphrodites were synchronized at the L1 stage by leaving them overnight in M9. L1s animals (30-50% of which were male) were added to each RNAi plate and grown for approximately 48 hours at 20-22°C. 0-2 hour adults were scored using a fluorescent dissecting scope (Leica). Clones were either newly created by cloning into the L4440 vector, or were

already published clones from the Ahringer feeding library (Fraser et al., 2000; Kamath et al., 2003).

Germline transformation and rescue experiments

Germline transformation was carried out as previously described (Mello et al., 1991). For GFP expression analysis, all plasmids were injected into *unc-119*(*ed3*) III; *him-8*(*e1489*) IV hermaphrodites with *unc-119*(+) (Maduro and Pilgrim, 1995) as a transformation marker. All plasmids were injected at between 1-50ng/ul. pBluescript (Agilent) was used to adjust the DNA concentration of injection mixtures if necessary. For rescue studies, animals were picked under a fluorescent dissecting microscope (Leica) the previous night as L3s with YFP- or mCherry-expressing linker cell to a new RNAi plate and scored the following day.

Linker cell survival, migration, and GFP expression assays

Late L4-stage males were analyzed for linker cell defects as previously described (Blum et al., 2012). Linker cell migration defect was calculated by dividing the number of inappropriately migrated linker cells (living or dying), by the total number of animals scored (with or without surviving linker cells). For GFP expression assays, 0-2 hour adults containing the *let-70*pro::*let-70*::gfp (*nsIs241*) or *ubq-1*pro::*ubq-1*::gfp (*nsIs386*) transgenes were scored for the presence or absence of GFP expression in the linker cell. The fraction of animals expressing GFP was divided by the fraction of animals with surviving linker cells in order to obtain an accurate measure of linker cell expression. This method was verified by looking at GFP expression of reporters with a *lag-2*pro::mCherry coinjection marker; results using the two different methodologies showed similar expression patterns.

cDNA isolation of *C. briggsae* and *C. elegans*

Total RNA was extracted using TRIzol (Life Technologies) using standard protocols (Bacaj et al., 2008). 1μg of cDNAs was reverse transcribed from day one adult *C. briggsae* using the SuperScript II Reverse Transcriptase (Life Technologies). *C. briggsae let-70* cDNA with silent mutations was generated using GeneArt® Gene Synthesis (Life Technologies) and cloned into plasmid using standard conditions. C85S point mutation was generated using Pfu turbo polymerase (Agilent) and DpnI digest (NEB) using standard Quikchange protocol (Agilent).

qRT-PCR

1μL of cDNA was used for RT-PCR reaction, which utilized the LightCycler480 SYBR green I master (Roche) on a Roche Applied Science LightCycler 480 System. Reactions were carried out in triplicate, and the values were normalized to four different loading controls: *lmn-1*, *rpl-28*, *cdc-42* and *Y45F10D.4.* Primers used: *pqn-41* 1: 5'-ACAGTCACAGGCTCAACAGCAG, 5'-CGGCTGCGAGTTGTTGGTTATG; *pqn-41* 2: 5'-CAACAACAACAACAACAGCAAA, 5'-CACCGAGCAAATGAGCAAT; *pqn-41* 3: 5'-TCCGCAGAATCTGATCTCGT, 5'-TTGTTGCTCCTGGAGTCGTT; *eor-1*: 5'-TGACACCTAACTTGGTGATGAGA, 5'-TTGTGGATCAGAGTTTGTGGA; *tir-1*: 5'-ACGACACCGACCACCAAAGAAATG, 5'-TTGTGGTCTGCCACCGTTGTTG; *hpk-1*: 5'-TATCCGGCGAGGGAGAATATCAGC, 5'-CCACTTGTCCGAAAGTACCCTTGC; *rpn-11*: 5'-AACGTTCGGAGCCAATCCACAG, 5'-CAGCAACGCCAGCGAAGAAATG;
mig-5: 5'-AGTTTGGGTAGAAACCGCTGTGC, 5'-TAGTTGCCGTTTGCTCCTGTGG; *lin-29:* 5'-AATGGAGAACGAGCTCCTGGGTTC, 5'-TGACCCGTTGTAGCGTTGGATG; *siah-*

1: 5'-TCTGCTCGAACTGCAGACCAAAG, 5'-AGGTTGCGGACAGAAGGAGTTG; *hsf-1*: 5'-TCCTGCTTCAGGAGGACCATCTAC and 5'-CCGAATAGTCTTGTTGCGGCTGAG.

Microscopy

Linker cell death and GFP expression were scored using conventional fluorescence microscopy. An Axioplan II compound microscope (Zeiss) equipped with an AxioCam CCD camera (Zeiss) was used to take images on AxioVision software (Zeiss). For electron microscopy, 0-2 hour adult *let-70*(RNAi) males confirmed to have a surviving linker cell were imaged using the Axioplan II (Zeiss). Linker cell position relative to the animal tail-tip was calculated using the AxioVision software (Zeiss). Animals were fixed, stained, embedded in resin, and serially sectioned using previously described methods (Lundquist et al., 2001). Images were taken using an FEI Technai G2 Spirit BioTwin transmission electron microscope with a Gatan 4K X 4K digital camera.

Statistical methods

An unpaired T test was used for GFP quantification in *rde-1* knockdown animals (Figure S1). Fisher's exact tests were used for quantification of linker cell death experiments as well as quantification of GFP+ linker cells.

CRISPR/Cas9-mediated mutagenesis

Co-CRISPR was conducted as described (Arribere et al., 2014). 21 N2 animals were injected with pDD162(50ng/µl) + pJA58 (50ng/µl) + P61S sgRNA (50ng/µl) + *dpy-10*(*cn64*) oligo (5'-AAACCTCGTGGTGCCTATGGTAGC) (20ng/µl) + P61S oligo (5'-

TTAAATTTATTTTTTTCCAATTTCGATCAATACCTTTGGTGGTTTAAATGAATAGTCT GTTGGGAAGTGGATAGTGAGGAAGAAGACACCTCCCTGATAGG) (20ng/μl) diluted in injection buffer (20mM potassium phosphate, 3mM potassium citrate, 2% PEG, pH 7.5). Animals were picked off on to individual plates and placed at 25°C for 2 days; the resulting DpyRol animals were picked off and PCR genotyped for point mutations.

Yeast two-hybrid assay

Two separate yeast two-hybrid assays were performed with identical results. The first assay utilized the strain and vectors from the DUALHybrid Kit (Dualsystems Biotech). *let-70*, *siah-1*, *rbx-1*, *tir-1b*, and *pqn-41*C fragments were cloned into pLexA and pGAD vectors and co-transformed into the NMY51 yeast strain using the lithium acetate method. Selection was performed on SD medium lacking adenine, histidine, leucine and tryptophan. The second assay used vectors and yeast strains as previously described (Tang et al., 1997). *let-70*, *siah-1*, *rbx-1* and *pqn-41*C were cloned into pJG4-5 and pEG202 vectors (Gift from Russ Finley; NBRP Yeast). Bait and prey were cotransformed using the lithium acetate method into the yeast strain EGY48 carrying the pSH18-34 plasmid. Selection was performed using SD medium lacking histidine, tryptophan and uracil.

Purification of 6x-His-tagged proteins

cDNA of the gene of interest (*let-70, siah-1, bar-1, hpk-1, skr-1, sel-10*) in the vector pET28b(+) (Novagen) was transformed into BL21(DE3) cells (LifeTechnologies) using heat shock. Cells were induced overnight with 500mM IPTG at 25°C overnight. Purification was performed using a previously described protocol (Sandu et al., 2010).

In vitro ubiquitination assay

Proteins used were recombinant *Drosophila* Uba1, Diap1, and ubiquitin (Gift from C. Sandu); and *C. elegans* His-LET-70 (purified as above). Ubiquitination assay was conducted as previously described (Sandu et al., 2010). For the SCF in vitro assay, purified SCF was obtained from EMD Millipore.

Transfection of S2 cells

Cells were split at $1x10^6$ cells per mL, and 8mL were added to a 10-cm plate. The next day, a transfection mix of 500μL of Opti-MEM® (Life Technologies), 5μg of DNA per construct and 40μL of FuGENE HD® Transfection Reagent (Promega) were mixed and added to each plate.

Immunoprecipitation from S2 Cells

48 hours after transfection, the cells were harvested by addition of IP lysis buffer (600mM Tris pH 8.0; 1% NP-40, 10% glycerol, complete Protease Inhibitor Cocktail Tablets (Roche)). Cells were spun at 4000RPM for 1 minute resuspended in lysis buffer, transferred to Eppendorf tubes and rotated at 4°C for 30 minutes. Lysate was spun at max speed and supernatant was added to 20μL of myc-agarose beads (Genetex) and rotated at 4°C for two hours. Beads were washed three times using lysis buffer and eluted with 40μL of sample buffer. 10μL were loaded per well and analyzed by western blot. Membranes were probed for myc (rabbit polyclonal, 1:5000, Abcam AB9106) and HA (rat anti-HA peroxidase, 1:2000, Roche 3F10).

Nuclear fractionation experiments

Four peptone plates of worms were washed in M9 and resuspended in 2 volumes of cold hypotonic buffer (10mM KCl, 1.5 mM $MgCl_2$, 1mM EDTA, 1mM EGTA, 1mM DTT, 0.1 mM phenlmethylsufolnyl fluoride, 250 mM sucrose). The suspension was dripped into $N_2(l)$, and the resulting balls were ground in a mortar. The powder was thawed on ice and sheared using a douncer (30 strokes, pistol B). The homogenates were centrifuged at 40*g* briefly to remove worm debris. The supernatant was centrifuged twice at 750*g* for 10 minutes and the resulting pellets were pooled as the nuclear fraction. The supernatant was further centrifuged at 100,000*g* for 1 hour. One-fifth of each fraction was used for immunoblotting analysis. Rabbit polyclonal antibody directed against human H3 (Abcam, 1:10,000) was used as a marker for the nuclear fraction.

Transgenic strains

Transgene	Constructs	Reference
nsEx3669, nsEx3670, nsEx3671, nsEx3672	*mig-24*pro::*let-70 C. briggsae* cDNA silently point mutated to avoid RNAi + *unc-119(+)* + *lag-2*p::yfp	This work
nsEx3683, nsEx3684	*mig-24*pro::*let-70 C. briggsae* cDNA C85S + *lag-2*pro::yfp + *unc-119*(+)	This work
nsEx3081	*mig-24*pro::*rde-1* cDNA::SL2::mCherry + *lag-2*p::mCherry	(Blum et al., 2012)
nsEx3680, nsEx3681, nsEx3682,	*mig-24*pro::*let-70* cDNA + *lag*-2pro::mCherry + *unc-119*(+)	This work
nsEx3667, nsEx3668,	*mig-24*pro::*let-70* cDNA::SL2::*pqn-41C* cDNA+ *lag-2*pro::mCherry + *unc-119*(+)	This work
nsEx3662, nsEx3663, nsEx3664, nsEx3665, nsEx3666	*mig-24*pro::*let-70* cDNA + *mig-24*pro::*pqn-41C* cDNA + *lag-2*pro::*mCherry* + *unc-119*(+)	This work
nsEx3733	*mig-24*pro::*let-70* cDNA+ *mig-24*pro::*pqn-41*B cDNA + *lag-2*pro::*mCherry* + *unc-119*(+)	This work
nsEx4101, nsEx4012	*mig-24*pro::*ubq-1*cDNA + *lag-2*pro::yfp + *unc-119*(+)	This work
nsEx4103, nsEx4134	*mig-24*pro::*ubq-1*::SL2::*let-70* + *lag-2*pro::yfp + *unc-119*(+)	This work
nsEx3887	*mec-7*pro::*let-70* cDNA + *rol-6*	This work
nsEx3717	*mec-7*pro::*let-70* cDNA::SL2::*pqn-41C* cDNA + *rol-6*	This work
nsEx3721	*mec-7*pro::*let-70* cDNA::SL2::gfp + *mec-7*pro::*pqn-41C* cDNA + *unc-119*(+)	This work
nsEx3722, nsEx3723	*mec-7*pro::*let-70* cDNA::SL2::*pqn-41C* cDNA + *mec-7*pro::gfp + *un-119*(+)	This work
nsEx2866,	pJAZ002 (*let-70*(1.5kb)pro::GFP) + *unc-119*(+)	This work
nsEx2864, nsEx2865	pJAZ001 (*let-70*(1.5kb)pro::*let-70*::GFP + *unc-119*(+)	This work
nsEx3284	*let-70*(1.5kb)pro::*let-70::*GFP::*let-70* 3'UTR + *unc-119*(+)	This work
nsEx3285	*let-70*(1.5kb)pro::GFP::*let-70* 3'UTR + *unc-119*(+)	This work
nsEx4197,	*rbx-1*pro::GFP + *unc-119*(+)	This work
nsEx3889	*ubq-1*pro::GFP + *unc-119*(+)	This work

Transgene	Constructs	Reference
nsEx3950, nsEx3952, nsEx3993, nsEx3994	*ubq-1*pro::*ubq-1* first monomer::GFP + *unc-119*(+)	This work
nsEx3845	*mig-24*pro::GFP::*siah-1* cDNA + *unc-119*(+)	This work
nsEx3755, nsEx3756	*ubq-1*pro::*ubq-1* first monomer::mCherry + *unc-119*(+)	This work
nsEx3851, nsEx3870, nsEx3891	*ubq-1*pro::mCherry + *unc-119*(+)	This work
sEx10785	*cul-3*pro::GFP + *pCeh361* (*dpy-5* (+))	(McKay et al., 2003)
sEx10148	*rpn-3*pro::GFP + *pCeh361* (*dpy-5* (+))	(McKay et al., 2003)
nsEx4475	*siah*-1::GFP fosmid + *unc-119*(+)	(Sarov et al., 2012), This work
nsEx4111	*let-70* rescue fosmid (WRM0617dB10- Vancouver Fosmid Library) + *lag-2*pro::mCherry + pBlueScript	This work
nsEx4108	*rbx*-1pro::GFP fosmid	(Sarov et al., 2012), This work
nsEx4818, nsEx4819, nsEx4834	*eor-1*pro::*eor-1*::gfp + *lag-2*pro::mCherry + *odr-1*pro::mCherry + pUC19	(Howard and Sundaram, 2002), This work
csEx126	*eor-1*::GFP + *ttx-3*::GFP	(Howard and Sundaram, 2002)

Plasmid Construction

All primer sequences written 5' to 3'

Construct	Description	Notes
pJAZ001	*let-70*::gfp in pPD95_75	N2 genomic sequence was amplified using primers: 5'-GATTGGGCATGCTTTCCATATCTCTTG and 5'-GTTAGGGTACCCACATAGCGTACTTTTGCGTCC, and ligated into pPD95.75 (Andrew Fire) as an SphI/KpnI fragment.
pJAZ002	*let-70*pro::gfp in pPD95_75	N2 genomic sequence was amplified using primers: 5'-GATTGGGCATGCTTTCCATATCTCTTG and 5'-CTTTTGGTACCCATGTTGGTGTTCTGATTTGCTG, and ligated into pPD95.75 (Andrew Fire) as an SphI/KpnI fragment.
pJAZ005	*siah-1* RNAi in L4440	cDNA library was amplified using primers: 5'-GCGCGGCCGCAAACGATGGCCAGAGTTCAG and 5'-GCGCGTCGACTCCAAGGTTTCCGTTTTCTG. This XbaI/XmaI fragment was ligated into L4440 (Julie Ahringer).
pJAZ006	*let-70* RNAi in L4440	The entire *let-70* cDNA sequence was amplified from a cDNA library using 5'-GCGCTCTAGATCCATTGGCAAGCTACGATT and 5'-GCGCGGTACCCCATTCTCTCGCCAATTGAT. This XbaI/KpnI fragment was ligated into L4440 (Julie Ahringer).
pJAZ007/JAZ023	*let-70*::gfp + *let-70* 3'UTR in pPD95_75 (in JAZ020)	N2 DNA was amplified using primers 5'-GATTGGGCATGCTTTCCATATCTCTTG and 5'-GTTAGGGTACCCACATAGCGTACTTTTGCGTCC. The fragment was inserted into pJAZ020 using SphI/KpnI.
pJAZ008	*let-70* 3'UTR RNAi in L4440 (RNAi C)	N2 genomic sequence was amplified using 5'-GGCGGCCGCGAGGCTAACACCATTCATACAAGA and 5'-GGGTCGACATGCAGTGGGCTCTTCAGTAATTTATTCAGGATTCTCAGACC. This NotI/SalI fragment was ligated into L4440.

Construct	Description	Notes
pJAZ009	*nhr-67/let-70* RNAi in L4440	cDNA library was amplified using 5'-GGCCTCTAGAGGATCCTCTCCTAATTCGCC and 5'-GGCCCCCGGGTGTTGTGGTGGCTTGAACAT. This XbaI/XmaI fragment was ligated into an L4440 already containing *let-70* RNAi between sites HindIII/XhoI.
pJAZ012	*set-16/let-70* RNAi in L4440	cDNA library was amplified using 5'-GCGCTCTAGATGCAATCATAAAGCAGCGTCand 5'-GCGCCCCGGGGCGTCACTTGATCTGAG. This XbaI/XmaI fragment was ligated into an L4440 already containing *let-70* RNAi between HindIII and XhoI (*pJAZ021)*.
pJAZ013	*nhr-67* RNAi in L4440	cDNA library was amplified using 5'-GGCCTCTAGAGGATCCTCTCCTAATTCGCC and 5'-GGCCCCCGGGTGTTGTGGTGGCTTGAACAT. This XbaI/XmaI fragment was ligated into L4440.
pJAZ015	*set-16* RNAi in L4440	cDNA library was amplified using 5'-GCGCTCTAGATGCAATCATAAAGCAGCGTCand 5'-GCGCCCCGGGGCGTCACTTGATCTGAG. This XbaI/XmaI fragment was ligated into L4440.
pJAZ018	*tir-1* RNAi in L4440	cDNA library was amplified using 5'-GCGCTCTAGAATCGGATACGATGAAGCTGG and 5'-GCGCCCCGGGCCGATGAGTAATCAGCAGCA. This XbaI/XmaI fragment was ligated into L4440.
pJAZ019	*tir-1/let-70* RNAi in L4440	cDNA library was amplified using 5'-GCGCTCTAGAATCGGATACGATGAAGCTGG and 5'-GCGCCCCGGGCCGATGAGTAATCAGCAGCA. This XbaI/XmaI fragment was ligated into an L4440 already containing *let-70* RNAi between HindIII and XhoI (*pJAZ021)*.
pJAZ021	*let-70* RNAi in L4440	cDNA library was amplified using 5'-GCGCAAGCTTTCCATTGGCAAGCTACGATT and 5'-GCGCCTCGAGCCATTCTCTCGCCAATTGAT, and inserted into L4440 using HindIII/XhoI.

Construct	Description	Notes
pJAZ022	*let-70*p::gfp with *let-70 3'UTR*	N2 genomic sequence was amplified using primers: 5'-GATTGGGCATGCTTTCCATATCTCTTG and 5'-CTTTTGGTACCCATGTTGGTGTTCTGATTTGCTG, and ligated into pJAZ020 as an SphI/KpnI fragment.
pJAZ024	*rbx-1/let-70* RNAi in L4440	cDNA library was amplified using 5'-GCGCTCTAGAATGGCCCAAGCAAGCGACAG and 5'-GCGCCCCGGGTTAGTGTCCGTACTTTTGGA. This XbaI/XmaI fragment was ligated into an L4440 already containing *let-70* RNAi between HindIII and XhoI (*pJAZ021)*.
pJAZ025	*gpd-2/let-70* RNAi in L4440	cDNA library was amplified using 5'-GCGCTCTAGATGTGGGTTGAGTGAGATGGA and 5'-GCGCCCCGGGAATTTTCAGCCATGCCAAAG. This XbaI/XmaI fragment was ligated into an L4440 already containing *let-70* RNAi between HindIII and XhoI (*pJAZ021)*.
pJAZ026	*swd-2.2/let-70* RNAi in L4440	cDNA library was amplified using 5'-GCGCTCTAGATTTGTTAATTCCGGGTTTGC and 5'-GCGCCCCGGGCGGAGCTTCCCACCATAATA. This XbaI/XmaI fragment was ligated into an L4440 already containing *let-70* RNAi between HindIII and XhoI (*pJAZ021)*.
pJAZ027	*mCherry/let-70* RNAi in L4440	mCherry genomic sequence was amplified using 5'-GCGCTCTAGAAAGGGCGAGGAGGATAACAT and 5'-GCGCCCCGGGTTGACCTCAGCGTCGTAGTG. This XbaI/XmaI fragment was ligated into an L4440 already containing *let-70* RNAi between HindIII and XhoI (*pJAZ021)*.
pJAZ029	*swd-2.2* RNAi in L4440	cDNA library was amplified using 5'-GCGCTCTAGATTTGTTAATTCCGGGTTTGC and 5'-GCGCCCCGGGCGGAGCTTCCCACCATAATA. This XbaI/XmaI fragment was ligated into an L4440 vector.

Construct	Description	Notes
pJAZ030	*rpn-3* RNAi in L4440	cDNA library was amplified using 5'-GCGCTCTAGAACAATGATCTTGCCCGCTAC and 5'-GCGCCCCGGGGGACAGGGATCTCGATTTGA. This XbaI/XmaI fragment was ligated into an L4440 vector.
pJAZ031	*rpn-3/let-70* RNAi in L4440	cDNA library was amplified using 5'-GCGCTCTAGAACAATGATCTTGCCCGCTAC and 5'-GCGCCCCGGGGGACAGGGATCTCGATTTGA. This XbaI/XmaI fragment was ligated into an L4440 already containing *let-70* RNAi between HindIII and XhoI (*pJAZ021)*.
pJAZ033	*rbx-1* RNAi in L4440	cDNA library was amplified using 5'-GCGCTCTAGAATGGCCCAAGCAAGCGACAG and 5'-GCGCCCCGGGTTAGTGTCCGTACTTTTGGA. This XbaI/XmaI fragment was ligated into an L4440 vector.
pJAZ034	*gpd-2* RNAi in L4440	cDNA library was amplified using 5'-GCGCTCTAGATGTGGGTTGAGTGAGATGGA and 5'-GCGCCCCGGGAATTTTCAGCCATGCCAAAG. This XbaI/XmaI fragment was ligated into an L4440 vector.
pJAZ035	*lin-29* RNAi in L4440	cDNA library was amplified using 5'-GCGCTCTAGAAGAGCACAGATTTTTGAACGAAG and 5'-GCGCCCCGGGATTTAATTTTACAGCCGATGGGT. This XbaI/XmaI fragment was ligated into an L4440 vector.
pJAZ036	*lin-29/let-70* RNAi in L4440	cDNA library was amplified using 5'-GCGCTCTAGAAGAGCACAGATTTTTGAACGAAG and 5'-GCGCCCCGGGATTTAATTTTACAGCCGATGGGT. This XbaI/XmaI fragment was ligated into an L4440 already containing *let-70* RNAi between HindIII and XhoI (*pJAZ021)*.
pJAZ038	*mig-24*pro::*let-70 briggsae* C85S	pJAZ042 was mutagenized using Quikchange primers: 5'-ATTAACTCGAACGGATCGATTTCCCTCGATATTCTCCGATCACA and 5'-TGTGATCGGAGAATATCGAGGGAAATCGATCCGTTCGAGTTAAT using site-directed mutagenesis kit (Stratagene)

Construct	Description	Notes
pJAZ039	*mig-24*pro::*let-70* cDNA::SL2::*pqn-41C* cDNA	pEB28 was amplified using 5'-GCGCTCGAGATGGCGGCTGCAATAAA and 5'-CGCGGAATTCTCATCGTCCATTCGGCA. This XhoI/EcoRI fragment was ligated into pJAZ043.
pJAZ040	*mig-24*pro::*let-70* cDNA	cDNA library was amplified using 5'-GCGCGGTACCGGTAGAAAAAATGGCTC TCAAAAGAATCCA and 5'-GCGCGAATTCCAGACGCTCTTCAGTAA TTT. The KpnI/EcoRI fragment was ligated into a *mig-24*p::mCherry vector.
pJAZ041	*cdh-3*pro::*let-70* cDNA	cDNA library was amplified using 5'-CGCGTTAATTAATTTATCAGTTATCAGC AAGCAGAGA and 5'-CCGGGGTACCGCCATTTTAATAAAATT GTGTA. This PacI/KpnI fragment was ligated into pJAZ041 vector.
pJAZ042	*mig-24*pro::*let-70 briggsae* cDNA point mutated rescue	*let-70* cDNA carrying point mutations and flanked by KpnI/EcoRI was engineered via GeneArt Gene Synthesis (Life Technologies). The fragment was digested and inserted into a *mig-24*p::mCherry vector using KpnI/EcoRI.
pJAZ045	*ubq-1*::mCherry	N2 genomic sequence was amplified using 5'-GCGCGAGCTCCAGTTGCATGACGAGAA AAAAGA and 5'-GGTACCCCAATGTCTCCTCCGCGAAGA CGAAGAACG. This SacI/KpnI fragment was ligated into a *mig-24*p::mCherry vector.
pJAZ047	*cdh-3*pro::*let-70* cDNA::SL2::*pqn-41C* cDNA	pJAZ041 was amplified using 5'-CGCGGAGCTCTTTATCAGTTATCAGCAA GCAGAGA and 5'-CGCGGGCCCGAGCTTTAGAACATTAAA AAA. The SacI/XbaI fragment was ligated into pJAZ039.
pJAZ048	*mec-7*pro::*let-70* cDNA	pJAZ040 was amplified using 5'-GCGCGGTACCGGTAGAAAAAATGGCTC TCAAAAGAATCCA and 5'-CGCGATATCTCACATAGCGTACTTTTGC GTCC. The KpnI/EcoRV fragment was ligated into the pPD52_102 vector (Fire lab).

Construct	Description	Notes
pJAZ049	*LexA*::*let-70* cDNA	pJAZ040 was amplified using 5'-CGGGTACCATGGCTCTCAAAAGAATCCAGAAGG and 5'-CGCCGCGGTCACATAGCGTACTTTTGCGTCCATT. This KpnI/SacII fragment was ligated into pLexA-N (DUALHybrid).
pJAZ050	*GAD*::*let70* cDNA	pJAZ040 was amplified using 5'-CGCCCCGGGGATGGCTCTCAAAAGAATCCAGAAGG and 5'-CGCTCTAGATCACATAGCGTACTTTTGCGTCCATT. This XmaI/XbaI fragment was ligated into pGAD-HA(DUALHybrid).
pJAZ051	*LexA*::*tir-1B* cDNA	*tir-1b* cDNA clone from *C. elegans* ORFeome library was amplified using 5'-CGGGTACCATGTGTGCCCTAGTCTCATCTCCAA and 5'-CGCCGCGGTTAATTCCGATCGGAAGTTGTGGATG. This KpnI/SacII fragment was ligated into pLexA-N (DUALHybrid).
pJAZ052	*GAD*::*tir-1B* cDNA	*tir-1b* cDNA clone from *C. elegans* ORFeome library was amplified using 5'-CGCCCCGGGGATGTGTGCCCTAGTCTCATCTCCAA and 5'-CGCGTCTAGATTAATTCCGATCGGAAGTTGTGGATG. This XmaI/XbaI fragment was ligated into pGAD-HA(DUALHybrid).
pJAZ053	*LexA*::*siah-1* cDNA	cDNA library was amplified using 5'-GCGGTACCGGTAGAAAAAATGAGTAATCGGAACGGTGGT and 5'-CGCCGCGGCTAGTCGTACTCGAGATCAGAATTTT. This KpnI/SacII fragment was ligated into pLexA-N (DUALHybrid).
pJAZ054	*GAD*::*siah-1* cDNA	cDNA library was amplified using 5'-CGCCCCGGGGATGAGTAATCGGAACGGTGGTGGAG and 5'-CGCTCTAGACTAGTCGTACTCGAGATCAGAATTTT. This XmaI/XbaI fragment was ligated into pGAD-HA(DUALHybrid).
pJAZ055	*mec-7*pro::*pqn-41C* cDNA ("QC" has KpnI cut site removed from between *mec-7* and *pqn*)	pEB28 was amplified using 5'-GCGGGTACCATGGCGGCTGCAATAAATGAAGCAACGCGA and 5-GCGCGATATCTCATCGTCCATTCGGCATTTGCGGCGGCTT. This KpnI/EcoRV fragment was ligated into pPD52_102 (Fire lab).

Construct	Description	Notes
pJAZ056	*mec-7*pro::*let-70* cDNA::SL2::*pqn-41C* cDNA	KpnI cut site mutagenized out of *mec-7::let-70* using primers 5'-AGGAGGACCCTTGGCTAGCGTCGACGGTTCCGGTAGAAAAAATGGCTCTC and 5'-GAGAGCCATTTTTTCTACCGGAACCGTCGACGCTAGCCAAGGGTCCTCCT. Resulting vector was amplified using primers 5'-GCGCATGCAATGTAAACCTGTCATTTCTGTGTATTTCAGC and 5'-CGCGGTACCTCACATAGCGTACTTTTGCGTCCATTCTCTCG. The resulting SphI/KpnI fragment was ligated into pJAZ039.
pJAZ057	*mec-7*pro::*let-70* cDNA::SL2::GFP	pJAZ056 was digested using SphI/KpnI. The resulting fragment was ligated into pSM-SL2-GFP vector.
pJAZ059	*mec-7*pro::gfp	pPD52_102 was digested using XbaI/XmaI (Fire lab). This fragment was ligated into pPD95_75 (Fire lab).
pJAZ060	*6xHis*::*let-70* cDNA in pET28b(+)	*pJAZ040* was used as a template for amplification using the primers 5'-GCGGGATCCATGGCTCTCAAAAGAATCCAG and 5'-GCGGCCGCTCACATAGCGTACTTTTGCG The fragment was ligated into *pET28b(+)* (Novagen) using BamHI and NotI.
pJAZ061	*6xHis*::FLAG::*siah-1* cDNA in pET-28b(+)	N2 cDNA library was used to amplify fragment and add external FLAG tag. Primers used were 5'-CGCGGATCCGATTACAAGGATGACGATGACAAGATGAGTAATCGGAACGG and 5'-GCGGCCGCCTAGTCGTACTCGAGATCAGAATTTTCCA. Fragment was ligated into *pET28b(+)* (Novagen) using BamHI and NotI.

Construct	Description	Notes
pJAZ066	*mig-24*pro::GFP::*siah-1* cDNA	N2 cDNA library was used to amplify *siah-1* fragment using primers 5'-GCGGATCCGGTAGAAAAAATGAGTAATCGGAACGGTGGT and 5'-GCGGTACCCCGTCGTACTCGAGATCAGAATTTTC. Fragment was inserted into pPD95.75 (Andrew Fire) using BamHI and KpnI. *mig-24*pro was amplified from *mig-24*::mCherry vector using primers 5'-CGGTCGACAGCTTTAGAACATTAAAAAA and 5'-CGGGATCCCCCATTTTAATAAAATTGTGTAAGATGAC and was cloned into *siah-1*::GFP using SalI and BamHI.
pJAZ067	*ubq-1*pro::mCherry	N2 genomic sequence was amplified using primers 5'-GCGCGAGCTCCAGTTGCATGACGAGAAAAAAGA and 5'-GCGGGTACCGATTGCTGAAAAAATAGAAAATGAGTGCG. The SacI/KpnI fragment was ligated into a *mig-24*p::mCherry vector.
pJAZ068	*ubq-1*pro::*ubq-1*::GFP	N2 genomic sequence was amplified using primers 5'-GCGCGCATGCCAGTTGCATGACGAGAAAAAAGA and 5'-GGTACCCCAATGTCTCCTCCGCGAAGACGAAGAACG. The SphI/KpnI fragment was ligated into pPD95.75.
pJAZ069	*ubq-1*pro::GFP	pJAZ045 was amplified using primers 5'-GCGCGCATGCCAGTTGCATGACGAGAAAAAAGA and 5'-GCGGGTACCGATTGCTGAAAAAATAGAAAATGAGTGCG. The SphI/KpnI fragment was ligated into pPD95.75.
pJAZ073	LexA::*siah-1* RING domain	pJAZ053 was amplified using 5'-GCGGGTACCAGCAGTGCAGAGATCTTGTCGGTGTTT and 5'-CGCCGCGGCTAGCCCAGGTTGCGGACAGAAGGAGTTG. The KpnI/SacII fragment was ligated into pLexA-N (DUALHybrid).

Construct	Description	Notes
pJAZ074	GAD::*siah-1* RING domain	pJAZ053 was amplified using 5'-CGCGCCCGGGGAGCAGTGCAGAGATCTTGTCGGTGTTT and 5'-GGCCTCTAGATCAGCCCAGGTTGCGGACAGAAGGAGTTG. The XmaI/XbaI site was ligated into pGAD-HA(DUALHybrid).
pJAZ075	LexA::*siah-1* SIAH domain	pJAZ053 was amplified using 5'-GCGGGTACCCGCAACCTGGGCCTCGAGAAGATC and 5'-CGCCGCGGCTAGATATCCTCGCCTTGAAGCGTCGTGAT. The KpnI/SacII fragment was ligated into pLexA-N (DUALHybrid).
pJAZ076	GAD::*siah-1* SIAH domain	pJAZ053 was amplified using 5'-CGCGCCCGGGGCGCAACCTGGGCCTCGAGAAGATC and 5'-GGCCTCTAGATCAGATATCCTCGCCTTGAAGCGTCGTGAT. The XmaI/XbaI fragment was ligated into pGAD-HA(DualHybrid).
pJAZ078	GAD::*let-70* UBC fold	pJAZ049 was amplified using 5'-CGCCCCGGGGATGGCTCTCAAAAGAATCCAGAAGG and 5'-GGCCTCTAGATCATGGATCACAGAGCAGCGAGCAGATCG. The XmaI/XbaI fragment was ligated into pGAD-HA(DualHybrid).
pJAZ079	LexA::*let-70* UBC fold	pJAZ049 was amplified using 5'- and 5'-CGCCGCGGTCATGGATCACAGAGCAGCGAGCAGATCG. This The KpnI/SacII fragment was ligated into pLexA-N (DUALHybrid).
pJAZ081	LexA::*siah-1* Siah binding domain (SBD)/TRAF-like	pJAZ053 was amplified using 5'-CGCGGGTACCGGAGCCACCGACGACAGCAGTGCA and 5'-CGCGCCGCGGCTAGTCGTACTCGAGATCAGA. This KpnI/SacII fragment was ligated into pLexA-N(DUALHybrid).
pJAZ082	GAD::*siah-1* Siah binding domain (SBD)/TRAF-like	pJAZ053 was amplified using 5'-CGCGCCCGGGGGGAGCCACCGACGACAGCAGTGCA and CGCGTCTAGACCTAGTCGTACTCGAGATCA. This XmaI/XbaI fragment was ligated into pGAD-HA (DUALHybrid).

Construct	Description	Notes
pJAZ084	*mig-24*pro::*ubq-1*cDNA	N2 cDNA library was amplified using 5'-GCGCGGTACCCATGCAAATCTTCGTCA and 5'-GCGCGGAATTCTCACCCAATGTCTCCTCCGCGAAG. This KpnI/EcoRI fragment was ligated into pJAZ040.
pJAZ086	*AC*pro::myc::let-*70 cDNA*	pJAZ040 was amplified using primers 5'-CGCGGCGGCCGCATGGCTCTCAAAAGAATCCAGAA and 5'-CGCGGCGGCCGCATGGCTCTCAAAAGAATCCAGAA. The NotI/ApaI fragment was inserted into pGO119 (Drosophila actin 5c promoter vector, gift from Grigorios Oikonomou (Oikonomou et al., 2011).
pJAZ087	*AC*pro::HA::*siah-1 cDNA*	cDNA library was amplified using primers 5'-CGCGGCGGCCGCATGAGTAATCGGAACGGTGGTGG and 5'-CGCGGGGCCCCTAGTCGTACTCGAGATCAGAATTT. The NotI/ApaI fragment was inserted into pGO123 (Grigorios Oikonomou).
pJAZ088	*AC*pro::HA::*siah-1* RING domain	cDNA library was amplified using primers 5'-CGCGGCGGCCGCAGCAGTGCAGAGATCTTGTCGGT and 5'-CGCGGGGCCCCTAGCCCAGGTTGCGGACAGAA. The NotI/ApaI fragment was inserted into pGO123 (Grigorios Oikonomou).
pJAZ089	*AC*pro::HA::*siah-1* SIAH domain	cDNA library was amplified using primers 5'-CGCGGCGGCCGCCGCAACCTGGGCCTCGAGAAGAT and 5'-CGCGGGGCCCGCTAGATATCCTCGCCTTGAAGCGT. The NotI/ApaI fragment was inserted into pGO123 (Grigorios Oikonomou).
pJAZ090	*AC*pro::HA::*siah-1* SBD/TRAF domain	cDNA library was amplified using primers 5'-CGCGGCGGCCGCGGAGCCACCGACGACAGCAGTGC and 5'-CGCGGGGCCCCTAGTCGTACTCGAGATCAGAATTT. The NotI/ApaI fragment was inserted into pGO123 (Grigorios Oikonomou).
pJAZ091	*AC*pro::HA::*rbx-1 cDNA*	cDNA library was amplified using primers 5'-CGCGGCGGCCGCATGGCCCAAGCAAGC and 5'-CGCGGGGCCCTTAGTGTCCGTACTTTTGG. The NotI/ApaI fragment was inserted into pGO123 (Grigorios Oikonomou).

Construct	Description	Notes
pJAZ092	GAD::rbx-*1* cDNA	N2 cDNA library was amplified using 5'-CGCGCCCGGGGATGGCCCAAGCAAGCGACAGCACAGCT and 5'-CGCGTCTAGATTAGTGTCCGTACTTTTGGAATTC. This XmaI/XbaI fragment was ligated into pGAD-HA(DUALHybrid).
pJAZ093	LexA::rbx-*1* cDNA	N2 cDNA library was amplified using 5'-CGCGGGTACCATGGCCCAAGCAAGCGACAGCA and 5'-GCGCCCGCGGTTAGTGTCCGTACTTTTGGAATTCCC. This KpnI/SacII fragment was ligated into pLexA-N (DUALHybrid).
pJAZ094	*mig-24*pro::*ubq-1*::SL2::*let-70*	pJAZ040 was amplified using 5'-CGCGCTCGAGATGGCTCTCAAAAGAATCCAGA and 5'-CGCGGAATTCTCACATAGCGTACTTTTGCGTCCA. This EcoRI/BamHI fragment was ligated into pJAZ084.
pJAZ097	*let-70* cDNA in pJG4-5	pJAZ040 was amplified using primers 5'-CGCGGAATTCATGGCTCTCAAAAGAATCCAGAAG and 5'-CGCGCTCGAGTCACATAGCGTACTTTTGCGTCCA. The XhoI/EcoRI fragment was inserted into pJG45(gift, R. Finley).
pJAZ098	*siah-1* cDNA in pJG4-5	N2 cDNA library was amplified using primers 5'-GCGCGAATTCATGAGTAATCGGAACGGTGGTGGA and 5'-CGCGCTCGAGCCTAGTCGTACTCGAGATCAGAAT. The XhoI/EcoRI fragment was inserted into pJG45(gift, R. Finley).
pJAZ099	UBC domain (*let-70*) cDNA in pJG4-5	pJAZ040 was amplified using primers 5'-CGCGGAATTCATGGCTCTCAAAAGAATCCAGAAG and 5'-CGCGCTCGAGTCATGGATCACAGAGCAGCGAGCA. The XhoI/EcoRI fragment was inserted into pJG45 (gift, R. Finley).
pJAZ100	RING domain (*siah-1*) cDNA in pJG4-5	pJAZ098 was amplified using primers 5'-CGCGGAATTCAGCAGTGCAGAGATCTTGTCGGTG and 5'-CGCGCTCGAGCTAGCCCAGGTTGCGGACAGAAGG. The XhoI/EcoRI fragment was inserted into pJG45 (gift, R. Finley).

Construct	Description	Notes
pJAZ101	SIAH domain (*siah-1*) cDNA in pJG4-5	pJAZ098 was amplified using primers 5'-CGCGCCCGGGCGCAACCTGGGCCTCGAGAAGATC and 5'-CGCGGGGCCCCTAGATATCCTCGCCTTGAAGCG. The XmaI/ApaI fragment was inserted into pJG45(gift, R. Finley).
pJAZ102	SBD/TRAF domain (*siah-1*) cDNA in pJG4-5	pJAZ098 was amplified using primers 5'-CGCCCCGGGGGAGCCACCGACGACAGCAGTGCA and 5'-CGCGGGGCCCCTAGTCGTACTCGAGATCAGAAT. The XmaI/ApaI fragment was inserted into pJG45(gift, R. Finley).
pJAZ103	*pqn-41C* cDNA in pJG4-5	pEB28 was amplified using primers 5'-CGCGGAATTCATGGCGGCTGCAATAAATGAAGCA and 5'-CGCGCTCGAGTCATCGTCCATTCGGCATTTGCGG. The XhoI/EcoRI fragment was inserted into pJG45(gift, R. Finley).
pJAZ104	*rbx-1* cDNA in pJG4-5	N2 cDNA library was amplified using primers 5'-CGCGGAATTCATGGCCCAAGCAAGCGACAGCACA and 5'-CGCGCTCGAGTTAGTGTCCGTACTTTTGGAATTC. The XhoI/EcoRI fragment was inserted into pJG45(gift, R. Finley).
pJAZ105	*let-70* cDNA in pEG202	Fragment from pJAZ097 was inserted into pEG202 (NBRP Yeast) following digest with EcoRI/XhoI.
pJAZ106	*siah-1* cDNA in pEG202	Fragment from pJAZ098 was inserted into pEG202 (NBRP Yeast) following digest with EcoRI/XhoI.
pJAZ107	UBC domain (*let-70*) cDNA in pEG202	Fragment from pJAZ099 was inserted into pEG202 (NBRP Yeast) following digest with EcoRI/XhoI.
pJAZ108	RING domain (*siah-1*) cDNA in pEG202	Fragment from pJAZ100 was inserted into pEG202 (NBRP Yeast) following digest with EcoRI/XhoI.
pJAZ109	SIAH domain (*siah-1*) cDNA in pEG202	Fragment from pJAZ101 was inserted into pEG202 (NBRP Yeast) following digest with EcoRI/XhoI.
pJAZ110	SBD/TRAF domain (*siah-1*) cDNA in pEG202	Fragment from pJAZ102 was inserted into pEG202 (NBRP Yeast) following digest with EcoRI/XhoI.

Construct	Description	Notes
pJAZ111	*pqn-41C* cDNA in pEG202	Fragment from pJAZ103 was inserted into pEG202 (NBRP Yeast) following digest with EcoRI/XhoI.
pJAZ112	*rbx-1* cDNA in pEG202	Fragment from pJAZ104 was inserted into pEG202 (NBRP Yeast) following digest with EcoRI/XhoI.
pJAZ113	6xHis::FLAG::*rbx-1* cDNA in pET28b(+)	pJAZ104 was amplified using primers 5'-CGCGGGATCCCGATTACAAGGATGACGATGACAAGATGGCCCAAGCAAGCGACAGCACAGCTAT and 5'-CGCCGCGGGCCGCTTAGTGTCCGTACTTTTGGAATTCCCACT. The BamHI/NotI fragment was ligated into pET28b(+) (Novagen).
pJAZ114	6xHis::HA::*bar-1* cDNA in pET28b(+)	The vector was assembled using the Gibson protocol as previously described (Gibson et al., 2009). *bar-1* primers 5'-TCAGTGGTGGTGGTGGTGCTCGAGTGCTTAAAATCGACTATTCCTAGAAGG and 5'-CGAATTCGAGCTCCGATGGAGTACCCATACGAC. pET28b(+):5'-GTCGACGGAGCTCGAATTCGGATCCCGACCCATTT and 5'-GCGGCCGCACTCGAGCACCACCACCACCACCACT. All fragments were DpnI digested prior to assembly.
pJAZ117	*rbx-1*pro::GFP	N2 DNA was amplified using primers 5'-CGCGGCATGCATGCTTATCATGCCTTTCTAGGTAAA and 5'-CGCGGGTACCGGTTTCTGGAAAAAATACAAATGAGAATAA. The SphI/KpnI fragment was inserted into pPD95.75 (Andrew Fire).
pJAZ121	RING domain (*siah-1*-extra aa's) cDNA in pJG4-5	pJAZ098 was amplified using primers 5'-CGCGCCCGGGCCAATCGGCGGCGGTGGAGCCACCGACGAC and 5'-CGCGGGGCCCCTAAAAGCGGACGGTGTTGGCGATCTTCTC. The XmaI/ApaI fragment was inserted into pJG45(gift, R. Finley).
pJAZ122	RING domain (*siah-1*-extra aa's) cDNA in pEG202	Fragment from pJAZ121 was inserted into pEG202 (NBRP Yeast) following digest with EcoRI/XhoI.
pJAZ123	*siah-1* cDNA (aa's 146-	Fragment from pJAZ124 was inserted into

	400) in pEG202	pEG202 (NBRP Yeast) following digest with EcoRI/XhoI.
pJAZ124	*siah-1* cDNA (aa's 146-400) in pJG4-5	pJAZ098 was amplified using primers 5'-CGCGCCCGGGAGCAGTGCAGAGATCTTGTCGGTGT and 5'-CGCGGGGCCCCTACCTTGACGTTGATTCCAAGGTTTCCGTTTTCT. The XmaI/ApaI fragment was inserted into pJG45(gift, R. Finley).
pJAZ127	6xHis::HA::*hpk-1B* cDNA in pET28b(+)	The vector was assembled using the Gibson protocol as previously described (Gibson et al., 2009). *hpk-1b* was amplified off cDNA clone from *C. elegans* ORFeome library of using primers 5'-CGCGGGATCCCATGGAGTACCCATACGACGTACCAGATATGAATTTCCAT and 5'-GCGGCCGCTTAGTTAAAAGCTCTGGGAATATGAGAT. pET28b(+):5'-GTCGACGGAGCTCGAATTCGGATCCCGACCCATTT and 5'-GCGGCCGCACTCGAGCACCACCACCACCACCACT. All fragments were DpnI digested prior to assembly.
pJAZ132	*AC*pro::*siah-1* cDNA::HA	pJAZ087 was amplified using the following primers: 5'-CGCGGGTACCAAAATGAGTAATCGGAACGGTGGTGG and 5'-CGCGGGGCCCTAAGCGTAATCTGGAACATCGTATGGGTACATGTCGTACTCGAG. The KpnI/ApaI fragment was ligated into pJAZ087.
pJAZ133	*AC*pro::*rbx-1* cDNA::HA	pJAZ091 was amplified using the following primers: 5'-CGCGGGTACCAAAATGGCCCAAGCAAGCGACAGC and 5'-CGCGGGGCCCTTAAGCGTAATCTGGAACATCGTATGGGTACATGTGTCCG. The KpnI/ApaI fragment was ligated into pJAZ087.
pJAZ139	*let-70/hpk-1* RNAi in L4440	pJAZ127 was amplified using 5'-CGCGTCTAGATGAGAAAGTCTGTGGCGTTGATGCAA and 5'-CGCGCCCGGGCGAAATAATCCTTGGCTTGCCGTTC. The XbaI/XmaI fragment was ligated into pJAZ021.
pJAZ151	*cul-1/let-70* RNAi in	N2 cDNA library was amplified using primers

	L4440	5'-CGCGTCTAGAGAAGACGGTCGAGCAGAATC and 5'-CGCGCCCGGGGCATGAATCCTGGCTCATTT. The XbaI/XmaI fragment was inserted into pJAZ021.
pJAZ155	*cul-3* RNAi in L4440 (XbaI/XmaI)	N2 cDNA library was amplified using 5'-CGCGTCTAGAggccacaatagacgagcaat and 5'-CGCGCCCGGGccggtactgtcaccgaatc. The XbaI/XmaI fragment was ligated into L4440.
pJAZ156	*siah-1* RNAi in L4440 (Xho/HindIII)	pJAZ005 was amplified using 5'-GCGCAAGCTTGGCCGCAAACGATGGCCAGAGTTCAG and 5'-GCGCCTCGAGGTCGACTCCAAGGTTTCCGTTTTCTG. This HindIII/XhoI fragment was ligated into L4440.
pJAZ157	*cul-3*/*siah-1* RNAi in L4440	pJAZ155 was digested using XbaI/XmaI and inserted into pJAZ156.
pJAZ158	*sel-10* RNAi in L4440 (Xho/HindIII)	N2 cDNA library was amplified using 5'-CGCGAAGCTTTCACAATTTAACCGGATATGACC and 5'-CGCGCTCGAGGGGTATACAGCATCAAAGTCGAG. This HindIII/XhoI fragment was ligated into L4440.
pJAZ159	*cul-1/sel-10* RNAi in L4440	pJAZ151 was digested using XbaI/XmaI and inserted into pJAZ158.
pJAZ160	*cul-1* RNAi in L4440 (XhoI/HindIII)	N2 cDNA library was amplified using 5'-CGCGAAGCTTGAAGACGGTCGAGCAGAATC and 5'-CGCGCTCGAGGCATGAATCCTGGCTCATTT. The XhoI/HindIII fragment was ligated into L4440.
pJAZ161	*cul-1/cul-3* RNAi in L4440	pJAZ155 was digested using XbaI/Xma and ligated into pJAZ160.
pJAZ162	*lin-23* RNAi in L4440 (Xba/Xma)	N2 cDNA library was amplified using 5'-CGCGTCTAGAAGTCGAGACATGTCAGTGCG and 5'-CGCGCCCGGGGCAGAGGCATATTTCCGAAG. This XbaI/XmaI fragment was ligated into L4440.
pJAZ163	*lin-23/sel-10* RNAi in L4440	pJAZ162 was digested using XbaI/XmaI and ligated into pJAZ158.
pJAZ165	*cul-3/sel-10* RNAi in L4440	pJAZ155 was digested using XbaI/XmaI and ligated into pJAZ158.
pJAZ166	*cul-1/lin-23* RNAi in L4440	pJAZ151 was digested with XbaI/XmaI and ligated into pJAZ162.

pJAZ167	*cul-1/siah-1* RNAi in L4440	pJAZ151 was digested with XbaI/XmaI and ligated into pJAZ156.
pJAZ168	*rbx-1/cul-1* RNAi in L4440	pJAZ033 was digested with XbaI/XmaI and ligated into pJAZ160.
pJAZ171	*mig-24*pro::*eor-1* cDNA	C. elegans cDNA was amplified using primers 5'-CGCGGGTACCGGTAGAAAAAATGACATTAGTAGCTAGTTCCGAAA and 5'-CGCGGAATTCTTATTGTACATTCCACGGATTCCATG. The KpnI/EcoRI fragment was inserted into mig-24p::mCherry.
pJAZ175	*AC*pro::HA::*eor-1* cDNA	N2 cDNA library was amplified using 5'-CGCGGCGGCCGCATGACATTAGTAGCTAGTTCCGAA and 5'-CGCGGGGCCCTTATTGTACATTCCACGGATTCCATGC. The NotI/ApaI fragment was ligated into pJAZ091.
pJAZ176	*AC*pro::myc::*cul-3* cDNA	N2 cDNA library was amplified using 5'-GATAGCGGCCGCATGAGCGGACGCTCCGGTAATGGT and 5'-GGGCCCCTAGGCAATGTATTGATAGGCACGATG. The NotI/ApaI fragment was ligated into pJAZ086.
pJAZ190	*AC*pro::myc::*eor-1* cDNA	pJAZ175 was digested with NotI/ApaI and ligated into pJAZ086.
pJAZ191	*AC*pro::HA::*cul-3* cDNA	pJAZ176 was digested with NotI/ApaI and ligated into pJAZ091.
pJAZ195	*AC*pro::myc::*eor-2* cDNA	N2 cDNA library was amplified using 5'-GCTTGCGGCCGCCATGGATCAACGTAATCA and 5'-CGAAGGGCCCTTACACATCGCGAAACTCGT. The NotI/ApaI fragment was ligated into pJAZ086.
pJA42 + let-70	*let-70* sgRNA	pJA42 was mutagenized using Quikchange primers: 5'-AAGACATCTCGCAATAGGAGGTGTTTATATAGGGGCAACACAA and 5'-CTATTGCGAGATGTCTTGATGGATAGTCTGTTGGGAAGGTTTTAGAGCTAGAAATAGCAAG.

APPENDIX, or Potential leads

A1. Mutations in the Homeodomain Interacting Protein Kinase HPK-1 rescue *let-70*(LC-RNAi)-induced linker cell survival

While performing a yeast two-hybrid screen for interactors with the poly-glutamine repeat protein PQN-41, Lena Kutscher, a graduate student in the lab, identified the homeodomain-interacting protein kinase HPK-1 as an inhibitor of linker cell death, as *hpk-1*(*pk1393*) mutants are able to rescue survival caused by other linker cell death mutants (L. Kutscher, unpublished observations). We wondered whether *hpk-1*(*pk1393*) could rescue the linker cell survival detected in *let-70* RNAi animals. Though *hpk-1*(*pk1393*); *let-70*(RNAi) animals fail to rescue the *let-70*(RNAi) linker cell survival defect, *hpk-1* RNAi is able to rescue survival in a linker cell-specific *let-70* RNAi background (Appendix Table 1). Two possible causes underlie the data observed: 1) HPK-1 acts to inhibit LET-70 function, in a manner that is not visible in *hpk-1*(*pk1393*); *let-70*(RNAi) animals due to off-target metabolic effects induced by systemic loss of *hpk-1* function. 2) HPK-1 does not inhibit LET-70 function, and the "rescue" observed in linker-cell specific *hpk-1*(RNAi); *let-70*(RNAi) animals is actually the output of inefficient *let-70* RNAi execution possibly due to expressing two siRNAs from the same plasmid. More work is needed to determine which of these causes is the reason behind the phenotypes observed.

Appendix Table 1. HPK-1 inhibits LET-70 in *let-70*(cell specific RNAi) animals

Genotype	**% Surviving LCs**	**% LCs with migration defect**
let-70 RNAi	78 ± 4	79 ± 4
hpk-1(*pk1393*)	4 ± 2	1 ± 1
hpk-1(*pk1393*); *let-70* RNAi	81 ± 4	91 ± 3
hpk-1 RNAi	10 ± 2	3 ± 1
*rde-1; mig-24*p::*rde-1*; *hpk-1* RNAi; *let-70* RNAi	11 ± 2	1 ± 1
*rde-1; mig-24*p::*rde-1*; *let-70* RNAi	21 ± 3	1 ± 1

[a]All animals contained the *him-5*(*e1490*) mutations and a *lag-2*::gfp (*qIs56*) reporter gene to identify the linker cell, except in the LC-only experiments in which the *mig-24* promoter was used to drive an *rde-1* cDNA in *rde-1*(*ne219*); *him-8*(*e1489*); *qIs56* mutants. *rde-1*(*ne219*) mutants have 12 ± 1 % LC survival. Error, SEM.

[b]N>70

A2. *siah-1* mutants do not enhance mutations in GAPDH/*gpd-2*

Previous experiments conducted in mammalian systems have implicated SIAH-1 homologs in the regulation of cell death. In vitro coimmunoprecipitation experiments suggest that Siah1 interacts with the glycolytic enzyme glyceraldehyde 3-phosphate dehydrogenase (GAPDH) and the Huntington's disease protein Huntingtin in a complex that is localized to the nucleus in fractionation experiments (Bae et al., 2006). Intrigued by this data, we wondered whether GAPDH is required for linker cell death in *C. elegans*. We performed RNAi knockdown of all known GAPDH homologs in *C. elegans*, and found that we observe weak but significant linker cell survival following *gpd-2* knockdown, indicating that *gpd-2* may play a role in linker cell death. *gpd-2* RNAi performed in a *siah-1(tm1968)* mutant background causes no further increase in cell survival above what is observed with *gpd-2* RNAi or *siah-1(tm1968)* alone, indicating that either *siah-1* works in the same pathway as GAPDH to promote cell death, or that the survival observed by *gpd-2* RNAi is an artifact caused by issues with RNAi (Appendix Table 2). Combined knockdown of *let-70* and *gpd-2* using RNAi causes no further increase in linker cell survival above the *let-70* RNAi defect, nor does *let-70* and *gpd-2* RNAi performed in a *siah-1(tm1968)* genetic background. While the survival defect is too weak to conclude anything, it is possible that GAPDH may play a role in linker cell death.

Appendix Table 2: *siah-1* may act with GAPDH to promote linker cell death

Genotype (RNAi sensitized)[a]	**% Surviving Linker Cells, 0-2 hr adults**[b]	**% Migration Defect**
let-70 RNAi	45 ± 2	58 ± 6
siah-1(*tm1968*)	14 ± 2	2 ± 1
gpd-1 RNAi	6 ± 2	0 ± 0
gpd-2 RNAi	10 ± 1	3 ± <1
gpd-3 RNAi	3 ± 2	1 ± 1
gpd-4 RNAi	2 ± 1	0 ± 0
gpd-2 RNAi, *let-70* RNAi	33 ± 8	22 ± 8
siah-1(*tm1968*)*; gpd-2* RNAi	9 ± 8	3 ± 0
siah-1(*tm1968*)*; gpd-2* RNAi; *let-70* RNAi	27 ± 2	15 ± 2

[a]strains analyzed contained *rrf-3*(*pk1426*); *him-8*(*e1489*) mutations and a *lag-2*::gfp (*qIs56*) reporter gene to identify the linker cell. Error, SEM.

[b]n>63

A3. *pqn-41*(*ns294*) acts in the same pathway as *siah-1*

A previous screen conducted by Elyse Blum and Mary Abraham identified the polyQ repeat gene *pqn-41* as an important regulator of linker cell death. As such, we wondered if the polyQ gene *pqn-41* acts with *siah-1*, which might indicate that the molecular biology underlying linker cell death shares some similarity with neurodegenerative cell death. *siah-1*(*tm1968*); *pqn-41*(*ns294*) double mutants show no increase in linker cell survival compared to *pqn-41*(*ns294*), indicating that the two do not genetically interact. Though this finding is promising, it is unlikely that SIAH-1 and PQN-41 bind directly to promote death, as SIAH-1 and PQN-41 fail to physically interact in a yeast two-hybrid assay (Appendix Table 3, Table 3.3).

A4. *pqn-41*(*ns294*) shows a synergistic increase in linker cell survival in *pqn-41*(*ns294*); *nhr-67*(RNAi) animals

As *let-70*(RNAi); *nhr-67*(RNAi) animals exhibit a synergistic increase in linker cell survival, we wondered whether *nhr-67* also synergizes with other mutants required for linker cell death. Like *let-70*(RNAi); *nhr-67*(RNAi) animals, *pqn-41*(*ns294*); *nhr-67*(RNAi) animals also exhibit a synergistic increase in cell survival compared to *nhr-67*(RNAi) or *pqn-41*(*ns294*) alone (Appendix Table 3).

Appendix Table 3: *pqn-41* acts with *siah-1*, but not *nhr-67*, to promote linker cell death

Genotype (RNAi sensitized)[a]	**% Surviving Linker Cells, 0-2 hr adults**[b]	**% Migration Defect**
siah-1(*tm1968*)	14 ± 2	2 ± 1
pqn-41(*ns294*)	25 ± 1	6 ± <1
siah-1(*tm1968*); *pqn-41*(*ns294*)	24 ± 1	7 ± 2
nhr-67 RNAi	63 ± 5	78 ± 4
nhr-67 RNAi; *pqn-41*(*ns294*)	86 ± 4	91 ± 4

[a]strains analyzed contained *him-8*(*e1490*) mutations and a *lag-2*::gfp (*qIs56*) reporter gene to identify the linker cell. Error, SEM.

[b]n>63

A5. RNAi against 16 individual Skp genes causes no inappropriate linker cell survival

We wondered whether other components of the SCF complex such as Skp proteins were required for linker cell death. RNAi against 16 of the 22 Skps in the *C. elegans* genome produces no inappropriate linker cell survival, indicating that they are either not required for linker cell death, or that RNAi knockdown is insufficient to perturb the Skp required for death (Appendix Table 4).

A6. The cullin CUL-1 and the F-box proteins SEL-10 and LIN-23 may be required for linker cell death

Although none of the Skps produce inappropriate linker cell survival when knocked down by RNAi (Appendix Table 4), we wondered whether any other cullins or F-box proteins were required for linker cell death. RNAi against the *cul-1* gene produces weak but significant linker cell survival (Appendix Table 5). Simultaneous RNAi against *cul-1* and *cul-3* produces a synergistic increase in linker cell survival above that observed with *cul-1*(RNAi) or *cul-3*(RNAi), indicating that perhaps *cul-1* and *cul-3* work redundantly to promote death (Appendix Table 5). However, linker cell-specific *cul-1* RNAi causes no defect above that observed in *rde-1* mutant animals, indicating that either the survival is real but RNAi is inefficient in *rde-1*(*ne219*) animals, or that the linker cell survival observed during systemic *cul-1* RNAi is itself an artifact (Appendix Table 5).

In order to determine whether F-box proteins were required for linker cell death, we performed RNAi against homologs against the known SCF component Fbw7 (Koepp et al., 2001). RNAi against *lin-23* and *sel-10* produces weak linker cell survival, which shows no further increase when both are knocked down (Appendix Table 5). Therefore, either the weak

survival exhibited by *lin-23*(RNAi) and *sel-10*(RNAi) animals is an artifact, or both F-box genes are weakly required for linker cell death.

We sought to understand which proteins worked with CUL-1 or CUL-3 to promote death. With the exception of *cul-1*(RNAi); *cul-3*(RNAi) animals, RNAi against any two SCF genes caused no increase in linker cell survival compared to RNAi against any single gene observed (Appendix Table 5). Thus, either all of the genes somehow work together to promote death, or the survival observed might be an artifact caused by unintended effects of the RNAi.

Nonetheless, we wondered whether LET-70 was capable of interacting with an SCF complex to promote death. As we did not know the identity of the CUL-1 SCF complex required for death, we obtained a purified human SCF complex consisting of Skp1, Cul1, Rbx1 and Fbw7 to test in our in vitro assay (EMD Millipore). Purified LET-70 is able to ubiquitinate the human SCF complex, indicating that LET-70 is capable of interacting with Rbx1 to transfer ubiquitin to a substrate (in this case, Cul1). Despite the fact that the E2 and E3 used came from different organisms, the ubiquitination reaction still was successfully completed, indicating that LET-70 and UBE2D2 may be functionally conserved (Appendix Figure 1).

Appendix Table 4. RNAi against Skp-related genes produces no inappropriate linker cell survival

Genotype[a]	**% LC survival, 0-2 hr adults**[b]
No RNAi	3 ± <1
let-70 RNAi	45 ± 2
rbx-1 RNAi	15 ± 2
skr-1 RNAi	7 ± 4
skr-2 RNAi	5 ± 2
skr-3 RNAi	4 ± 2
skr-5 RNAi	5 ± 2
skr-6 RNAi	4 ± 2
skr-8 RNAi	1 ± 1
skr-9 RNAi	5 ± 2
skr-11 RNAi	4 ± 2
skr-12 RNAi	6 ± 2
skr-13 RNAi	2 ± 2
skr-15 RNAi	6 ± 3
skr-16 RNAi	7 ± 3
skr-17 RNAi	8 ± 3
skr-19 RNAi	5 ± 2
skr-20 RNAi	3 ± 2
skr-21 RNAi	7 ± 2

[a]All animals contained *rrf-3*(*pk1426*); *him-8*(*e1489*) mutations and a *lag-2*p::gfp (*qIs56*) reporter gene to identify the linker cell. Error, SEM.

[b]LC, linker cell. n>41

Appendix Table 5. Components of the SCF complex are weakly required for linker cell death

Genotype (RNAi sensitized)	**% Surviving Linker Cells, 0-2 hr adults**
lin-23 RNAi	14 ± 2
sel-10 RNAi	8 ± 2
lin-23 RNAi*; sel-10* RNAi	14 ± 4
cul-1 RNAi	14 ± 1
cul-1 LC-specific RNAi	13 ± 1
cul-1 RNAi; *lin-23* RNAi	17 ± 3
cul-3 RNAi	24 ± 4
sel-10 RNAi; *cul-3* RNAi	13 ± 5
rbx-1 RNAi	21 ± 3
cul-1 RNAi*; rbx-1* RNAi	11 ± 1
cul-1 RNAi; *cul-3* RNAi	39 ± 2
siah-1(*tm1968*)	14 ± 2
siah-1(*tm1968*); *sel-10* RNAi	17 ± 4
siah-1(*tm1968*); *lin-23* RNAi	25 ± 6

[a]All animals contained *rrf-3(pk1426); him-8*(*e1489*) mutations and a *lag-2*::gfp (*qIs56*) reporter gene to identify the linker cell, , except in the LC-only experiments in which the *mig-24* promoter was used to drive an *rde-1* cDNA in *rde-1*(*ne219*); *him-8*(*e1489*); *qIs56* mutants. *rde-1*(*ne219*) mutants have 12 ± 1 % LC survival, Error, SEM.

[b]LC, linker cell. n>56

Appendix Figure 1. LET-70 is capable of ubiquitinating the human SCF complex in an in vitro ubiquitination assay. (A) red *= mono-ub Cul1, **= di-ub Cul1, Addition of purified LET-70 to *Drosophila* UBA1, *Drosophila* HA-ubiquitin, and human SCF^{Fbw7} causes auto-ubiquitination of HA-Cul1 that is visible by Coommassie staining. Blue *= poly-ub-DIAP1 (B) Western blot of gel from (A) with anti-HA antibody (Roche). *=ubq-Cul1 (C) Western blot of gel from (A) with anti-ubiquitin antibody (Sigma). *=ubq-Cul1 (D) Western blot of gel from (A) with anti-Cul1 antibody (Abcam). *=ubq-Cul1

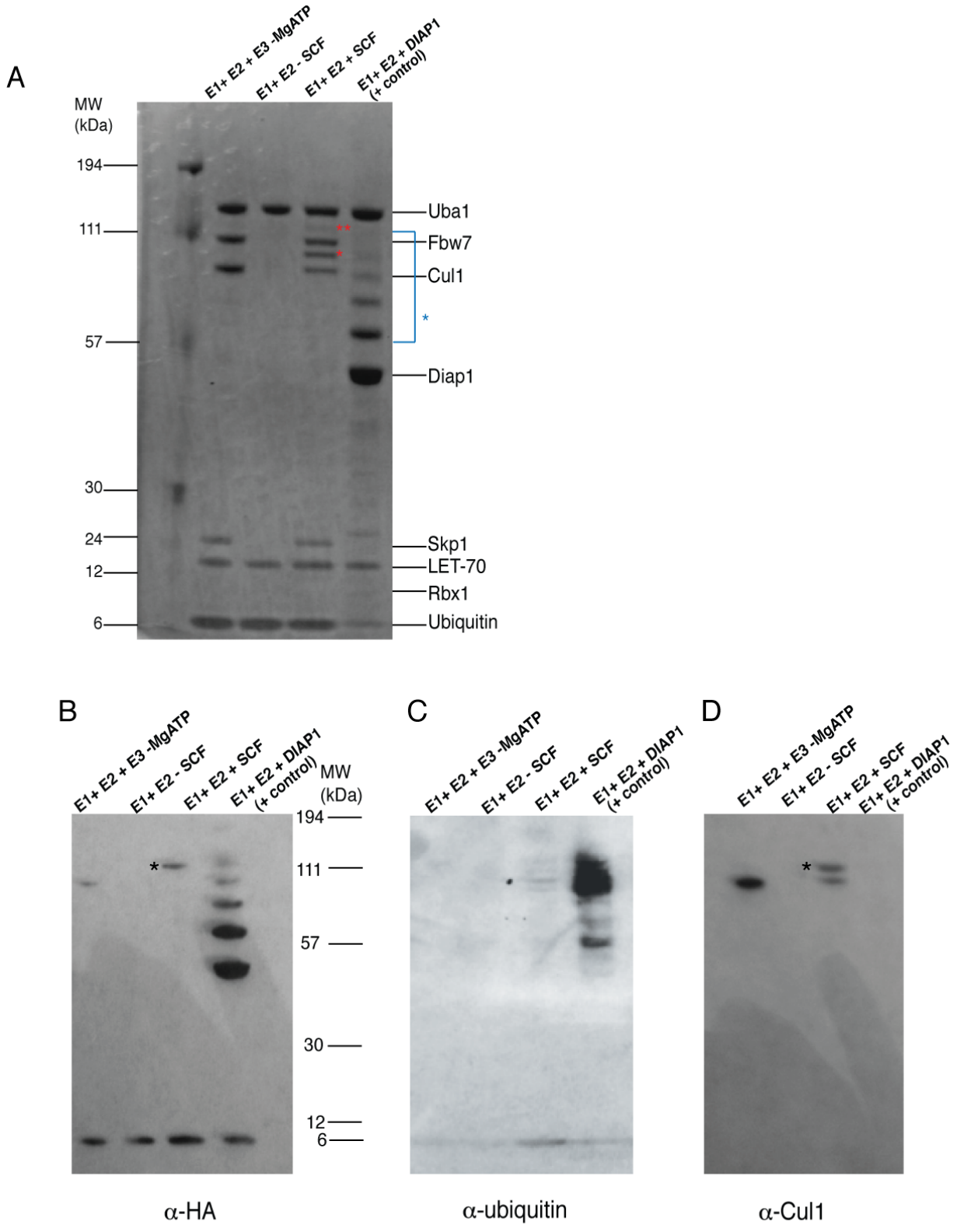
A
E1+ E2 + E3 -MgATP
E1+ E2 - SCF
E1+ E2 + SCF
E1+ E2 + DIAP1 (+ control)
MW (kDa)
194
111
57
30
24
12
6
Uba1
Fbw7
Cul1
Diap1
Skp1
LET-70
Rbx1
Ubiquitin
B
C
D
α-HA
α-ubiquitin
α-Cul1

REFERENCES

Abraham, M.C., Lu, Y., and Shaham, S. (2007). A morphologically conserved nonapoptotic program promotes linker cell death in Caenorhabditis elegans. Developmental Cell *12*, 73–86.

Acehan, D., Jiang, X., Morgan, D.G., Heuser, J.E., Wang, X., and Akey, C.W. (2002). Three-dimensional structure of the apoptosome: implications for assembly, procaspase-9 binding, and activation. Molecular Cell *9*, 423–432.

Agianian, B., Leonard, K., Bonte, E., Van der Zandt, H., Becker, P.B., and Tucker, P.A. (1999). The glutamine-rich domain of the Drosophila GAGA factor is necessary for amyloid fibre formation in vitro, but not for chromatin remodelling. J. Mol. Biol. *285*, 527–544.

Ambros, V., and Horvitz, H.R. (1984). Heterochronic mutants of the nematode Caenorhabditis elegans. Science (New York, NY) *226*, 409–416.

Antonsson, B., Conti, F., Ciavatta, A., Montessuit, S., Lewis, S., Martinou, I., Bernasconi, L., Bernard, A., Mermod, J.J., Mazzei, G., et al. (1997). Inhibition of Bax channel-forming activity by Bcl-2. Science (New York, NY) *277*, 370–372.

Arama, E., Agapite, J., and Steller, H. (2003). Caspase activity and a specific cytochrome C are required for sperm differentiation in Drosophila. Developmental Cell *4*, 687–697.

Arama, E., Bader, M., Rieckhof, G.E., and Steller, H. (2007). A ubiquitin ligase complex regulates caspase activation during sperm differentiation in Drosophila. PLoS Biol *5*, e251.

Arribere, J.A., Bell, R.T., Fu, B.X.H., Artiles, K.L., Hartman, P.S., and Fire, A.Z. (2014). Efficient Marker-Free Recovery of Custom Genetic Modifications with CRISPR/Cas9 in Caenorhabditis elegans. Genetics *198*, 837–846.

Aruscavage, P.J., Hellwig, S., and Bass, B.L. (2010). Small DNA Pieces in C. elegans Are Intermediates of DNA Fragmentation during Apoptosis. Plos One 1–7.

Ayad, N.G., Rankin, S., Ooi, D., Rape, M., and Kirschner, M.W. (2005). Identification of ubiquitin ligase substrates by in vitro expression cloning. Meth Enzymol *399*, 404–414.

Bacaj, T., Tevlin, M., Lu, Y., and Shaham, S. (2008). Glia are essential for sensory organ function in C. elegans. Science (New York, NY) *322*, 744–747.

Bader, M., Arama, E., and Steller, H. (2010). A novel F-box protein is required for caspase activation during cellular remodeling in Drosophila. Development *137*, 1679–1688.

Bae, B.-I., Hara, M.R., Cascio, M.B., Wellington, C.L., Hayden, M.R., Ross, C.A., Ha, H.C., Li, X.-J., Snyder, S.H., and Sawa, A. (2006). Mutant huntingtin: nuclear translocation and cytotoxicity mediated by GAPDH. Proc Natl Acad Sci USA *103*, 3405–3409.

Basanez, G., and Sharpe, J.C. (2002). Bax-type Apoptotic Proteins Porate Pure Lipid Bilayers through a Mechanism Sensitive to Intrinsic Monolayer Curvature. J Biol Chem 1–7.

Baum, J.S., Arama, E., Steller, H., and McCall, K. (2007). The Drosophila caspases Strica and Dronc function redundantly in programmed cell death during oogenesis. Cell Death and Differentiation *14*, 1508–1517.

Belote, J.M., and Zhong, L. (2009). Duplicated proteasome subunit genes in Drosophila and their roles in spermatogenesis. Heredity (Edinb) *103*, 23–31.

Bianchi, L., Gerstbrein, B., Frøkjaer-Jensen, C., Royal, D.C., Mukherjee, G., Royal, M.A., Xue, J., Schafer, W.R., and Driscoll, M. (2004). The neurotoxic MEC-4(d) DEG/ENaC sodium channel conducts calcium: implications for necrosis initiation. Nat Neurosci *7*, 1337–1344.

Bloss, T.A., Witze, E.S., and Rothman, J.H. (2003). Suppression of CED-3-independent apoptosis by mitochondrial betaNAC in Caenorhabditis elegans. Nature *424*, 1066–1071.

Blum, E.S., Abraham, M.C., Yoshimura, S., Lu, Y., and Shaham, S. (2012). Control of Nonapoptotic Developmental Cell Death in Caenorhabditis elegans by a Polyglutamine-Repeat Protein. Science (New York, NY) *335*, 970–973.

Boldin, M.P., Goncharov, T.M., Goltsev, Y.V., and Wallach, D. (1996). Involvement of MACH, a novel MORT1/FADD-interacting protease, in Fas/APO-1- and TNF receptor-induced cell death. Cell *85*, 803–815.

Borsello, T., Mottier, V., Castagné, V., and Clarke, P.G.H. (2002). Ultrastructure of retinal ganglion cell death after axotomy in chick embryos. J Comp Neurol *453*, 361–371.

Breckenridge, D.G., Kang, B.-H., and Xue, D. (2009). Bcl-2 proteins EGL-1 and CED-9 do not regulate mitochondrial fission or fusion in Caenorhabditis elegans. Current Biology : CB *19*, 768–773.

Breckenridge, D.G., Kang, B.-H., Kokel, D., Mitani, S., Staehelin, L.A., and Xue, D. (2008). Caenorhabditis elegans drp-1 and fis-2 regulate distinct cell-death execution pathways downstream of ced-3 and independent of ced-9. Molecular Cell *31*, 586–597.

Brenner, S. (1974). The genetics of Caenorhabditis elegans. Genetics *77*, 71–94.

Budhavarapu, V.N., White, E.D., Mahanic, C.S., Chen, L., Lin, F.-T., and Lin, W.-C. (2012). Regulation of E2F1 by APC/C Cdh1 via K11 linkage-specific ubiquitin chain formation. Cell Cycle *11*, 2030–2038.

Canning, P., Cooper, C.D.O., Krojer, T., Murray, J.W., Pike, A.C.W., Chaikuad, A., Keates, T., Thangaratnarajah, C., Hojzan, V., Ayinampudi, V., et al. (2013). Structural basis for Cul3 protein assembly with the BTB-Kelch family of E3 ubiquitin ligases. Journal of Biological Chemistry *288*, 7803–7814.

Carthew, R.W., and Rubin, G.M. (1990). seven in absentia, a Gene Required for Specification of R7 Cell Fate in the Drosophila Eye. Cell *63*, 561–577.

Chautan, M., Chazal, G., Cecconi, F., Gruss, P., and Golstein, P. (1999). Interdigital cell death

can occur through a necrotic and caspase-independent pathway. Current Biology : CB *9*, 967–970.

Chen, C.Y., Pajak, L., Tamburlin, J., Bofinger, D., and Koury, S.T. (2002). The effect of proteasome inhibitors on mammalian erythroid terminal differentiation. Exp. Hematol. *30*, 634–639.

Chen, F., Hersh, B.M., Conradt, B., Zhou, Z., Riemer, D., Gruenbaum, Y., and Horvitz, H.R. (2000). Translocation of C. elegans CED-4 to nuclear membranes during programmed cell death. Science (New York, NY) *287*, 1485–1489.

Chen, P., Nordstrom, W., Gish, B., and Abrams, J.M. (1996a). grim, a novel cell death gene in Drosophila. Genes & Development *10*, 1773–1782.

Chen, P., Rodriguez, A., Erskine, R., Thach, T., and Abrams, J.M. (1998). Dredd, a novel effector of the apoptosis activators reaper, grim, and hid in Drosophila. Developmental Biology *201*, 202–216.

Chen, Y.R., Wang, X., Templeton, D., Davis, R.J., and Tan, T.H. (1996b). The role of c-Jun N-terminal kinase (JNK) in apoptosis induced by ultraviolet C and gamma radiation. Duration of JNK activation may determine cell death and proliferation. J Biol Chem *271*, 31929–31936.

Chen, Z., Brand, N.J., Chen, A., Chen, S.J., Tong, J.H., Wang, Z.Y., Waxman, S., and Zelent, A. (1993). Fusion between a novel Krüppel-like zinc finger gene and the retinoic acid receptor-alpha locus due to a variant t(11;17) translocation associated with acute promyelocytic leukaemia. The EMBO Journal *12*, 1161–1167.

Chien, S.-C., Brinkmann, E.-M., Teuliere, J., and Garriga, G. (2013). Caenorhabditis elegans PIG-1/MELK acts in a conserved PAR-4/LKB1 polarity pathway to promote asymmetric neuroblast divisions. Genetics *193*, 897–909.

Chinnaiyan, A.M., O'Rourke, K., Tewari, M., and Dixit, V.M. (1995). FADD, a novel death domain-containing protein, interacts with the death domain of Fas and initiates apoptosis. Cell *81*, 505–512.

Chinnaiyan, A., Chaudhary, D., O'Rourke, K., Koonin, E.V., and Dixit, V.M. (1997a). Role of CED-4 in the activation of CED-3. Nature 1–2.

Chinnaiyan, A., O'Rourke, K., Lane, B.R., and Dixit, V.M. (1997b). Interaction of CED-4 with CED-3 and CED-9: A Molecular Framework for Cell Death. Science (New York, NY) 1–6.

Chiorazzi, M., Rui, L., Yang, Y., Ceribelli, M., Tishbi, N., Maurer, C.W., Ranuncolo, S.M., Zhao, H., Xu, W., Chan, W.-C.C., et al. (2013). Related F-box proteins control cell death in Caenorhabditis elegans and human lymphoma. Proceedings of the National Academy of Sciences.

Ciechanover, A., Heller, H., Elias, S., Haas, A.L., and Hershko, A. (1980). ATP-dependent conjugation of reticulocyte proteins with the polypeptide required for protein degradation. Proc

Natl Acad Sci USA *77*, 1365–1368.

Cizeau, J., Ray, R., Chen, G., Gietz, R.D., and Greenberg, A.H. (2000). The C. elegans orthologue ceBNIP3 interacts with CED-9 and CED-3 but kills through a BH3- and caspase-independent mechanism. Oncogene *19*, 5453–5463.

Clem, R.J., Fechheimer, M., and Miller, L.K. (1991). Prevention of apoptosis by a baculovirus gene during infection of insect cells. Science (New York, NY) *254*, 1388–1390.

Colussi, P.A., Quinn, L.M., Huang, D.C., Coombe, M., Read, S.H., Richardson, H., and Kumar, S. (2000). Debcl, a proapoptotic Bcl-2 homologue, is a component of the Drosophila melanogaster cell death machinery. J Cell Biol *148*, 703–714.

Conforti, L., Wilbrey, A., Morreale, G., Janeckova, L., Beirowski, B., Adalbert, R., Mazzola, F., Di Stefano, M., Hartley, R., Babetto, E., et al. (2009). Wld S protein requires Nmnat activity and a short N-terminal sequence to protect axons in mice. J Cell Biol *184*, 491–500.

Conradt, B., and Horvitz, H.R. (1999). The TRA-1A sex determination protein of C. elegans regulates sexually dimorphic cell deaths by repressing the egl-1 cell death activator gene. Cell *98*, 317–327.

Conradt, B., and Horvitz, H.R. (1998). The C. elegans protein EGL-1 is required for programmed cell death and interacts with the Bcl-2-like protein CED-9. Cell *93*, 519–529.

Cordes, S., Frank, C.A., and Garriga, G. (2006). The C. elegans MELK ortholog PIG-1 regulates cell size asymmetry and daughter cell fate in asymmetric neuroblast divisions. Development *133*, 2747–2756.

Coucouvanis, E., and Martin, G.R. (1995). Signals for death and survival: a two-step mechanism for cavitation in the vertebrate embryo. Cell *83*, 279–287.

Cummings, C.J., Reinstein, E., Sun, Y., Antalffy, B., Jiang, Y., Ciechanover, A., Orr, H.T., Beaudet, A.L., and Zoghbi, H.Y. (1999). Mutation of the E6-AP ubiquitin ligase reduces nuclear inclusion frequency while accelerating polyglutamine-induced pathology in SCA1 mice. Neuron *24*, 879–892.

Davies, S.W., Turmaine, M., Cozens, B.A., DiFiglia, M., Sharp, A.H., Ross, C.A., Scherzinger, E., Wanker, E.E., Mangiarini, L., and Bates, G.P. (1997). Formation of neuronal intranuclear inclusions underlies the neurological dysfunction in mice transgenic for the HD mutation. Cell *90*, 537–548.

De Arras, L., Seng, A., Lackford, B., Keikhaee, M.R., Bowerman, B., Freedman, J.H., Schwartz, D.A., and Alper, S. (2013). An evolutionarily conserved innate immunity protein interaction network. J Biol Chem *288*, 1967–1978.

de Pril, R., Fischer, D.F., Roos, R.A.C., and van Leeuwen, F.W. (2007). Ubiquitin-conjugating enzyme E2-25K increases aggregate formation and cell death in polyglutamine diseases. Mol Cell Neurosci *34*, 10–19.

del Peso, L., Gonzalez, V.M., and Nuñez, G. (1998). Caenorhabditis elegans EGL-1 disrupts the interaction of CED-9 with CED-4 and promotes CED-3 activation. J Biol Chem *273*, 33495–33500.

del Peso, L., Gonzalez, V.M., Inohara, N., Ellis, R.E., and Nuñez, G. (2000). Disruption of the CED-9.CED-4 complex by EGL-1 is a critical step for programmed cell death in Caenorhabditis elegans. J Biol Chem *275*, 27205–27211.

Denning, D.P., Hatch, V., and Horvitz, H.R. (2012). Programmed elimination of cells by caspase-independent cell extrusion in C. elegans. Nature 1–6.

Desai, C., Garriga, G., McIntire, S.L., and Horvitz, H.R. (1988). A genetic pathway for the development of the Caenorhabditis elegans HSN motor neurons. Nature *336*, 638–646.

Deshaies, R.J., and Joazeiro, C.A.P. (2009). RING domain E3 ubiquitin ligases. Annu. Rev. Biochem. *78*, 399–434.

Deveraux, Q.L., Roy, N., Stennicke, H.R., Van Arsdale, T., Zhou, Q., Srinivasula, S.M., Alnemri, E.S., Salvesen, G.S., and Reed, J.C. (1998). IAPs block apoptotic events induced by caspase-8 and cytochrome c by direct inhibition of distinct caspases. The EMBO Journal *17*, 2215–2223.

Deveraux, Q.L., Takahashi, R., Salvesen, G.S., and Reed, J.C. (1997). X-linked IAP is a direct inhibitor of cell-death proteases. Nature *388*, 300–304.

DiFiglia, M., Sapp, E., Chase, K.O., Davies, S.W., Bates, G.P., Vonsattel, J.P., and Aronin, N. (1997). Aggregation of huntingtin in neuronal intranuclear inclusions and dystrophic neurites in brain. Science (New York, NY) *277*, 1990–1993.

Dimitrova, Y.N., Li, J., Lee, Y.-T., Rios-Esteves, J., Friedman, D.B., Choi, H.-J., Weis, W.I., Wang, C.-Y., and Chazin, W.J. (2010). Direct ubiquitination of beta-catenin by Siah-1 and regulation by the exchange factor TBL1. J Biol Chem *285*, 13507–13516.

Ditzel, M., Broemer, M., Tenev, T., Bolduc, C., Lee, T.V., Rigbolt, K.T.G., Elliott, R., Zvelebil, M., Blagoev, B., Bergmann, A., et al. (2008). Inactivation of effector caspases through nondegradative polyubiquitylation. Molecular Cell *32*, 540–553.

Donaldson, K.M., Li, W., Ching, K.A., Batalov, S., Tsai, C.-C., and Joazeiro, C.A.P. (2003). Ubiquitin-mediated sequestration of normal cellular proteins into polyglutamine aggregates. Proc Natl Acad Sci USA *100*, 8892–8897.

Dorstyn, L., Colussi, P.A., Quinn, L.M., Richardson, H., and Kumar, S. (1999). DRONC, an ecdysone-inducible Drosophila caspase. Proc Natl Acad Sci USA *96*, 4307–4312.

Dorstyn, L., Mills, K., Lazebnik, Y., and Kumar, S. (2004). The two cytochrome c species, DC3 and DC4, are not required for caspase activation and apoptosis in Drosophila cells. J Cell Biol *167*, 405–410.

Driscoll, M., and Chalfie, M. (1991). The mec-4 gene is a member of a family of Caenorhabditis elegans genes that can mutate to induce neuronal degeneration. Nature *349*, 588–593.

Du, C., Fang, M., Li, Y., Li, L., and Wang, X. (2000). Smac, a mitochondrial protein that promotes cytochrome c-dependent caspase activation by eliminating IAP inhibition. Cell *102*, 33–42.

Duda, D.M., Borg, L.A., Scott, D.C., Hunt, H.W., Hammel, M., and Schulman, B.A. (2008). Structural insights into NEDD8 activation of cullin-RING ligases: conformational control of conjugation. Cell *134*, 995–1006.

Ellis, H., and Horvitz, H.R. (1986). Genetic control of programmed cell death in the nematode C. elegans. Cell *44*, 817–829.

Ellis, R.E., Yuan, J.Y., and Horvitz, H.R. (1991a). Mechanisms and functions of cell death. Annu. Rev. Cell Biol. *7*, 663–698.

Ellis, R.E., and Horvitz, H.R. (1991). Two C. elegans genes control the programmed deaths of specific cells in the pharynx. Development *112*, 591–603.

Ellis, R.E., Jacobson, D.M., and Horvitz, H.R. (1991b). Genes required for the engulfment of cell corpses during programmed cell death in Caenorhabditis elegans. Genetics *129*, 79–94.

Enari, M., and Sakahira, H. (1998). A caspase-activated DNase that degrades DNA during apoptosis, and its inhibitor ICAD. Nature 1–9.

Fairlie, W.D., Perugini, M.A., Kvansakul, M., Chen, L., Huang, D.C.S., and Colman, P.M. (2006). CED-4 forms a 2 : 2 heterotetrameric complex with CED-9 until specifically displaced by EGL-1 or CED-13. Cell Death and Differentiation *13*, 426–434.

Fernandes-Alnemri, T., Armstrong, R.C., Krebs, J., Srinivasula, S.M., Wang, L., Bullrich, F., Fritz, L.C., Trapani, J.A., Tomaselli, K.J., Litwack, G., et al. (1996). In vitro activation of CPP32 and Mch3 by Mch4, a novel human apoptotic cysteine protease containing two FADD-like domains. Proc Natl Acad Sci USA *93*, 7464–7469.

Flach, K., Ramminger, E., Hilbrich, I., Arsalan-Werner, A., Albrecht, F., Herrmann, L., Goedert, M., Arendt, T., and Holzer, M. (2014). Axotrophin/MARCH7 acts as an E3 ubiquitin ligase and ubiquitinates tau protein in vitro impairing microtubule binding. Biochim Biophys Acta *1842*, 1527–1538.

Fraser, A.G., and Evan, G.I. (1997). Identification of a Drosophila melanogaster ICE/CED-3-related protease, drICE. The EMBO Journal *16*, 2805–2813.

Fraser, A.G., Kamath, R.S., Zipperlen, P., Martinez-Campos, M., Sohrmann, M., and Ahringer, J. (2000). Functional genomic analysis of C. elegans chromosome I by systematic RNA interference. Nature *408*, 325–330.

Galindo, K.A., Lu, W.-J., Park, J.H., and Abrams, J.M. (2009). The Bax/Bak ortholog in Drosophila, Debcl, exerts limited control over programmed cell death. Development *136*, 275–283.

Galvin, B.D., Kim, S., and Horvitz, H.R. (2008). Caenorhabditis elegans genes required for the engulfment of apoptotic corpses function in the cytotoxic cell deaths induced by mutations in lin-24 and lin-33. Genetics *179*, 403–417.

Gartner, A., Milstein, S., Ahmed, S., Hodgkin, J., and Hengartner, M.O. (2000). A conserved checkpoint pathway mediates DNA damage--induced apoptosis and cell cycle arrest in C. elegans. Molecular Cell *5*, 435–443.

Gavrieli, Y., Sherman, Y., and Ben-Sasson, S.A. (1992). Identification of programmed cell death in situ via specific labeling of nuclear DNA fragmentation. J Cell Biol *119*, 493–501.

Gerlach, B., Cordier, S.M., Schmukle, A.C., Emmerich, C.H., Rieser, E., Haas, T.L., Webb, A.I., Rickard, J.A., Anderton, H., Wong, W.W.-L., et al. (2011). Linear ubiquitination prevents inflammation and regulates immune signalling. Nature *471*, 591–596.

Gibson, D.G., Young, L., Chuang, R.-Y., Venter, J.C., Hutchison, C.A., and Smith, H.O. (2009). Enzymatic assembly of DNA molecules up to several hundred kilobases. Nature Methods *6*, 343–345.

Goyal, L., McCall, K., Agapite, J., Hartwieg, E., and Steller, H. (2000). Induction of apoptosis by Drosophila reaper, hid and grim through inhibition of IAP function. The EMBO Journal *19*, 589–597.

Grether, M.E., Abrams, J.M., Agapite, J., White, K., and Steller, H. (1995). The head involution defective gene of Drosophila melanogaster functions in programmed cell death. Genes & Development *9*, 1694–1708.

Group, T.H.D.C.R. (1993). A novel gene containing a trinucleotide repeat that is expanded and unstable on Huntington“s disease chromosomes. The Huntington”s Disease Collaborative Research Group. Cell *72*, 971–983.

GuhaThakurta, D., Palomar, L., Stormo, G.D., Tedesco, P., Johnson, T.E., Walker, D.W., Lithgow, G., Kim, S., and Link, C.D. (2002). Identification of a novel cis-regulatory element involved in the heat shock response in Caenorhabditis elegans using microarray gene expression and computational methods. Genome Res. *12*, 701–712.

Gumienny, T.L., Brugnera, E., Tosello-Trampont, A.C., Kinchen, J.M., Haney, L.B., Nishiwaki, K., Walk, S.F., Nemergut, M.E., Macara, I.G., Francis, R., et al. (2001). CED-12/ELMO, a novel member of the CrkII/Dock180/Rac pathway, is required for phagocytosis and cell migration. Cell *107*, 27–41.

Gumienny, T.L., Lambie, E., Hartwieg, E., Horvitz, H.R., and Hengartner, M.O. (1999). Genetic control of programmed cell death in the Caenorhabditis elegans hermaphrodite germline. Development *126*, 1011–1022.

Guo, P., Hu, T., Zhang, J., Jiang, S., and Wang, X. (2010). Sequential action of Caenorhabditis elegans Rab GTPases regulates phagolysosome formation during apoptotic cell degradation. Proceedings of the National Academy of Sciences *107*, 18016–18021.

Haas, A.L., Baboshina, O., Williams, B., and Schwartz, L.M. (1995). Coordinated induction of the ubiquitin conjugation pathway accompanies the developmentally programmed death of insect skeletal muscle. J Biol Chem *270*, 9407–9412.

Hajdu-Cronin, Y.M., Chen, W.J., and Sternberg, P.W. (2004). The L-type cyclin CYL-1 and the heat-shock-factor HSF-1 are required for heat-shock-induced protein expression in Caenorhabditis elegans. Genetics *168*, 1937–1949.

Hall, D.H., Gu, G., García-Añoveros, J., Gong, L., Chalfie, M., and Driscoll, M. (1997). Neuropathology of degenerative cell death in Caenorhabditis elegans. J Neurosci *17*, 1033–1045.

Hausmann, G., O'Reilly, L.A., van Driel, R., Beaumont, J.G., Strasser, A., Adams, J.M., and Huang, D.C. (2000). Pro-apoptotic apoptosis protease-activating factor 1 (Apaf-1) has a cytoplasmic localization distinct from Bcl-2 or Bcl-x(L). J Cell Biol *149*, 623–634.

Hay, B.A., Wassarman, D.A., and Rubin, G.M. (1995). Drosophila homologs of baculovirus inhibitor of apoptosis proteins function to block cell death. Cell *83*, 1253–1262.

Hedgecock, E.M., Sulston, J.E., and Thomson, J.N. (1983). Mutations affecting programmed cell deaths in the nematode Caenorhabditis elegans. Science (New York, NY) *220*, 1277–1279.

Hegde, R., Srinivasula, S.M., Zhang, Z., Wassell, R., Mukattash, R., Cilenti, L., DuBois, G., Lazebnik, Y., Zervos, A.S., Fernandes-Alnemri, T., et al. (2002). Identification of Omi/HtrA2 as a mitochondrial apoptotic serine protease that disrupts inhibitor of apoptosis protein-caspase interaction. J Biol Chem *277*, 432–438.

Hengartner, M.O., and Horvitz, H.R. (1994). Activation of C. elegans cell death protein CED-9 by an amino-acid substitution in a domain conserved in Bcl-2. Nature 1–3.

Hengartner, M.O., Ellis, R.E., and Horvitz, H.R. (1992). Caenorhabditis elegans gene ced-9 protects cells from programmed cell death. Nature *356*, 494–499.

Hershko, A., Ciechanover, A., and Rose, I.A. (1979). Resolution of the ATP-dependent proteolytic system from reticulocytes: a component that interacts with ATP. Proc Natl Acad Sci USA *76*, 3107–3110.

Hershko, A., Heller, H., Elias, S., and Ciechanover, A. (1983). Components of ubiquitin-protein ligase system. Resolution, affinity purification, and role in protein breakdown. J Biol Chem *258*, 8206–8214.

Hershko, A., Leshinsky, E., Ganoth, D., and Heller, H. (1984). ATP-dependent degradation of ubiquitin-protein conjugates. Proc Natl Acad Sci USA *81*, 1619–1623.

Hirose, T., and Horvitz, H.R. (2013). An Sp1 transcription factor coordinates caspase-dependent and -independent apoptotic pathways. Nature *500*, 354–358.

Hirose, T., and Horvitz, H.R. (2014). The translational regulators GCN-1 and ABCF-3 act together to promote apoptosis in C. elegans. PLoS Genet *10*, e1004512.

Hirose, T., Galvin, B.D., and Horvitz, H.R. (2010). Six and Eya promote apoptosis through direct transcriptional activation of the proapoptotic BH3-only gene egl-1 in Caenorhabditis elegans. Proceedings of the National Academy of Sciences *107*, 15479–15484.

Hockenbery, D., Nuñez, G., Milliman, C., Schreiber, R.D., and Korsmeyer, S.J. (1990). Bcl-2 is an inner mitochondrial membrane protein that blocks programmed cell death. Nature *348*, 334–336.

Hodgkin, J., Horvitz, H.R., and Brenner, S. (1979). Nondisjunction Mutants of the Nematode CAENORHABDITIS ELEGANS. Genetics *91*, 67–94.

Hoeppner, D.J., Hengartner, M.O., and Schnabel, R. (2001). Engulfment genes cooperate with ced-3 to promote cell death in Caenorhabditis elegans. Nature *412*, 202–206.

Hoeppner, D.J., Spector, M.S., Ratliff, T.M., Kinchen, J.M., Granat, S., Lin, S.-C., Bhusri, S.S., Conradt, B., Herman, M.A., and Hengartner, M.O. (2004). eor-1 and eor-2 are required for cell-specific apoptotic death in C. elegans. Developmental Biology *274*, 125–138.

Honarpour, N., Du, C., Richardson, J.A., Hammer, R.E., Wang, X., and Herz, J. (2000). Adult Apaf-1-deficient mice exhibit male infertility. Developmental Biology *218*, 248–258.

Hong, K., and Driscoll, M. (1994). A transmembrane domain of the putative channel subunit MEC-4 influences mechanotransduction and neurodegeneration in C. elegans. Nature *367*, 470–473.

Horvitz, H.R. (2003). Nobel lecture. Worms, life and death.

House, C.M., Frew, I.J., Huang, H.-L., Wiche, G., Traficante, N., Nice, E., Catimel, B., and Bowtell, D.D.L. (2003). A binding motif for Siah ubiquitin ligase. Proc Natl Acad Sci USA *100*, 3101–3106.

House, C.M., Hancock, N.C., Möller, A., Cromer, B.A., Fedorov, V., Bowtell, D.D.L., Parker, M.W., and Polekhina, G. (2006). Elucidation of the substrate binding site of Siah ubiquitin ligase. Structure *14*, 695–701.

Howard, R.M., and Sundaram, M.V. (2002a). C. elegans EOR-1/PLZF and EOR-2 positively regulate Ras and Wnt signaling and function redundantly with LIN-25 and the SUR-2 Mediator component. Genes & Development *16*, 1815–1827.

Howard, R.M., and Sundaram, M.V. (2002b). C. elegans EOR-1/PLZF and EOR-2 positively regulate Ras and Wnt signaling and function redundantly with LIN-25 and the SUR-2 Mediator component. Genes & Development *16*, 1815–1827.

Howell, K., Arur, S., Schedl, T., and Sundaram, M.V. (2010). EOR-2 is an obligate binding partner of the BTB-zinc finger protein EOR-1 in Caenorhabditis elegans. Genetics *184*, 899–913.

Hsu, H., Xiong, J., and Goeddel, D.V. (1995). The TNF receptor 1-associated protein TRADD signals cell death and NF-kappa B activation. Cell *81*, 495–504.

Hu, S., and Yang, X. (2003). Cellular inhibitor of apoptosis 1 and 2 are ubiquitin ligases for the apoptosis inducer Smac/DIABLO. J Biol Chem *278*, 10055–10060.

Huang, W., Jiang, T., Choi, W., Qi, S., Pang, Y., Hu, Q., Xu, Y., Gong, X., Jeffrey, P.D., Wang, J., et al. (2013). Mechanistic insights into CED-4-mediated activation of CED-3. Genes & Development *27*, 2039–2048.

Inohara, N., Gourley, T.S., Carrio, R., Muñiz, M., Merino, J., Garcia, I., Koseki, T., Hu, Y., Chen, S., and Nuñez, G. (1998). Diva, a Bcl-2 homologue that binds directly to Apaf-1 and induces BH3-independent cell death. J Biol Chem *273*, 32479–32486.

Irmler, M., Hofmann, K., Vaux, D., and Tschopp, J. (1997). Direct physical interaction between the Caenorhabditis elegans `death proteins' CED-3 and CED-4. FEBS Lett *406*, 189–190.

Jagasia, R., Grote, P., Westermann, B., and Conradt, B. (2005). DRP-1-mediated mitochondrial fragmentation during EGL-1-induced cell death in C. elegans. Nature *433*, 754–760.

Jiang, H.-S., and Wu, Y.-C. (2014). LIN-3/EGF promotes the programmed cell death of specific cells in Caenorhabditis elegans by transcriptional activation of the pro-apoptotic gene egl-1. PLoS Genet *10*, e1004513.

Jin, Z., Li, Y., Pitti, R., Lawrence, D., Pham, V.C., Lill, J.R., and Ashkenazi, A. (2009). Cullin3-based polyubiquitination and p62-dependent aggregation of caspase-8 mediate extrinsic apoptosis signaling. Cell *137*, 721–735.

Joshi, P., and Eisenmann, D.M. (2004). The Caenorhabditis elegans pvl-5 Gene Protects Hypodermal Cells from ced-3-Dependent, ced-4-Independent Cell Death. Genetics 1–14.

Kaiser, W.J., Vucic, D., and Miller, L.K. (1998). The Drosophila inhibitor of apoptosis D-IAP1 suppresses cell death induced by the caspase drICE. FEBS Lett *440*, 243–248.

Kalchman, M.A., Graham, R.K., Xia, G., Koide, H.B., Hodgson, J.G., Graham, K.C., Goldberg, Y.P., Gietz, R.D., Pickart, C.M., and Hayden, M.R. (1996). Huntingtin is ubiquitinated and interacts with a specific ubiquitin-conjugating enzyme. J Biol Chem *271*, 19385–19394.

Kale, A., Li, W., Lee, C.-H., and Baker, N.E. (2015). Apoptotic mechanisms during competition of ribosomal protein mutant cells: roles of the initiator caspases Dronc and Dream/Strica. Cell Death and Differentiation.

Kamath, R.S., Fraser, A.G., Dong, Y., Poulin, G., Durbin, R., Gotta, M., Kanapin, A., Le Bot, N., Moreno, S., Sohrmann, M., et al. (2003). Systematic functional analysis of the Caenorhabditis elegans genome using RNAi. Nature *421*, 231–237.

Kamura, T., Koepp, D.M., Conrad, M.N., Skowyra, D., Moreland, R.J., Iliopoulos, O., Lane, W.S., Kaelin, W.G., Elledge, S.J., Conaway, R.C., et al. (1999). Rbx1, a component of the VHL tumor suppressor complex and SCF ubiquitin ligase. Science (New York, NY) *284*, 657–661.

Kanda, H., Igaki, T., Kanuka, H., Yagi, T., and Miura, M. (2002). Wengen, a member of the Drosophila tumor necrosis factor receptor superfamily, is required for Eiger signaling. J Biol Chem *277*, 28372–28375.

Kanuka, H., Sawamoto, K., Inohara, N., Matsuno, K., Okano, H., and Miura, M. (1999). Control of the cell death pathway by Dapaf-1, a Drosophila Apaf-1/CED-4-related caspase activator. Molecular Cell *4*, 757–769.

Kato, M., and Sternberg, P.W. (2009). The C. elegans tailless/Tlx homolog nhr-67 regulates a stage-specific program of linker cell migration in male gonadogenesis. Development *136*, 3907–3915.

Keck, S., Nitsch, R., Grune, T., and Ullrich, O. (2003). Proteasome inhibition by paired helical filament-tau in brains of patients with Alzheimer's disease. J Neurochem *85*, 115–122.

Kelekar, A., and Thompson, C.B. (1998). Bcl-2-family proteins: the role of the BH3 domain in apoptosis. Trends in Cell Biology 1–7.

Kelly, W.G., Xu, S., Montgomery, M.K., and Fire, A. (1997). Distinct requirements for somatic and germline expression of a generally expressed Caernorhabditis elegans gene. Genetics *146*, 227–238.

Kerr, J.F., Wyllie, A.H., and Currie, A.R. (1972). Apoptosis: a basic biological phenomenon with wide-ranging implications in tissue kinetics. Br J Cancer *26*, 239–257.

Kim, D.H., Feinbaum, R., Alloing, G., Emerson, F.E., Garsin, D.A., Inoue, H., Tanaka-Hino, M., Hisamoto, N., Matsumoto, K., Tan, M.-W., et al. (2002). A conserved p38 MAP kinase pathway in Caenorhabditis elegans innate immunity. Science (New York, NY) *297*, 623–626.

Kim, H., Rafiuddin-Shah, M., Tu, H.-C., Jeffers, J.R., Zambetti, G.P., Hsieh, J.J.-D., and Cheng, E.H.-Y. (2006). Hierarchical regulation of mitochondrion-dependent apoptosis by BCL-2 subfamilies. Nat Cell Biol *8*, 1348–1358.

Kimble, J., and Hirsh, D. (1979). The postembryonic cell lineages of the hermaphrodite and male gonads in Caenorhabditis elegans. Developmental Biology *70*, 396–417.

Kinchen, J.M., and Ravichandran, K.S. (2010). Identification of two evolutionarily conserved genes regulating processing of engulfed apoptotic cells. Nature *464*, 778–782.

Kinchen, J.M., Doukoumetzidis, K., Almendinger, J., Stergiou, L., Tosello-Trampont, A., Sifri, C.D., Hengartner, M.O., and Ravichandran, K.S. (2008). A pathway for phagosome maturation during engulfment of apoptotic cells. Nat Cell Biol *10*, 556–566.

Kipreos, E.T. (2005). Ubiquitin-mediated pathways in C. elegans. WormBook 1–24.

Kischkel, F.C., Hellbardt, S., Behrmann, I., Germer, M., Pawlita, M., Krammer, P.H., and Peter, M.E. (1995). Cytotoxicity-dependent APO-1 (Fas/CD95)-associated proteins form a death-inducing signaling complex (DISC) with the receptor. The EMBO Journal *14*, 5579–5588.

Kitada, T., Asakawa, S., Hattori, N., Matsumine, H., Yamamura, Y., Minoshima, S., Yokochi, M., Mizuno, Y., and Shimizu, N. (1998). Mutations in the parkin gene cause autosomal recessive juvenile parkinsonism. Nature *392*, 605–608.

Koepp, D.M., Schaefer, L.K., Ye, X., Keyomarsi, K., Chu, C., Harper, J.W., and Elledge, S.J. (2001). Phosphorylation-dependent ubiquitination of cyclin E by the SCFFbw7 ubiquitin ligase. Science (New York, NY) *294*, 173–177.

Komander, D., and Rape, M. (2012). The ubiquitin code. Annu. Rev. Biochem. *81*, 203–229.

Kornbluth, S., and White, K. (2005). Apoptosis in Drosophila: neither fish nor fowl (nor man, nor worm). Journal of Cell Science *118*, 1779–1787.

Korswagen, H.C., Park, J.H., Ohshima, Y., and Plasterk, R.H. (1997). An activating mutation in a Caenorhabditis elegans Gs protein induces neural degeneration. Genes & Development *11*, 1493–1503.

Krajewski, S., Tanaka, S., Takayama, S., Schibler, M.J., Fenton, W., and Reed, J.C. (1993). Investigation of the subcellular distribution of the bcl-2 oncoprotein: residence in the nuclear envelope, endoplasmic reticulum, and outer mitochondrial membranes. Cancer Res. *53*, 4701–4714.

Kulkarni, M., and Smith, H.E. (2008). E1 ubiquitin-activating enzyme UBA-1 plays multiple roles throughout C. elegans development. PLoS Genet *4*, e1000131.

Kurz, T., Pintard, L., Willis, J.H., Hamill, D.R., Gönczy, P., Peter, M., and Bowerman, B. (2002). Cytoskeletal regulation by the Nedd8 ubiquitin-like protein modification pathway. Science (New York, NY) *295*, 1294–1298.

Laundrie, B., Peterson, J.S., Baum, J.S., Chang, J.C., Fileppo, D., Thompson, S.R., and McCall, K. (2003). Germline cell death is inhibited by P-element insertions disrupting the dcp-1/pita nested gene pair in Drosophila. Genetics *165*, 1881–1888.

Lee, J.T., Wheeler, T.C., Li, L., and Chin, L.S. (2007). Ubiquitination of -synuclein by Siah-1 promotes -synuclein aggregation and apoptotic cell death. Human Molecular Genetics *17*, 906–917.

Leroy, E., Boyer, R., Auburger, G., Leube, B., Ulm, G., Mezey, E., Harta, G., Brownstein, M.J., Jonnalagada, S., Chernova, T., et al. (1998). The ubiquitin pathway in Parkinson's disease. Nature *395*, 451–452.

Ley, R., Balmanno, K., Hadfield, K., Weston, C., and Cook, S.J. (2003). Activation of the ERK1/2 signaling pathway promotes phosphorylation and proteasome-dependent degradation of the BH3-only protein, Bim. J Biol Chem *278*, 18811–18816.

Li, P., Nijhawan, D., Budihardjo, I., Srinivasula, S.M., Ahmad, M., Alnemri, E.S., and Wang, X. (1997). Cytochrome c and dATP-dependent formation of Apaf-1/caspase-9 complex initiates an apoptotic protease cascade. Cell *91*, 479–489.

Liani, E., Eyal, A., Avraham, E., Shemer, R., Szargel, R., Berg, D., Bornemann, A., Riess, O., Ross, C.A., Rott, R., et al. (2004). Ubiquitylation of synphilin-1 and alpha-synuclein by SIAH and its presence in cellular inclusions and Lewy bodies imply a role in Parkinson's disease. Proc Natl Acad Sci USA *101*, 5500–5505.

Liu, H., Strauss, T.J., Potts, M.B., and Cameron, S. (2006). Direct regulation of egl-1 and of programmed cell death by the Hox protein MAB-5 and by CEH-20, a C. elegans homolog of Pbx1. Development 1–10.

Liu, J., Stevens, J., Rote, C.A., Yost, H.J., Hu, Y., Neufeld, K.L., White, R.L., and Matsunami, N. (2001). Siah-1 mediates a novel beta-catenin degradation pathway linking p53 to the adenomatous polyposis coli protein. Molecular Cell *7*, 927–936.

Liu, Q.A., and Hengartner, M.O. (1999). Human CED-6 encodes a functional homologue of the Caenorhabditis elegans engulfment protein CED-6. Current Biology : CB *9*, 1347–1350.

Liu, Q.A., and Hengartner, M.O. (1998). Candidate adaptor protein CED-6 promotes the engulfment of apoptotic cells in C. elegans. Cell *93*, 961–972.

Liu, X., Li, P., Widlak, P., Zou, H., Luo, X., Garrard, W.T., and Wang, X. (1998). The 40-kDa subunit of DNA fragmentation factor induces DNA fragmentation and chromatin condensation during apoptosis. Proc Natl Acad Sci USA *95*, 8461–8466.

Lomonosova, E., and Chinnadurai, G. (2008). BH3-only proteins in apoptosis and beyond: an overview. Oncogene *27 Suppl 1*, S2–S19.

Lorick, K.L., Jensen, J.P., Fang, S., Ong, A.M., Hatakeyama, S., and Weissman, A.M. (1999). RING fingers mediate ubiquitin-conjugating enzyme (E2)-dependent ubiquitination. Proc Natl Acad Sci USA *96*, 11364–11369.

Lu, N., Shen, Q., Mahoney, T.R., Liu, X., and Zhou, Z. (2011a). Three sorting nexins drive the degradation of apoptotic cells in response to PtdIns(3)P signaling. Molecular Biology of the Cell *22*, 354–374.

Lu, Y., Rolland, S.G., and Conradt, B. (2011b). A molecular switch that governs mitochondrial fusion and fission mediated by the BCL2-like protein CED-9 of Caenorhabditis elegans.

Proceedings of the National Academy of Sciences *108*, E813–E822.

Lundquist, E.A., Reddien, P.W., Hartwieg, E., Horvitz, H.R., and Bargmann, C.I. (2001). Three C. elegans Rac proteins and several alternative Rac regulators control axon guidance, cell migration and apoptotic cell phagocytosis. Development *128*, 4475–4488.

Mack, T.G., Reiner, M., Beirowski, B., Mi, W., Emanuelli, M., Wagner, D., Thomson, D., Gillingwater, T., Court, F., Conforti, L., et al. (2001). Wallerian degeneration of injured axons and synapses is delayed by a Ube4b/Nmnat chimeric gene. Nat Neurosci *4*, 1199–1206.

Maduro, M., and Pilgrim, D. (1995). Identification and cloning of unc-119, a gene expressed in the Caenorhabditis elegans nervous system. Genetics *141*, 977–988.

Maiuri, M.C., Le Toumelin, G., Criollo, A., Rain, J.-C., Gautier, F., Juin, P., Tasdemir, E., Pierron, G., Troulinaki, K., Tavernarakis, N., et al. (2007). Functional and physical interaction between Bcl-X(L) and a BH3-like domain in Beclin-1. The EMBO Journal *26*, 2527–2539.

Maloof, J.N., Whangbo, J., Harris, J.M., Jongeward, G.D., and Kenyon, C. (1999). A Wnt signaling pathway controls hox gene expression and neuroblast migration in C. elegans. Development *126*, 37–49.

Mangahas, P.M., Yu, X., Miller, K.G., and Zhou, Z. (2008). The small GTPase Rab2 functions in the removal of apoptotic cells in Caenorhabditis elegans. J Cell Biol *180*, 357–373.

Manjón, C., Sánchez-Herrero, E., and Suzanne, M. (2007). Sharp boundaries of Dpp signalling trigger local cell death required for Drosophila leg morphogenesis. Nat Cell Biol *9*, 57–63.

Mathew, R., Seiler, M.P., Scanlon, S.T., Mao, A.-P., Constantinides, M.G., Bertozzi-Villa, C., Singer, J.D., and Bendelac, A. (2012). BTB-ZF factors recruit the E3 ligase cullin 3 to regulate lymphoid effector programs. Nature *491*, 618–621.

Matsuzawa, S.I., and Reed, J.C. (2001). Siah-1, SIP, and Ebi collaborate in a novel pathway for beta-catenin degradation linked to p53 responses. Molecular Cell *7*, 915–926.

Maurer, C.W., Chiorazzi, M., and Shaham, S. (2007). Timing of the onset of a developmental cell death is controlled by transcriptional induction of the C. elegans ced-3 caspase-encoding gene. Development *134*, 1357–1368.

McKay, S.J., Johnsen, R., Khattra, J., Asano, J., Baillie, D.L., Chan, S., Dube, N., Fang, L., Goszczynski, B., Ha, E., et al. (2003). Gene expression profiling of cells, tissues, and developmental stages of the nematode C. elegans. Cold Spring Harbor Symposia on Quantitative Biology *68*, 159–169.

Mei, Y., Xie, C., Xie, W., Wu, Z., and Wu, M. (2007). Siah-1S, a novel splice variant of Siah-1 (seven in absentia homolog), counteracts Siah-1-mediated downregulation of beta-catenin. Oncogene *26*, 6319–6331.

Meier, P., Silke, J., Leevers, S.J., and Evan, G.I. (2000). The Drosophila caspase DRONC is

regulated by DIAP1. The EMBO Journal *19*, 598–611.

Mendes, C.S., Arama, E., Brown, S., Scherr, H., Srivastava, M., Bergmann, A., Steller, H., and Mollereau., B. (2006). Cytochrome c-d regulates developmental apoptosis in the Drosophila retina. EMBO Reports *7*, 933-939.

Metzstein, M.M., and Horvitz, H.R. (1999). The C. elegans cell death specification gene ces-1 encodes a snail family zinc finger protein. Molecular Cell *4*, 309–319.

Metzstein, M.M., Hengartner, M.O., Tsung, N., Ellis, R.E., and Horvitz, H.R. (1996). Transcriptional regulator of programmed cell death encoded by Caenorhabditis elegans gene ces-2. Nature *382*, 545–547.

Miller, T., Krogan, N.J., Dover, J., Erdjument-Bromage, H., Tempst, P., Johnston, M., Greenblatt, J.F., and Shilatifard, A. (2001). COMPASS: a complex of proteins associated with a trithorax-related SET domain protein. Proc Natl Acad Sci USA *98*, 12902–12907.

Mohan, M., Lin, C., Guest, E., and Shilatifard, A. (2010). Licensed to elongate: a molecular mechanism for MLL-based leukaemogenesis. Nat Rev Cancer *10*, 721–728.

Moore, D.J., West, A.B., Dawson, V.L., and Dawson, T.M. (2005). Molecular pathophysiology of Parkinson's disease. Annu. Rev. Neurosci. *28*, 57–87.

Moreno, E., Yan, M., and Basler, K. (2002). Evolution of TNF signaling mechanisms: JNK-dependent apoptosis triggered by Eiger, the Drosophila homolog of the TNF superfamily. Current Biology : CB *12*, 1263–1268.

Mori, H., Kondo, J., and Ihara, Y. (1987). Ubiquitin is a component of paired helical filaments in Alzheimer's disease. Science (New York, NY) *235*, 1641–1644.

Morishima-Kawashima, M., Hasegawa, M., Takio, K., Suzuki, M., Titani, K., and Ihara, Y. (1993). Ubiquitin is conjugated with amino-terminally processed tau in paired helical filaments. Neuron *10*, 1151–1160.

Muro, I., Berry, D.L., Huh, J.R., Chen, C.H., Huang, H., Yoo, S.J., Guo, M., Baehrecke, E.H., and Hay, B.A. (2006). The Drosophila caspase Ice is important for many apoptotic cell deaths and for spermatid individualization, a nonapoptotic process. Development *133*, 3305–3315.

Nagano, Y., Yamashita, H., Takahashi, T., Kishida, S., Nakamura, T., Iseki, E., Hattori, N., Mizuno, Y., Kikuchi, A., and Matsumoto, M. (2003). Siah-1 facilitates ubiquitination and degradation of synphilin-1. J Biol Chem *278*, 51504–51514.

Nakagawa, A., Shi, Y., Kage-Nakadai, E., Mitani, S., and Xue, D. (2010). Caspase-Dependent Conversion of Dicer Ribonuclease into a Death-Promoting Deoxyribonuclease. Science (New York, NY).

Nakano, K., and Vousden, K.H. (2001). PUMA, a novel proapoptotic gene, is induced by p53. Molecular Cell *7*, 683–694.

Nehme, R., Grote, P., Tomasi, T., Löser, S., Holzkamp, H., Schnabel, R., and Conradt, B. (2010). Transcriptional upregulation of both egl-1 BH3-only and ced-3 caspase is required for the death of the male-specific CEM neurons. Cell Death and Differentiation *17*, 1266–1276.

Neufeld, T.P., Tang, A.H., and Rubin, G.M. (1998). A genetic screen to identify components of the sina signaling pathway in Drosophila eye development. Genetics *148*, 277–286.

Neukomm, L.J., Burdett, T.C., Gonzalez, M.A., Züchner, S., and Freeman, M.R. (2014). Rapid in vivo forward genetic approach for identifying axon death genes in Drosophila. Proceedings of the National Academy of Sciences *111*, 9965–9970.

Nicholson, D.W., Ali, A., Thornberry, N.A., Vaillancourt, J.P., Ding, C.K., Gallant, M., Gareau, Y., Griffin, P.R., Labelle, M., and Lazebnik, Y.A. (1995). Identification and inhibition of the ICE/CED-3 protease necessary for mammalian apoptosis. Nature *376*, 37–43.

Nieto, C., Almendinger, J., Gysi, S., Gómez-Orte, E., Kaech, A., Hengartner, M.O., Schnabel, R., Moreno, S., and Cabello, J. (2010). ccz-1 mediates the digestion of apoptotic corpses in C. elegans. Journal of Cell Science *123*, 2001–2007.

Ohta, T., Michel, J.J., Schottelius, A.J., and Xiong, Y. (1999). ROC1, a homolog of APC11, represents a family of cullin partners with an associated ubiquitin ligase activity. Molecular Cell *3*, 535–541.

Oppenheim, R.W., Flavell, R.A., Vinsant, S., Prevette, D., Kuan, C.Y., and Rakic, P. (2001). Programmed cell death of developing mammalian neurons after genetic deletion of caspases. J Neurosci *21*, 4752–4760.

Osterloh, J.M., Yang, J., Rooney, T.M., Fox, A.N., Adalbert, R., Powell, E.H., Sheehan, A.E., Avery, M.A., Hackett, R., Logan, M.A., et al. (2012). dSarm/Sarm1 Is Required for Activation of an Injury-Induced Axon Death Pathway. Science (New York, NY).

Park, D., Jia, H., Rajakumar, V., and Chamberlin, H.M. (2006). Pax2/5/8 proteins promote cell survival in C. elegans. Development *133*, 4193–4202.

Parrish, A.B., Freel, C.D., and Kornbluth, S. (2013). Cellular mechanisms controlling caspase activation and function. Cold Spring Harbor Perspectives in Biology *5*.

Parrish, J., Li, L., Klotz, K., Ledwich, D., Wang, X., and Xue, D. (2001). Mitochondrial endonuclease G is important for apoptosis in C. elegans. Nature *412*, 90–94.

Parrish, J., Metters, H., Chen, L., and Xue, D. (2000). Demonstration of the in vivo interaction of key cell death regulators by structure-based design of second-site suppressors. Proc Natl Acad Sci USA *97*, 11916–11921.

Peden, E., Kimberly, E., Gengyo-Ando, K., Mitani, S., and Xue, D. (2007). Control of sex-specific apoptosis in C. elegans by the BarH homeodomain protein CEH-30 and the transcriptional repressor UNC-37/Groucho. Genes & Development *21*, 3195–3207.

Pérez-Garijo, A., Fuchs, Y., and Steller, H. (2013). Apoptotic cells can induce non-autonomous apoptosis through the TNF pathway. Elife *2*, e01004.

Phillips, M.E., and Platt, J.E. (1994). The use of ubiquitin as a marker of thyroxine-induced apoptosis in cultured Rana catesbeiana tail tips. Gen. Comp. Endocrinol. *95*, 409–415.

Pilar, G., and Landmesser, L. (1976). Ultrastructural differences during embryonic cell death in normal and peripherally deprived ciliary ganglia. J Cell Biol *68*, 339–356.

Poreba, M., Strozyk, A., Salvesen, G.S., and Drag, M. (2013). Caspase Substrates and Inhibitors. Cold Spring Harbor Perspectives in Biology 1–20.

Pourkarimi, E., Greiss, S., and Gartner, A. (2012). Evidence that CED-9/Bcl2 and CED-4/Apaf-1 localization is not consistent with the current model for C. elegans apoptosis induction. Cell Death and Differentiation 1–10.

Qadota, H., Inoue, M., Hikita, T., Köppen, M., Hardin, J.D., Amano, M., Moerman, D.G., and Kaibuchi, K. (2007). Establishment of a tissue-specific RNAi system in C. elegans. Gene *400*, 166–173.

Qi, S., Pang, Y., Hu, Q., Liu, Q., Li, H., Zhou, Y., He, T., Liang, Q., Liu, Y., Yuan, X., et al. (2010). Crystal Structure of the Caenorhabditis elegans Apoptosome Reveals an Octameric Assembly of CED-4. Cell *141*, 446–457.

Qiu, X.-B., Markant, S.L., Yuan, J., and Goldberg, A.L. (2004). Nrdp1-mediated degradation of the gigantic IAP, BRUCE, is a novel pathway for triggering apoptosis. The EMBO Journal *23*, 800–810.

Quinn, L., Coombe, M., Mills, K., Daish, T., Colussi, P., Kumar, S., and Richardson, H. (2003). Buffy, a Drosophila Bcl-2 protein, has anti-apoptotic and cell cycle inhibitory functions. The EMBO Journal *22*, 3568–3579.

Reddien, P.W., and Horvitz, H.R. (2000). CED-2/CrkII and CED-10/Rac control phagocytosis and cell migration in Caenorhabditis elegans. Nat Cell Biol *2*, 131–136.

Reddien, P.W., Andersen, E.C., Huang, M.C., and Horvitz, H.R. (2007). DPL-1 DP, LIN-35 Rb and EFL-1 E2F act with the MCD-1 zinc-finger protein to promote programmed cell death in Caenorhabditis elegans. Genetics *175*, 1719–1733.

Reddien, P.W., Cameron, S., and Horvitz, H.R. (2001). Phagocytosis promotes programmed cell death in C. elegans. Nature *412*, 198–202.

Ren, X., and Hurley, J.H. (2010). Ren_et_al-2010-The_EMBO_Journal. The EMBO Journal *29*, 1045–1054.

Rieser, E., Cordier, S.M., and Walczak, H. (2013). Linear ubiquitination: a newly discovered regulator of cell signalling. Trends Biochem Sci *38*, 94–102.

Riley, B.E., and Orr, H.T. (2006). Polyglutamine neurodegenerative diseases and regulation of transcription: assembling the puzzle. Genes & Development *20*, 2183–2192.

Rocheleau, C.E., Howard, R.M., Goldman, A.P., Volk, M.L., Girard, L.J., and Sundaram, M.V. (2002). A lin-45 raf enhancer screen identifies eor-1, eor-2 and unusual alleles of Ras pathway genes in Caenorhabditis elegans. Genetics *161*, 121–131.

Rodriguez, A., Oliver, H., Zou, H., Chen, P., Wang, X., and Abrams, J.M. (1999). Dark is a Drosophila homologue of Apaf-1/CED-4 and functions in an evolutionarily conserved death pathway. Nat Cell Biol *1*, 272–279.

Rott, R., Szargel, R., Haskin, J., Shani, V., Shainskaya, A., Manov, I., Liani, E., Avraham, E., and Engelender, S. (2008). Monoubiquitylation of alpha-synuclein by seven in absentia homolog (SIAH) promotes its aggregation in dopaminergic cells. J Biol Chem *283*, 3316–3328.

Roy, N., Deveraux, Q.L., Takahashi, R., Salvesen, G.S., and Reed, J.C. (1997). The c-IAP-1 and c-IAP-2 proteins are direct inhibitors of specific caspases. The EMBO Journal *16*, 6914–6925.

Ryoo, H.D., Bergmann, A., Gonen, H., Ciechanover, A., and Steller, H. (2002). Regulation of Drosophila IAP1 degradation and apoptosis by reaper and ubcD1. Nat Cell Biol *4*, 432–438.

Saeki, Y., Kudo, T., Sone, T., Kikuchi, Y., Yokosawa, H., Toh-e, A., and Tanaka, K. (2009). Lysine 63-linked polyubiquitin chain may serve as a targeting signal for the 26S proteasome. The EMBO Journal *28*, 359–371.

Sandu, C., Ryoo, H.D., and Steller, H. (2010). Drosophila IAP antagonists form multimeric complexes to promote cell death. J Cell Biol *190*, 1039–1052.

Sarov, M., Murray, J.I., Schanze, K., Pozniakovski, A., Niu, W., Angermann, K., Hasse, S., Rupprecht, M., Vinis, E., Tinney, M., et al. (2012). A genome-scale resource for in vivo tag-based protein function exploration in C. elegans. Cell *150*, 855–866.

Sasagawa, Y., Urano, T., Kohara, Y., Takahashi, H., and Higashitani, A. (2003). Caenorhabditis elegans RBX1 is essential for meiosis, mitotic chromosomal condensation and segregation, and cytokinesis. Genes Cells *8*, 857–872.

Scaglione, K.M., Zavodszky, E., Todi, S.V., Patury, S., Xu, P., Rodríguez-Lebrón, E., Fischer, S., Konen, J., Djarmati, A., Peng, J., et al. (2011). Ube2w and ataxin-3 coordinately regulate the ubiquitin ligase CHIP. Molecular Cell *43*, 599–612.

Schertel, C., and Conradt, B. (2007). C. elegans orthologs of components of the RB tumor suppressor complex have distinct pro-apoptotic functions. Development *134*, 3691–3701.

Schneider, P., Bodmer, J.L., Holler, N., Mattmann, C., Scuderi, P., Terskikh, A., Peitsch, M.C., and Tschopp, J. (1997). Characterization of Fas (Apo-1, CD95)-Fas ligand interaction. J Biol Chem *272*, 18827–18833.

Schulman, B.A., and Harper, J.W. (2009). Ubiquitin-like protein activation by E1 enzymes: the apex for downstream signalling pathways. Nat Rev Mol Cell Biol *10*, 319–331.

Schumacher, B., Schertel, C., Wittenburg, N., Tuck, S., Mitani, S., Gartner, A., Conradt, B., and Shaham, S. (2005). C. elegans ced-13 can promote apoptosis and is induced in response to DNA damage. Cell Death and Differentiation *12*, 153–161.

Schwartz, H.T., and Horvitz, H.R. (2007). The C. elegans protein CEH-30 protects male-specific neurons from apoptosis independently of the Bcl-2 homolog CED-9. Genes & Development *21*, 3181–3194.

Schwartz, L.M., and Truman, J.W. (1982). Peptide and steroid regulation of muscle degeneration in an insect. Science (New York, NY) *215*, 1420–1421.

Schwartz, L.M., Myer, A., Kosz, L., Engelstein, M., and Maier, C. (1990). Activation of polyubiquitin gene expression during developmentally programmed cell death. Neuron *5*, 411–419.

Schwartz, L.M., Smith, S.W., Jones, M.E., and Osborne, B.A. (1993). Do all programmed cell deaths occur via apoptosis? Proc Natl Acad Sci USA *90*, 980–984.

Selkoe, D.J. (1991). The molecular pathology of Alzheimer's disease. Neuron *6*, 487–498.

Seshagiri, S., and Miller, L.K. (1997). Caenorhabditis elegans CED-4 stimulates CED-3 processing and CED-3-induced apoptosis. Current Biology : CB *7*, 455–460.

Seshagiri, S., Chang, W.T., and Miller, L.K. (1998). Mutational analysis of Caenorhabditis elegans CED-4. FEBS Lett *428*, 71–74.

Seufert, W., and Jentsch, S. (1990). Ubiquitin-conjugating enzymes UBC4 and UBC5 mediate selective degradation of short-lived and abnormal proteins. The EMBO Journal *9*, 543–550.

Sevrioukov, E.A., Burr, J., Huang, E.W., Assi, H.H., Monserrate, J.P., Purves, D.C., Wu, J.N., Song, E.J., and Brachmann, C.B. (2007). Drosophila Bcl-2 proteins participate in stress-induced apoptosis, but are not required for normal development. Genesis *45*, 184–193.

Shaham, S., and Horvitz, H.R. (1996a). Developing Caenorhabditis elegans neurons may contain both cell-death protective and killer activities. Genes & Development *10*, 578–591.

Shaham, S., and Horvitz, H.R. (1996b). An alternatively spliced C. elegans ced-4 RNA encodes a novel cell death inhibitor. Cell *86*, 201–208.

Shirayama, M., Tóth, A., Gálová, M., and Nasmyth, K. (1999). APC(Cdc20) promotes exit from mitosis by destroying the anaphase inhibitor Pds1 and cyclin Clb5. Nature *402*, 203–207.

Siegfried, K.R., and Kimble, J. (2002). POP-1 controls axis formation during early gonadogenesis in C. elegans. Development *129*, 443–453.

Simmer, F., Tijsterman, M., Parrish, S., Koushika, S.P., Nonet, M.L., Fire, A., Ahringer, J., and Plasterk, R.H.A. (2002). Loss of the putative RNA-directed RNA polymerase RRF-3 makes C. elegans hypersensitive to RNAi. Current Biology : CB *12*, 1317–1319.

Skinner, P.J., Koshy, B.T., Cummings, C.J., Klement, I.A., Helin, K., Servadio, A., Zoghbi, H.Y., and Orr, H.T. (1997). Ataxin-1 with an expanded glutamine tract alters nuclear matrix-associated structures. Nature *389*, 971–974.

Sobhian, B., Shao, G., Lilli, D.R., Culhane, A.C., Moreau, L.A., Xia, B., Livingston, D.M., and Greenberg, R.A. (2007). RAP80 targets BRCA1 to specific ubiquitin structures at DNA damage sites. Science (New York, NY) *316*, 1198–1202.

Song, Q., Kuang, Y., Dixit, V.M., and Vincenz, C. (1999). Boo, a novel negative regulator of cell death, interacts with Apaf-1. The EMBO Journal *18*, 167–178.

Spector, M.S., Desnoyers, S., Hoeppner, D.J., and Hengartner, M.O. (1997). Interaction between the C. elegans cell-death regulators CED-9 and CED-4. Nature 1–4.

Srinivasula, S.M., Ahmad, M., Fernandes-Alnemri, T., Litwack, G., and Alnemri, E.S. (1996). Molecular ordering of the Fas-apoptotic pathway: the Fas/APO-1 protease Mch5 is a CrmA-inhibitable protease that activates multiple Ced-3/ICE-like cysteine proteases. Proc Natl Acad Sci USA *93*, 14486–14491.

Stevens, T. A. (1999) Characterization and developmental expression patterns of the ubiquitin-conjugating enzyme UBC-2 in the nematode *Caenorhabditis elegans*. (Doctoral dissertation) The University of British Columbia.

Stogios, P.J., and Prive, G.G. (2004). The BACK domain in BTB-kelch proteins. Trends Biochem Sci *29*, 634–637.

Sulston, J.E. (1976). Post-embryonic Development in the ventral cordof Caenorhabditis elegans. Philosophical Transactions of the Royal Society of London Series B, Biological Sciences 1–13.

Sulston, J.E., and Horvitz, H.R. (1977). Post-embryonic cell lineages of the nematode, Caenorhabditis elegans. Developmental Biology *56*, 110–156.

Sulston, J.E., Albertson, D.G., and Thomson, J.N. (1980). The Caenorhabditis elegans male: postembryonic development of nongonadal structures. Developmental Biology *78*, 542–576.

Sulston, J.E., Schierenberg, E., White, J.G., and Thomson, J.N. (1983). The embryonic cell lineage of the nematode Caenorhabditis elegans. Developmental Biology *100*, 64–119.

Suzuki, Y., Nakabayashi, Y., and Takahashi, R. (2001). Ubiquitin-protein ligase activity of X-linked inhibitor of apoptosis protein promotes proteasomal degradation of caspase-3 and enhances its anti-apoptotic effect in Fas-induced cell death. Proc Natl Acad Sci USA *98*, 8662–8667.

Syntichaki, P., Xu, K., Driscoll, M., and Tavernarakis, N. (2002). Specific aspartyl and calpain proteases are required for neurodegeneration in C. elegans. Nature *419*, 939–944.

Tabara, H., Sarkissian, M., Kelly, W.G., Fleenor, J., Grishok, A., Timmons, L., Fire, A., and Mello, C.C. (1999). The rde-1 gene, RNA interference, and transposon silencing in C. elegans. Cell *99*, 123–132.

Tait, S.W.G., de Vries, E., Maas, C., Keller, A.M., D'Santos, C.S., and Borst, J. (2007). Apoptosis induction by Bid requires unconventional ubiquitination and degradation of its N-terminal fragment. J Cell Biol *179*, 1453–1466.

Takacs-Vellai, K., Vellai, T., Puoti, A., Passannante, M., Wicky, C., Streit, A., Kovács, A.L., and Müller, F. (2005). Inactivation of the Autophagy Gene bec-1 Triggers Apoptotic Cell Death in C. elegans. Current Biology *15*, 1513–1517.

Tamai, K.K., and Nishiwaki, K. (2007). bHLH transcription factors regulate organ morphogenesis via activation of an ADAMTS protease in C. elegans. Developmental Biology *308*, 562–571.

Tan, F.J., Fire, A.Z., and Hill, R.B. (2007). Regulation of apoptosis by C. elegans CED-9 in the absence of the C-terminal transmembrane domain. Cell Death and Differentiation *14*, 1925–1935.

Tan, F.J., Zuckerman, J.E., Wells, R.C., and Hill, R.B. (2011). The C. elegans B-cell Lymphoma 2 (bcl-2) Homolog Cell Death Abnormal 9 (ced-9) Associates with and Remodels Lipid Membranes. Protein Science 1–13.

Tang, A.H., Neufeld, T.P., Kwan, E., and Rubin, G.M. (1997). PHYL acts to down-regulate TTK88, a transcriptional repressor of neuronal cell fates, by a SINA-dependent mechanism. Cell *90*, 459–467.

Thellmann, M., Hatzold, J., and Conradt, B. (2003). The Snail-like CES-1 protein of C. elegans can block the expression of the BH3-only cell-death activator gene egl-1 by antagonizing the function of bHLH proteins. Development *130*, 4057–4071.

Thornberry, N.A. (1992). A novel heterodimeric cysteine protease is required for interleukin-1b processing in monocytes. Nature 1–7.

Tofaris, G.K., Razzaq, A., Ghetti, B., Lilley, K.S., and Spillantini, M.G. (2003). Ubiquitination of -Synuclein in Lewy Bodies Is a Pathological Event Not Associated with Impairment of Proteasome Function. Journal of Biological Chemistry *278*, 44405–44411.

Tongaonkar, P., Beck, K., Shinde, U.P., and Madura, K. (1999). Characterization of a temperature-sensitive mutant of a ubiquitin-conjugating enzyme and its use as a heat-inducible degradation signal. Anal. Biochem. *272*, 263–269.

Trauth, B.C., Klas, C., Peters, A.M., Matzku, S., Möller, P., Falk, W., Debatin, K.M., and Krammer, P.H. (1989). Monoclonal antibody-mediated tumor regression by induction of

apoptosis. Science (New York, NY) *245*, 301–305.

Treinin, M., and Chalfie, M. (1995). A mutated acetylcholine receptor subunit causes neuronal degeneration in C. elegans. Neuron *14*, 871–877.

Trent, C., Tsuing, N., and Horvitz, H.R. (1983). Egg-laying defective mutants of the nematode Caenorhabditis elegans. Genetics *104*, 619–647.

Umebayashi, K., Stenmark, H., and Yoshimori, T. (2008). Ubc4/5 and c-Cbl continue to ubiquitinate EGF receptor after internalization to facilitate polyubiquitination and degradation. Molecular Biology of the Cell *19*, 3454–3462.

Venegas, V., and Zhou, Z. (2007). Two Alternative Mechanisms That Regulate the Presentation of Apoptotic Cell Engulfment Signal in Caenorhabditis elegans. Molecular Biology of the Cell 1–13.

Verhagen, A.M., Ekert, P.G., Pakusch, M., Silke, J., Connolly, L.M., Reid, G.E., Moritz, R.L., Simpson, R.J., and Vaux, D.L. (2000). Identification of DIABLO, a mammalian protein that promotes apoptosis by binding to and antagonizing IAP proteins. Cell *102*, 43–53.

Verma, S., Zhao, L.J., and Chinnadurai, G. (2001). Phosphorylation of the pro-apoptotic protein BIK: mapping of phosphorylation sites and effect on apoptosis. J Biol Chem *276*, 4671–4676.

Vucic, D., Kaiser, W.J., and Miller, L.K. (1998). Inhibitor of apoptosis proteins physically interact with and block apoptosis induced by Drosophila proteins HID and GRIM. Molecular and Cellular Biology *18*, 3300–3309.

Vucic, D., Kaiser, W.J., Harvey, A.J., and Miller, L.K. (1997). Inhibition of reaper-induced apoptosis by interaction with inhibitor of apoptosis proteins (IAPs). Proc Natl Acad Sci USA *94*, 10183–10188.

Wang, L., Du, F., and Wang, X. (2008). TNF-alpha induces two distinct caspase-8 activation pathways. Cell *133*, 693–703.

Wang, X., Yang, C., Chai, J., Shi, Y., and Xue, D. (2002). Mechanisms of AIF-mediated apoptotic DNA degradation in Caenorhabditis elegans. Science (New York, NY) *298*, 1587–1592.

Wang, Y., Matthewman, C., Han, L., Miller, T., Miller, D.M., and Bianchi, L. (2013). Neurotoxic unc-8 mutants encode constitutively active DEG/ENaC channels that are blocked by divalent cations. J. Gen. Physiol. *142*, 157–169.

Wefes, I., Mastrandrea, L.D., Haldeman, M., Koury, S.T., Tamburlin, J., Pickart, C.M., and Finley, D. (1995). Induction of ubiquitin-conjugating enzymes during terminal erythroid differentiation. Proc Natl Acad Sci USA *92*, 4982–4986.

White, K., Grether, M.E., Abrams, J.M., Young, L., Farrell, K., and Steller, H. (1994). Genetic

control of programmed cell death in Drosophila. Science (New York, NY) *264*, 677–683.

Wilson, R., Goyal, L., Ditzel, M., Zachariou, A., Baker, D.A., Agapite, J., Steller, H., and Meier, P. (2002). The DIAP1 RING finger mediates ubiquitination of Dronc and is indispensable for regulating apoptosis. Nat Cell Biol *4*, 445–450.

Wolter, K.G., Hsu, Y.T., Smith, C.L., Nechushtan, A., Xi, X.G., and Youle, R.J. (1997). Movement of Bax from the cytosol to mitochondria during apoptosis. J Cell Biol *139*, 1281–1292.

Woo, J.-S., and Jung, J.-S. (2003). Unique structural features of a BCL-2 family protein CED-9 and biophysical characterization of CED-9/EGL-1 interactions. Cell Death and Differentiation 1–10.

Wu, D., Wallen, H.D., Inohara, N., and Nuñez, G. (1997). Interaction and regulation of the Caenorhabditis elegans death protease CED-3 by CED-4 and CED-9. J Biol Chem *272*, 21449–21454.

Wu, Y.C., and Horvitz, H.R. (1998). The C. elegans cell corpse engulfment gene ced-7 encodes a protein similar to ABC transporters. Cell *93*, 951–960.

Wu, Y.C., Stanfield, G.M., and Horvitz, H.R. (2000). NUC-1, a caenorhabditis elegans DNase II homolog, functions in an intermediate step of DNA degradation during apoptosis. Genes & Development *14*, 536–548.

Wu, Y.C., Tsai, M.C., Cheng, L.C., Chou, C.J., and Weng, N.Y. (2001). C. elegans CED-12 acts in the conserved crkII/DOCK180/Rac pathway to control cell migration and cell corpse engulfment. Developmental Cell *1*, 491–502.

Xu, K., Tavernarakis, N., and Driscoll, M. (2001). Necrotic cell death in C. elegans requires the function of calreticulin and regulators of Ca(2+) release from the endoplasmic reticulum. Neuron *31*, 957–971.

Xu, L., Wei, Y., Reboul, J., Vaglio, P., Shin, T.-H., Vidal, M., Elledge, S.J., and Harper, J.W. (2003). BTB proteins are substrate-specific adaptors in an SCF-like modular ubiquitin ligase containing CUL-3. Nature *425*, 316–321.

Xu, P., Duong, D.M., Seyfried, N.T., Cheng, D., Xie, Y., Robert, J., Rush, J., Hochstrasser, M., Finley, D., and Peng, J. (2009). Quantitative Proteomics Reveals the Function of Unconventional Ubiquitin Chains in Proteasomal Degradation. Cell *137*, 133–145.

Xue, D., and Horvitz, H.R. (1995). Inhibition of the Caenorhabditis elegans cell-death protease CED-3 by a CED-3 cleavage site in baculovirus p35 protein. Nature *377*, 248–251.

Xue, D., Shaham, S., and Horvitz, H.R. (1996). The Caenorhabditis elegans cell-death protein CED-3 is a cysteine protease with substrate specificities similar to those of the human CPP32 protease. Genes & Development *10*, 1073–1083.

Xue, D., and Horvitz, H.R. (1997). Caenorhabditis elegans CED-9 protein is a bifunctional cell-death inhibitor. Nature *390*, 305–308.

Yamamoto, Y., and Henderson, C.E. (1999). Patterns of programmed cell death in populations of developing spinal motoneurons in chicken, mouse, and rat. Developmental Biology *214*, 60–71.

Yan, N., Chai, J., Lee, E.-S., Gu, L., Liu, Q., He, J., Wu, J.W., Kokel, D., Li, H., Hao, Q., et al. (2005). Structure of the CED-4–CED-9 complex provides insights into programmed cell death in Caenorhabditis elegans. Nat Cell Biol *437*, 831–837.

Yan, N., Gu, L., Kokel, D., Chai, J., Li, W., Han, A., Chen, L., Xue, D., and Shi, Y. (2004). Structural, biochemical, and functional analyses of CED-9 recognition by the proapoptotic proteins EGL-1 and CED-4. Molecular Cell *15*, 999–1006.

Yan, N., Wu, J.-W., Chai, J., Li, W., and Shi., Y. (2004b). Molecular mechanisms of DrICE inhibition by DIAP1 and removal of inhibition by Reaper, Hid and Grim. Nat Struc Mol Bio *11,* 420-428.

Yang, X., Chang, H.Y., and Baltimore, D. (1998). Essential Role of CED-4 Oligomerization in CED-3 Activation and Apoptosis. Science (New York, NY) 1–4.

Ye, Y., and Rape, M. (2009). Building ubiquitin chains: E2 enzymes at work. Nat Rev Mol Cell Biol *10*, 755–764.

Yu, X., Wang, L., Acehan, D., Wang, X., and Akey, C.W. (2006). Three-dimensional structure of a double apoptosome formed by the Drosophila Apaf-1 related killer. J. Mol. Biol. *355*, 577–589.

Yuan, J., and Horvitz, H.R. (1990). The Caenorhabditis elegans Genes ced-3 and ced-4 Act Cell Autonomously to Cause Programmed Cell Death. Developmental Biology 1–9.

Yuan, J., and Horvitz, H.R. (1992). The Caenorhabditis elegans cell death gene ced-4 encodes a novel protein and is expressed during the period of extensive programmed cell death. Development *116*, 309–320.

Yuan, J., Shaham, S., Ledoux, S., Ellis, H., and Horvitz, H.R. (1993). The C. elegans cell death gene ced-3 encodes a protein similar to mammalian interleukin-1 beta-converting enzyme. Cell *75*, 641–652.

Zander, C., Takahashi, J., Hachimi, El, K.H., Fujigasaki, H., Albanese, V., Lebre, A.S., Stevanin, G., Duyckaerts, C., and Brice, A. (2001). Similarities between spinocerebellar ataxia type 7 (SCA7) cell models and human brain: proteins recruited in inclusions and activation of caspase-3. Human Molecular Genetics *10*, 2569–2579.

Zhai, Q., Wang, J., Kim, A., Liu, Q., Watts, R., Hoopfer, E., Mitchison, T., Luo, L., and He, Z. (2003). Involvement of the ubiquitin-proteasome system in the early stages of wallerian degeneration. Neuron *39*, 217–225.

Zhen, M., Heinlein, R., Jones, D., Jentsch, S., and Candido, E.P.M. (1993). The ubc-2 gene of Caenorhabditis elegans encodes a ubiquitin-conjugating enzyme involved in selective protein degradation. Molecular and Cellular Biology *13*, 1371–1377.

Zhen, M., Schein, J.E., Baillie, D.L., and Candido, E.P. (1996). An essential ubiquitin-conjugating enzyme with tissue and developmental specificity in the nematode Caenorhabditis elegans. The EMBO Journal *15*, 3229–3237.

Zhou, Z., Caron, E., Hartwieg, E., Hall, A., and Horvitz, H.R. (2001a). The C. elegans PH domain protein CED-12 regulates cytoskeletal reorganization via a Rho/Rac GTPase signaling pathway. Developmental Cell *1*, 477–489.

Zhou, Z., Hartwieg, E., and Horvitz, H.R. (2001b). CED-1 is a transmembrane receptor that mediates cell corpse engulfment in C. elegans. Cell *104*, 43–56.

Zou, H., and Niswander, L. (1996). Requirement for BMP signaling in interdigital apoptosis and scale formation. Science (New York, NY) *272*, 738–741.

Zou, H., Henzel, W.J., Liu, X., Lutschg, A., and Wang, X. (1997). Apaf-1, a human protein homologous to C. elegans CED-4, participates in cytochrome c-dependent activation of caspase-3. Cell *90*, 405–413.